# Whole Exome Sequencing in Children with Rare Endocrine Disorders

A thesis submitted by

**Dr Dinesh Chand Giri Harirambapu**

For the degree of Doctorate in Medicine from the University of Liverpool

Institute in the Park

Alder Hey Children's NHS Foundation Trust

Department of Women's and Children's Health

University of Liverpool

September 2017

# ACKNOWLEDGEMENTS

Firstly, I would express my sincere thanks to Dr Senthil Senniappan for his excellent supervision and continuous support throughout my MD. His optimism, patience, enthusiasm and motivation have been my inspiration throughout. I extend my thanks to my co-supervisors, Professor Paul McNamara and Professor Matthew Peak for their constant encouragement, guidance and support.

I am grateful to Dr Carles Gaston-Massuet, Queen Mary University of London, for his collaboration and kindly hosting me to do the functional work and laboratory studies. I also thank his excellent team- Maria Liilina Vignola, Angelica Gualtieri and Valeria Scagliotti for teaching me various molecular biology techniques. I am also grateful for the help offered by Dr John Scott from the University of Melbourne, Australia on some of the functional studies related to my project. I thank Dr Roger Mountford, Molecular Genetics laboratory, Liverpool Women's Hospital for his support and Dr Pia Koldkjaer, Dr Christiane Hertz-Fowler, Dr Sam Heldenby, Dr Xuan Liu from the centre of genomic research, University of Liverpool for their help with sequencing and bioinformatics.

I owe my kind regards to Dr Mo Didi, Dr Jo Blair, Dr Poonam Dharmaraj, Dr Urmi Das & Dr Renuka Ramakrishnan from the department of Paediatric Endocrinology, Alder Hey Children's NHS Foundation Trust for their help and encouragement. I thank Dr Julie Park for her friendship and cheerful encouragement during my time in the department.

I thank Sandoz(UK) limited for gracefully funding my MD.

I extend my thanks to Dr Bala Palanisami and his family for their warmth and support especially over the last couple of years. My sincere thanks to my parents for their love and blessings. My heartfelt thanks to my wife, Jaishri for her perseverance, immense support, encouragement and of course, my 5-year-old daughter, Vibusha for her patience, understanding and sparing me the time over the last 2 years to accomplish this endeavour.

# DECLARATION OF WORK

I, Dr Dinesh Chand Giri Harirambapu, confirm that the work presented in this thesis is my own. Where information has been derived from other sources, I confirm that this has been indicated in the thesis.

# ABSTRACT

**Background**
Congenital Hyperinsulinism (CHI) is characterized by unregulated secretion of insulin in the presence of hypoglycaemia. Mutations in eleven different genes *ABCC8, KCNJ11, GLUD1, GCK, HADH, UCP2, HNF4A, HNF1A, MCT1, HK1* and *PGM1* have been associated with genetic forms of CHI. However, the genetic cause for many CHI patients (nearly 50%) remains elusive. Mutations in transcription factors such as *HESX1, PROP1, POU1F1, LHX3, LHX4, PITX1, PITX2, OTX2, SOX2* and *SOX3* have been associated with congenital hypopituitarism(CH) in mouse and humans. However, these mutations account only for a small proportion with the majority of patients having an unknown genetic cause for their symptoms. The use of next generation sequencing in children with undiagnosed or unidentified syndromic disorders is becoming more popular in recent years, increasing the diagnostic ability and discovery of novel genes and mutations contributing to novel clinical phenotypes.

**Aims**
1. To identify novel genetic mechanisms in patients with rare endocrine disorders.
2. To functionally characterize a transcription factor associated with pituitary and pancreatic development and to characterize a novel gene associated with CHI.

**Patients**
Six patients with varied phenotypes such as CHI and CH(n=1), CHI(n=1), primary IGF1 deficiency with dysmorphic features (n=1), severe short stature with dysmorphic features(n=1), severe short stature(n=1), hypercalcemia and glomerular disease(n=1) were recruited into this study.

**Methods**
Whole exome sequencing(WES) was performed on the genomic DNA in trios (patient and the biological parents) for 5 patients. In one of the patients where the DNA sample was not possible to obtain from the biological father, WES was performed on the genomic DNA from the patient and the biological mother. mRNA expression during murine embryogenesis was studied using *in situ* hybridization and the protein expression in human embryos was demonstrated by immunohistochemistry. The pathogenic effect of the variant on protein function was further demonstrated by transcriptional activation assays using luciferase and quantification of protein expression using western blot.

**Results**
1. WES identified a *de novo* heterozygous mutation in *FOXA2* (c.505T>C, p.S169P) in a highly conserved residue within the DNA binding domain in a patient with CHI and CH. A strong expression of *Foxa2* mRNA was found in the developing hypothalamus, pituitary, pancreas, lungs and oesophagus of mouse embryos using *in situ* hybridization. Expression profiling on human embryos by immunohistochemistry showed strong expression of hFOXA2 in the neural tube, third ventricle, diencephalon and in the pancreas. Transient transfection of HEK293T cells with Wt (Wild type) hFOXA2 or mutant hFOXA2 showed an impairment in transcriptional reporter activity by the mutant hFOXA2. Further analyses using western blot assays showed that the *FOXA2* p.(S169P) variant is pathogenic resulting in lower expression levels when compared with Wt hFOXA2.

2. A novel compound heterozygous mutation (p.R989G, p.K1026N) in *ASXL3* contributing to Bainbridge Ropers syndrome in association with primary IGF1 deficiency was found in a patient with severe short stature with dysmorphism.
3. A *de novo* heterozygous frameshift mutation (p.G539fs*4) was found in *CaMKK2* isoform-7 in a patient with persistent CHI, negative for mutations in known genes. On expressing the pG539fs*4 mutant in COS7 cells a significantly higher basal and $Ca^{2+}$-CaM dependent kinase activity was noted when compared with WT (Wild Type) isoform-7. Both isoform-7 and the pG539fs*4 mutant have elevated basal kinase activity compared with isoform-1, the major CaMKK2 isoform expressed in most tissues.
4. A heterozygous splicing mutation in *B3GAT3* was found in a patient with short stature, congenital heart defects, facial dysmorphism and skeletal abnormalities.
5. A homozygous mutation in the promoter region of *GH1* was identified in a patient with severe short stature and low IGF1.

In one patient, no relevant genetic variant segregating with the phenotype was identified.

**Conclusions**

*FOXA2* mutation can cause a complex congenital syndrome with hypopituitarism, and hyperinsulinism. Frameshift mutation in *CaMKK2* is a potential novel cause of persistent CHI.WES has helped to identify the underlying genetic etiology in 5 out of 6 families recruited in the study.

## TABLE OF CONTENTS


Acknowledgements ii
Declaration of Work iii
Abstract iv
Table of Contents vi
List of Figures xiii
List of Tables xvi
Abbreviations xvii

**CHAPTER 1**

**PROMISE OF WHOLE EXOME SEQUENCING IN PAEDIATRIC ENDOCRINOLOGY**

1.1 Summary of Chapter 1 2
1.2 Whole Exome Sequencing(WES) 3
1.2.1 Introduction 3
1.2.2 Exome Sequencing 3
1.2.3 WES in Medicine 4
1.2.4 WES in Paediatric Endocrinology 7
1.2.4.1 WES in Growth and Pubertal Disorders 7
1.2.4.2 WES in Disorders of Adrenal gland and Endocrine Neoplasia 9
1.2.4.3 WES in Familial Glucocorticoid Deficiency 9
1.2.4.4 WES in Thyroid Disorders 10
1.2.4.5 WES in Juvenile Osteoporosis 11
1.2.4.6 WES in 46XY Disorders of Sexual Differentiation 11
1.2.4.7 WES in Clinical Endocrinology
1.2.5 Disadvantages in WES 14
1.2.6 WES, GWAS and Whole Genome Sequencing (WGS) 15

**CHAPTER 2**

**PITUITARY GLAND-EMBRYOLOGY, DEVELOPMENTAL TRANSCRIPTION FACTORS, CONGENITAL HYPOPITUITARISM, DIAGNOSIS AND MANAGEMENT**

2.1 Summary of Chapter 2 17
2.2 Pituitary Gland 18
2.2.1 Embryology and Development of Pituitary Gland 19
2.2.1.1 Early Developmental Genes and Signals 21
2.3 Syndromic Forms of Hypopituitarism 23
2.3.1 Septo-optic Dysplasia(SOD) 23

2.3.2 *HESX1* mutations and SOD 24
2.3.3 *SOX2* and *SOX3* Mutations 25
2.3.4 Holoprosencephaly 25
2.3.5 *LHX3* mutations 26
2.3.6 *LHX4* mutations 26
2.3.7 *OTX2* mutations 27
2.3.8 Axenfield-Rieger syndrome (*PITX2* mutations) 27
2.4 Non-syndromic forms of Hypopituitarism 28
2.4.1 *PROP1* mutations 28
2.4.2 *POU1F1(PIT1)* mutations 29
2.4.3 *TBX19* mutations 29
2.5 Isolated Hormone Deficiencies due to Mutations in Specific Cell Type:
GH1 mutations 30
2.6 Clinical Manifestations of Hypopituitarism 31
2.7 Investigations in Hypopituitarism 32
2.7.1 ACTH Deficiency 32
2.7.2 TSH Deficiency 33
2.7.3 GH Deficiency 33
2.7.4 Gonadotropin Deficiency 33
2.7.5 ADH Deficiency (Diabetes Insipidus) 34
2.7.6 The Role of Neuroradiology 34
2.8 Management of Hypopituitarism 35

## CHAPTER 3

## CONGENITAL HYPERINSULINISM-MOLECULAR MECHANISMS, DIAGNOSIS AND MANAGEMENT

3.1 Summary of Chapter 3 37
3.2 Congenital Hyperinsulinism(CHI) 38
3.3. Insulin Secretion and Pancreatic β-cell Physiology 38
3.3.1 Structure of $K_{ATP}$ Channel 39
3.3.2 $K_{ATP}$ Channel Independent Insulin Secretion 42
3.4 Etiology of CHI 42
3.4.1 CHI due to Defects in Pancreatic β-cell $K_{ATP}$ Channels 43
3.4.1.2 Molecular Basis of *ABCC8* and *KCNJ11* Recessive Mutations 44
3.4.2 Defects in Biogenesis and Turnover 44
3.4.3 Trafficking Defects 45
3.4.4 Defects in Channel Regulation 45

3.4.5 Dominant Activating KATP Channel Mutations 45
3.4.6 CHI due to Gain of Function Mutations in *GLUD1* 46
3.4.7 CHI due to Mutations in *HADH* 47
3.4.8 CHI due to Gain of Function Mutations in *GCK* 48
3.4.9 CHI due to Mutations in Transcription Factors-*HNF4A* and *HNF1A* 49
3.4.10 Exercise-induced Hyperinsulinism 50
3.4.11 CHI due to Mutations in *UCP2* 51
3.4.12 CHI due to Mutations in *HK1* 51
3.4.13 CHI due to *PGM1* Mutations 52
3.5 CHI-Histological Subtypes 54
3.5.1 Differentiation between Diffuse and Focal Hyperinsulinism 55
3.6 Clinical Presentation of CHI 56
3.7 Diagnosis of CHI 57
3.8 Medical Management of CHI 58
3.8.1 Glucagon 58
3.8.2 Diazoxide 59
3.8.3 Octreotide 60
3.8.4 Newer Medical Therapies for CHI 60
3.9 Surgical Management of CHI 61
3.10 **Aims of the Project** 62
3.11 **Patient Recruitment** 63
3.12 **Ethics** 64

**CHAPTER 4**

**GENERAL METHODS**

4.1 Summary of Chapter 4 67
4.2 Genomic DNA Extraction from Blood 68
4.2.1 Quantification of DNA 69
4.2.2 DNA Quality Control: Bioanalyzer or Fragment Analyzer
Principle of Fragment Analyzer 70
4.3 Whole Exome Sequencing 73
4.3.1 Workflow of Exome Sequencing 73
4.3.1.1 Sample Preparation 73
4.3.1.2 Hybridization 75
4.3.1.3 Indexing and Sample Processing of Multiplexed Sequencing 75
4.3.1.4 Sequencing 76
4.4 Bioinformatics 77
4.4.1 Processing and Quality Assessment of the Sequencing Data 77

4.4.2 Alignment of Reads to the Reference Genome 79
4.4.3 Variant Detection 81
4.4.4 Identifying Causal Alleles 81
4.5 Approaches Towards Identifying Causal Alleles 82
4.5.1 Discrete Filtering 82
4.5.2 Stratifying the Candidate Genes After Discrete Filtering 83
4.5.3 In Silico Tools: SIFT and PolyPhen 83
4.5.4 Pedigree Information 84
4.5.5 Technical and Analytical Limitations of Exome Sequencing 85

**CHAPTER 5**

**CLINICAL PHENOTYPE AND WHOLE EXOME SEQUENCING RESULTS (FAMILY A)**

5.1 Summary of Chapter 5 87
5.2 Clinical Information (Proband A) 88
5.3 Whole Exome Sequencing Results (Family A) 94

**CHAPTER 6**

**FOXA2 (FORKHEAD BOX A2): DESCRIPTION OF GENE FUNCTION, FOXA2 MUTATION (c.505T>C, p. S169P) & FUNCTIONAL ANALYSIS**

6.1 Summary of Chapter 6 99
6.2 Role of *FOXA2* in the Development of Central Nervous System 100
6.2.1 *FOXA2* and its interaction with Shh signalling pathway 101
6.3 Role of Foxa2 in mouse pancreas 104
6.4 Description of *FOXA2* mutation(c.505T>C, p.S169P) 105
6.4.1 Factors Supporting Pathogenicity of the Variant 107
6.5 Functional Analysis of *FOXA2*(c.505T>C, p.S169P) 109
6.5.1 Mice 111
6.5.2 Fixation, Embedding and Sectioning of Mouse Embryos 111
6.5.2.1 Fixation 111
6.5.2.2 Dehydration 112
6.5.2.3 Embedding 112
6.5.2.4 Sectioning of Paraffin Embedded Tissue 113
6.5.3 Bacterial Transformation and Purification of Mouse Foxa2 Plasmid 114
6.5.3.1 Bacterial Transformation 114
6.5.3.2 Started Cultures and Midiprep 115
6.5.4 Preparation of *Foxa2* mRNA Probe and Labelling 117

6.5.4.1 Linearization of Plasmid 117
6.5.4.2 Digoxigenein(DIG) Labelled RNA Antisense Probe Transcription 118
6.5.4.3 Probe Purification 119
6.5..5 *In Situ* Hybridization 120
6.5.5.1 Pre-Hybridization Treatment 120
6.5.5.2 Hybridization 121
6.5.5.3 Post Hybridization Washing 121
6.5.5.4 Antibody Detection 122
6.5.6 Immunohistochemistry 123
6.5.6.1 Deparrafinisation and Rehydration 123
6.5.6.2 Heat Induced Antigen Retrieval 124
6.5.6.3 Addition of Primary Antibody 124
6.5.6.4 Addition of Secondary Antibody 125
6.5.7 Human *FOXA2* Plasmid 126
6.5.7.1 Verification of Plasmid by Sequencing 128
6.5.8 Mutagenic Primer Designing 129
6.5.9 Site-Directed Mutagenesis(SDM) 130
6.5.9.1 SDM reaction 130
6.5.9.2 Digestion 132
6.5.9.3 Transformation 132
6.5.9.4 Inoculating Agar Plates 132
6.5.9.5 Started Cultures, Midiprep and Double Digestion 133
6.5.10 Dual Luciferase Reporter(DLR) Assay-Principle 134
6.5.10.1 Cell Culture and Transfection 137
6.5.10.1.1 Cell Culture 138
6.5.10.1.2 Transfection 139
6.5.10.1.3 Preparation of Cell Lysates 139
6.5.10.1.4 Preparation of Luciferase Assay Reagent II(LAR II) 139
6.5..10.1.5 Preparation of Stop and Glo Reagent 140
6.6 Brief description of specific methods 142
6.6.1 *In situ* Hybridization 142
6.6.2 Immunohistochemistry 143
6.6.3 Plasmids and Site Directed Mutagenesis 143
6.6.4 Cell Culture and Luciferase Assays 144
6.6.5 Western Blotting 144
6.6.6 Immunocytofluorescence 145

6.7 Results from in vitro studies 146
6.7.1 *Foxa2* mRNA Expression during Murine Embryonic Development 147
6.7.2 FOXA2 expression during Human Embryonic Development 149
6.7.3 Immunocytofluorescence 151
6.7.4 Dual Luciferase Transcriptional Assay 152
6.7.5 Western Blot Assay 154
6.8 Discussion 156

**CHAPTER 7**

**CLINICAL PHENOTYPE AND WHOLE EXOME SEQUENCING RESULTS (FAMILY B)**

7.1 Summary of Chapter 7 164
7.2 Clinical Information(Proband B) 165
7.3 Whole Exome Sequencing Results(Family B) 168
7.4 Bainbridge-Ropers Syndrome(BRPS) 174
7.5 *ASXL3*:Gene Description 175
7.6 Exome Sequencing 177
7.7 Bioinformatics 178
7.8 *ASXL3* mutations in proband B 179
7.8.1 Description of *ASXL3* Compound Heterozygous Mutations 180
7.8.2 Bioinformatic Analysis of *ASXL3* mutations 183
7.9 Association with Primary IGF1 Deficiency 185
7.10 Conclusion 185

**CHAPTER 8**

**CLINICAL ASPECTS AND WHOLE EXOME SEQUENCING RESULTS (FAMILY C)**

8.1 Summary of Chapter 8 187
8.2 Clinical Information (Proband C) 188
8.3 Whole Exome Sequencing Results (Family C) 189
8.4 $Ca^{2+}$/calmodulin-dependent protein kinase 2(CaMKK2)
and Effect of Mutation 194
8.4.1 *CaMKK2* 194
8.4.2 Role of *CaMKK2* in Insulin Secretion 194
8.5 Methods 197
8.5.1 Plasmid 197
8.5.2 Expression of human *CaMKK2* isoforms and pGly539fs*mutant 197
8.5.3 CaMKK2 Assay 198

8.5.4 Immunoblotting 199
8.5.5 *CaMKK2* isoform-7(c.1611_1614dupAAAA)(pGly539fs*4) mutation 199
8.6 Discussion 205

**CHAPTER 9**

**CLINICAL PHENOTYPES AND WHOLE EXOME SEQUENCING RESULTS (FAMILIES D, E, F)**

9.1 Summary of Chapter 9 212
9.2 Clinical Information (Proband D) 213
9.3 Whole Exome Sequencing Results (Family D) 216
9.4 *B3GAT3* 218
9.4.1 *B3GAT3* mutation 219
9.4.2 Biological Function of *B3GAT3* 219
9.5 Discussion 222
9.6 Clinical Information (Proband E) 224
9.7 Whole Exome Sequencing Results (Family E) 225
9.8 *GH1* gene 231
9.8.1 *GH1* Promoter Variant(c.-93delG) 232
9.9 Clinical Information (Proband F) 234
9.10 Whole Exome Sequencing Results (Family F) 236

**CHAPTER 10**

**GENERAL DISCUSSION, CONCLUSIONS & FUTURE DIRECTIONS**

10.1 General Discussion 244
10.2 Conclusions 250
10.3 Future Directions 251

**CHAPTER 11**

References 253

**CHAPTER 12**

**APPENDIX**

Ethics approval 290
R & D approval 291
Patient/Guardian Information Sheets 292
Consent Forms 310
List of Publications 312
Abstracts and PDF of accepted manuscripts 315

# LIST OF FIGURES

## CHAPTER 1

Figure 1.1: WES and its impact in medicine 6

## CHAPTER 2

Figure 2.1: Stages in mouse pituitary development 20
Figure 2.2: Pituitary signalling cascade and differentiation of cell types 22

## CHAPTER 3

Figure 3.1: Mechanism of insulin release from pancreatic ß-cell 41
Figure 3.2: Role of various genes in insulin secretion 53
Figure 3.3 (A & B): Focal and Diffuse forms of CHI 55
Figure 3.4:Flowchart of Patient Recruitment 64

## CHAPTER 4

Figure 4.1: Gel image of the DNA samples 71
Figure 4.2: Electropherogram traces of the DNA samples 72
Figure 4.3: Sample preparation for exome sequencing 74
Figure 4.4: SureSelect target enrichment 76
Figure 4.5: Read length distributions of samples after trimming 78
Figure 4.6: Parent-Child trio 84

## CHAPTER 5

Figure 5.1: Sagittal view of MRI scan of brain of proband A 90
Figure 5.2: Linear growth curve of proband A and response to GH 92
Figure 5.4: Pedigree chart of Family A 93
Figure 5.4: De Novo variant analysis of proband A 94

## CHAPTER 6

Figure 6.1: Schematic representation of *FOXA2* gene with its domains 102
Figure 6.2: Interaction between Shh signalling pathway and *FOXA2* 103
Figure 6.3: Electropherogram showing the point mutation in *FOXA2*(c.505 T>C) 107
Figure 6.4: Evolutionary conservation of serine amino acid residue 108
Figure 6.5: Agarose gel image showing DNA yield from purified plasmid 116
Figure 6.6: Agarose gel image showing Mouse Foxa2 linearized plasmid 117
Figure 6.7: Agarose gel image showing the probe after transcription 119
Figure 6.8: Physical map of plasmid pCMV3 with *FOXA2* insert 127
Figure 6.9: Agarose gel image depicting PCR product 131

Figure 6.10: Bioluminescent reaction-Firefly luciferase 135
Figure 6.11: Bioluminescent reaction-Renilla luciferase 135
Figure 6.12: Comparison of luminescent signals generated by firefly and Renilla luciferase 136
Figure 6.13: Sequential steps inside the luminometer 141

Figure 6.14: mRNA expression of *Foxa2* during mouse embryonic development 148
Figure 6.15: FOXA2 expression during human embryonic development 150
Figure 6.16: Double immunofluorescence using anti-FOXA2 antibody 151
Figure 6.17: Dual luciferase transcriptional assay 153
Figure 6.18: Western blot assay 155
Figure 6.19: Schematic representation of regulation of genes involved in insulin secretion by *FOXA2* 160

**CHAPTER 7**

Figure 7.1: Growth chart depicting height and weight of proband B 167
Figure 7.2: Pedigree chart of Family B 167
Figure 7.3: *De Novo* variant analysis of proband B 168
Figure 7.4: Recessive variant analysis of proband B 171
Figure 7.5: *ASXL3* gene with its domains 176
Figure 7.6: Electropherogram showing compound heterozygous mutations(c.2695 C>G) and c.3078G>C 179
Figure 7.7: *ASXL3* gene with previous reported mutations 181

**CHAPTER 8**

Figure 8.1 Pedigree chart of Family C 188
Figure 8.2: De Novo variant analysis of proband c 189
Figure 8.3: Mechanism of insulin release from ß-cell via the $Ca^{2+}$-CaM kinase cascade 196
Figure 8.4A: Schematic representation of *CaMKK2* isoforms 1, isoform 7 and mutant isoform 7 p.G539fs*4 202
Figure 8.4B Immunoblotting with rabbit anti-Flag antibody showing the expression of pG539fs*4 mutant in COS7 cells at a similar level as wild-type 203

Figure 8.4C Graph showing $Ca^{2+}$-Calmodulin dependent kinase activities with *CaMKK2* isoform 1, isoform 7 and isoform 7 pG539fs*4 204
Figure 8.5: Schematic representation of excess insulin release from ß-cell via increased activation of the kinase cascade by *CaMKK2* isoform 7 pG539fs*4 209

**CHAPTER 9**

Figure 9.1: Pedigree chart of Family D 215
Figure 9.2: Growth chart of Proband D 215
Figure 9.3: *De Novo* variant analysis of Family D 216
Figure 9.4: Pedigree chart of Family E 224
Figure 9.5: Growth chart of Proband E 225
Figure 9.6: *De Novo* variant analysis of Family E 226
Figure 9.7: Recessive variant analysis of Family E 229
Figure 9.8: Pedigree chart of Family F 235
Figure 9.9: *De Novo* variant analysis of Family F 236
Figure 9.10:Recessive variant analysis of Family F 240

# LIST OF TABLES


Table 1.1: Summary of genes found by WES in some endocrine disorders 12

Table 3.1: Summary of the phenotypes of recruited patients 65

Table 4.1: Summary of raw and trimmed sequence data 78

Table 4.2: Summary of sequence alignments 80

Table 5.2: Summary of clinical features of proband A 93

Table 5.3: List of *de novo* variants in proband A 95

Table 6.1: Human *FOXA2* insert in pCMV3 126

Table 6.2: Mutagenic primers used to insert mutations in *FOXA2* 130

Table 6.3: SDM reaction preparation 130

Table 6.4: PCR settings for SDM reaction 131

Table 6.5: Quantity of reagents added to each well in 24-well plates 138

Table 7.1: List of *de novo* variants in proband B 169

Table 7.2: List of compound heterozygous/homozygous variants in proband B 172

Table 7.3: Comparison of phenotypic features of proband B with patients with BRPS reported in literature 182

Table 8.1: List of *de novo* variants in proband C 190

Table 8.2: $Ca^{2+}$-CaM stimulated activities of CaMKK2.1 (isoform 1), CaMKK2.7 (isoform 7) and pG539*fs4 mutant measured over a range of CaM concentrations 201

Table 9.1: Summary of investigations in proband D following 19-hour fast 214

Table 9.2: List of variants in proband D 217

Table 9.3: Comparison of clinical features between proband D and patients with *B3GAT3* mutations reported in literature 220

Table 9.4: List of *de novo* variants in proband E 227

Table 9.5: List of recessive variants in proband E 230

Table 9.6: Summary of investigations in proband F 235

Table 9.7: List of *de novo* variants in proband F 237

Table 9.8: List of recessive variants in proband F 241

# ABBREVIATIONS

| | |
|---|---|
| ACTH | Adrenocorticotropic Hormone |
| ALS | Acid-labile subunit |
| AMPK | AMP- activated protein kinase |
| ASXL3 | Additional Sex Combs Like 3, Transcriptional Regulator |
| AVP | Arginine Vasopressin |
| B3GAT3 | β-1,3-glucuronyltransferase 3 |
| BMP4 | Bone Morphogenetic Protein 4 |
| BQSR | Base quality score recalibration |
| BRPS | Bainbridge-Ropers syndrome |
| Buffer AL | Lysis buffer |
| Buffer AW1 | Wash buffer 1 |
| Buffer AE | elution buffer |
| $Ca^{2+}$ | Calcium |
| CaMKK2 | $Ca^{2+}$/calmodulin-dependent protein kinase 2 |
| cDNA | Complementary deoxyribonucleic acid |
| CGH | Comparative genomic hybridisation |
| CHI | Congenital Hyperinsulinism |
| CNPAS | congenital nasal pyriform aperture stenosis |
| CPHD | Combined Pituitary Hormone Deficiency |
| CRISPR/CAS9 | Clustered Regularly Interspaced Short Palindromic Repeats/ CRISPR associated system |
| CS | Carnegie stage |
| ddH2O | double distilled water |
| DEPC | diethyl pyrocarbonate |
| DIG | Digoxigenein |

| | |
|---|---|
| DLR | Dual-Luciferase Reporter |
| DMEM | Dulbecco modified Eagle medium |
| E(number) | Embryonic day |
| ELM | Eukaryotic Linear Motifs |
| ExAc | Exome Aggregation Consortium |
| $^{18}$F-DOPA PET | 18F-fluro-L-dihydroxyphenylalanine Positron Emission Tomography |
| Fgf | Fibroblast growth factor signalling |
| FISH | Fluorescent In situ Hybridization |
| FOXA2 | Forkhead Box A2 |
| FSH | Follicular Stimulating Hormone |
| GABA | Glutamate decarboxylase |
| GATK | Genome Analysis Tool Kit |
| GAG | Glycosaminoglycan |
| GCK | Glucokinase |
| GDH | Glutamate Dehydrogenase |
| GH | Growth Hormone |
| GLP-1 | glucagon like peptide-1 |
| GLUT-2 | Glucose transporter 2 |
| GlcAT-I | β-1,3-glucuronyltransferase 3 |
| GnRH | Gonadotropin Releasing Hormone |
| GWAS | Genome Wide Association Studies |
| HADH | Hydroxyacyl-Coenzyme A dehydrogenase |
| hCG | Human chorionic gonadotropin |
| HEK | Human Embryonic Kidney |
| HPA | Hypothalamo-pituitary axis |
| HPE | Holoprocencephaly |

| | |
|---|---|
| IGF-1 | Insulin Growth Factor-1 |
| IGHD | Isolated Growth Hormone Deficiency |
| IGFBP-1 | Insulin-like growth factor-binding protein 1 |
| KATP | ATP-sensitive potassium channels |
| Kir6.2 | Inward rectifying potassium channel pore forming |
| LARII | Luciferase Assay Reagent |
| LH | Luteinizing Hormone |
| MAF | minor allele frequency |
| MCT1 | Monocarboxylate transporter |
| MSH | Melanin Stimulating Hormone |
| mTOR | mammalian target of rapamycin inhibitor |
| NBF | Nucleotide Binding Fold |
| NBT | Nitro blue tetrazolium |
| PTCH1 | Patched-1 |
| PBS | Phosphate buffered saline |
| phGT2 | plasmid with human GLUT2 reporter |
| POMC | Pro-opiomelanocortin |
| PPARα | peroxisomal proliferator-activated receptor alpha |
| PR-DUB | Polycomb repressive deubiquitination |
| PRL | Prolactin |
| PVA | Polyvinyl alcohol |
| qPCR | quantitative polymerase chain reaction |
| rGH | recombinant growth hormone |
| RFU | relative fluorescence unit |
| rIGF1 | recombinant IGF1 |
| RP | Rathke’s Pouch |

| | |
|---|---|
| Shh | Sonic Hedgehog |
| SIFT | Sorting intolerant from tolerant |
| SOD | Septo-optic dysplasia |
| SSC | saline sodium citrate |
| SMO | smoothened |
| SNV | single nucleotide variant |
| SUR1 | sulfonylurea receptor 1 |
| Ttf1 | Thyroid Transcription Factor 1 |
| TMD | Transmembrane Domain |
| Ub1 | mono-ubiquitin |
| UCSC | University of California Santa Cruz |
| VQSR | Variant Quality Recalibration Score |
| WES | Whole Exome Sequencing |

# CHAPTER 1

# PROMISE OF WHOLE EXOME SEQUENCING IN PAEDIATRIC ENDOCRINOLOGY

## 1.1 SUMMARY OF CHAPTER 1

Chapter 1 provides an introduction to Whole Exome Sequencing (WES). This chapter begins with a brief description of WES in medicine followed by the usefulness of WES in diagnosing various conditions in paediatric endocrinology.

## 1.2 WHOLE EXOME SEQUENCING

### 1.2.1 Introduction

The sequencing technologies have been constantly evolving over the last decade since the completion of Human Genome Project (1). They include individual gene based approach (Sanger sequencing), large scale genome wide analysis to determine genetic determinants of disease, whole exome and whole genome sequencing (2). Whole exome sequencing is one such major advancement in the field of genomic medicine (3) and is a highly effective form of genetic analysis as this allows the sequencing of the majority (>90%) of the protein coding portion of an individual's DNA (4).

### 1.2.2 Exome Sequencing

The human genome is vast and comprises of 3 billion base pairs that contains both the coding and the non-coding regions (5). Approximately 1% of the entire human genome constitute the protein coding region or exomes that harbours about 85% of the disease causing mutations (5). Therefore, sequencing of exomes has the potential to discover the underlying genetic causes of not only rare diseases but also in determining predisposing variants in cancers and common diseases (4). The cost to sequence the whole exome is about six fold less when compared to the cost involved to sequence the whole genome and therefore WES is a cost-effective method to identify the disease causing mutations (6), especially in rare diseases. WES is performed after the exomes or the coding part are captured from the genomes using specific probes and by high-throughput technologies (2). The sequence is then compared with human reference sequence, where by the use of computer tools, the differences in alignment are identified to determine the potential genetic variants (4).

Some of the limitations of WES include its inability to assess the non-coding alleles, the limitations in coverage of the regulatory regions of the genome and limitations in capturing the entire exome (2). WES has been promising in identifying novel genes and underlying genetic pathways of diseases despite the above limitations.

### 1.2.3 WES in Medicine

WES as a research tool has facilitated the understanding of the molecular basis of genetic diseases. The earliest report of the utility of WES was published in 2009 (7) when *MYH3* was identified as a disease causing gene in individuals with Freeman-Sheldon syndrome (FSS; OMIM193700). Another example is the exome sequencing studies in individuals with Kabuki syndrome where the sequencing identified *KMT2D* (formally known as *MLL2*) in >50% of patients in this syndrome, characterized by wide phenotypic variability and multiple congenital malformations (8). These kind of studies uncover the genetic basis of the rare disorders and help in the management of the patients.

In addition to identifying genetic causes for rare diseases, WES can serve as a potentially useful tool in screening, prenatal diagnosis and disease treatment (5). The applicability of WES in prenatal diagnosis was demonstrated using fetal DNA in maternal serum in finding aneuploidies (9). These methods are non-invasive when compared with other methods such as amniocentesis or chorionic villi biopsy (10, 11).

The underlying molecular basis is known only in two-thirds of the described monogenic disorders (5). The discovery of the causative gene contributes massively to the understanding of the pathogenesis of the disease process. The identification of a novel genetic cause for a rare disease depends on a number of factors such as identification of similar variant in the gene in other patients with similar clinical phenotype and

absence or rarity of the variant present in control population. In rare diseases, where the finding of similar affected phenotypes can be difficult, functional experiments on the identified variant to determine the pathological impact of the variant on protein function is crucial to understand the biological pathways associated with the disease and to validate the variant as pathogenic. WES can therefore be a powerful tool in finding the genetic etiology for Mendelian disorders (12).

Besides monogenic disorders, WES can identify common genetic variants associated with complex and common diseases with multigenic traits (13). With the emerging rare variants-common disease hypothesis, WES will have a bigger role in common diseases along with the main driving force, genome-wide association studies (GWAS) (14). WES has made promising advances in common diseases such as cardiovascular disease, hypertension, obesity, diabetes and also has massively aided in detailed understanding of molecular mechanisms and pathways in cancer (5).

For genetically heterogeneous disorders, the use of targeted exome sequencing, which involves sequencing of many known disease associated genes rather than the whole exome can be sufficient (15). This also confers other advantages such as reduced cost, better depth of sequencing and reduced diagnostic time. For example there are a number of genes associated with heterogeneous conditions such as learning difficulties and congenital hearing loss in which targeted sequencing of the implied genes has better diagnostic abilities with reduced cost (5).

**Figure 1.1:** WES and its impact on health improvement. In both research and clinical settings, WES is used in common diseases, cancer and rare diseases. This potentially leads to the establishment of gene networks, new Single nucleotide polymorphisms(SNPs), new mutation detection and discovery of new genes (5).

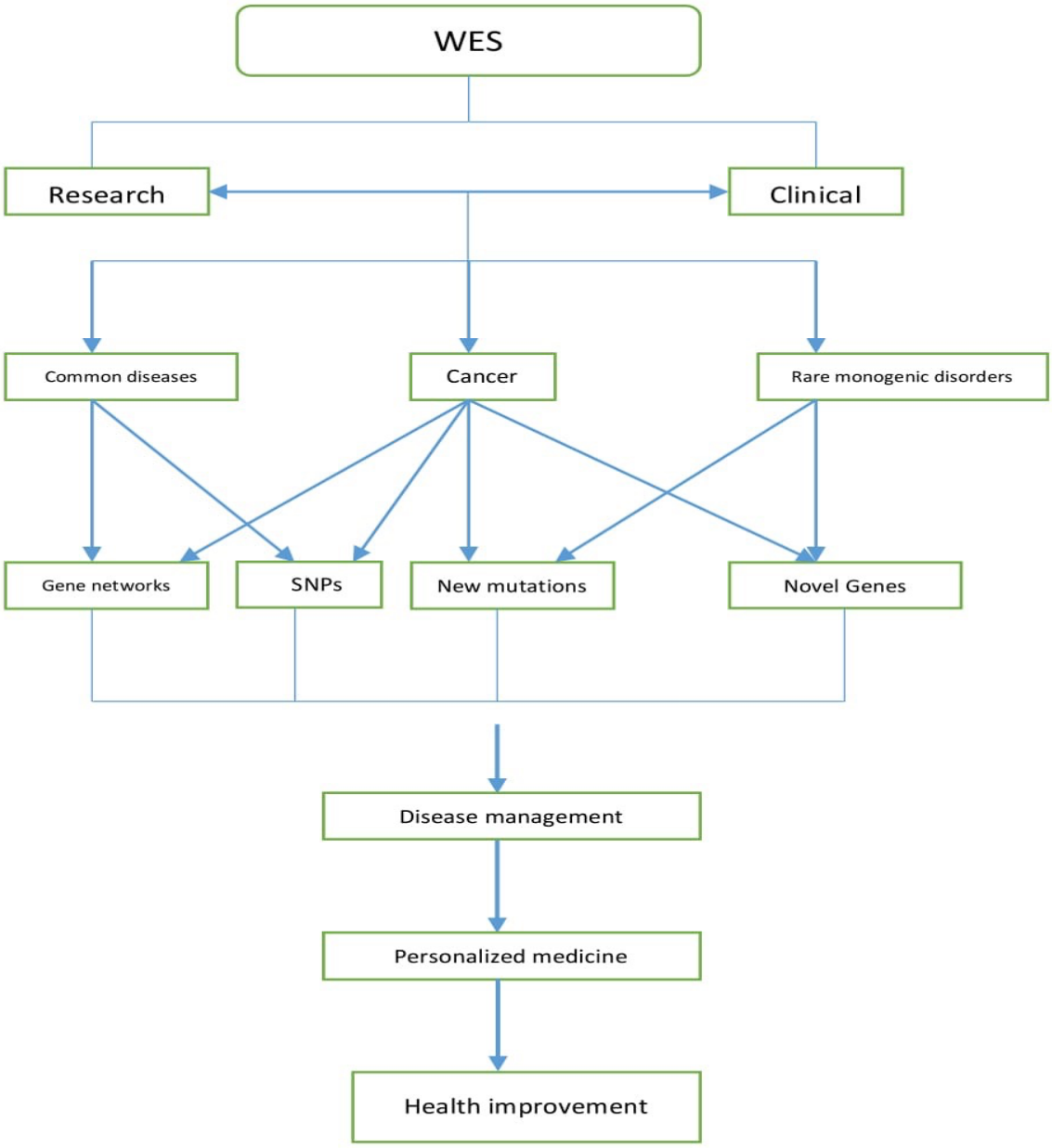

### 1.2.4 WES in Paediatric Endocrinology

Paediatric endocrinology consists of many rare diseases. Although the clinical phenotype and management has been established in many of these conditions, the underlying genetic etiology remains unidentified. WES has enabled to uncover the molecular diagnosis and shed valuable insights in understanding the novel genetic pathways in many disorders involving growth, puberty, adrenal gland, type 2 diabetes mellitus and a variety of genetic syndromes with predominant endocrine involvement (2). Besides, WES based studies have opened up new insights in understanding the pathogenesis of neuroendocrine tumours (2). Clinical endocrinologists often treat children with multitude of endocrine related problems that have a suspected underlying genetic etiology. The large number of potentially relevant genes in many of these conditions makes candidate gene sequencing difficult. WES in such patients is helpful in identifying the underlying genetic cause. The unbiased approach of sequencing the coding regions of approximately 20,000 genes simultaneously confers the major benefit to WES (3).

#### 1.2.4.1 WES in Disorders Involving Growth and Puberty

Although common genetic variants associated with height have been found in more than 400 genomic loci in GWAS population studies, many of these variants do not directly account for short stature (16, 17). However, they highlight the fact that there are multiple potentially novel pathways that govern growth. WES in individuals from the same family with idiopathic short stature can be a helpful tool in identifying the potential genetic cause. For example, a WES based study, identified novel heterozygous mutations in *ACAN*, in individuals with idiopathic short stature from three affected families. *ACAN* encodes aggrecan which is a proteoglycan in the extracellular matrix of the growth plate with a role in the linear growth (18).

Puberty is a complex process which is initiated by the release of gonadotropins from the pituitary gland which is under the control of the hypothalamic gonadotrophin releasing hormone that functions as a pulse generator. The biological and genetic mechanisms that govern this process and the timing of puberty have not been clearly understood (19). WES based studies in individuals with familial central precocious puberty have identified a loss-of-function mutation in *MKRN3*, an imprinted gene that encodes for probable E3 ubiquitin-protein-ligase makorin-3 (20). Expression studies on murine embryos demonstrated the reduced *MKRN3* mRNA expression in the hypothalamus before the pubertal onset (20). Thus by WES, the novel genetic pathway underlying *MKRN3*, a repressor of pubertal onset was identified and the finding of similar mutations in further studies have not only confirmed the important findings but also brings a question if differential expression of *MKRN3* can explain the variability in pubertal onset in children (21). WES has also been useful in understanding some of the genetic mechanisms underlying Kallmann syndrome, characterised by hypogonadotropic hypogonadism with or without anosmia, where homozygous loss of function mutations in *FEZF1*, a gene involved in the migration of the olfactory receptor neurons in mice was found in four individuals with Kallmann syndrome from two independent families (22, 23). Novel mutations in genes involved in ubiquitination pathway such as *RNF216*, *OTUD4* and *STUB1* have been identified to cause Gordon Holmes syndrome, a neurodegenerative disorder characterised by ataxia and hypogonadism (24, 25). Moreover, WES based studies have identified novel genes such as *STAG3, PSMC3IP, EIF4ENIF1* and *SYCE1*, associated with familial premature ovarian failure and gonadal dysgenesis (26-29).

### 1.2.4.2 WES in Disorders of Adrenal gland and Endocrine Neoplasia

Various WES based studies in patients with adrenal hypercortisolism due to adrenal tumour have significantly advanced the understanding of the adrenocortical disease. Somatic mutation(p.Leu206Arg) in *PRKACA*, the cAMP dependent protein kinase A catalytic subunit causes an increase in cAMP signalling and has been identified in adrenal tumours by WES based studies on adrenal tumour-blood pairs in patients with adrenal Cushing syndrome (30-33). Similarly, mutations in *DOTIL* and *CLASP2* have been found to be involved in macronodular hyperplasia and adrenocortical oncocytomas (31). Inactivating mutations in *ARMC5*, have been reported in majority of patients (both familial and isolated) with bilateral macro nodular hyperplasia (34). *ARMC5* has a potential role in steroidogenesis, gene transcription, cell growth and survival as demonstrated by in-vitro studies (35).

The role of WES in endocrine neoplasia has enabled the identification of novel germline mutations, such as *DICER1*, which predisposes an individual to an increased risk of endocrine tumour in later life and also somatic mutations (36). In many cases, WES is performed in pairs where the sequencing of tumour cells and normal biopsy tissue (or unaffected lymphocytes) is done simultaneously to identify the tumour initiating mutation (2). When such paired sequencing is performed in cohort of patients with similar type of tumour, the common genetic etiology governing the pathophysiology of the tumour is likely to be identified (2).

### 1.2.4.3 WES in Familial Glucocorticoid Deficiency

Familial Glucocorticoid Deficiency (FGD) is an autosomal recessive disease characterised by glucocorticoid deficiency due to the hereditary unresponsiveness to adrenocorticotropic hormone (ACTH) (37). The underlying genetic mechanisms of FGD is not completely understood as mutations in ACTH receptor, *MC2R* constitute

only 25% of cases and mutations in its accessory protein MRAP, accounts for a further 15-20% of cases with FGD (37). With the advent of WES, novel pathways involved in the mitochondrial detoxification of reactive oxygen species have been identified to cause FGD(38). Homozygous mutations in *TXNRD2*, encoding thioredoxin reductase 2 have been found to cause FGD in seven individuals from a consanguineous family (39). An increase in susceptibility to oxidative stress due to a significant increase in reactive oxygen species production was demonstrated in the *TXNRD2* knock-down adrenocortical cell line when compared with the controls (39). Mutations in nicotinamide nucleotide transhydrogenase (*NNT*) gene have been found to reduce the amount of NADPH production, required for p450 related oxidative-reductive reactions in the adrenal cortex, thereby leading to FGD (40). Mutations in *MCM4*, encoding minichromosome maintenance deficient 4, that has a role in DNA replication and cell cycle regulation have been associated with adrenal insufficiency, natural killer cell deficiency and short stature (41). Homozygosity mapping in recessive conditions can help in the localisation of the candidate region of the genome in genetically isolated populations that harbour the causal mutations. This was used by the investigators in genetically isolated populations with FGD and enabled identification of the target candidate regions, sequencing of which identified *NNT* and *MCM4* mutations (40, 41).

#### 1.2.4.4 WES in Thyroid Disorders

Mutations in *IGSF1*, encoding the immunoglobulin superfamily member 1 protein, were identified by WES studies to cause a novel X-linked disease causing central hypothyroidism, macro-orchidism and short stature (42). The *IGSF1* plasma membrane glycoprotein is expressed in the anterior pituitary gland and plays a vital role in trafficking of the protein to the cell surface (43). WES also identified a homozygous missense mutation in *SLC26A4* (also associated with thyroid

dyshormonogenesis), in a consanguineous family with thyroid dysgenesis, thereby expanding the clinical spectrum (44).

#### 1.2.4.5 WES in Juvenile Osteoporosis

Mutations in *PLS3*, encoding plastin-3, a protein involved in the formation of filamentous actin bundles were identified by WES in a study involving five families with X-linked osteoporosis and fractures (45). Although the underlying biological mechanism for osteoporosis and increased fracture risk is unknown, it has been proposed that *PLS3* mutation can cause altered mechanosensing by the osteocytes leading to the effects on bone remodelling (45).

#### 1.2.4.6 WES in 46 XY Disorders of Sex Development

The formation of bipotential gonad is followed by a series of complex and coordinated genetic programmes and signals that determine the formation of either the testis or the ovary (46). Once the sex determination occurs, the circulating sex hormones along with genetic mechanisms act together in the differentiation of internal and external genitalia. Disorders of sex development (DSD) occurs as a result of disruption in the process of sex determination or differentiation which can cause a discrepancy between the phenotypic sex and chromosomal sex (47). However, many patients with DSD do not receive a genetic diagnosis. In particular, in some individuals with 46XY DSD, loss of function in *SRY* or *NR5A1* results in disruption of the process of testis determination and can result in gonadal dysgenesis (48, 49). However, mutations in *SRY* or *NR5A1* account for only 10-15% cases of 46XY DSD (46). Likewise, 46XY DSD due to disruption in the process of testis differentiation is not always explained by mutations in the gene encoding the androgen receptor (50). Hence in majority of patients with 46XY DSD, the diagnosis is not reached at the genetic level. WES in this

group of patients has the potential to uncover the underlying genetic etiology. In a study, the investigators adopted WES based approach in 46XY DSD individuals without genetic diagnosis and found that a genetic diagnosis was found in 35% of cases (14 of 40 cases) and six patients had variants of unknown significance who may be reclassified in the future as the literature evolves (46).

**Table 1.1: Summary of genes found by WES in some endocrine disorders**

| **Endocrine disorder** | **Gene** |
|---|---|
| Central precocious puberty | *MKRN3* |
| Hypogonadotropic hypogonadism(Kallmann syndrome) | *FEZF1* |
| Hypogonadotropic hypogonadism & ataxia | *RNF216/OTUD4* |
| Premature ovarian failure | *STAG3, PSMC3IP, EIF4ENIF1 and SYCE1* |
| Familial glucocorticoid deficiency | *TXNRD2, NNT* |
| Central hypothyroidism, testicular enlargement | *IGSF1* |
| Juvenile osteoporosis | *PLS3* |
| 46XY disorder of sexual development | *FOG2* |

#### 1.2.4.7 WES in Clinical Endocrinology

Overall, WES has the potential to change and enhance the diagnostic approach in patients with rare endocrine diseases with a suspected genetic etiology. The use of WES has been very promising in the field of endocrinology but has a widespread use in the field of neurology, particularly for children with neurodevelopmental issues and congenital anomalies (51). It has been reported that almost quarter of the patient population within the field of neurology with neurodevelopmental issues can be diagnosed by using WES (52).

Among the large number of variants identified in WES, a majority of them are common in the general population and unlikely to have a causative role in the disease. The frequency of occurrence of any variant can be found in the publicly available data bases such as the 1000 Genomes Project, the National Heart, Lung, and Blood Institute Exome Variant Server and the Exome Aggregation Consortium browser (ExAC).

Trio sequencing, which involves sequencing of the patient sample along with the biological parents optimises interpretation (4). Trio sequencing helps in the identification of *de novo*, heterozygous, homozygous and compound heterozygous variants and also in the identification of variant with autosomal recessive and dominant modes of inheritance (2).

### 1.2.5 Disadvantages in WES

The use of WES in the diagnosis of rare diseases is based on the assumption that these patients have highly penetrant genetic variants and follow a classic Mendelian pattern of inheritance (53). Although this approach has several advantages and is currently the most tractable approach for the analysis of exome sequencing data, there are some limitations in this approach. The possibility of genetic mutations in multiple genes contributing to short stature is overlooked by this approach. Only the rare variants with population minor allele frequency of <1%are analysed by this approach. Although it is unlikely that common variants (minor allele frequency>1% in reference databases) will have a large effect on the linear growth, their analysis does not form a part in this approach. The synonymous variants are ignored in this approach and only the non-synonymous variants are analysed. It is possible that synonymous changes also perturb the gene function or expression. WES has disadvantages of not be able to analyse the noncoding regions of the genome(introns), somatic or non-germline changes, epigenetic changes and copy number variations. WES, in addition to identifying the disease causing variants, can also identify incidental findings, such as *BRCA1* or *BRCA2* have the predisposition to cancer. The American College of Medical Genetics has published guidelines and includes a list of 57 genes that is recommended by the clinical laboratories to report on incidental findings (54). However, this recommendation is a subject of controversy as the true clinical impact of finding novel or rare variants is not known and identifying these variants may not necessarily have a positive effect on the health (2).

Despite these limitation, in the current setting, WES has been successfully used in establishing genetic diagnosis in children with undiagnosed rare diseases. With time,

WES will be used more by the clinicians which will help in the identification of increasing number of pathogenic variants with a wealth of molecular database (2).

### 1.2.6 WES, GWAS and Whole Genome Sequencing (WGS)

GWAS searches for SNPs that are more prevalent in population with particular disease than those without it. GWAS study looks at many loci at the same time. GWAS is used to pinpoint genes that may contribute to the development of a common disease. WES is however used to identify the underlying genetic etiology in rare diseases. WES, although a cost-effective way to identify disease-related variants, it has its limitations as described above. With the decreasing sequencing cost and accumulating knowledge of the human genome, whole genome sequencing has the potential to identify important variants in regulatory regions typically inaccessible for exome sequencing.

# CHAPTER 2

# PITUITARY GLAND-EMBRYOLOGY, DEVELOPMENTAL TRANSCRIPTION FACTORS, CONGENITAL HYPOPITUITARISM, DIAGNOSIS AND MANAGEMENT

## 2.1 SUMMARY OF CHAPTER 2

Chapter 2 provides an introduction to the embryological development of pituitary gland, role of transcription factors and mutations in congenital hypopituitarism. This chapter opens with a brief description on the embryology and genes involved in the pituitary gland development. This then leads into detailed description of the clinical condition “congenital hypopituitarism”, its genetic causes, clinical presentation, diagnosis, and management.

## 2.2 PITUITARY GLAND

The pituitary gland, located within the sella turcica at the base of the brain is the master regulator of growth, puberty, metabolism, response to stress, reproduction and lactation (55). The pituitary gland consists of three lobes: the anterior, the intermediate and the posterior lobes. The anterior and the intermediate lobe (involutes in the adult) comprise the adenohypophysis and the posterior lobe comprises the neurohypophysis (56). The adenohypophysis or the anterior part of the pituitary gland secrete six different hormones produced from five different cell types: growth hormone (GH) from somatotrophs, thyroid stimulating hormone (TSH) or thyrotrophin from the thyrotrophs, adrenocorticotropic hormone (ACTH) from corticotrophs, prolactin (PRL) from lactotrophs, follicular stimulating hormone (FSH) and luteinizing hormone (LH) from gonadotrophs (57). The intermediate lobe consists of melanotrophs that secrete pro-opiomelanocortin (POMC), which is a precursor to melanocyte-stimulating hormone (MSH) and endorphins (57). Within the posterior lobe, arginine vasopressin (AVP) and oxytocin are secreted which are synthesised magnocellular neurones of the paraventricular and supra-optic nuclei within the hypothalamus (57). Secretory and inhibitory peptides that regulate the secretion of hormones from the anterior pituitary gland are produced from the hypothalamus. The infundibulum or the pituitary stalk not only carries the neural tracts from the hypothalamus to the posterior pituitary gland but also carries the portal blood delivering the hypothalamic regulating hormones to the anterior pituitary gland (57).

### 2.2.1 Embryology and Development of Pituitary Gland

The oral ectoderm gives rise to the formation of the anterior and intermediate lobes of the pituitary while the posterior pituitary is derived from the neural ectoderm (57). The development of the pituitary gland has been extensively studied in mouse which occurs in a sequential, well defined and coordinated manner that involves the formation of the pituitary placode, rudimentary Rathke's pouch, definitive Rathke's pouch and the mature pituitary gland (58). The developmental cascade of murine pituitary gland reflects that of humans (58). At embryonic stage, E7.5 in the mouse, the roof of the oral ectoderm thickens and gives rise to the pituitary placode, which by E9.0, invaginates to form the rudimentary Rathke's pouch that then forms into the definitive Rathke's pouch by E10.5 (59). The Rathke's pouch then gives rise to the anterior and the intermediate lobes of the pituitary gland (55). The neural ectoderm evaginates at the base of the ventral diencephalon to give rise to the infundibulum and the posterior pituitary (55). At E12.5, there is separation of Rathke's pouch from the oral ectoderm (55). The various stages of pituitary gland development in the rodent are depicted in figure 2.1 (55). The hormone-secreting progenitor cells proliferate between E12.5 and E15.5 followed by spatial and temporal differentiation of the various cell types (55), starting from the thyrotrophs and corticotrophs, followed by the somatotrophs, gonadotrophs and lactotrophs that each secrete their respective hormones (60, 61).

**Figure 2.1:** Stages in mouse pituitary gland development. (a) Oral ectoderm. (b) Rudimentary pouch. (c) Definitive pouch. (d) Adult pituitary gland. I-Infundibulum; NP-neural plate; N-notochord; PP-pituitary placode; OM-oral membrane; H-heart; F-Forebrain; MB-midbrain; HB-hindbrain; RP-Rathke's pouch; AN-anterior neural pore; O-oral cavity; PL-posterior lobe; OC-optic chiasm; P-pontine flexure; PO-pons; IL-intermediate lobe; AL-anterior lobe; DI-diencephalon; SC-sphenoid cartilage (56).

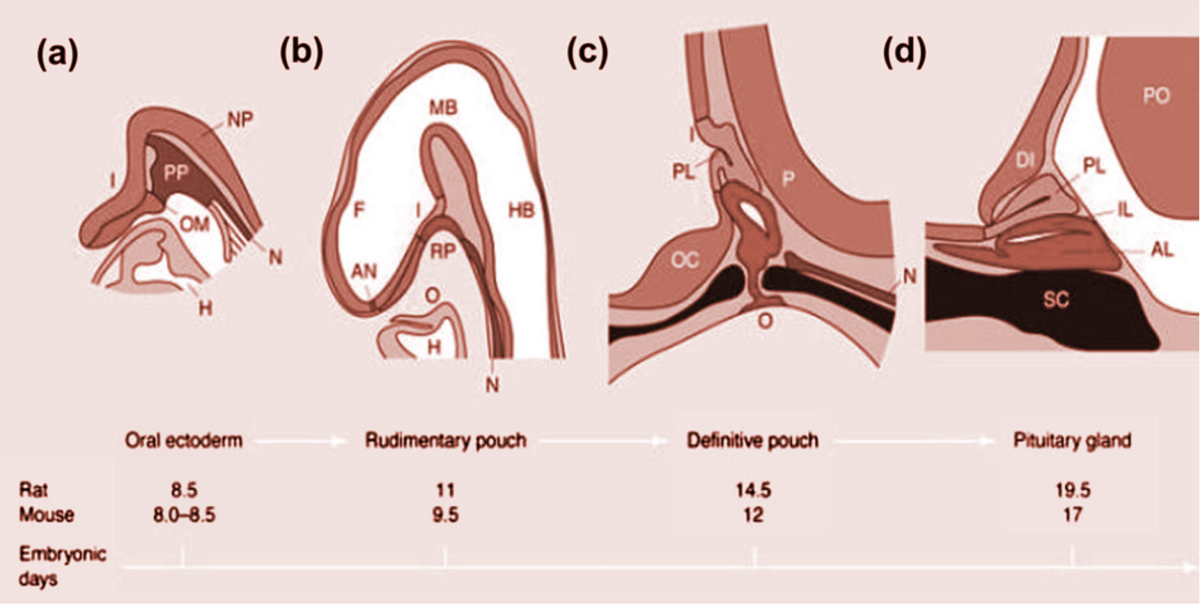

#### 2.2.1.1 Early Developmental Genes and Signals in Pituitary Development

The development of the pituitary gland is orchestrated by a series of well-co-ordinated cascade of morphogenetic signalling molecules and transcription factors that play a vital role in the process of organ commitment, cell proliferation, patterning and differentiation (56). The formation of the rudimentary Rathke's pouch(RP), is initiated by the signalling molecules such as Bone Morphogenetic Protein 4(Bmp4) and thyroid transcription factor (Ttf1) from the ventral diencephalon combined with the Sonic Hedgehog (Shh) from the oral ectoderm (62). The invagination of the RP and further pituitary progenitor cell proliferation is directed by the co-ordination of Fibroblast growth factor signalling (Fgf8 and Fgf10) and Wnt5a along with early transcription factors such as *Gli1*, *Gli2, Lhx3, Ptx1* and *Ptx2* (62).The expression of *Hesx1* and *Prop1*(prophet of Pit-1) in RP leads to differentiation of specific pituitary cell types.*Prop1* in-turn induces the expression of *Pou1f1*, leading to the terminal differentiation of somatotrophs, lactotrophs and thyrotrophs (63). The gonadotrophs differentiation is induced by the expression of *Gata2* and steroidogenic factor 1(*sf1*) (63). The differentiation of corticotrophs is regulated by the expression of Tbx19 from the POMC-producing cells (63).

The development of pituitary is a carefully co-ordinated complex process which requires the expression of the signalling molecules during critical periods of development. The genes that are expressed early are not only involved in the organ commitment but also play an important role in the activation and expression of downstream signalling molecules that have a specific role in the differentiation of progenitor cells (56).The differentiation of various pituitary cell types from the various transcription factors is shown in figure 2.2 (55).

**Figure 2.2**: Schematic representation of pituitary developmental cascade with sequential expression of pituitary transcription factors and genes (56). A cascade of signalling molecules and transcription factors such as Bmp4, Sf1, Lhx4, Prop1, Pitx1, Pit1 play a crucial role in organ commitment, cell proliferation, patterning, and terminal differentiation of the cells that secrete hypothalamic regulatory peptides (GHRH, TRH, GnRH) and the pituitary hormones (ACTH, PRL, GH, TSH, LH and FSH).

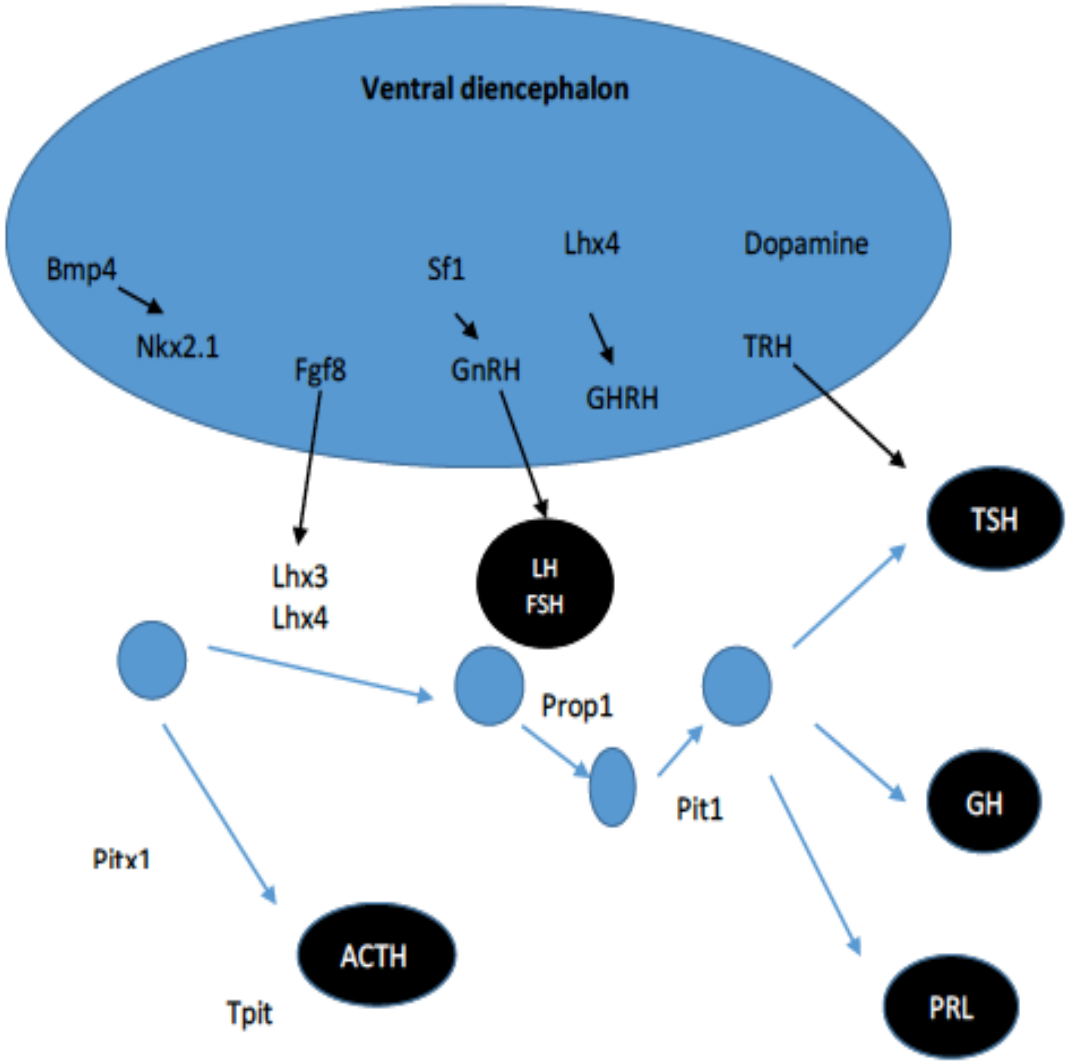

The understanding of human pituitary disease has been significantly enhanced by studying the effects of induced mutations and gene knock outs in the murine models. This has led to the identification of mutations in a number of genes that give rise to the phenotype of hypopituitarism in humans. Mutations in transcription factors such as *Hesx1, Lhx3, Lhx4, Prop1, Pou1f1, Pitx2* and *Tbx19* have been implicated to cause hypopituitarism in both the mice and the humans (57). Hypopituitarism is the deficiency of one or more hormones secreted by the pituitary gland. Congenital hypopituitarism comprises of a spectrum of disorders with variable phenotypes that can range in severity, from isolated hormone deficiency [IGHD being the most common] to combined pituitary hormone deficiency (CPHD) when two or more pituitary hormones are deficient (57). Congenital hypopituitarism may present as part of a syndrome with abnormalities in structures that share a common embryological origin with the pituitary gland (57).

The mutations in the known transcription factors implicated in the etiology of syndromic and non-syndromic hypopituitarism are described below:

## 2.3 SYNDROMIC FORMS OF HYPOPITUITARISM

### 2.3.1 Septo-Optic Dysplasia

De Morsier syndrome or septo-optic dysplasia(SOD) is a rare condition with a reported incidence of 1 in 10,000 newborns and is equally prevalent in both sexes (64). SOD is heterogeneous congenital anomaly and is characterised by the presence of at least two of the three features: hypopituitarism (one or more pituitary hormone deficiency), hypoplasia of the optic nerve and defects of the midline structures of the forebrain such as absent septum pellucidum or agenesis of corpus callosum (64). While the presence of all the three features occurs only in about 30% of the patients,

hypopituitarism and midline brain abnormalities can be a feature in 62% and 60% of the patients respectively (55). SOD has multifactorial etiologies such as genetic, viral infections, alcohol, drugs, vascular and environmental teratogens. Mutations in *HESX1, SOX2* and *SOX3* have been implicated in SOD (65, 66). However, the proportion of patients with SOD having mutations in these genes is very small, implying that there may be other unidentified genetic factors that may account for SOD (65, 66).

Any disruption occurring during the development of forebrain and the pituitary between 3-6 weeks of gestation can account for SOD (55). Disturbances in visual axis, squint or nystagmus secondary to unilateral or bilateral (majority) optic nerve hypoplasia can be the presenting feature of SOD (66). The pituitary hormone deficiencies may not be always present in patients with SOD but may evolve later in life, thus requiring life-long follow-up. The commonest pituitary hormone deficiency is GH followed by TSH, ACTH and gonadotropins (66). Posterior pituitary involvement and diabetes insipidus are rare. There also may be associated neurological manifestations such as cerebellar hypoplasia, schizencephaly, seizures and global developmental delay (67).

### 2.3.2 *HESX1* mutations and SOD

*HESX1* is critical transcription factor that has a central role in the early differentiation and determination of the forebrain and the pituitary gland (55). Expression studies during mouse embryogenesis show that *Hesx1* is one of the earliest markers of the pituitary primordium, first expressed in the anterior midline visceral endoderm and its continued expression in this area plays a vital role in the development of the forebrain, ventral diencephalon, anterior pituitary and the presumptive hypothalamus (55). Evidence from murine studies show that targeted disruption of *Hesx1* causes forebrain abnormalities, micropthalmia and absent optic vesicles, the features which are in line

with SOD in humans (68). The first homozygous missense mutation (Arg160Cys) was found in the homeobox of *HESX1* in two siblings with SOD with optic nerve hypoplasia, absent corpus callosum and septum pellucidum, an ectopic/undescended posterior pituitary and anterior pituitary hypoplasia with hypopituitarism (68). Subsequently homozygous and heterozygous mutations have been reported to cause variable phenotype ranging from IGHD to SOD. Only minority of patients with SOD (<1%) have *HESX1* mutations, implying that there are potential unidentified genes contributing to this complex disorder (69, 70).

### 2.3.3 *SOX2* and *SOX3* Mutations

The expression of *SOX2* and *SOX3* are important for the differentiation of progenitor stem cells and pituitary development (71, 72). *SOX2* mutations have been described in association with anterior pituitary hypoplasia, hypogonadotropic hypogonadism, hippocampal and corpus callosum abnormalities (73, 74). *SOX3* causes X linked hypopituitarism in males and may consist of abnormalities of corpus callosum, hypoplasia of the infundibulum, isolated or combined hormonal deficiencies (75, 76). The phenotype may be associated with learning difficulties (77).

### 2.3.4 Holoprosencephaly (HPE)

HPE is a heterogeneous condition with multifactorial etiology resulting from the abnormal cleavage of the forebrain and may be associated with pituitary, corpus callosum, nasal and ocular abnormalities (78). The most common endocrine manifestation in HPE is cranial diabetes insipidus (55). The transcription factor *GLI2* mediates the signal from the Sonic Hedgehog(*SHH*) signalling pathway, the mutation of which has been implicated in the development of HPE sequence (79). *GLI2*

mutations have been associated with hypopituitarism, partial agenesis of corpus callosum, single central maxillary incisor, post axial polydactyly and single nares (55).

### 2.3.5 *LHX3* mutations: Hypopitutarism with Spine Abnormalities

*Lhx3* or the LIM homeobox is an important early development gene detected in the Rathke's pouch and the developing nervous system, the continuous expression of which helps in the proliferation of gonadotrophs, thyrotrophs, somatotrophs and lactotrophs (80). Homozygous targeted disruption of this gene from mouse causes pituitary aplasia and results in their death, shortly after birth (81). Patients with homozygous *LHX3* mutations have deficiencies of GH, PRL, TSH, LH,FSH and also sometimes ACTH deficiencies with small to an enlarged anterior pituitary with a lesion suggestive of microadenoma (82, 83). There also can be an association of short rigid cervical spine with limitation of neck movement and sensorineural hearing loss (83-85).

### 2.3.6 *LHX4* mutations

The expression of *Lhx4* is closely related to that of *Lhx3* (86). The expression pattern of *Lhx4* is found throughout the invaginating Rathke's pouch at very early mouse embryonic stage but by E15.5 its expression is predominantly found in the anterior lobe of the pituitary (55). Targeted *Lhx4* deletion in mice results in hypoplastic pituitary due to reduction in cell numbers (58). Experiments involving *Lhx3* and *Lhx4* gene dosage in murine models demonstrate that a single allele of *Lhx3* or *Lhx4* is sufficient for the formation of definitive Rathke's Pouch (58). With targeted deletion of *Lhx3* and *Lhx4* in mouse, the progression from rudimentary to definitive Rathke's pouch does not occur (58). Variable degrees of hypopituitarism involving GH, ACTH, TSH and gonadotropin deficiencies with ectopic posterior pituitary, hypoplastic sella, cerebellar

abnormalities and Chiari malformation have been reported in patients with heterozygous *LHX4* mutations (83, 87, 88). *LHX4* is required for the activation and expression of *GH1*, therefore *LHX4* mutations result in short stature due to GH deficiency (89).

### 2.3.7 *OTX2* mutations

*OTX2* is another important transcription factor required for the formation of forebrain and its maintenance (90, 91). In humans, mutations in *OTX2* have been described in patients with hypopituitarism and bilateral anophthalmia with a normal or small anterior pituitary and an ectopic posterior pituitary. *OTX2* mutations can also cause hypopituitarism without associated ocular abnormalities (92). Among the anophthalmia/micropthalmia syndromes, 2-3% of the underlying genetic aetiology is due to a mutation in *OTX2* (93, 94).

### 2.3.8 Axenfield-Rieger syndrome (*PITX2* mutations)

In the mouse, *Pitx2* is initially expressed in the oral ectoderm and then in the Rathke's pouch. It is also expressed in the mesenchyme near the optic eminence, forelimbs and the domains of the abdominal cavity (57). It is required at multiple stages of the pituitary development after the commitment of the definitive Rathke's pouch. Targeted *Pitx2* mutations in mice causes hypopituitarism with hypoplastic anterior pituitary (95). Heterozygous mutations in *PITX2* (OMIM 601542 also known as *RIEG1*) are implicated in Axenfield-Rieger syndrome, an autosomal dominant condition that comprises of malformation of the anterior segment of eye, dental hypoplasia, protuberant umbilicus and brain abnormalities (96, 97). Pituitary abnormalities due to *PITX2* mutation in humans are yet to be described.

## 2.4 NON-SYNDROMIC FORMS OF HYPOPITUITARISM

### 2.4.1 *PROP1* Mutations

In the mouse embryo, the transcription factor *Prop1* is expressed within the Rathke's pouch from E10, in a region overlapping the *Hesx1* expression domain (55). The expression of *Prop1* starts to decrease after E12 and disappears at E15.5 (98). This decline in *Prop1* expression is important as overexpression can result in delay in the differentiation of gonadotrophs leading to transient gonadotrophin deficiency and delayed puberty (55). *Prop1* regulates the expression of *Hesx1* and *Pou1f1* by acting as transcriptional repressor of the former and transcriptional activator for the latter (99). Therefore the appropriate and timely suppression of *Prop1* is important for *Pou1f1* determination and in the establishment of other cell lineages (100). Naturally occurring *Prop1* mutations in Ames dwarf mice cause GH,PRL,TSH and gonadotrophin deficiencies due to failure in determination of *Pou1f1* lineage which determines the differentiation of somatotrophs, lactotrophs and thyrotrophs (55). In humans, *PROP1* is located at chromosome 5q and consists of three exons and a protein product of 226 amino acids (56). The most common mutations in *PROP1* are recessive mutations associated with GH, TSH, PRL and gonadotropin deficiencies (101). ACTH deficiency is uncommon but has been reported in patients with *PROP1* mutations (102). The degree of TSH and gonadotropin deficiencies is variable. The gonadotropin deficiency may range from micropenis, undescended testes, delayed puberty and infertility (101).

### 2.4.2 *POU1F1*(*PIT1*) Mutations

*POUIFI* (previously PIT-1), is a transcription factor that is expressed at E14.5 during the mouse pituitary development and persists throughout the postnatal period and in the adult pituitary (55). The differentiation of somatotrophs, lactotrophs and thyrotrophs depends on the *Pou1f1* expression (55). *POU1F1* mutations in humans are mostly autosomal recessive but dominant mutations have been described (103). The phenotype consists of GH and PRL deficiencies in early life and TSH deficiency occurring in late childhood with normal sized or small anterior pituitary and a normal posterior pituitary with no midline abnormalities (104).

### 2.4.3 *TBX19* mutations (OMIM 604614. Previously known as *TPIT*)

*TBX19* belongs to T-box family of transcription factors and is expressed from E11.5 within the developing anterior pituitary and the ventral diencephalon in mouse embryos (105). In the adult mouse pituitary, *TBX19* expression is detected in corticotrophs in anterior lobe that express POMC and in the melanotrophs forming the intermediate lobe (106). *TBX19* mutations are thus associated with isolated ACTH deficiency (107). Homozygous and compound heterozygous mutations in *TBX19* have been described implying a recessive mode of inheritance (107). ACTH deficiency can present in the neonatal period with severe hypoglycaemia, jaundice or seizures (108).

## 2.5 ISOLATED HORMONE DEFICIENCY DUE TO MUTATION IN SPECIFIC CELL TYPE: *GH1* MUTATIONS

In addition to mutations in the developmental genes, causing combined pituitary hormonal deficiencies, there are genetic mutations that contribute to isolated hormone deficiencies. An example is mutations in *GH1.*

Growth hormone is encoded by GH1 gene, the mutations of which are estimated in up to 12.5% of patients with isolated GH deficiency although the true incidence is difficult to ascertain owing to geographical and ethnic differences (109). Isolated GH deficiency(IGHD) due to *GH1* mutations consists of three types: Type 1a is the severest form due to the deletion of GH1 gene in which patients will not have any detectable serum GH and respond well to recombinant GH, although some patients develop anti-GH neutralizing antibodies (110). Type 1b IGHD is due to homozygous splice site mutation in *GH1* and is characterized by low but detectable GH after provocative stimulation (110). Type 2 IGHD is the common form and is due to splice site and missense mutations in *GH1* and is an autosomal dominant condition. Type 3 IGHD, an X-linked recessive disorder is associated with X-linked agammaglobulinemia (110).

A mutation leading to the absence of a disulphide bridge in *GH1* results in the decreased binding of GH to its receptor and subsequent downstream signalling, causing a high serum GH levels with low serum IGF-1 concentration leading to short stature (111).Patients with IGHD can also develop additional pituitary hormonal deficiencies later in life and therefore require life-long monitoring. In addition to *GH1* mutations, several other mutations in genes encoding GHRHR, TSH, LH and FSH have been known to cause specific hormonal deficiencies (112-114).

## 2.6 CLINICAL MANIFESTATIONS OF HYPOPITUITARISM

Establishing the diagnosis of congenital hypopituitarism is important as untreated hypopituitarism can result in serious morbidities such as global developmental delay due to prolonged undetected hypoglycaemia and untreated hypothyroidism, significant reduction in final height and morbidities related to water and electrolyte imbalance.

The clinical spectrum of hypopituitarism is dependent on the combination of hormonal deficits. The clinical manifestations may be non-specific in the neonatal period such as poor feeding, temperature instability, jitteriness, poor weight gain and prolonged jaundice (115). Early diagnosis in this age group can be challenging due to factors such as prematurity, associated neonatal comorbidities, lack of data appropriate for gestation and immaturity of hypothalamic-pituitary axis (55). Neonates can also present with associated developmental defects such as ocular, midline, genital abnormalities or syndromes associated with hypopituitarism. Presence of fixed squint, nystagmus in a neonate can be due to underlying optic nerve hypoplasia which can be isolated or a part of the spectrum of septo optic dysplasia. Such patients will need life- long follow up and assessment of endocrine function, even if their initial endocrine investigations are normal (116). Congenital hypopituitarism can be life threatening in neonates due to an underlying ACTH deficiency and may present as sepsis, seizures or conjugated hyperbilirubinaemia (117).

Growth failure can occur in infancy in severe GHD (118). Male neonates may present with micropenis or undescended testes as the penile growth is dependent on normal LH secretion during the second and third trimester (56). Diabetes insipidus can present as polyuria, polydipsia but may be masked in patients with ACTH deficiency as cortisol is essential to excrete the water load. Hydrocortisone replacement may unmask

diabetes insipidus and hence vigilance is essential in patients with suspected hypopituitarism with or without midline defects when being treated with hydrocortisone therapy for cortisol deficiency.

## 2.7 INVESTIGATIONS IN HYPOPITUITARISM

The investigations of hypopituitarism comprise of stimulation or provocative tests to check the adequacy of the hypothalamic-pituitary axis (HPA) and neuroradiology.

### 2.7.1 ACTH Deficiency

In neonates, ACTH deficiency can be life threatening. It is however challenging to assess the intactness of the hypothalamic-pituitary-adrenal axis as the circadian rhythm of cortisol is not well established during the first six months of life (119). The usefulness of baseline serum cortisol samples in the morning or evening are limited in this age group. Multiple cortisol measurements during the various points during the day and night can be challenging and may not reveal definitive information on the integrity of the axis. Hypoglycaemia induced cortisol stimulation is contraindicated in the age group but standard synacthen test is safe and easy to perform in this age group. However the standard synacthen test is limited by sensitivity of 80% and therefore false negative results are a possibility despite ACTH deficiency (117). In older children, after the establishment of circadian rhythm , 08:00 am cortisol of 175nmol/L or more combined with a 30 minute stimulated level of more than 540nmol/L on a standard synacthen test has a sensitivity of 69% and specificity of 100% in excluding ACTH deficiency (117).

### 2.7.2 TSH Deficiency

TSH deficiency is normally characterised by a low or inappropriately normal TSH combined with a low serum free thyroxine. Isolated TSH deficiency is rare but can occur in combination of other pituitary hormone deficiencies (120). Provocative test such as thyrotropin releasing hormone(TRH) test is generally not required to establish the diagnosis of central hypothyroidism (121).

### 2.7.3 GH Deficiency

Severe GH deficiency can present in the neonatal period as hypoglycaemia. The provocative tests to assess the hypothalamic-pituitary-growth axis are contraindicated in children less than one year of age. The diagnosis of GH deficiency in this age group is normally suggested by low plasma GH concentration in response to spontaneous hypoglycaemia, low plasma IGF-1 and/or the presence of additional hormonal deficiencies (122).In older age groups the diagnosis is based on the faltering growth velocity, low IGF1, suboptimal GH response to GH provocation test and/or the presence of a structural anomaly in the pituitary gland detected on MRI.

### 2.7.4 Gonadotropin Deficiency

Males with gonadotropin deficiency can present with micropenis with or without undescended testes. The physiological postnatal surge in LH, FSH and testosterone is detected up to 6 months in males and about 2 years in females (123). A combination of GnRH (gonadotropin releasing hormone) and hCG (human chorionic gonadotropin) stimulation tests are useful in the earlier detection of hypogonadotropic hypogonadism (HH) in infants where a low baseline gonadotropin concentrations (LH & FSH) and blunted response to stimulation with GnRH are found (124).

### 2.7.5 ADH Deficiency (Diabetes Insipidus(DI))

Early morning paired serum and urine osmolality, hypernatraemia along with symptoms such as polyuria, weight loss may be helpful in the diagnosis as water deprivation test can be dangerous in this age group. The symptoms of DI can be masked in patients with ACTH deficiency as cortisol is important for water excretion from the kidneys.

### 2.7.6 The Role of Neuroradiology

In infants with suspected or diagnosed hypopituitarism, MRI of the pituitary and brain can help to assess the size of anterior pituitary, the location of posterior pituitary, the morphologies of infundibulum, corpus callosum, septum pellucidum, optic nerves, optic chiasma and associated brain abnormalities (125). The neuro radiological abnormalities are usually related to the severity or the evolution of hypopituitarism (126). In patients with ectopic posterior pituitary, the risk of hypopituitarism is much greater than patients with normally positioned pituitary. Neonates with optic nerve hypoplasia and small anterior pituitary will require a lifelong follow-up despite their initial normal endocrine function as hypopituitarism may evolve over a period of time (126).

## 2.8 MANAGEMENT OF CONGENITAL HYPOPITUITARISM

The management of congenital hypopituitarism is multidisciplinary and requires a lifelong follow-up. The management should not only focus on optimizing the hormone replacement but also to monitor carefully for the evolvement of potential hormonal deficiencies in the future. In syndromic forms of hypopituitarism, it is also vital to address the wider issues such as visual and neuro-developmental issues and offer appropriate genetic counselling (55).

While replacing hormones in suspected combined pituitary hormone deficiency, it is important to assess the adequacy of cortisol secretion and replacing with hydrocortisone when the cortisol secretion is suboptimal before commencing on thyroxine (55). As mentioned above, patients on cortisol replacement should be carefully monitored for symptoms of DI.

Overall, the mainstay of treatment of congenital hypopituitarism is to identify the existing and evolving hormonal deficits optimizing their replacement.

# CHAPTER 3

# CONGENITAL HYPERINSULINSIM-MOLECULAR MECHANISMS, DIAGNOSIS AND MANAGEMENT

## 3.1 SUMMARY OF CHAPTER 3

Chapter 3 provides an introduction to glucose physiology, regulation of insulin secretion, ATP-sensitive potassium channels ($K_{ATP}$), and congenital hyperinsulinism(CHI). This chapter opens with a brief description on insulin secretion and pancreatic β-cell physiology, followed by introduction to $K_{ATP}$ channels. This then leads into detailed description of the clinical condition “congenital hyperinsulinism”, its causes, clinical presentation, diagnosis, histological subtypes and management.

## 3.2 CONGENITAL HYPERINSULINISM (CHI)

Congenital hyperinsulinism (CHI) is a condition in which there is an unregulated insulin secretion from the β-cells of the pancreas (127). This unregulated insulin secretion suppresses the production of glucose by inhibiting gluconeogenesis and glycogenolysis leading to severe and persistent hypoglycaemia (128). In the absence of glucose, the brain normally utilises the ketone bodies as an alternative source of energy. However, in CHI, the metabolic actions of the excess insulin inhibit ketogenesis and lipolysis depriving the brain of both glucose and ketones as energy source leading to hypoglycaemic brain injury. During the neonatal, infancy and childhood periods, CHI is an important cause of hyperinsulinaemic hypoglycaemia and requires early recognition, diagnosis and immediate and appropriate management to prevent or reduce the neurological injury (129).

## 3.3 INSULIN SECRETION AND PANCREATIC β-CELL PHYSIOLOGY

Insulin is the key regulator of blood glucose concentration and its secretion is tightly linked to the metabolism of glucose, intricately translated into signals in pancreatic β-cells (130). Glucose enters the pancreatic β-cells mainly via glucose transporter 2 (*GLUT 2*) situated in the cell membrane. The transport of glucose across the pancreatic β-cell membrane in proportion to the blood glucose concentration is facilitated by the high affinity($K_m$) for glucose with *GLUT2* (131). Once transported, the glucose is converted to glucose-6-phosphate by an islet specific enzyme, glucokinase. Glucokinase acts like a sensor to the β-cell, increasing its activity during high blood glucose concentration and reducing its activity when the blood glucose concentration falls low (132). These activities in-turn guide the signals regulating the insulin production in the pancreatic β-cells.

The β-cell membrane has ATP-sensitive $K^+$ channel ($K_{ATP}$ channel) that plays a fundamental role in maintaining the glucose homeostasis (133). These channels couple the glucose metabolism to β-cell's electrical excitability and insulin secretion (133).

### 3.3.1 Structure of $K_{ATP}$ Channel

The $K_{ATP}$ channel is a hetero-octameric complex arranged in a 4:4 stoichiometry. This model was first suggested by Inagaki and colleagues on the basis of optimum activity of $K_{ATP}$ channels when SUR1 and Kir6.2 subunits were co expressed with a molar ratio of 1:1 (134). The channel comprises of two types of subunits consisting of four inward rectifying potassium channel pore forming (Kir6.2) subunits and four high affinity sulfonylurea receptor 1 (SUR 1) subunits (an ATP binding cassette transporter) (134). The Kir6.x subunits belong to the superfamily of weak inwardly rectifying, voltage independent potassium (K+) channels that allow a large influx of K+ flux at negative potentials (135). The channel is arranged in such a way that the Kir6.2 subunit forms the inner core and the SUR1 is a regulatory subunit and forms the outer part (134). This assembly is unique and the correct assembly is vital for the transport and subsequent expression of the channel on the surface of the cell membrane.

The Kir6.2 forms the core of the channel whilst the SUR1 (an ATP binding cassette transporter) acts as a regulatory subunit. $K_{ATP}$ channels can only function if they are assembled and correctly transported to the cell membrane surface (trafficking) (136). The assembly and trafficking of $K_{ATP}$ channels are intricately linked processes (136). Each Kir6.2 subunit consists of two transmembrane domains (TM1 and TM2) linked by an extracellular pore-forming region H5 that serves as a potassium selectivity filter

(137). The TM2 domains from all the four Kir6.2 subunits form the pore of the channel. Both the aminoacid and carboxyl terminals are found in the cytoplasm and are responsible for ATP binding and channel gating (137).

Each SUR1 subunit consists of 17 transmembrane regions organized into three domains (137). The TMD1 and TMD2 comprise of the transmembrane regions from TM6-11 and TM12-17 respectively. The TMD0 that comprises of the regions from TM1-5 plays an important role in trafficking the Kir subunit to the surface of the cell membrane (137). The subunit also comprises of two nucleotide binding folds (NBFs) on the cytoplasmic side (138). The NBF-1 is found between TMD1 and TMD2 and NBF-2 is present after TMD2 (139).

Both the subunits (Kir6.2 and SUR1) have to be co-expressed on the surface of the cell membrane in order to function. The trafficking of either subunit in the absence of other is prevented by the presence of an endoplasmic reticulum (ER) retention signal in the C terminal region of Kir6.2 and between TM11 and NBF-1 in SUR1 (136). Mutations causing the truncation of the Kir6.2 C-terminus results in deletion of the retention signal and causes its expression in the absence of SUR1 (140).

When blood glucose level is low, the $K_{ATP}$ channels in pancreatic β-cell remain open to allow the diffusion of potassium that maintains the resting membrane potential at a hyperpolarized state and keeps the voltage gated calcium channels closed. With an increase in the blood glucose concentration, the production of ATP increases and raises the intracytosolic ATP/ADP ratio which inhibits the SUR1. This results in the closure of the KATP channels leading to membrane depolarization. This in-turn causes $Ca^{2+}$ influx into the pancreatic β-cell via the voltage gated $Ca^{2+}$ channels.

The increase in the intracellular calcium concentration triggers the exocytosis and the release of insulin(141). The mechanism of insulin release is depicted in the figure 3.1.

**Figure 3.1:** Mechanism of release of insulin from the pancreatic β-cell:The glucose enters via GLUT2 (Glucose Transporter 2) is phosphorylated. This increases the ATP/ADP ratio which causes the closure of the $K_{ATP}$ channel resulting in the membrane depolarisation, resulting in the opening of the voltage gated calcium channels. The entry of calcium results in exocytosis and subsequent insulin release.

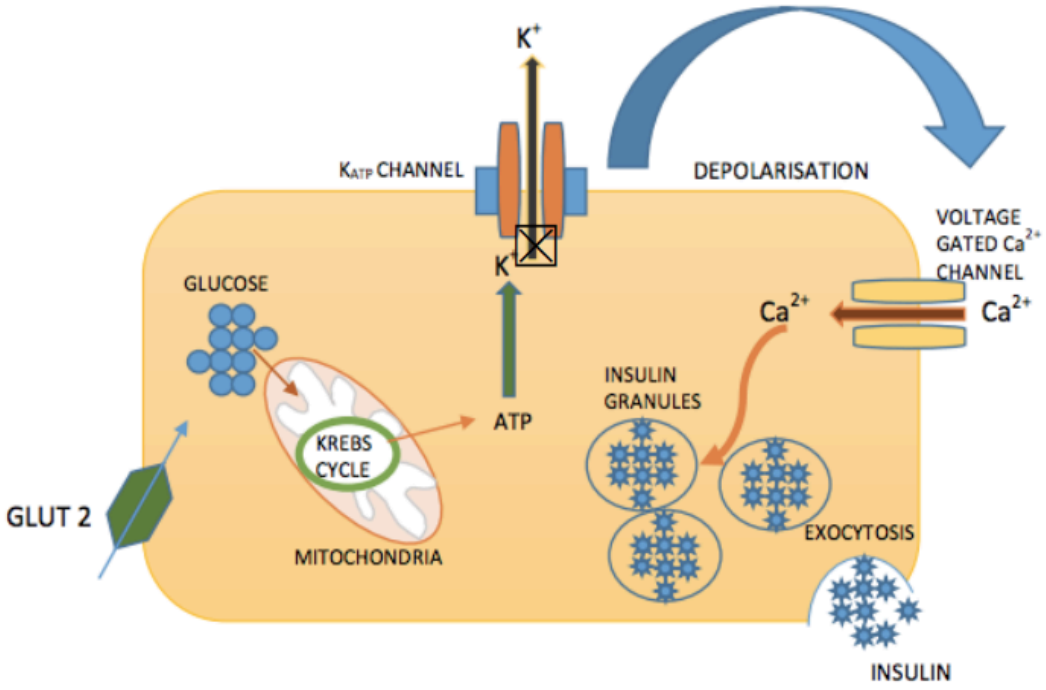

### 3.3.2 $K_{ATP}$ Channel Independent Insulin Secretion

The key mechanism of insulin release from the pancreatic β-cell is the glucose stimulated insulin secretion by triggering the $K_{ATP}$ channel dependent signals. However, there are evidences to suggest that the insulin release from the pancreatic β-cell can occur independent of the $K_{ATP}$ channels (142-144).Gembal et al. demonstrated that the depolarisation of the β-cell membrane on the mouse islets, by increasing the extracellular potassium concentration triggered calcium influx and the resultant insulin release despite diazoxide (143). They also demonstrated that the insulin secretion proportionately increased by increasing glucose concentration. This is suggestive of potential $K_{ATP}$ channel independent mechanism that operates in glucose mediated insulin secretion. Straub et al. demonstrated glucose stimulated insulin secretion without an increase in the intracellular free calcium on islets on a patient with mutation in the $K_{ATP}$ channel (144).The insulinotropic action of glucose in $Ca^{2+}$ depleted rat pancreatic islets occurred in the presence of a phorbol ester (phorbol 12-myristate 13-acetate; PMA) and forskolin (adenylate cyclase activator) (145).

## 3.4 ETIOLOGY OF CHI

Hyperinsulinaemic hypoglycaemia can have an underlying monogenic etiology or can be transient secondary to intra-uterine growth retardation (IUGR) and maternal diabetes mellitus (gestational or insulin dependent), birth asphyxia and can be associated with several developmental syndromes (such as Beckwith-Wiedemann, Kabuki and Turner syndromes) and rare metabolic conditions such as congenital disorders of glycosylation (CDG) syndromes (146).

Mutations in 11 genes are associated with genetic forms of CHI (*ABCC8, KCNJ11, GLUD1, GCK, HADH1, UCP2, MCT1, HNF4A, HNF1A, HK1, PGM1*) (147). *ABCC8* or *KCNJ11* mutations constitute the majority of causes of monogenic CHI (147).

### 3.4.1 CHI due to Defects in Pancreatic β-cell $K_{ATP}$ Channels

The Kir6.2 and SUR1 subunits are encoded by the genes *KCNJ11* and *ABCC8* respectively. The first link between CHI and $K_{ATP}$ channels was suggested with the help of linkage analysis in 15 families (12 Ashkenazi Jewish, 2 consanguineous Arab and 1 non-Jewish Caucasian) where the region responsible to cause CHI was mapped to 11p14-15.1 (148). By fluorescence *in situ* hybridization (FISH), Thomas et al. mapped the gene encoding SUR to this region and identified splice site mutations in individuals from nine different families (149). Subsequently, a homozygous missense mutation (L147P) in Kir6.2 was reported in a child with CHI (150).

The most common causes of CHI are recessive mutations involving *ABCC8* or *KCNJ11*, that diminish or completely abolish the activity of KATP channel which results in constant membrane depolarization and an unregulated release of insulin despite the presence of hypoglycaemia (151). In about half of the patients with CHI, germline mutations are found in *ABCC8* or *KCNJ11* (152). The majority of the reported mutations are in *ABCC8* (about 150 homozygous, compound heterozygous and inactivating heterozygous) and in *KCNJ11*, about 24 mutations have been reported (152).

#### 3.4.1.1 Molecular Basis of *ABCC8* and *KCNJ11* Recessive Mutations

The mutations involving the genes encoding $K_{ATP}$ channels can cause defects in the biogenesis and turnover of the channel, defects in the trafficking of the channel from the endoplasmic reticulum and Golgi apparatus to the plasma membrane or defects causing altered response to nucleotide activation and open state (153-155). The loss of function mutations contributing to these defects are of two types: class I mutations are those that cause defects in trafficking and class II mutations result in reduced $K_{ATP}$ channel response to nucleotide activation or reduced intrinsic channel open probability (130).

The recessive homozygous mutations abolish the activity of $K_{ATP}$ channel completely resulting in severe CHI, unresponsive to diazoxide treatment. Recessive compound heterozygous mutations can cause a milder phenotype that can respond to treatment with diazoxide (156).

### 3.4.2 Defect in Biogenesis and Turnover

The biogenesis and turnover of SUR1 and KiR6.2 were studied with pulse-labelling methods by Crane et al. and it was found that SUR1, when expressed alone had a half-life of approximately 25.5 hours. On the other hand, Kir6.2 had biphasic turnover with a half-life of 36 minutes for the first 60% and 26 hours for the remaining (157). The co-expression of SUR1 and Kir6.2 prevented the fast degradation of Kir6.2 and the combined estimated half-life was about 7.3 hours. Mutations involving the channels such as Kir6.2 W91R and SUR1$\Delta$F1388 result in rapid degradation and affect the biogenesis and turnover (157).

### 3.4.3 Trafficking Defects

The masking of the endoplasmic retention signal is an important requirement to allow correct trafficking and co-expression of the $K_{ATP}$ channels on the surface of the β-cell membrane. The endoplasmic retention signal comprises of a three peptide sequence (RKR; Arg-Lys-Arg), present in both the SUR1 and Kir6.2 (136, 140). Mutations affecting the trafficking can cause CHI.The phenyl alanine at the position 1388 in SUR1 is critical for normal trafficking, and SUR1ΔF1388 causes CHI (153). The other mutations that have been demonstrated to affect trafficking include SUR1 L1544P and SUR1 R1394H (154, 158).

### 3.4.4 Defects in Channel Regulation

The nucleotide binding folds (NBF-1 and NBF-2) of SUR1 regulate the conductance of Kir6.2 and several mutations (R1420C, T1139M and R1215Q) can alter the sensitivity to changes in ATP/ADP ratio and can result in loss of ADP dependent KATP channel function and constitutive release of insulin (139, 155).

### 3.4.5 Dominant Activating $K_{ATP}$ Channel Mutations

Dominant $K_{ATP}$ channel mutations can cause CHI which may either be diazoxide responsive or unresponsive depending on the response of Kir 6.2 and SUR1 to the ADP or diazoxide. Dominant $K_{ATP}$ mutations do not affect the trafficking of the channels. Huopio et al. identified diazoxide responsive heterozygous mutations in seven patients and their mothers (159). Pinney et al. described dominantly inherited KATP mutations in 14 patients (11 *ABCC8* and 3 *KCNJ11* mutations) (160).The functional studies indicated that the mutations had significantly decreased channel opening probability and also reduced response to MgADP and diazoxide (160). The presence of WT *ABCC8* or *KCNJ11* allele in heterozygous conditions resulted in

partial response to alterations in ATP/ADP ratio suggesting that the dominant mutations result in milder phenotype compared to the recessive ones (160). Flanagan et al. reported diazoxide unresponsive dominant mutations in *ABCC8* either as *de novo* or inherited from one of the parents (161). MacMullen et al. reported 13 missense *ABCC8* heterozygous mutations associated with diazoxide-unresponsive disease (162). Expression of these mutations in COSm6 cells revealed normal trafficking of channels but severely impaired responses to MgADP or diazoxide (162).

### 3.4.6 CHI due to Gain of Function Mutations in *GLUD 1*

Gain of function mutations in *GLUD1* causes hyperinsulinism-hyperammonemia (HI/HA) syndrome, which is the second most common cause of monogenic CHI after KATP channel mutations (127). *GLUD1* is mapped to chromosome 10q23.3 and encodes a mitochondrial matrix enzyme, glutamate dehydrogenase (GDH). This enzyme catalyses the oxidative deamination of glutamate to alpha-ketoglutarate and ammonia, resulting in ATP production. GDH is allosterically inhibited by GTP and activated by leucine (163). Mutations in *GLUD1* reduce the allosteric inhibition of GDH by ATP and GTP, resulting in the increase in the enzyme activity. The increased enzyme activity in the pancreatic β-cells, causes an increase in the ATP/ADP ratio which consequently activates $K_{ATP}$ channels, resulting in cell depolarization and insulin release (164). In addition to pancreatic β-cells, GDH is also expressed in other organs such as pancreas, liver, brain, kidney, heart and lungs (165).

The first reports of patients with HI/HA syndrome were identified by Zammarchi et al. and Weinzimer et al. in a group of patients who were noted to have an increased GDH activity in their lymphoblasts derived from peripheral blood lymphocytes (166, 167).

The phenotype of patients with *GLUD1* mutations is milder compared to other forms of CHI and is characterised by fasting hypoglycaemia and hypoglycaemia following protein rich meals (165). The patients also have asymptomatic hyperammonemia. The hyperammonemia is mild to moderate and is resistant to treatment with detoxification agents and protein restriction diet (168). A small percentage of patients with *GLUD1* mutations have been reported to have normal serum ammonia level but still demonstrate leucine hypersensitivity(165). Using animal models, the source of high ammonia production in majority of *GLUD1* mutations have been shown to be from kidneys due to the increased renal GDH activity (169).

The patients with HI/HA syndrome have greater incidence of epilepsy when compared with the other forms of CHI (165). *GLUD 1* mutations occurring in the GTP binding site have been found to have increased frequency of epilepsy (165). The reason for the increased frequency of neurological complications in these patients in unclear but various potential mechanisms such as recurrent hypoglycaemia, chronic elevated high ammonia causing brain injury have been suggested (164). The elevated GDH activity in the brain reduces the availability of glutamate for the glutamate decarboxylase and GABA synthesis, resulting in decreased GABA concentration (170). Although this is an interesting potential mechanism, the measurement of GABA and other neurotransmitters in the CSF of these patients have been normal (170).

### 3.4.7 CHI due to mutations in *HADH*

Mutations in HADH are responsible for recessive form of CHI (171). *HADH* is a mitochondrial gene encoding the enzyme 3-hydroxyacyl-coenzyme A dehydrogenase that catalyses the penultimate reaction in the beta oxidation of fatty acids and converts L3-hydroxyacyl CoAs of variable chain length to their corresponding 3- ketoacyl CoAs

(172). Although *HADH* is expressed in many tissues, the highest level of expression is found in the islets of Langerhans (172). The patients with *HADH* mutation are protein sensitive. Protein sensitivity had been demonstrated in *HADH* knock out mice (173).These findings suggest that an amino acid triggered pathway of insulin release might be a potential underlying cause (174). It is also hypothesised that *HADH* mutations may cause a loss of inhibitory regulation of GDH by HADH and leading to increased GDH activity and CHI (173, 175). Most of the reported patients to date are from consanguineous families. The biochemistry profile of these patients may show an increased level of plasma hydroxyl-butyryl- carnitine and urinary 3-hydroxyglutarate levels (174). The patients with *HADH* mutations are diazoxide responsive and hence it is recommended to test for this gene mutation in those diazoxide responsive patients from consanguineous families with negative KATP gene mutations (176).

### 3.4.8 CHI due to Gain of Function Mutations in *GCK*

*GCK* encodes the glycolytic enzyme, glucokinase which acts like a pancreatic β-cell sensor and has a key role as a rate limiting enzyme in the metabolism of glucose (177). It converts the transported glucose into glucose-6-phosphate. Glucokinase has low affinity for glucose, a key property that helps in maintaining the plasma glucose at physiological concentrations by governing the glucose stimulated insulin secretion (178).

Activating or gain of function *GCK* mutations increase the affinity of glucokinase for glucose which lowers the threshold for glucose stimulated insulin secretion. The increased affinity results in an increased ATP/ADP ration within the pancreatic β-cell, causing the closure of KATP channel, depolarization and consequent insulin release (178). The phenotype of *GCK* activating mutations are variable ranging from

asymptomatic hypoglycaemia, medically unresponsive CHI and CHI with some variable responses to diazoxide (178-180).

### 3.4.9 CHI due to Mutations in Transcription Factors-*HNF4A* and *HNF 1A*

*HNF4A* belongs to the nuclear hormone receptor superfamily and codes for hepatocyte nuclear factor 4α. It is a transcription factor that plays an important role in regulating the expression of genes involved in glucose stimulated insulin secretion (181). While the heterozygous inactivating mutations in *HNF4A* and *HNF1A* is associated with maturity-onset diabetes of the young (MODY 1 & MODY 3 respectively), heterozygous mutations in these transcription factor have also been implicated in CHI (182). The mechanism of causation of CHI by *HNF4A* mutation is not precisely known. One of the proposed mechanisms is: *HNF4A* reduces the levels of PPARα (peroxisomal proliferator-activated receptor alpha) (181, 183). The transcription factor PPARα is known to control the expression of genes involved in the beta oxidation of fatty acids and PPARα null mice develop fasting hypoglycaemia. *HNF4A*, by reducing the levels of PPARα, reduces the beta-oxidation of fatty acids (183). This reduction in beta-oxidation of fatty acids results in lipid accumulation in the cytoplasm. Malonyl-CoA is one such lipid, the accumulation of which potentially inhibits the enzyme carnitine-palmitoyltransferase I which then causes an increase in the long-chain-acyl-CoA in the cytoplasm which in turn signals the release of insulin (181, 184).

The other possible mechanism by which *HNF4A* mutation causes CHI is that it may potentially cause a reduction in the expression of Kir 6.2 subunits. *HNF4A* knockout mouse had 60% reduction in the expression of KiR6.2 subunit (181). Patients with *HNF4A* mutations developing CHI are characterised by large birth weight (185, 186).

The severity of hyperinsulinism may vary from transient form to persistent form requiring diazoxide treatment (187). The mutations in these transcription factors (*HNF4A* and *HNF1A*) can also affect the function and development of other organs and may result in extra pancreatic manifestations (147). Renal fanconi syndrome and hepatic glycogen storage disorders have been associated with *HNF4A* mutation in addition to CHI (188). The affected children are at increased risk of developing monogenic diabetes, responsive to oral sulfonylureas later in life. The underlying mechanisms responsible for the early unregulated excess insulin secretion which later switches to a state of insulin deficiency is unclear.

### 3.4.10 Exercise-induced Hyperinsulinism(EIHI)

Exercise-induced hyperinsulinism (EIHI) is inherited in an autosomal dominant fashion and is characterised by inappropriate insulin secretion following or during anaerobic exercise leading to hypoglycaemia. Heterozygous activating mutations in *SLC16A1* (solute carrier family 16, member 1) encoding monocarboxylate transporter (*MCT1*) have been implicated in EIHI (189-191). Strenuous exercise causes a build-up of lactate and pyruvate which under normal physiological conditions, are not transported across the pancreatic β-cells since the pyruvate transporter (*MCT1*) is not expressed in β-cells (190). However, a gain of mutation in the promoter region of *SLC16A1*, causes an increased expression of *MCT1* in the β-cells, rendering the plasma membrane permeable to pyruvate and lactate (190). The increased uptake of lactate and pyruvate by the β-cells in these patients during exercise, stimulates the release of insulin despite low blood glucose levels. The affected patients do not experience fasting hypoglycaemia. Avoidance of strenuous exercise in these patients usually prevents the hypoglycaemic episodes.

### 3.4.11 CHI due to Uncoupling Protein 2 (*UCP2*) Mutations

*UCP2* is implicated to downregulate the insulin secretion from the pancreatic β-cells and is expressed in many tissues. *UCP2* knock out mice has been shown to develop hyperinsulinism (192). *UCP2* also has a role in the metabolism of fatty acids and protection against oxidative stress. Vozza et al. demonstrated that *UCP2* suppresses the glucose oxidation and stimulates glutamine oxidation in the mitochondrial matrix (193). Dominant loss of function mutation in *UCP2* have been reported to cause diazoxide responsive CHI, presumably by enhancing the glucose oxidation, facilitating pyruvate entry and triggering the insulin release (193).

### 3.4.12 CHI due to Mutations in Hexokinase 1(*HK1*)

*HK1* encodes for the enzyme hexokinase 1 which has high affinity for glucose (low-$K_m$) and in normal individuals there is a very little or no expression in the pancreatic β-cells. *HK1* is mapped to a region in the chromosome 10q (194). Henquin et al. demonstrated the presence of low-$K_m$ hexokinase-I in β-cells of hyper functional islets in 5 patients with CHI who were negative for $K_{ATP}$ channel mutations (195). The authors proposed that the inappropriate insulin secretion to hypoglycaemia can be due to *HK-1* substituting glucokinase for the phosphorylation of glucose (194). Although the precise mechanism that allows the expression of *HK1* in the β-cells is not known, it is hypothesised that a somatic genetic event during the pancreas development could have affected the factor or the mechanism responsible for the normal repression of *HK1* in the β-cells. Mice lacking PKC-λ in their β-cells demonstrated increased expression of *HK-I* and excessive insulin secretion at low glucose levels, which was reversed by re-expression of the simultaneously decreased *Foxa2*, implying that the transcription factor *Foxa2* has a role in regulating *HK1* expression (196).

### 3.4.13 CHI due to Phosphoglucomutase 1(*PGM1*) Mutations

Phosphoglucomutase 1 (*PGM1*) is essential for glycogen degradation as it converts glucose-6-phosphate to glucose-1-phosphate. Inactivating mutations in *PGM1* have been reported in children with abnormal glycosylation and hypoglycaemia (197). The phenotype consisted of fasting ketotic hypoglycaemia, postprandial hyperinsulinaemic hypoglycaemia, short stature, cleft lip and palate (197).

The various genetic mechanisms controlling the release of insulin from the pancreatic β-cell is shown in figure 3.2.

**Figure 3.2:** Role of different genes in enhancing the insulin secretion from pancreatic β-cell: Kir6.2 & SUR-1(encoded by *KCNJ11 & ABCC8*) regulate the $K_{ATP}$ channel. Mutations in these channels can diminish their opening or cause complete closure resulting in constant depolarisation of the cell membrane and constant insulin release despite hypoglycaemia. Mutations in genes such as *GCK, MCT1, HADH* (encoding SCHAD), *UCP2* cause an increase in the ATP/ADP ratio by different mechanisms which causes closure of the $K_{ATP}$ channel resulting in membrane depolarisation.

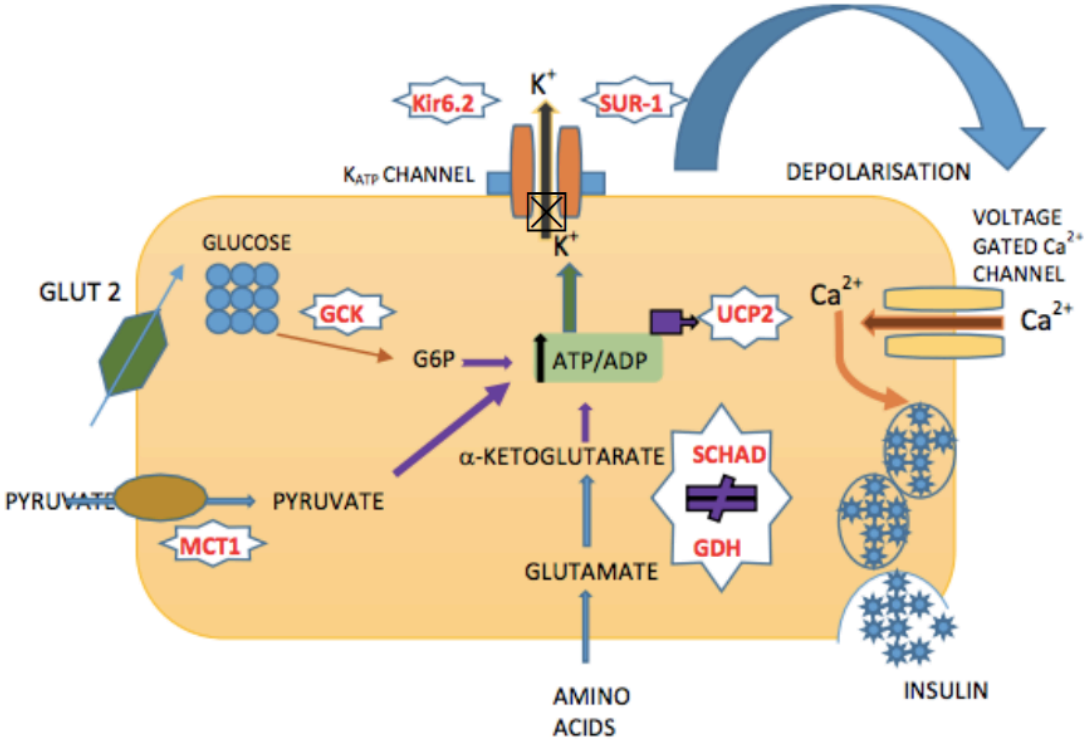

### 3.5 CHI-HISTOLOGICAL SUBTYPES

The two main types of CHI in relation to the histopathology are diffuse and focal. Diffuse form of CHI is characterised by the presence of hyperfunctioning islets that secrete excess insulin in the whole of the pancreas (198). The most common genetic etiologies for diffuse CHI are mutations in *ABCC8* and *KCNJ11*. Diffuse CHI due to the inactivating mutations in *ABCC8* or *KCNJ11* do not respond to diazoxide (Figure 3.3).

Focal form of CHI is characterised by nodular hyperplasia involving small localized regions of the pancreas measuring 2-10 mm in diameter. The areas of nodular hyperplasia in the islets consist of ductoinsular complexes and giant β-cell nuclei surrounded by normal pancreatic tissue (197). The focal disease is sporadic in origin. Two independent genetic events contribute to the etiology. The first event involves a mutation in paternally inherited *ABCC8* or *KCNJ11* genes. The second event involves a loss of heterozygosity, where there is a somatic loss of the maternal 11p allele involving the *ABCC8* and *KCNJ11* region (11p15.1 to 11p15.5) within the focal lesion(199). The resultant uniparental isodisomy causes the paternally inherited ABCC8 or *KCNJ11* mutation to be fully expressed contributing to increased insulin secretion. There is also altered expression of the adjacent Beckwith-Wiedemann syndrome(BWS) locus containing imprinted genes-*IGF2, H19* and *CDKN1C* that lead to increased proliferation of β-cells evolving into focal adenomatous hyperplasia(200). The focal forms of CHI usually do not respond to diazoxide.

### 3.5.1 Differentiation between Diffuse and Focal forms of Hyperinsulinism

Focal form of CHI is curable by surgery by excising the lesion of adenomatous hyperplasia. However, medically unresponsive diffuse form of CHI will require a near total pancreatectomy. A non-invasive technique to differentiate between the diffuse and the focal lesion was first described by Otonkoski et al in 2006, where the use of 18F-fluro-L-dihydroxyphenylalanine Positron Emission Tomography ($^{18}$F-DOPA PET) has proved to be beneficial in locating the small focal lesions of adenomatous hyperplasia (201). This technique is based on the principle of measuring the DOPA decarboxylase activity, which is expressed in islet cells. When the pancreatic islets take up L-DOPA, it is converted into dopamine by DOPA decarboxylase (201). The diffuse and focal lesions have high DOPA decarboxylase activity. The focal and diffuse uptake of DOPA on PET CT scan is depicted in figure 3.3.

**Figure 3.3:** Focal and Diffuse forms of CHI. A-Focal CHI; B-diffuse CHI [adapted from Arya, VB; (2015) Understanding the novel genetic mechanisms of congenital hyperinsulinaemic hypoglycaemia. Doctoral thesis, UCL (University College London]

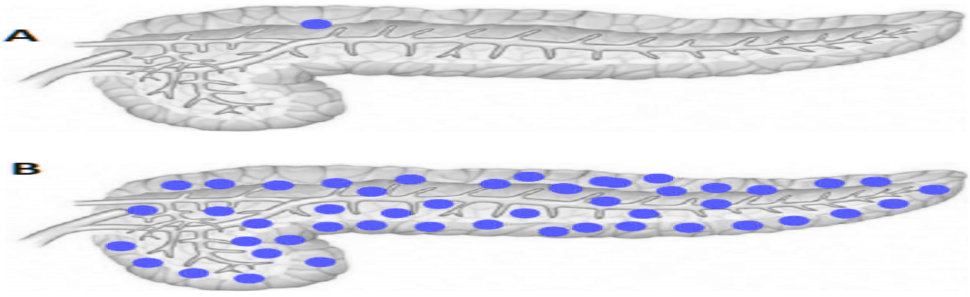

### 3.6 CLINICAL PRESENTATION OF CHI

Hyperinsulinaemic hypoglycaemia (HH) usually presents during the neonatal period and can be severe. The symptoms may be non-specific such as poor feeding, jitteriness, lethargy and in severe cases may involve seizures. HH during the neonatal period can be transient in infants who had intra uterine growth restriction(IUGR) or those who sustained perinatal asphyxia. Transient HH is also observed in babies born to diabetic mothers (insulin dependent or gestational). These infants typically have a large birth weight. The transient form of HH can take many weeks and months to resolve and may require treatment with diazoxide.

HH is an associated feature in some of the syndromes such as Kabuki syndrome, Soto's syndrome, Turner syndrome, Beckwith-Wiedemann syndrome(BWS) and also in metabolic conditions such as congenital disorder of glycosylation (127). BWS is an overgrowth syndrome characterised by prenatal and/or postnatal overgrowth, organomegaly, macroglossia, anterior abdominal wall defects, hemihypertrophy, ear lobe creases and helical pits (202). BWS is the commonest developmental syndrome associated with HH. HH in BWS is usually transient but may require treatment.

CHI can be a late presenting feature, especially in patients with *GLUD1* mutations (HI/HA syndrome) as the hypoglycaemia in these patients is not as severe as seen in patient with KATP channel mutations. These patients have asymptomatic mild to moderate hyperammonaemia and develop symptoms of hypoglycaemia following a protein-rich meal (167). In patients with a history of intestinal surgery or bowel resection, hyperinsulinaemic hypoglycaemia develops as a part of the dumping syndrome. Patients with *SLC1A1* mutations develop exercise induced hypoglycaemia after 30 minutes of anaerobic exercise (189).

### 3.7 DIAGNOSIS OF CHI

The early diagnosis of CHI is important in order to reduce or prevent hypoglycaemia induced brain injury. Since the symptoms of hypoglycaemia can often be subtle and non-specific in the neonatal period, it is important to have a low threshold in order to investigate these patients. Persistence of hypoglycaemia despite intravenous glucose administration and an intravenous glucose load of >8mg/kg/min (normal range:4-6mg/kg/min) is highly suggestive of CHI (128). The characteristic plasma biochemistry profile in CHI is that of hypoketonaemic, hypofattyacidaemic hypoglycaemia with a detectable insulin concentration. The severity of hypoglycaemia has no correlation with the level of serum insulin concentration (127). A high c-peptide concentration may also help to establish the diagnosis. Other investigations that can support the diagnosis of CHI include an elevation of blood glucose concentration>1.5mmol/L following an intramuscular/intravenous dose of glucagon (127). A positive glycaemic response to subcutaneous dose of octreotide with decreased plasma concentration of insulin-like growth factor-binding protein 1(IGFBP-1) may also aid diagnosis in some cases as the high concentration of circulating insulin suppresses the transcription of IGFBP-1 gene (203-205).

Elevated plasma ammonia concentration in a patient with hyperinsulinism may suggest the possibility of HI/HA syndrome. However, some patients with HI/HA syndrome can have normal plasma ammonia concentration (164). Provocative testing using a protein/leucine load may be helpful to establish a diagnosis in patients with suspected HI/HA syndrome (164).

Elevated plasma hydroxybutyrylcarnitine and urinary 3-hydroxyglutarate in a patient with CHI may be suggestive of HADH deficiency (173). Patients with exercise induced hyperinsulinism will require a formal exercise or a pyruvate loading test to demonstrate hypoglycaemia.

### 3.8 MEDICAL MANAGEMENT OF CHI

The aim of treatment is to achieve and sustain normoglycaemia (blood glucose level of 3.5-6mmol/L). In neonates with CHI, a central venous access is often required to deliver a high concentration of intravenous glucose infusion. It is important to maintain orality with some oral feeds(alone or in combination with glucose polymer-Maxijul or Polycal) to avoid a disturbed feeding pattern that may develop as feed aversion in these babies (128).

#### 3.8.1 Glucagon

Infants with CHI can have extremely difficult venous access. In such situations, administration of intramuscular glucagon(0.5-1mg) can be a temporary measure to improve the blood glucose levels. This is followed by intravenous glucose infusion to prevent rebound hypoglycaemia. During the acute management of CHI, glucagon can be given either intravenously or by subcutaneous infusion to improve the blood glucose levels. Glucagon acts by promoting glycogenolysis and gluconeogenesis. It also has effect on ketogenesis and lipolysis.

### 3.8.2 Diazoxide

Diazoxide is the mainstay of medical treatment in hyperinsulinism and is usually effective in all forms of CHI except those caused by inactivating mutations in *ABCC8* and *KCNJ11* (129). Patients with activating mutations in *GCK* demonstrate a variable response to diazoxide (180). Patients with focal forms of hyperinsulinism do not generally respond to diazoxide treatment. Diazoxide is a KATP channel agonist that binds and opens the intact $K_{ATP}$ channels and reduces the insulin secretion. It is administered orally (5-15mg/kg/day) and the responsiveness is noted by normoglycaemia, age appropriate fasting tolerance with undetectable insulin at the end of the fast and feeding with normal volume and frequency (129). The main side effects are that of hypertrichosis and fluid retention, especially in the newborns. The use of diazoxide in conjunction with thiazide diuretic chlorothiazide (5-10mg/kg/day) reduces the side effect of fluid retention. The other side effects include leukopenia, hyperuricaemia, tachycardia and feeding problems.

Genetic analysis on patients who do not respond to the maximum dose of diazoxide, helps in the identification of those who may need $^{18}$F-DOPA-PET CT scan to search for a focal lesion. Patients with paternally inherited mutation in *ABCC8* and *KCNJ11* (or those with no mutations in these genes) potentially have focal disease (206). Patients with homozygous or compound heterozygous mutations in *ABCC8* and *KCNJ11* will have a diffuse disease and will need alternative treatment options (206).

### 3.8.3 Octreotide

Octreotide is a somatostatin that is used as a second line medical therapy in the management of CHI. It acts by activating the somatostatin receptor-2 and -5 and also by restricting the movement of calcium in the pancreatic β-cells. It is administered as a subcutaneous injection every 6-8 hours(5-30μg/kg/day). The use of octreotide is associated with tachyphylaxis requiring higher doses(desensitisation occurring after 2-3 doses) (207). Octreotide is used cautiously in neonates as life threatening necrotising enterocolitis can occur as an adverse side effect (208).

### 3.8.4 Newer Medical Therapies for CHI

The long acting somatostatin preparation, lanreotide has been reported to be successful in patients with CHI (209). Lanreotide is given subcutaneously as once monthly injection (210).

Exendin-(9-39) is a GLP-1 receptor(glucagon like peptide-1) anatagonist and has been shown to treat hypoglycaemia and improve the fasting glucose in mouse model of $K_{ATP}$ HI(SUR-$1^{-/-}$) when administered by chronic subcutaneous infusion(211). In a randomized, open-labelled pilot study involving human subjects, it was demonstrated that administration of exendin-(9-39) resulted in significantly higher blood glucose nadir levels when compared to placebo (212).

Recently, the use of immunosuppressive mammalian target of rapamycin inhibitor(mTOR), sirolimus, in four consecutive infants with diazoxide unresponsive HI resulted in improved glycaemia (213). However, long-term safety of sirolimus, in young infants with CHI, is not fully established.

### 3.9 SURGICAL MANAGEMENT OF CHI

The indications for surgery in patients with CHI include severe form of diffuse CHI unresponsive to medical therapy and those with focal disease. The patients with diffuse disease require near total pancreatectomy (214). This is associated with post-operative complications such as persisting hypoglycaemia requiring additional feeding, diazoxide or octreotide, high incidence of diabetes mellitus and exocrine pancreatic insufficiency. For the focal disease, localisation of the focal lesion by $^{18}$F-DOPA-PET/CT helps in excision of the focal adenomatous lesion (214, 215). The newer approach of laparoscopic pancreatectomy is associated with lesser complications and a faster recovery than open laparotomy (216).

### 3.10 AIMS OF THE PROJECT

Mutations in transcription factors such as *HESX1, PROP1, POU1F1, LHX3, LHX4, PITX1, PITX2, OTX2, SOX2* and *SOX3* have been associated with congenital hypopituitarism in mouse and humans. However, these mutations account only for a small proportion with the majority of patients having an unknown genetic cause for their condition.

Mutations in genes *ABCC8, KCNJ11, GLUD1, GCK, HADH, UCP2, HNF4A, HNF1A, MCT1, HK1* and *PGM1* have been associated with genetic forms of CHI. However, the genetic cause for many CHI patients (nearly 50%) remains elusive (217).

The aims of this project were:

1. To recruit patients with complex phenotypes such as congenital hypopituitarism, congenital hyperinsulinism and severe short stature with or without dysmorphism with no identified genetic etiology for detailed clinical and biochemical phenotyping.

2. To study these patients with whole-exome sequencing to identify potential novel genetic etiology and/or novel genetic pathways underlying their condition based on the available biological information.

3. To functionally characterize the identified mutation by appropriate laboratory techniques.

### 3.11 PATIENT RECRUITMENT

A cohort of 6 patients from 6 families were recruited into this project over a period of two years. All these patients were managed at Alder Hey Children's NHS Foundation Trust, Liverpool. Personal data (name, date of birth, gender and ethnic background) and detailed phenotypic and laboratory data were collected on these patients. The patients were identified by experienced Consultant Endocrinologists as likely to have a high chance of an underlying monogenic etiology for their endocrine problems. The recruitment of the patients and their families into the study and obtainment of informed and written consents were done by me. All the six recruited patients had microarray to look for copy number changes. Trio sequencing was performed on the affected patient along with both the biological parents where possible. In one of the patients (proband D), where it was not possible to obtain DNA sample from the biological father, sequencing was performed on the patient and the biological mother. Two of the six patients had CHI (proband A and proband C) and had molecular genetic testing done for genetic mutations in known CHI genes: *KCNJ11, ABCC8, GLUD1, GCK, HADH, HNF4A, INSR, SLC16A1, TRMT10A* and *HNF1A* at University of Exeter Medical School, Exeter and were negative for mutations in these genes associated with the clinical phenotype. The flowchart for patient recruitment is shown below in the figure 5.1. The summary of the clinical phenotypes of the recruited patients is shown in the table 5.1.

### 3.12 ETHICS

The study was given favourable ethical opinion by the North West - Liverpool Central Research Ethics Committee (REC Reference: 15/NW/0758) and site study approval was granted by the Clinical Research Business Unit at Alder Hey Children's NHS Foundation Trust, Liverpool, UK.

**Figure 3.4:** Flowchart of Patient Recruitment

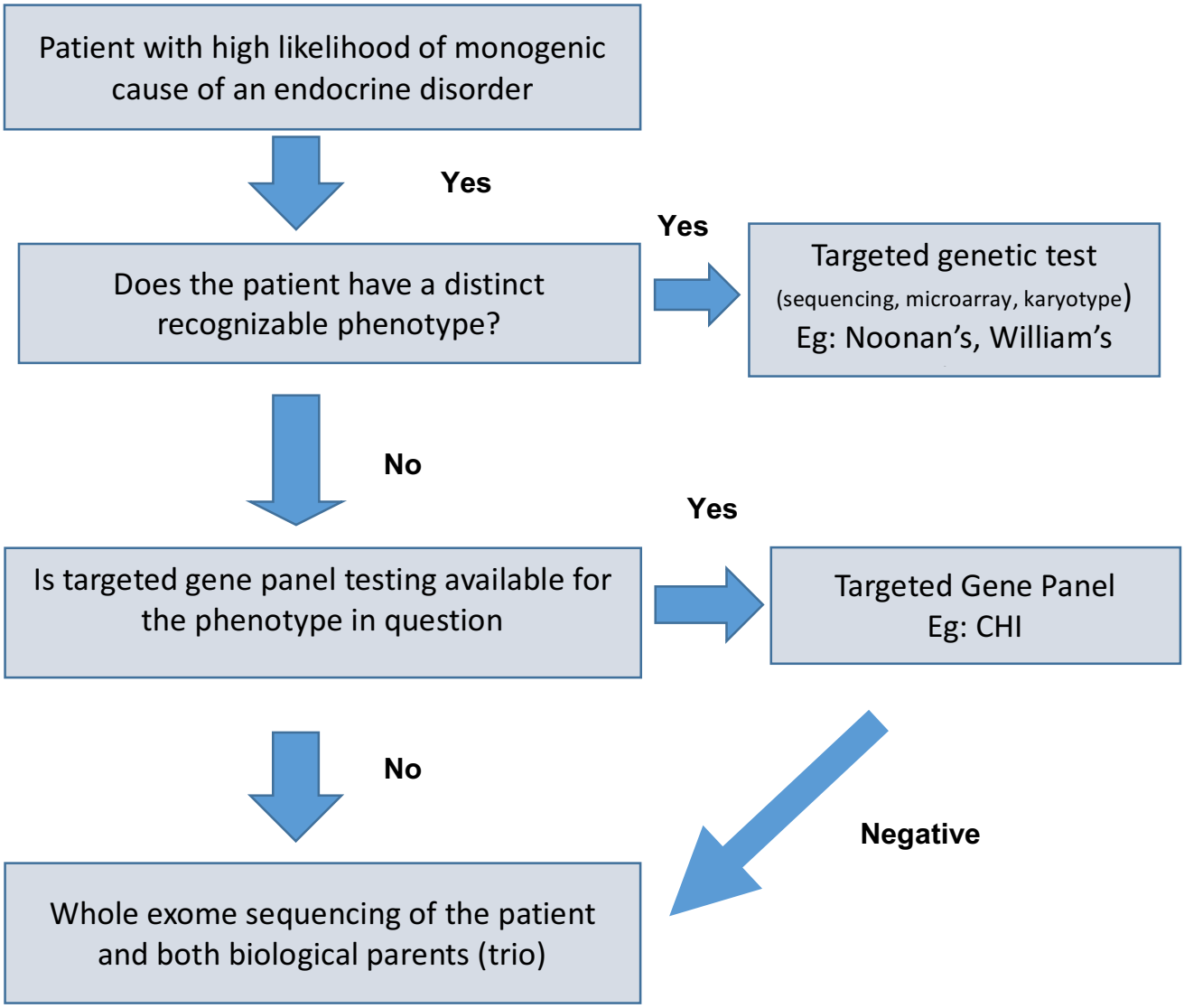

**Table 3.1:** Summary of the Recruited Patient Phenotypes

| PROBANDS | PHENOTYPES |
|---|---|
| **A** | Persistent mutation negative congenital hyperinsulinism, hypopituitarism with GH,ACTH,TSH deficiency, coloboma, pulmonary stenosis and developmental delay |
| **B** | Primary IGF1 deficiency, craniosynostosis<br>severe short stature, dysmorphic features, complex learning problems |
| **C** | Persistent mutation negative congenital hyperinsulinism |
| **D** | Severe short stature, recurrent hypoglycaemia ,congenital Deafness, posterior Cloaca, growth Hormone deficiency, cardiac defects, facial dysmorphism, hypermobile joints |
| **E** | Severe short stature, low IGF1 |
| **F** | Persistent Hypercalcemia, high PTH(mutations negative for FHH and primary hyperparathyroidism), glomerulonephritis |

# CHAPTER 4

# GENERAL METHODS

## 4.1 SUMMARY OF CHAPTER 4

In chapter 4, various techniques used in the general methodology for this project such as DNA extraction and quantification, whole-exome sequencing, bioinformatics pipeline, and variant filtering are discussed. The DNA extraction was performed by me at the institute of child health laboratory in Liverpool. Whole exome sequencing and bioinformatics were performed at the Centre for Genomic Research, University of Liverpool. Analysis of the VCF (variant calling files) data, variant filtering and segregation of the likely pathogenic variants were performed by me by using the ingenuity variant analysis software (QIAGEN Bioinformatics).

## 4.2 GENOMIC DNA EXTRACTION FROM BLOOD

DNA was obtained from blood samples of the child and both the biological parents (trio) using the QIAmp DNA blood Midi Kit (Qiagen, Hilden, Germany) as per the manufacturer's instructions.

The steps are described briefly:

1. One ml of whole blood was added to 100µl of QIAGEN protease (proteinase K) and 1.2ml of Buffer AL (Lysis buffer).

2. The mixture was mixed thoroughly to yield a homogenous solution and incubated at 70 degrees Celsius for 10 minutes.

3. After 10 minutes of incubation, 1ml of 96-100% ethanol was added to the sample and mixed thoroughly to yield a homogeneous solution.

4. This solution was transferred to QIAmp Midi column and centrifuged at 3000 rpm for 3 minutes.

5. The filtrate was discarded and 2 ml of Buffer AW1(wash buffer 1) was added to the QIAmp Midi column and centrifuged at 5000 rpm for 1 minute followed by the addition of 2 ml Buffer AW2(wash buffer 2) and centrifuging the mixture at 5000 rpm for 15 minutes.

6. After discarding the filtrate, the purified genomic DNA was eluted from the QIAmp midi spin column and 200 µl of Buffer AE (elution buffer) was added and centrifuged for 2 minutes at 8000 rpm. The extracted DNA was stored in Buffer AE at -30 degrees Celsius for long term use.

### 4.2.1 Quantification of DNA

The quantity of the DNA was estimated by using NanoDrop Nucleic Acid Quantification method (Thermo Fisher Scientific). The NanoDrop instruments utilize a patented sample retention system that allows the quantification of nucleic acids from 1–2µL samples.

Using the 'NanoDrop' 2000c Spectrophotometer, the DNA concentration was measured as follows:

1. The NanoDrop sensor was blanked by using blanking solution-distilled water, 1.5 µL and a routine wavelength verification check was completed with the help of the inbuilt computer software.

2. Following this, 1.5 µL of the DNA sample was added onto the NanoDrop sensor and the concentration was analysed using the software.

3. The 260/280 calculation ratio gives a measurement of output of wavelength vs absorbance. A ratio of >1.8 was generally accepted as pure for DNA. The DNA concentration was measured as ng/ µL.

### 4.2.2 DNA Quality Control: Bioanalyzer or Fragment analyzer

**Principle of Fragment Analyzer**

Further quality control of the extracted DNA was performed using the Fragment Analyzer™ system. The instrument consists of a multiplex of capillary electrophoresis and is used to perform high throughput, automated separation and quantification of nucleic acids. The separation of DNA is through the application of an electric field through an array of fused silica capillaries filled with conductive gel. With the application of high voltage, the DNA molecules migrates through the gel in relation to their length or size, with the smaller fragments migrating faster than the larger fragments (Figure 4.1). When the nucleic acid molecules migrate and reach the end of the capillary, detection is facilitated by fluorescence of a sensitive dye present in the gel matrix. The fluorescence can be monitored using the relative fluorescence unit (RFU) intensity as a function of time during the capillary electrophoresis separation. This information can be used to produce digital electropherogram traces representative of the DNA content of the entire samples (Figure 4.2).

**Figure 4.1:** Gel image of the DNA samples representing the relative sizes of the DNA molecules against the standard ladder

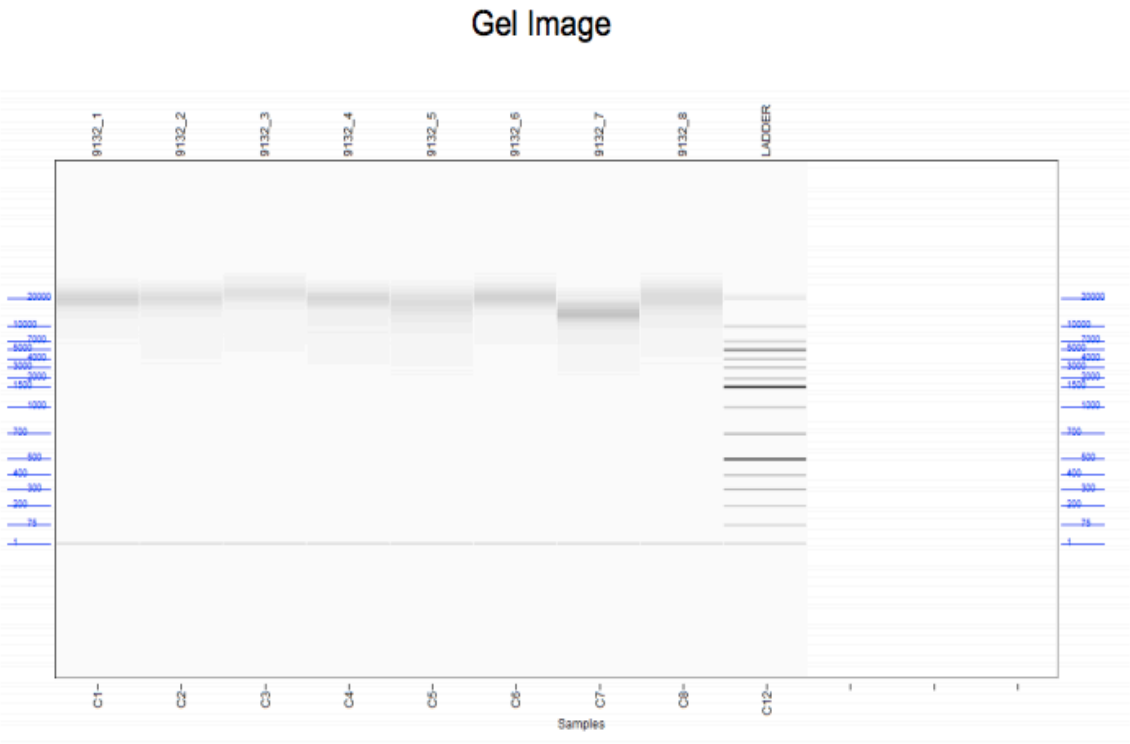

**Figure 4.2:** Electropherogram Traces showing the relative fluorescence unit of various genomic DNA samples(peaks) indicating the integrity of the samples

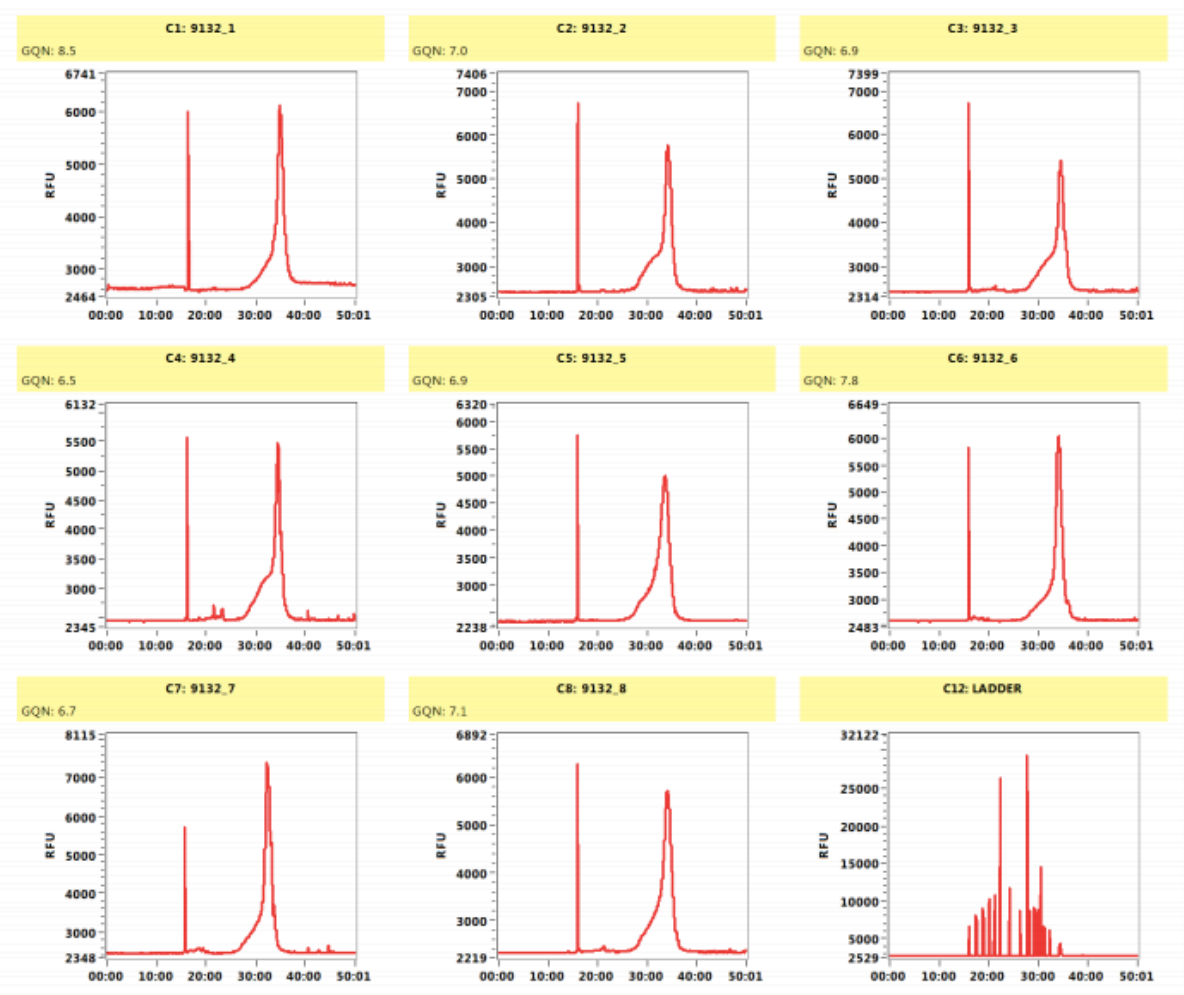

## 4.3 WHOLE EXOME SEQUENCING

### 4.3.1 Workflow for Exome Sequencing

The basic steps for exome sequencing include the following:

1 Sample preparation

2. Hybridization and capture

3. Indexing and processing for multiplexed sequencing

4. Sequencing

#### 4.3.1.1 Sample Preparation

Samples were sheared with the Picoruptor to a size of approximately 150-200 bp and the samples were cleaned with 1.8x AMPure beads (Agencourt). The target size of the DNA fragments (150-200 bp) was confirmed using the 2100 Bioanalyzer. The ends of the sheared DNA were repaired with T4 DNA Polymerase and Klenow enzyme and further purified by using AMPure XP beads (Figure 4.3). This was followed by addition of ‘A’ bases to the 3´ ends of the DNA fragments and purified again by AMPure XP beads. The DNA fragments with 3´ overhanging ‘A’ bases were ligated by using T4DNA ligase buffer and SureSelect Adaptor Oligo Mix. The sample was further purified using AMPure XP beads. The adaptor-ligated library was amplified by 5 rounds of PCR using Herculase II fusion DNA polymerase and again purified with AMPure XP beads. The libraries were checked on an Agilent HS 2100 Bioanalyser chip for fragment size peak of approximately 225 to 275 bp and quantified by Qubit assay. 750 ng of pre-capture library in a volume of 3.4µL (initial concentration of 221 ng/ µL was used for the hybridization reaction.

**Figure 4.3:** Sample preparation for Exome sequencing showing genomic DNA shearing, end repair of DNA fragments, addition of 3' A overhangs, adapter ligation and PCR amplification [adapted from Arya, VB; (2015) Understanding the novel genetic mechanisms of congenital hyperinsulinaemic hypoglycaemia. Doctoral thesis, UCL (University College London].

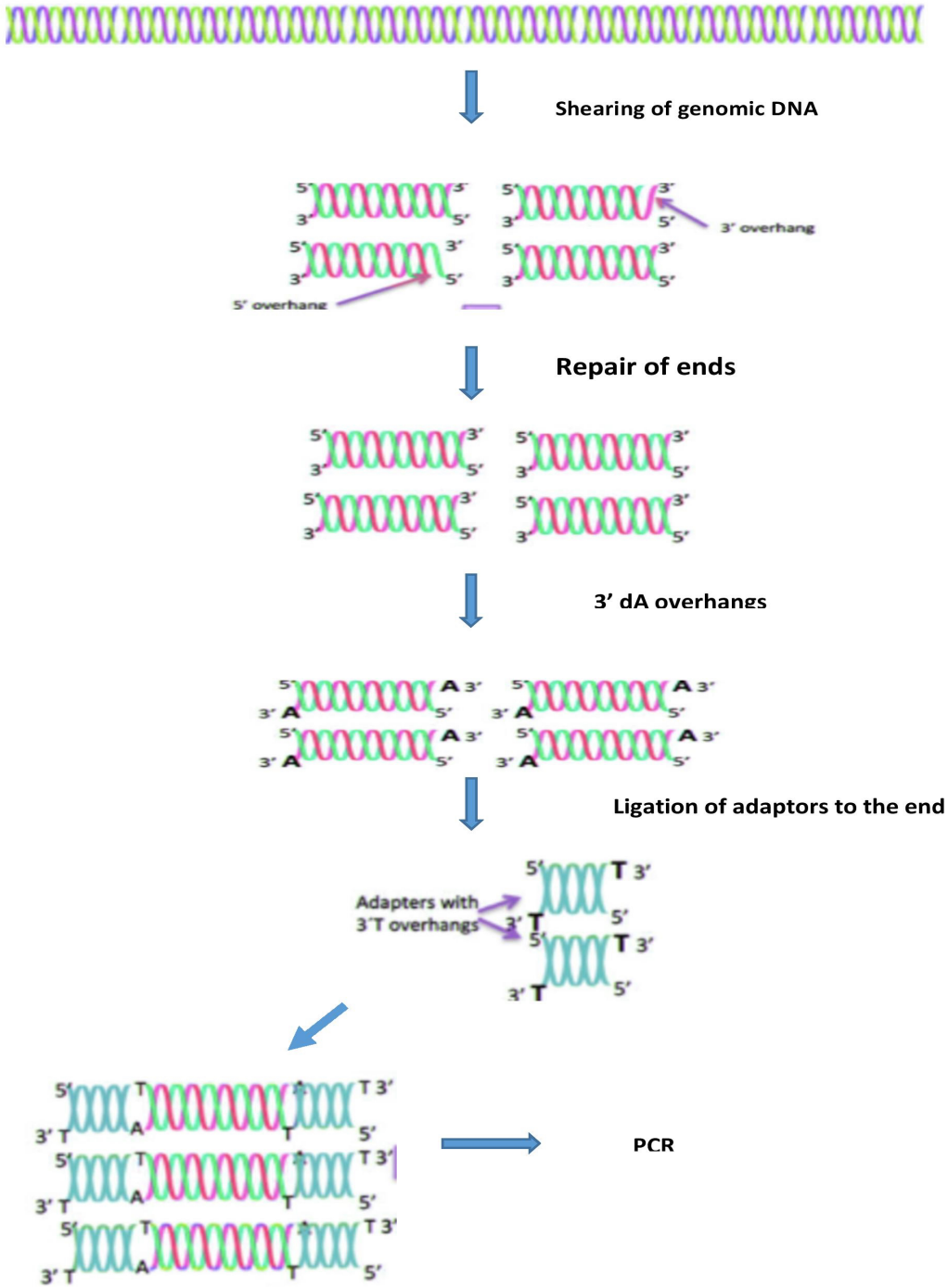

#### 4.3.1.2 Hybridization

The pre-capture libraries (genomic DNA) obtained in the previous step were then mixed with SureSelect hybridisation mix (Biotinylated RNA Library Baits) along with hybridization buffers and incubated for 24 hours at 65°C. RNA Baits will hybridize with the complementary DNA fragments present in the genomic DNA sample.

Following this, the samples (hybridized DNA) were mixed with washed streptavidin beads (Dynabeads MyOne Streptavidin T10). Streptavidin has an extraordinarily high affinity for biotin. The captured products were washed according to the protocol attached to the beads and the RNA is digested. (Figure 4.4)

#### 4.3.1.3 Indexing and Sample Processing for Multiplexed Sequencing

The SureSelect-enriched captured DNA libraries from the previous step are PCR amplified in 10 cycles of PCR reactions with 8 bp indexing primers (forward and reverse) using Herculase II fusion DNA polymerase with Herculase II reaction buffer. The amplified post-capture libraries were purified using AMPure XP beads. The quantity and quality of the post-capture indexed libraries were assessed by Agilent 2100 Bioanalyzer for the peak DNA fragment size positioned between 250 and 350 bp. Following this, the quantity of each index-tagged library was assessed by qPCR using the Agilent QPCR NGS library quantification kit from Kapa on a Roche Light Cycler LC480II according to manufacturer's instructions. The template DNA was denatured according to the protocol described in the Illumina cBot User guide and loaded at 300 pM concentrations.

#### 4.3.1.4 Sequencing

The sequencing was carried out on one lane of an Illumina HiSeq4000 at 2x150 bp paired-end sequencing with v1 chemistry. The read files (Fastq) were generated from the sequencing platform via the manufacturer's proprietary software.

**Figure 4.4:** Target enrichment using SureSelect [adapted from Agilent SureSelectXT Target enrichment for Illumina user guide]

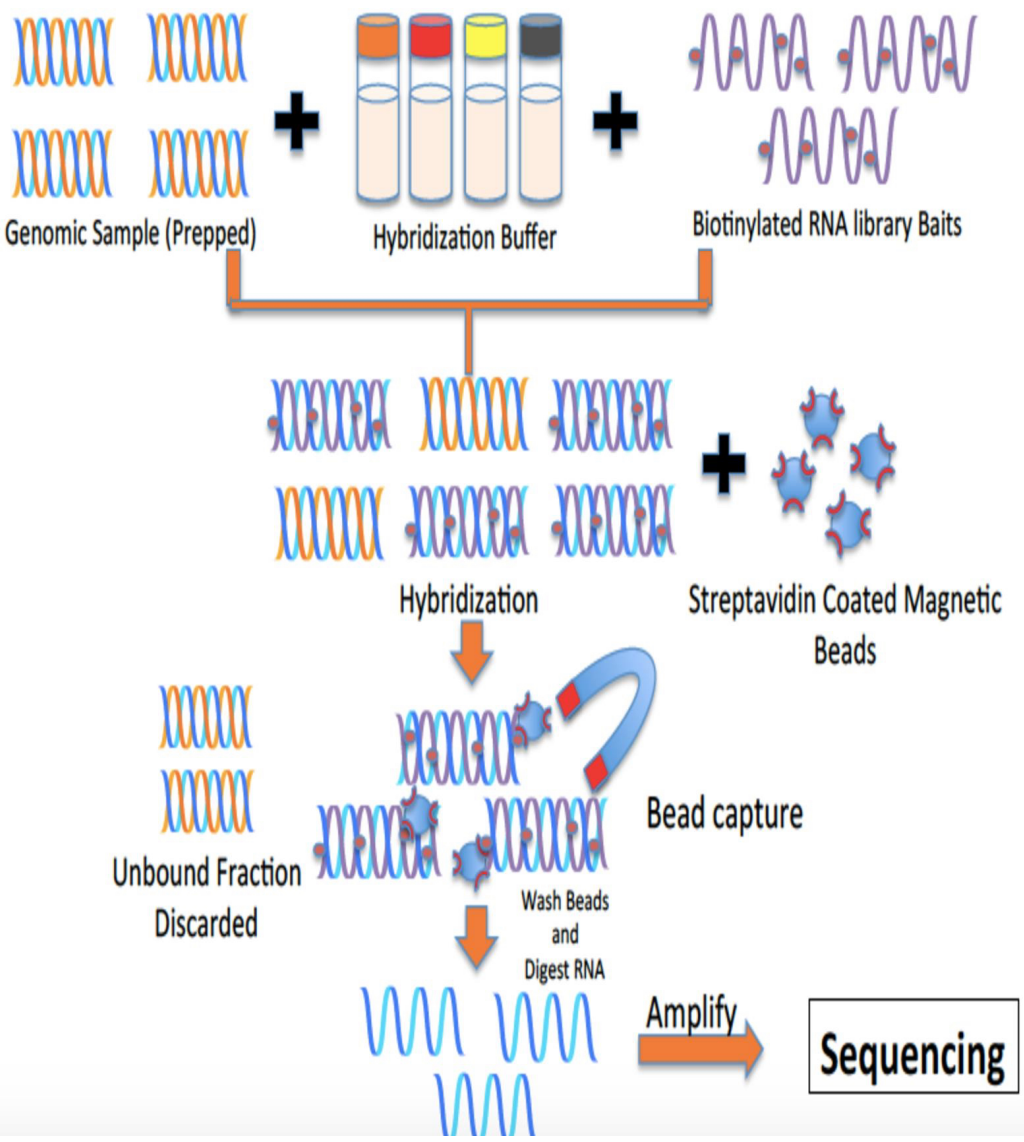

## 4.4 BIOINFORMATICS

The bioinformatics pipeline briefly consists of the following steps:

1. Processing and quality assessment of the sequence data
2. Alignment of reads to the reference sequence
3. Variant detection

### 4.4.1 Processing and Quality Assessment of Sequence Data

Initial processing and quality assessment of the sequence data was performed using an in-house pipeline (developed by Dr Richard Gregory). Briefly, basecalling and de-multiplexing of indexed reads was performed by CASAVA version 1.8.2 (Illumina) to produce samples in FASTQ format. The raw FASTQ files were trimmed to remove Illumina adapter sequences using Cutadapt version 1.2.1. The reads were further trimmed to remove low quality bases, with a minimum window quality score of 20. The raw trimmed sequence data are shown in table 4.1. The reads shorter than 10 bp were removed. The forward reads are indicated as R1, the reverse reads as R2 and the unpaired reads as R0. Table 4.2 summarises the read counts before and after adapter and quality trimming. Figure 4.5 shows the read length distributions after adapter and quality trimming. Note that R0 (unpaired) reads are trimmed more than paired reads as they more often represent poor quality sequence. Later analysis uses only R1 and R2 reads, which show a very little adapter/quality trimming.

All trimmed read data, as well as detailed statistics on the read trimming are available from the following URLs:

http://cgr.liv.ac.uk/illum/LIMS9132_80e653e1bc84f8a9

http://www.cgr.liv.ac.uk/illum/LIMS10697Results_8399f2b3f8c45af5/

**Table 4.1:** Summary of raw and trimmed sequence data of DNA samples

| Sample | Family ID | Untrimmed reads | Trimmed reads | R1/R2 pairs | R0 reads |
|---|---|---|---|---|---|
| Sample_1-L1512928 | I | 107,468,390 | 106,511,341 (99.11) | 52,778,930 | 953,481 (0.90) |
| Sample_2-L1512929 | I | 70,545,702 | 69,913,097 (99.10) | 34,641,451 | 630,195 (0.90) |
| Sample_3-L1512930 | I | 98,535,662 | 97,907,497 (99.36) | 48,640,949 | 625,599 (0.64) |
| Sample_4-L1513634 | G | 84,073,414 | 83,435,096 (99.24) | 41,399,781 | 635,534 (0.76) |
| Sample_5-L1513636 | G | 90,750,270 | 89,878,881 (99.04) | 44,505,794 | 867,293 (0.96) |
| Sample_6-L1514366 | D | 83,142,054 | 82,565,645 (99.31) | 40,995,695 | 574,255 (0.70) |
| Sample_7-L1514368 | D | 95,567,088 | 94,772,605 (99.17) | 46,990,660 | 791,285 (0.83) |
| Sample_8-L1514530 | D | 86,488,340 | 85,854,636 (99.27) | 42,611,693 | 631,250 (0.74) |

| Sample | Family ID | Untrimmed reads | TrimmedReadNumber (% of raw) | TrimmedPairNumber | TrimmedSingletonNumber (% of trimmed) |
|---|---|---|---|---|---|
| 1-L1605487 | 1 | 83,516,670 | 82,843,473 (99.19) | 41,086,569 | 670,335 (0.81) |
| 2-L1607210 | 1 | 67,344,304 | 66,912,873 (99.36) | 33,241,725 | 429,423 (0.64) |
| 3-L1607170 | 1 | 88,844,076 | 88,431,351 (99.54) | 44,010,365 | 410,621 (0.46) |
| 4-L1601222 | 3 | 67,042,998 | 66,455,447 (99.12) | 32,935,078 | 585,291 (0.88) |
| 5-L1601227 | 3 | 82,715,640 | 82,186,985 (99.36) | 40,830,398 | 526,189 (0.64) |
| 6-L1601228 | 3 | 82,077,336 | 81,560,684 (99.37) | 40,523,192 | 514,300 (0.63) |
| 7-L1601229 | 2 | 76,448,998 | 75,952,316 (99.35) | 37,728,954 | 494,408 (0.65) |
| 8-L1601236 | 2 | 68,371,366 | 68,014,879 (99.48) | 33,829,986 | 354,907 (0.52) |
| 9-L1601235 | 2 | 89,328,150 | 88,655,857 (99.25) | 43,993,188 | 669,481 (0.76) |

**Figure 4.5:** Read length distributions of samples after adapter and quality trimming

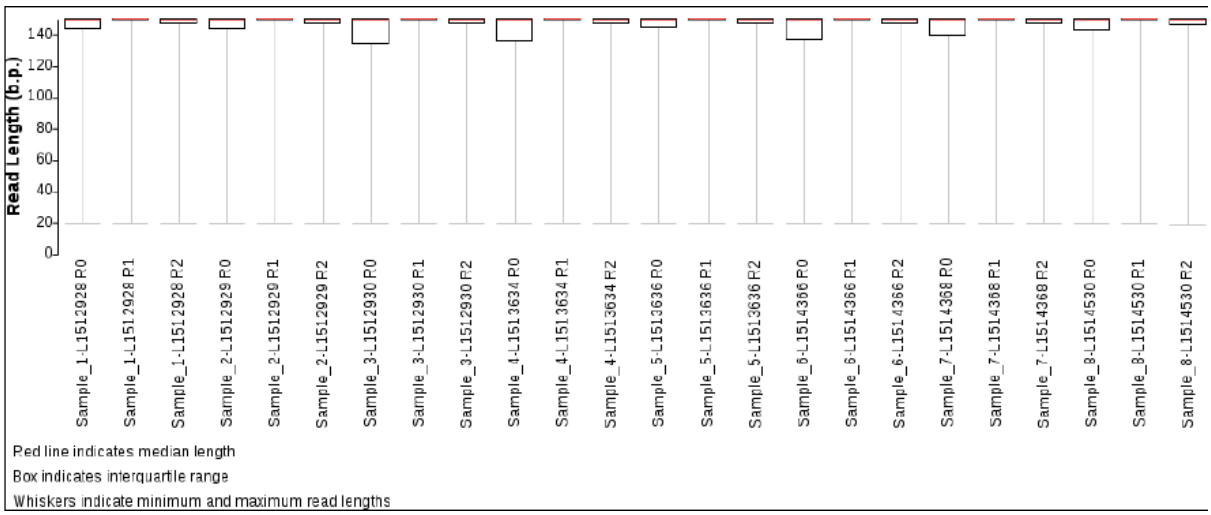

### 4.4.2 Alignment of Reads to the Reference Genome

R1/R2 read pairs were aligned to the human genome reference with decoy sequences (ftp.broadinstitute.org/bundle/2.8/b37/human_g1k_v37_decoy.fasta). This comprises the GRCh37 primary assembly (chromosomal plus unlocalised and unplaced contigs), the rCRS mitochondrial sequence (AC:NC_012920), Human herpesvirus 4 type 1(AC:NC_007605) and the concatenated decoy sequences. Reads were mapped to the reference sequences using BWA mem version 0.7.5a (218) with default parameters. To retain only confidently aligned reads, alignments were filtered to remove reads with a mapping quality lower than 10, which equates to a 10% chance that the read was derived from another genomic location. Misalignment caused by small insertions / deletions (indels) can lead to false SNP calls. To avoid this, the mapped reads were locally re-aligned to improve the alignments around small insertions/deletions (indels) using the Genome Analysis Tool Kit (GATK) version 2.1.13 (219, 220). Duplicate reads arising from PCR amplification can bias variant calling. To avoid this, read duplicates were identified and filtered to retain only a single representative, using the Picard “MarkDuplicates” tool, version 1.85 (http://picard.sourceforge.net/)

The quality scores assigned to the individual base calls in each sequence read influence the variant calling algorithms. The scores represent the per-base estimates of error emitted by the sequencing machines which are subject to various sources of systematic technical error, leading to over- or under-estimated base quality scores in the data (https://gatkforums.broadinstitute.org/gatk/categories/methods). Hence, base quality score recalibration (BQSR) was applied for all the alignment files. BQSR is a module of GATK that applies machine learning to model these errors empirically and adjust the quality scores accordingly. BQSR firstly builds a model of covariation based

on the data and a set of known variants (i.e. dbSNP), then it adjusts the base quality scores in the data based on the model. This will create more accurate base qualities, which in turn improves the accuracy of our variant calls.

**Table 4.2:** Summary of sequence alignments (before and after filtering to remove reads with low mapping quality and redundant duplicate reads) for various DNA samples with mean depth of coverage

| Sample | Reads to align [1] | Aligned reads after filtering (%)[2] | Number of bases in the capture regions with coverage more than 0(%)[3] | Mean Depth of Coverage for the bases with coverage more than 0 |
|---|---|---|---|---|
| Sample_1-L1512928 | 105,557,860 | 91,553,749(86.73%) | 49,901,837(99.03%) | 112.24x |
| Sample_2-L1512929 | 69,282,902 | 61,166,825(88.29%) | 49,901,223(99.03%) | 157.05x |
| Sample_3-L1512930 | 97,281,898 | 83,494,081(85.83%) | 50,090,890(99.41%) | 133.18x |
| Sample_4-L1513634 | 82,799,562 | 73,120,995(88.31%) | 49,905,274(99.04%) | 142.12x |
| Sample_5-L1513636 | 89,011,588 | 78,287,620(87.95%) | 49,917,767(99.06%) | 132.34x |
| Sample_6-L1514366 | 81,991,390 | 71,161,089(86.79%) | 50,101,073(99.43%) | 149.89x |
| Sample_7-L1514368 | 93,981,320 | 81,144,524(86.34%) | 49,912,857(99.05%) | 141.52x |
| Sample_8-L1514530 | 85,223,386 | 75,583,985(88.69%) | 50,095,529(99.41%) | 112.24x |

| Sample | Reads to align [1] | Aligned reads after filtering (%)[2] | Number of bases in the capture regions with coverage more than 0(%)[3] | Mean Depth of Coverage for the bases with coverage more than 0 |
|---|---|---|---|---|
| 1-L1605487 | 82,173,138 | 70,401,016 (85.67%) | 50,082,722 (99.39%) | 132.08x |
| 2-L1607210 | 66,483,450 | 57,871,298 (87.05%) | 50,061,715 (99.35%) | 112.12x |
| 3-L1607170 | 88,020,730 | 75,281,074 (85.53%) | 49,867,887 (98.96%) | 149.07x |
| 4-L1601222 | 65,870,156 | 58,051,049 (88.13%) | 50,084,049 (99.39%) | 108.11x |
| 5-L1601227 | 81,660,796 | 71,780,887 (87.90%) | 49,868,932 (98.96%) | 137.05x |
| 6-L1601228 | 81,046,384 | 69,866,457 (86.21%) | 50,094,093 (99.41%) | 132.60x |
| 7-L1601229 | 75,457,908 | 64,910,531 (86.02%) | 50,084,438 (99.39%) | 123.77x |
| 8-L1601236 | 67,659,972 | 59,519,122 (87.97%) | 49,851,203 (98.93%) | 116.60x |
| 9-L1601235 | 87,986,376 | 76,741,923 (87.22%) | 50,087,380 (99.40%) | 148.42x |

[1]Sum of all R1 and R2 reads used in the alignment

[2]Reads that align to the reference genome, before removing low mapping quality reads and redundant duplicate reads (% of all reads used in alignment)

[3]The size of the total capture regions is 50,390,601bp

### 4.4.3 Variant detection

Variant detection was performed using the GATK package. Single nucleotide polymorphisms (SNPs) and small insertions/deletions (INDELs) were identified in the same analysis step. In order to carry out the variants recalibration, which assigns a well-calibrated probability to each variant call in a call set, the VQSR (Variant Quality Recalibration Score) module in GATK was calibrated by combining the variants found in a random selection of 22 samples from the 1000 genome UK cohort along with the variants from the 8 samples in this project. Variants were outputted, and annotated using SnpEff version 3.2a (221). Finally, the phaseByTransmission module in GATK package was used for the trio analyses for the samples from the same family.

### 4.4.4 Identifying Causal Alleles

Whole exome sequencing on an average identifies ~24,000 single nucleotide variants (SNVs) in African American samples and ~20,000 in European American samples, among which 95% are known polymorphisms in human population(3). One of the main challenges in whole exome sequencing is the narrowing down and filtering of disease-related alleles from a huge background of polymorphisms that are non-pathogenic and errors related to sequencing.

The strategies for filtering the exome sequencing data and narrowing down to identify the alleles segregating with the phenotype depend on a number of factors such as the mode of inheritance of a trait; the pedigree or population structure; whether a phenotype arises owing to *de novo* or inherited variants; and the extent of locus heterogeneity for a trait(3).

## 4.5 APPROACHES TOWARDS IDENTIFYING CAUSAL ALLELES

### 4.5.1 Discrete Filtering:

The variants are filtered against polymorphisms available in publicly available databases such as dbSNP, 1000 Genomes Project, Exome Aggregation Consortium(ExAC) and those found in unaffected individuals such as unaffected biological parents or siblings. By this approach the non-causative polymorphisms are eliminated and the novel candidate genes are filtered. This is especially important because the number of candidate genes are drastically reduced because only a small fraction (~ 2% on average) of the single nucleotide variants (SNVs) identified in an individual by exome sequencing are novel(3). The assumption in this approach that the filter set may not contain alleles from individuals with the phenotype can be problematic for two reasons. First, dbSNP is 'contaminated' with a small but appreciable number of pathogenic alleles (3). Second, as the number of sequenced exomes and genomes increases, the filtering of observed alleles in dbSNP should take into account the minor allele frequency (MAF) as otherwise truly pathogenic alleles that are segregating in the general population at low but appreciable frequencies will be eliminated (3). This risk is especially relevant for recessive disorders, in which carrier status (heterozygous) will not result in a phenotype but will be present in the control population at a low frequency. Analysis of recessive disorders in which the maximum MAF is set at 1% is still well powered(3).

A lower MAF cut-off of 0.1% is helpful for dominant disorders, as the estimated prevalence of the disorder (generally well below 0.1%) provides an upper bound on the MAF(3). Additionally, the greater the number of novel variants with lower MAFs

that are present in a sample population, the more difficult it will be to home in on the causal gene (or genes) (6).

### 4.5.2 Stratifying the Candidate Genes After Discrete Filtering

1. After filtering for polymorphisms against the public databases mentioned above, further stratification was done based on the predicted impact on the protein function. Frameshift mutations, nonsense mutations and splice-site mutations which disrupt the canonical splice sites are more likely to be causal as compared to missense variants.
2. The stratification was further performed based on the available biological or functional information about a gene. This involves alleles with an existing or predicted role in a biological pathway or interacting with genes known to cause the phenotype.
3. Assessing evolutionary conservation among different species was also used to stratify the candidate genes. The mutations occurring in the sequences or amino acid residues that show high conservation among different species are likely to be pathogenic.
4. *In silico* tools such as SIFT, PolyPhen and Mutation Taster were used to further stratify the pathogenicity of the non-synonymous alleles.

### 4.5.3 *In Silico* Tools: SIFT and PolyPhen

Sorting intolerant from tolerant (SIFT) and polymorphism phenotyping (PolyPhen) are freely available as Web-based servers(222-224). SIFT and PolyPhen predict if the missense mutation is likely to be deleterious to the protein function by the use of sequence homology of related proteins and the degree of conservation of the affected base throughout evolution. PolyPhen uses annotated UniProt entries to predict

whether the amino acid substitution occurs within an important structural or functional site of the protein, for example, active or binding sites, and residues involved in disulphide bond formation(223). The predictive value of PolyPhen will therefore be reliant on the protein of interest having (i) a known, annotated crystal structure or (ii) the presence of a modelled protein of sufficient similarity in the UniProt database(225).

### 4.5.4 Pedigree Information

For Mendelian phenotypes, the pedigree information can be used to substantially narrow the genomic search space for candidate causal alleles. For identifying *de novo* coding mutations, an approach that involves sequencing of parent-child trios(Figure 4.6) is extremely efficient as it is highly unlikely that the proband will have multiple de novo events occurring within a specific gene (or within a gene family or pathway) (226, 227).

**Figure 4.6:** Parent-child trios for identifying *de novo* mutations

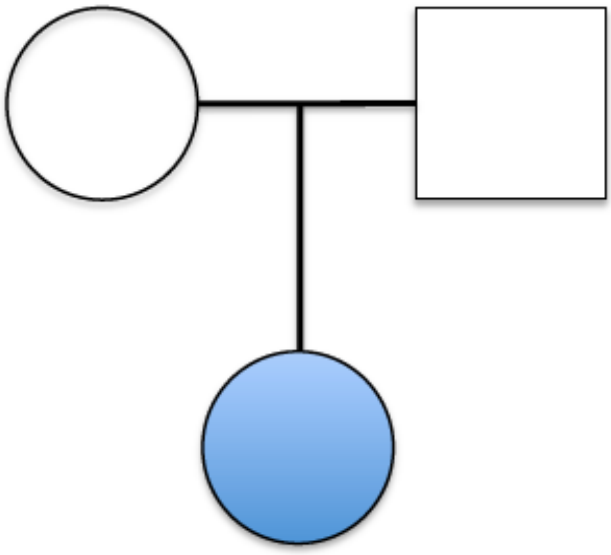

### 4.5.5 Technical and Analytical Limitations of Exome Sequencing:

Discrete filtering of the variants obtained from exome sequencing has been very successful in the identification of a novel disease gene(228-231). However, there are associated technical and analytical limitations that might hamper the process. This might either be due to inadequate capture of the exome which may contain part or all of the causative gene or inadequate depth of sequencing of the region that contains a causal variant (for example, because of poor capture or poor sequencing) (6).

It is also possible that due to the presence of small and complex indels, the causal variant may have been covered but not called(3). Genetic heterogeneity limits the power of discrete filtering. For example, if the disease is caused by mutations in a number of different genes (genetic heterogeneity), more than one gene in the sample population will have disease causing alleles (3).

# CHAPTER 5

# CLINICAL PHENOTYPE AND WHOLE EXOME SEQUENCING RESULTS (FAMILY A)

## 5.1 SUMMARY OF CHAPTER 5

Chapter 5 begins with the introduction of family A with a detailed description of the clinical phenotype and the whole exome sequencing results of proband A.

## 5.2 CLINICAL INFORMATION (PROBAND A)

A 5-year-old girl (Proband A), was born to non-consanguineous Caucasian British parents at 42 weeks' gestation with a birth weight of 4.185 Kg (+1.72 SDS). The pregnancy was normal and the 20-week antenatal scan showed polyhydramnios. The delivery was complicated by shoulder dystocia, needing resuscitation.

She was found to be persistently hypoglycaemic (glucose<2.6mmol/L) requiring a total glucose load of 25 mg/kg/min (normal: 4-6 mg/kg/min) to maintain normoglycaemia (plasma glucose>3.5mmol/L). She had low free thyroxine (FT4) (5.3 pmol/L) and suppressed thyroid-stimulating hormone (TSH) (<0.03 mu/L) that persisted even after the phase of acute severe illness. She also had an undetectable adrenocorticotropic hormone (ACTH) (<1.1 pmol/L) with no cortisol response to synacthen stimulation (peak cortisol to synacthen <50 nmol/L). Hydrocortisone replacement was commenced followed by levothyroxine therapy.

The MRI scan of the brain showed a hypoplastic anterior pituitary, absent posterior pituitary, interrupted pituitary stalk and a thin corpus callosum (Figure 5.2). The hypoglycaemia screen showed an inappropriately high plasma insulin (200 pmol/L) and c-peptide (1500 pmol/L) with suppressed plasma free fatty acid (<100 µmol/L) and beta hydroxyl butyrate (<100 µmol/L) during hypoglycaemia (plasma blood glucose: 1.2mmol/L) confirming the diagnosis of CHI.

A trial of diazoxide (5 mg/kg/day) with chlorothiazide resulted in a significant fluid retention. Commencement of octreotide (10 mcg/kg/day) caused a derangement of liver enzymes and therefore had to be discontinued after which the liver enzymes returned to normal plasma levels. She developed a significant feed intolerance due to severe gastroesophageal reflux which persisted despite maximum medical treatment.

A gastro-jejonostomy tube was inserted to support feeding. Normoglycaemia was maintained by continuous feed via the gastro-jejonostomy tube. Genetic analysis performed at the University of Exeter Medical School, Exeter was negative for *ABCC8, KCNJ11, HNF4A* and *GCK* mutations. The 18F-DOPA PET-CT scan of the pancreas suggested a diffuse pancreatic lesion.

**Figure 5.1:** Sagittal view of the MRI scan of the brain: The normal pituitary gland cannot be identified, the sella turcica is shallow and poorly defined with possibly a very hypoplastic anterior pituitary gland (arrowhead) Also, there is no evidence of the normal high signal of the posterior pituitary. There is a very short and thin pituitary stalk in its superior third (arrow) which is suggestive of an interrupted pituitary stalk. The corpus callosum is also noted to be thin (arrowhead)

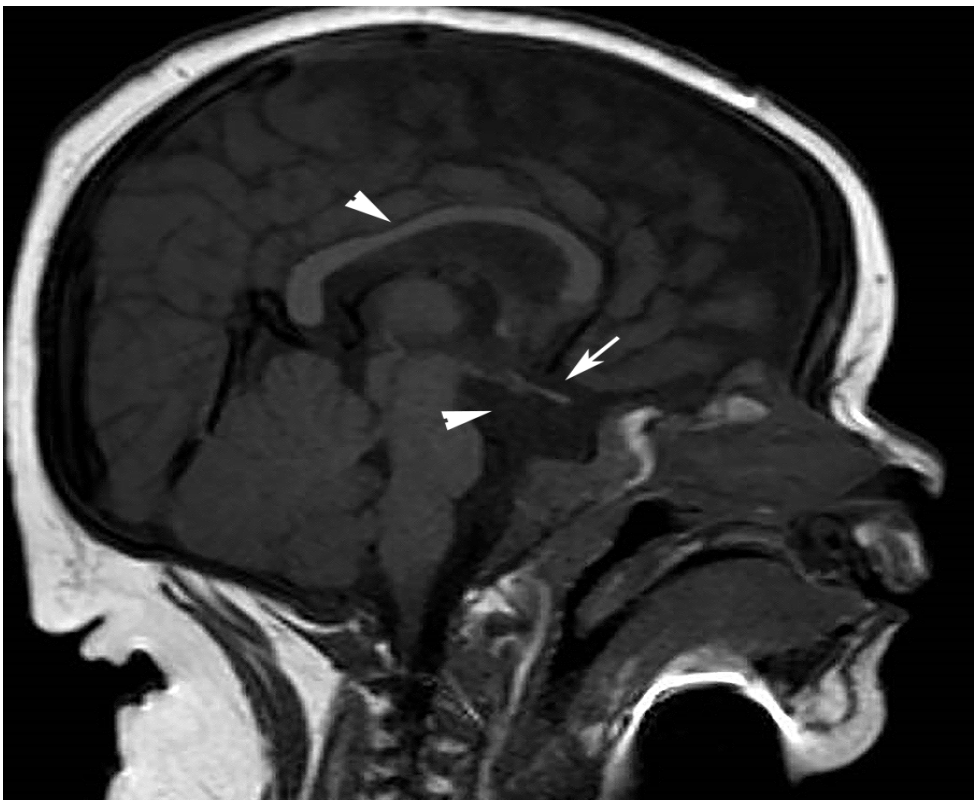

The facial dysmorphic features comprise of a single median maxillary central (SMMC) incisor, congenital nasal pyriform aperture stenosis (CNPAS), which was conservatively managed, and a left choroidal coloboma. She does not have any vision abnormalities. The cardiac echocardiogram revealed pulmonary stenosis which required balloon dilatation. She had a persistent oxygen requirement of unknown etiology (negative for respiratory infections, normal chest imaging and bronchoscopy) from birth, which gradually resolved at 5 months of age.

At 1.5 years of age she was diagnosed with growth hormone (GH) deficiency (height<3 SDS, IGF1<3.3 nmol/L and a peak GH of 1.1 µg/L (normal>7 µg/L) to arginine stimulation) and was commenced on rGH (recombinant GH) therapy. She demonstrated a good response to treatment with rGH (25 mcg/kg/day) with an improvement in the height velocity (Figure 5.3). She developed persistently elevated liver transaminases when she was 3 years old, with a negative autoimmune hepatitis and infection screen. The liver biopsy showed dense chronic inflammation with portal-portal bridging fibrosis. The clinical features are summarised in the table 5.2.

She is currently 5 years old, with persistent CHI, motor, speech and developmental delay and continues to be on rGH, levothyroxine and hydrocortisone replacements. She has shown response to the reintroduction of diazoxide (5 mg/kg/day) without any features of fluid retention, which has enabled her to come off her continuous feeds for 6 hours.

**Figure 5.2:** The patient's linear growth curve compared with British contemporary references. Recombinant growth hormone (25 mcg/kg/day) was started at 1.5 years of age when the linear height was -3SDS. A good response to the GH treatment was seen subsequently with an improvement in the height SDS

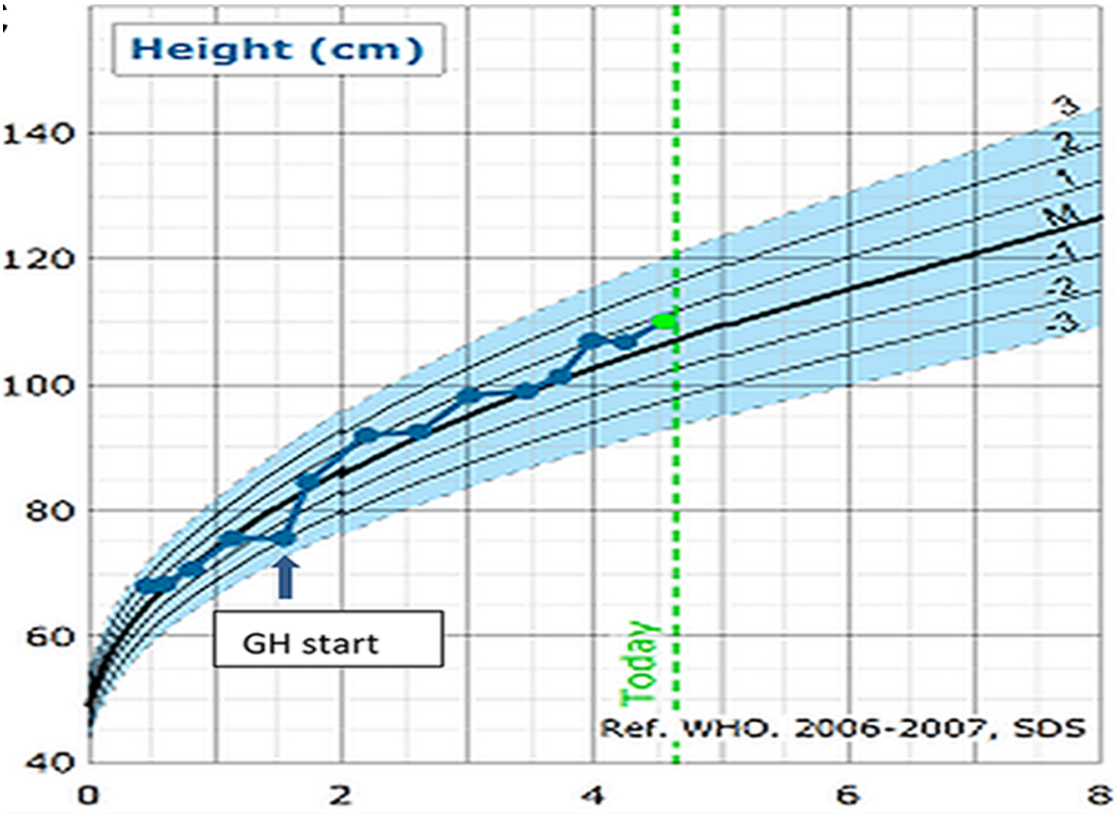

**Table 5.1:** Summary of clinical features (proband A):

| | |
|---|---|
| **Face** | Single median maxillary central incisor, congenital nasal pyriform aperture stenosis |
| **Eye** | Left choroidal coloboma |
| **Heart** | Supra-valvular pulmonary stenosis |
| **Gastrointestinal** | Feed intolerance, severe gastro-esophageal reflux disease requiring gastro-jejonostomy feeding |
| **Liver** | Mild portal-portal bridging fibrosis, elevated transaminases |
| **Lung** | Persistent oxygen requirement of unknown aetiology |
| **Pancreas** | Persistent form of hyperinsulinism |
| **Pituitary** | Hypopituitarism |
| **Neuro-developmental** | Speech and motor developmental delay |

**Figure 5.3**: Pedigree of Family A

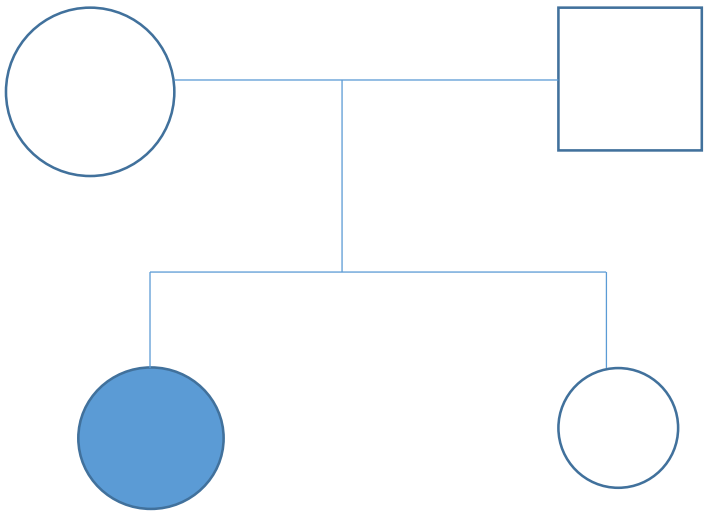

### 5.3 WHOLE EXOME SEQUENCING RESULTS (FAMILY A)

In this family, whole-exome sequencing was performed on the both the parents(unaffected) and the affected child. Assuming a *de novo* inheritance pattern, filters were applied to whole-exome data as shown in the figure 5.5. The potential candidate variants are listed in the table 5.3.

**Figure 5.4**

*De Novo* Variant Analysis of Proband A (* Novel variants include variants present in at least 5% minor allele frequency in 1000 Genomes Project, ExAC and NHLBI ESP exomes excluded; ** Predicted deleterious variants included nonsynonymous coding, splice site, frameshift, stop gain variants; *** Variants present in heterozygous state in the child and not present in both the parents; ****Variants with biological role related to the clinical phenotype of hyperinsulinaemic hypoglycaemia and hypopituitarism)

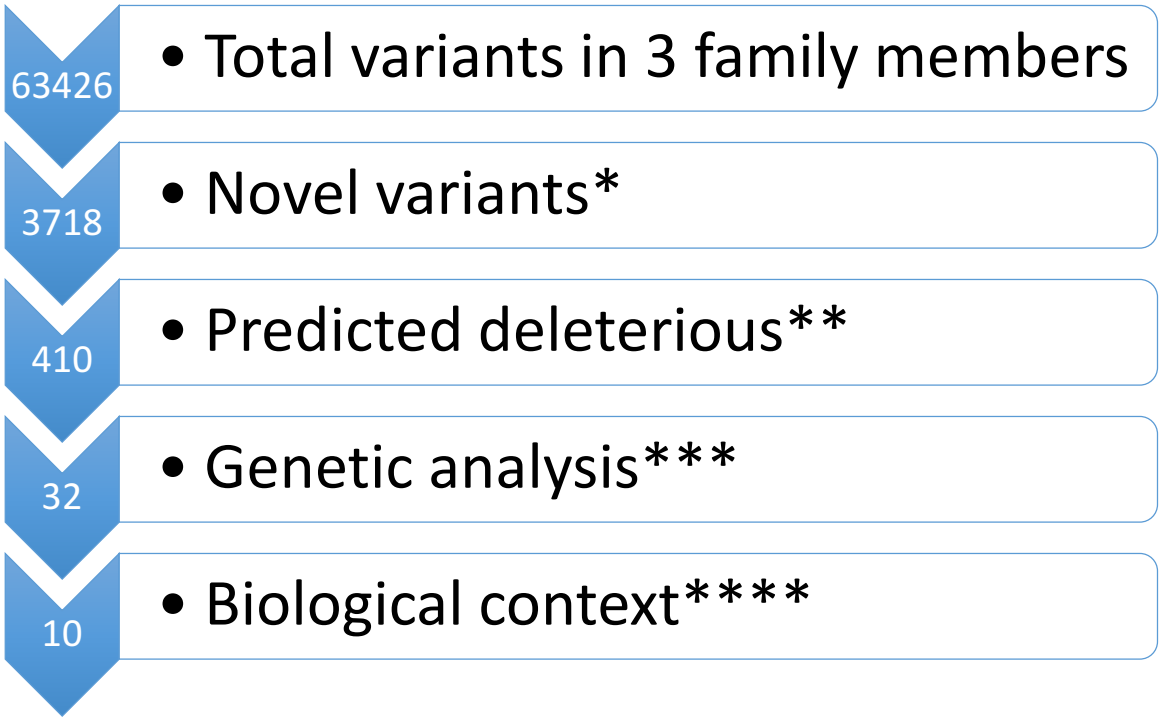

**Table 5.2:** List of *de novo* candidate gene variants and their locations in family A

| Chromosome | Gene | Gene region | Protein variant |
|---|---|---|---|
| 2 | *ALK* | Exonic | p.G924G |
| | | | |
| 2 | *PEL1* | Exonic | p.A68fs*10 |
| | | | |
| 7 | *HIP1* | Splice site | |
| | | | |
| 10 | *CHST15* | Exonic | p.R456fs*50 |
| | | | |
| 12 | *DUSP16* | Exonic | p.C136* |
| | | | |
| 12 | *CCNT1* | Splice site | |
| | | | |
| 16 | *KAT8* | Exonic | p.R448fs*9 |
| | | | |
| 17 | *FMNL1* | Exonic | p.P549L |
| | | | |
| 20 | ***FOXA2*** | Exonic | p.S169P |

A brief description on the biological function of the above genes is given below. The biological information on the genes were obtained from databases such as Uniprot and genecards.

***ALK*** (ALK Receptor Tyrosine Kinase)

*ALK* is involved in the development of specific neurons in the nervous system and *ALK* gene mutations are associated with anaplastic large cell lymphomas, neuroblastoma, and non-small cell lung cancer (232)

***PEL1*** (Phosphatidylglycerophosphate Synthase 1)

This gene catalyzes the synthesis of Phosphatidylglycerophosphate from CDP-diacylglycerol and glycerol 3-phosphate and functions as the committed and rate-limiting step in the biosynthesis of cardiolipin (233).

***CHST15*** (Carbohydrate Sulfotransferase 15)

The protein coded by this gene forms an important structural component of the extracellular matrix and which links to proteins to form proteoglycans (234).

***DUSP16*** (Dual Specificity Phosphatase 16)

This gene encodes a mitogen-activated protein kinase phosphatase. By using Northern blot analysis of mouse tissues, an abundant expression of this protein was found in in brain, kidney, intestine, and testis, and lower expression in thymus, spleen, and bone marrow (235).

***CCNT1***(Cyclin T1)

The protein encoded by this gene associates with cyclin-dependent kinase 9, and acts as a cofactor of human immunodeficiency virus type 1 (HIV-1) Tat protein, necessary for full activation of viral transcription (236).

***KAT8*** (Lysine Acetyltransferase 8)

This gene encodes a member of the MYST histone acetylase protein family which may be involved in transcriptional activation(237).

***FMNL1*** (Formin Like 1)

Formin-related proteins have been implicated in morphogenesis, cytokinesis, and cell polarity (238).

***FOXA2***(Forkhead Box A2)

*FOXA2* is a transcription factor with a critical role in early embryogenesis of various organs including central nervous system (238). Tissue specific deletion of *Foxa2* from the mice pancreatic β-cells leads to the development of CHI (249).

As *FOXA2* segregates with the clinical phenotype of proband A, this gene and the mutation (p.S169P) have been explored in detail in chapter 6.

# CHAPTER 6

# *FOXA2* (FORKHEAD BOX A2): DESCRIPTION OF THE GENE FUNCTION, DESCRIPTION OF THE MUTATION (c.505T>C, p. S169P) AND FUNCTIONAL ANALYSIS

## 6.1 SUMMARY OF CHAPTER 6

Chapter 6 begins with the introduction of *FOXA2*, discussion of the *FOXA2* mutation (c.505T>C, p.S169P) and detailed description of the results from various functional studies to demonstrate the pathogenicity of the mutation followed by a detailed discussion.

The manuscript of this chapter is accepted for publication. The pdf of the accepted version is attached in the appendix.

## 6.2 ROLE OF *FOXA2* IN THE DEVELOPMENT OF CENTRAL NERVOUS SYSTEM

*FOXA2* (formerly hepatocyte nuclear factor-3β, *HNF-3β*) belongs to the family of the Forkhead class of transcription factors and is localised to the cytogenic location 20p11.21(Figure 6.1). *FOXA2* regulates the critical developmental process and has been implicated in the development of liver bud, central nervous system, pancreas and endodermal tissues. An important role of *FOXA2* is its involvement in the development of axial mesoderm and formation of the notochord, node and floorplate which are important for the vertebrate body axis development (239, 240). Jin et.al. demonstrated that that *Foxa2* is important in the development of anterior forebrain structures, which have the same embryonic origin as the pituitary gland (241). Murine studies have shown a genetic interaction between *Foxa2* and Sonic Hedgehog (*Shh*) signalling pathway with overlapping expression pattern of *Foxa2* and *Shh* in the notochord and floor plate at E8.5. The development of central nervous system is dependent on several morphogenetic signals, one of which is the secretion of Shh by the notochord and floor plate (242).

### 6.2.1 *FOXA2* AND ITS INTERACTION WITH SHH SIGNALLING PATHWAY

The initiation of the Shh signalling pathway (Figure 6.2) starts with the binding of Shh protein to its receptor on target cell, PTCH1(Patched-1). This binding releases SMO(smoothened) which is normally under inhibitory control from PTCH-1. SMO is then active and enters the cytoplasm and activates Gli1, which is then phosphorylated, enters the nucleus and transcriptionally regulates the promoter regions of target genes such as *FOXA2* and *NKx2.2* (243-245). Mavromatakis et. al demonstrated that *Foxa2* plays an important role in modulation of *Shh* signalling, contributing to the specification of ventral motor neuron progenitor identity (246). Deletion of *Foxa2* is lethal as the *Foxa2* null embryos die during early gestation, at embryonic day 9.5, as a result of failure of formation of axial mesoderm (239).

**Figure 6.1:** *FOXA2* is localised at 20p11.21 and consists of 3 domains (Forkhead_N, FH and HNF_C). The variant (p. S169P) is located at the FH (DNA binding) domain

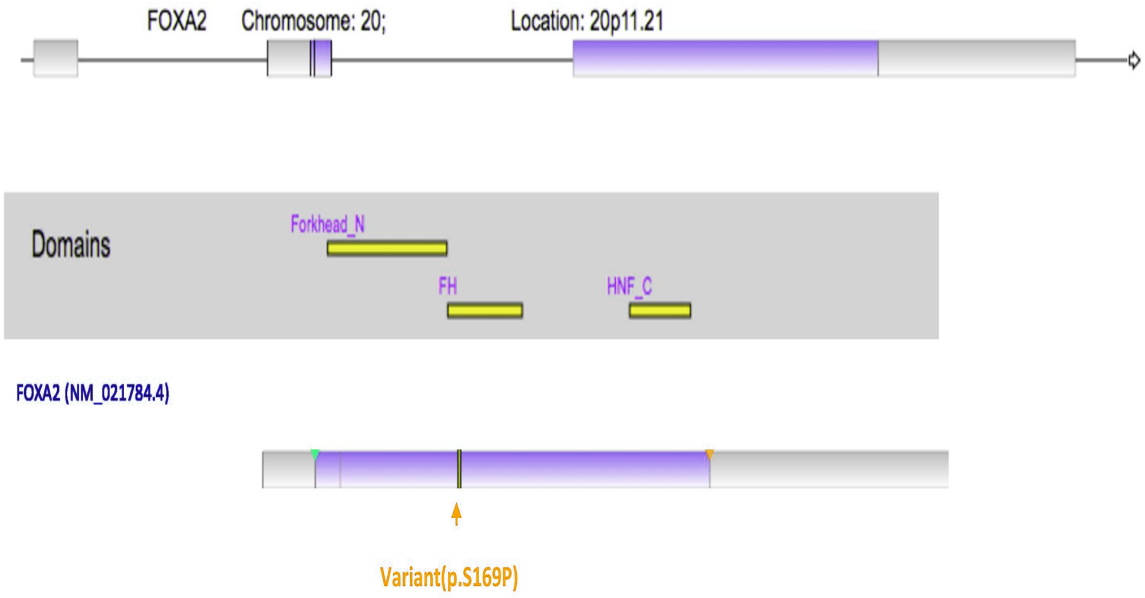

**Figure 6.2** Interaction between Shh signalling pathway and *FOXA2*. Shh: Sonic hedge hog; PTCH1: patched 1; SMO: smoothened. SMO is under the inhibitory control of the Shh cell surface receptor PTCH1.Binding of Shh to PTCH1 releases the inhibition and activates the downstream signalling pathway

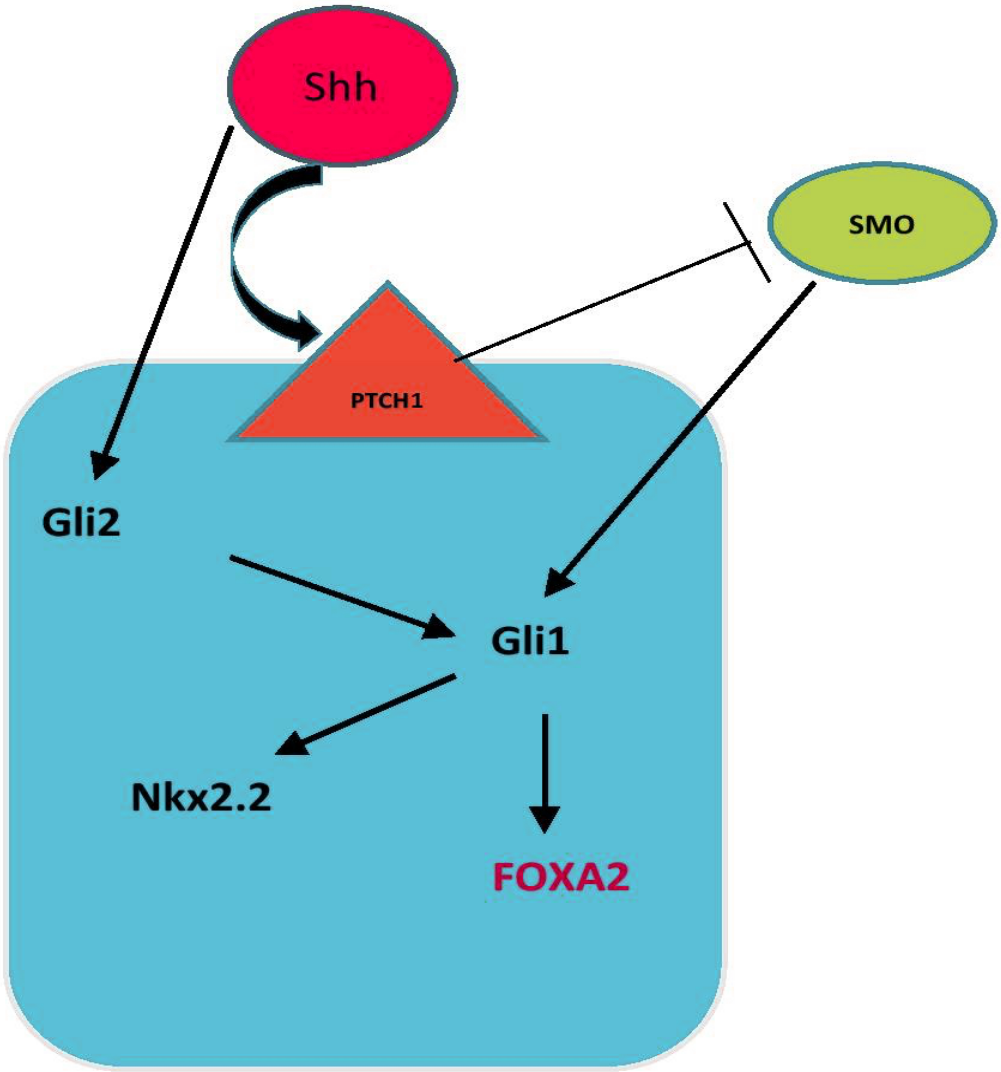

## 6.3 ROLE OF *FOXA2* IN MOUSE PANCREAS AND ENDODERM-DERIVED ORGANS

*Foxa2* co-operates with *Foxa1* and are required for the formation of endoderm-derived organs such as the liver (247), lung (248), pancreas (249) and gastrointestinal tract (250).

Sund et al. demonstrated that tissue-specific deletion of *Foxa2* from the pancreatic β-cells ($Foxa2^{loxp/loxp}$; Ins:Cre) leads to the development of CHI in mouse (251). *Foxa2* has been implicated to control multiple pathways involved in insulin secretion form the pancreatic ß cells (252). In the islet cells of mature pancreas, *Foxa2* has been shown to activate components of insulin secretion, such as sulfonylurea receptor1 [SUR1], encoding *ABCC8* (252) and the inward rectifier potassium channel member 6.2 [Kir 6.2], encoding *KCNJ11*(252). In humans, mutations in SUR1 (*ABCC8*) and Kir 6.2 (*KCNJ11*) (150, 253-256) are the most common causes of genetic forms of CHI.

Thus a mutation in this gene can potentially cause problems in the development of pituitary and pancreas, therefore segregates with the phenotype of proband A.

## 6.4 DESCRIPTION OF *FOXA2* MUTATION (c.505T>C, p.S169P)

A novel heterozygous *FOXA2* mutation (c.505T>C, p.S169P) was identified in the affected child but not in the parents. The mutation was confirmed by Sanger sequencing (Figure 6.3).

**Homo sapiens Forkhead box A2 (*FOXA2*), transcript variant 1, NM_021784.4, CDS with the position of point mutation highlighted in red**

***FOXA2*(c.505 T>C)**

ATGCACTCGGCTTCCAGTATGCTGGGAGCGGTGAAGATGGAAGGGCACGAGCCGTCCGACTGGAGCAGCT
ACTATGCAGAGCCCGAGGGCTACTCCTCCGTGAGCAACATGAACGCCGGCCTGGGGATGAACGGCATGAA
CACGTACATGAGCATGTCGGCGGCCGCCATGGGCAGCGGCTCGGGCAACATGAGCGCGGGCTCCATGAAC
ATGTCGTCGTACGTGGGCGCTGGCATGAGCCCGTCCCTGGCGGGGATGTCCCCCGGCGCGGGCGCCATGG
CGGGCATGGGCGGCTCGGCCGGGGCGGCCGGCGTGGCGGGCATGGGGCCGCACTTGAGTCCCAGCCTGAG
CCCGCTCGGGGGGCAGGCGGCCGGGGCCATGGGCGGCCTGGCCCCCTACGCCAACATGAACTCCATGAGC
CCCATGTACGGGCAGGCGGGCCTGAGCCGCGCCCGCGACCCCAAGACCTACAGGCGCAGCTACACGCACG
CAAAGCCGCCCTACTCGTACATCTCGCTCATCACCATGGCCATCCAGCAGAGCCCCAACAAGATGCTGAC
GCTGAGCGAGATCTACCAGTGGATCATGGACCTCTTCCCCTTCTACCGGCAGAACCAGCAGCGCTGGCAG
AACTCCATCCGCCACTCGCTCTCCTTCAACGACTGTTTCCTGAAGGTGCCCCGCTCGCCCGACAAGCCCG
GCAAGGGCTCCTTCTGGACCCTGCACCCTGACTCGGGCAACATGTTCGAGAACGGCTGCTACCTGCGCCG
CCAGAAGCGCTTCAAGTGCGAGAAGCAGCTGGCGCTGAAGGAGGCCGCAGGCGCCGCCGGCAGCGGCAAG
AAGGCGGCCGCCGGAGCCCAGGCCTCACAGGCTCAACTCGGGGAGGCCGCCGGGCCGGCCTCCGAGACTC
CGGCGGGCACCGAGTCGCCTCACTCGAGCGCCTCCCCGTGCCAGGAGCACAAGCGAGGGGGCCTGGGAGA
GCTGAAGGGGACGCCGGCTGCGGCGCTGAGCCCCCCAGAGCCGGCGCCCTCTCCCGGGCAGCAGCAGCAG
GCCGCGGCCCACCTGCTGGGCCCGCCCCACCACCCGGGCCTGCCGCCTGAGGCCCACCTGAAGCCGGAAC
ACCACTACGCCTTCAACCACCCGTTCTCCATCAACAACCTCATGTCCTCGGAGCAGCAGCACCACCACAG
CCACCACCACCACCAACCCCACAAAATGGACCTCAAGGCCTACGAACAGGTGATGCACTACCCCGGCTAC
GGTTCCCCCATGCCTGGCAGCTTGGCCATGGGCCCGGTCACGAACAAAACGGGCCTGGACGCCTCGCCCC
TGGCCGCAGATACCTCCTACTACCAGGGGGTGTACTCCCGGCCCATTATGAACTCCTCTTAA

**Aminoacid sequence of *FOXA2* with the point mutation at position 169(serine) highlighted in red**

***FOXA2* p.(S169P)**

```
atgcactcggcttccagtatgctgggagcggtgaagatggaagggcacgagccgtccgac
 M  H  S  A  S  S  M  L  G  A  V  K  M  E  G  H  E  P  S  D
tggagcagctactatgcagagcccgagggctactcctccgtgagcaacatgaacgccggc
 W  S  S  Y  Y  A  E  P  E  G  Y  S  S  V  S  N  M  N  A  G
ctggggatgaacggcatgaacacgtacatgagcatgtcggcggccgccatgggcagcggc
 L  G  M  N  G  M  N  T  Y  M  S  M  S  A  A  A  M  G  S  G
tcgggcaacatgagcgcgggctccatgaacatgtcgtcgtacgtgggcgctggcatgagc
 S  G  N  M  S  A  G  S  M  N  M  S  S  Y  V  G  A  G  M  S
ccgtccctggcggggatgtcccccggcgcgggcgccatggcgggcatgggcggctcggcc
 P  S  L  A  G  M  S  P  G  A  G  A  M  A  G  M  G  G  S  A
ggggcggccggcgtggcgggcatggggccgcacttgagtcccagcctgagcccgctcggg
 G  A  A  G  V  A  G  M  G  P  H  L  S  P  S  L  S  P  L  G
gggcaggcggccggggccatgggcggcctggccccctacgccaacatgaactccatgagc
 G  Q  A  A  G  A  M  G  G  L  A  P  Y  A  N  M  N  S  M  S
cccatgtacgggcaggcgggcctgagccgcgcccgcgaccccaagacctacaggcgcagc
 P  M  Y  G  Q  A  G  L  S  R  A  R  D  P  K  T  Y  R  R  S
tacacgcacgcaaagccgccctactcgtacatctcgctcatcaccatggccatccagcag
 Y  T  H  A  K  P  P  Y  S  Y  I  S  L  I  T  M  A  I  Q  Q
agccccaacaagatgctgacgctgagcgagatctaccagtggatcatggacctcttcccc
 S  P  N  K  M  L  T  L  S  E  I  Y  Q  W  I  M  D  L  F  P
ttctaccggcagaaccagcagcgctggcagaactccatccgccactcgctctccttcaac
 F  Y  R  Q  N  Q  Q  R  W  Q  N  S  I  R  H  S  L  S  F  N
gactgtttcctgaaggtgccccgctcgcccgacaagcccggcaagggctccttctggacc
 D  C  F  L  K  V  P  R  S  P  D  K  P  G  K  G  S  F  W  T
ctgcaccctgactcgggcaacatgttcgagaacggctgctacctgcgccgccagaagcgc
 L  H  P  D  S  G  N  M  F  E  N  G  C  Y  L  R  R  Q  K  R
ttcaagtgcgagaagcagctggcgctgaaggaggccgcaggcgccgccggcagcggcaag
 F  K  C  E  K  Q  L  A  L  K  E  A  A  G  A  A  G  S  G  K
aaggcggccgccggagcccaggcctcacaggctcaactcggggaggccgccgggccggcc
 K  A  A  A  G  A  Q  A  S  Q  A  Q  L  G  E  A  A  G  P  A
tccgagactccggcgggcaccgagtcgcctcactcgagcgcctccccgtgccaggagcac
 S  E  T  P  A  G  T  E  S  P  H  S  S  A  S  P  C  Q  E  H
aagcgaggggcctgggagagctgaaggggacgccggctgcggcgctgagccccccagag
 K  R  G  G  L  G  E  L  K  G  T  P  A  A  A  L  S  P  P  E
ccggcgccctctcccgggcagcagcagcaggccgcggcccacctgctgggcccgccccac
 P  A  P  S  P  G  Q  Q  Q  Q  A  A  A  H  L  L  G  P  P  H
cacccgggcctgccgcctgaggcccacctgaagccggaacaccactacgccttcaaccac
 H  P  G  L  P  P  E  A  H  L  K  P  E  H  H  Y  A  F  N  H
ccgttctccatcaacaacctcatgtcctcggagcagcagcaccaccacagccaccaccac
 P  F  S  I  N  N  L  M  S  S  E  Q  Q  H  H  H  S  H  H  H
caccaaccccacaaaatggacctcaaggcctacgaacaggtgatgcactaccccggctac
 H  Q  P  H  K  M  D  L  K  A  Y  E  Q  V  M  H  Y  P  G  Y
ggttcccccatgcctggcagcttggccatgggcccggtcacgaacaaaacgggcctggac
 G  S  P  M  P  G  S  L  A  M  G  P  V  T  N  K  T  G  L  D
gcctcgcccctggccgcagatacctcctactaccaggggggtgtactcccggcccattatg
 A  S  P  L  A  A  D  T  S  Y  Y  Q  G  V  Y  S  R  P  I  M
aactcctcttaa
 N  S  S  -
```

**Figure 6.3:** Sanger Sequencing showing the point mutation in *FOXA2* (c.505 T>C)

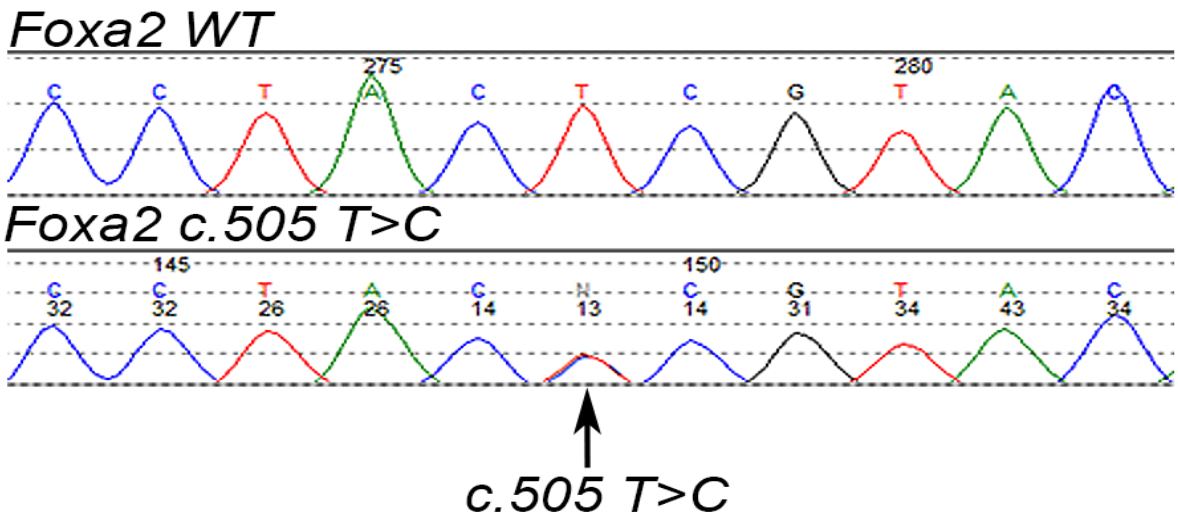


### 6.4.1 Factors Supporting Pathogenicity of the Variant

The variant is not present in control databases (ExAc, dbSNP, 1000 genome). Multiple sequence alignment shows that the serine residue at position 169 is highly conserved across different species, from drosophila, human, mouse, chicken to frog (Figure 6.4), suggesting that this residue is functionally important and has been maintained throughout evolution in different species.

Furthermore, the *FOXA2* mutation (c.505T>C, p.S169P) lies at the DNA binding domain of the transcription factor. In silico analysis using SIFT, PolyPhen, Mutation Taster predict this aminoacid substitution to have deleterious impact on the protein function.

**Figure 6.4:** The evolutionary conservation of the amino acid residue serine at position 169 is shown across different species such as drosophila, human, mouse, chicken and frog. DROME: drosophila; XENTR: Frog.

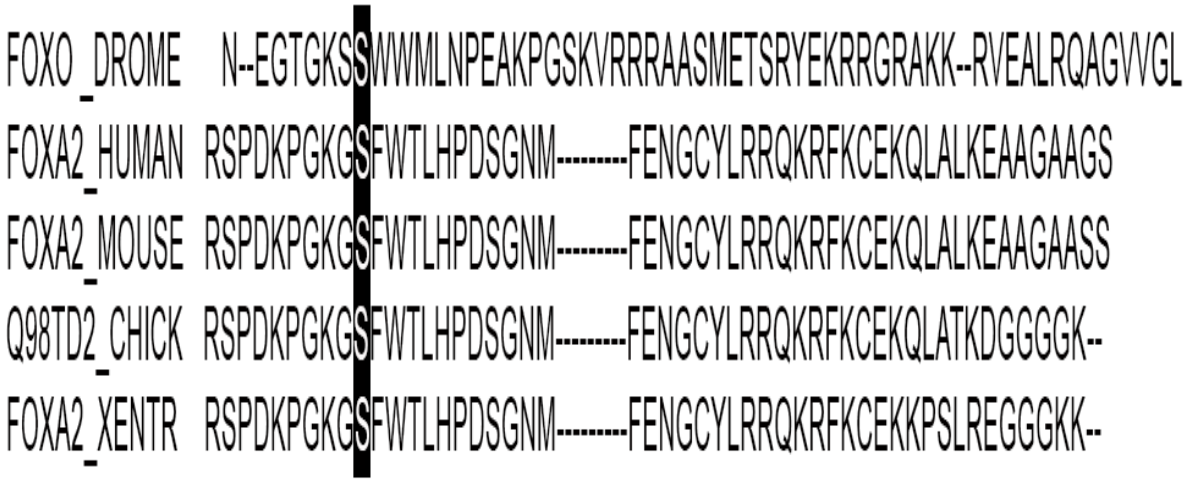

# 6.5 FUNCTIONAL ANALYSIS OF *FOXA2* (c.505T>C, p. S169P):

# *IN VITRO* EXPERIMENTS

This section describes a detailed description of various *in vitro* functional studies such as *in situ* hybridisation, immunohistochemistry, site-directed mutagenesis, dual luciferase assay, Immunocytofluorescence, western blot etc. *In vitro* studies were performed in the laboratory at the centre for endocrinology, William Harvey Research institute, London under the supervision of Dr Carles Gaston-Massuet and his team. The experiments (bacterial transformation, *in situ* hybridisation, immunohistochemistry, site-directed mutagenesis, luciferase assay and western blot) were performed by me under the guidance of research fellows-Lillina Vignola, Angelica Gualtieri and Valeria Scagliotti.

## 6.5 FUNCTIONAL ANALYSIS OF FOXA2(c.505 T>C, p.S169P)

### 6.5.1 Mice

All mice were housed with a 12-hour light/12-hour dark cycle in a temperature and humidity-controlled room (21°C, 55% humidity) with constant access to food and water. Timed pregnancies were achieved by mating females and males overnight and, the presence of vaginal plug the following morning, was considered as embryonic day (e) 0.5.

All experiments were conducted under the regulations, licenses and local ethical review of the UK Animals (Scientific Procedures) Act 1986.

### 6.5.2 Fixation, Embedding and Sectioning of Mouse Embryos

#### 6.5.2.1 Fixation

The embryos at stages E11.5, E12.5, E.13.5 and E15.5 were dissected and fixed in 4 % paraformaldehyde (prepared by adding 4 gram of paraformaldehyde to 100 ml of 1X PBS (phosphate buffered saline) and heating at 65°C with stirring to get a homogeneous mixture which is then cooled and filtered on 0.45um disposable filter).

**Reagents used:**

| |
|---|
| 0.85% saline (4.25g NaCl in 500ml ddH2O) |
| 50% ethanol |
| 70% ethanol |
| 4% formaldehyde in 1X PBS |

The steps for fixation are as follows:

1. The dissected embryos were rinsed well in PBS
2. The embryos were placed in labelled 20 ml snap-cap glass vials containing 4 % paraformaldehyde
3. The fixation was allowed to proceed at 4°C and incubated overnight.
4. The embryos were then washed twice with PBS at room temperature and decanted to remove as much solution as possible.
5. Following the previous step, the embryos were washed with 0.85% saline (4.25g NaCl in 500ml ddH2O) which helps remove phosphate from PBS to avoid it precipitating during ethanol dehydration.
6. The embryos were incubated for 15 minutes in 50% ethanol, at room temperature and then in 70% ethanol for 15 minutes and stored in 70% ethanol at 4°C.

#### 6.5.2.2 Dehydration

The 70% ethanol was decanted carefully without disturbing or damaging the embryos. Dehydration was carried out by adding 95% ethanol and incubating for 20 minutes at room temperature. This step was repeated twice. Following this, the 95% ethanol was decanted and 100% ethanol was added and incubated for 20 minutes twice. The 100% ethanol was replaced with xylenes and incubated for 10 minutes.

#### 6.5.2.3 Embedding

The Xylene from the previous step was poured off and 5ml fresh Xylene was added to each vial followed by addition of 5 ml of molten wax. The samples were mixed and left overnight at room temperature to harden the mixture and enable the paraffin to be

dissolved in xylene to start impregnation of the samples. The wax/xylene mixture was melted by transferring the samples to 60°C oven. The wax/xylene mixture was then poured off from the vials and fresh molten wax was immediately added to the vials with a hot glass pipette and transferred to 60°C heating block. The vials were incubated for 1 hour at 60°C in an oven. The samples were transferred to wax-filled embedding moulds and left at room temperature to harden.

#### 6.5.2.4 Sectioning of Paraffin Embedded Tissue

The paraffin-embedded tissue blocks were placed faced down on an ice block for 10 minutes. The microtome (Leica, Model RM2155) was set at a clearance angle of 5° to cut the blocks. The paraffin block was inserted and oriented appropriately and trimmed at an initial thickness of 10-30 µm initially to expose the tissue to the surface level. Once the tissue was exposed, the trimming was done at a thickness of about 4-5 µm. The cut sections were carefully placed on the surface of a pre-prepared water bath containing DEPC (diethyl pyrocarbonate) water at 40-45°C.The sections floating on the water-bath were picked up on to the surface of clean glass microscopic slides. The slides were then placed on warming block in a 65°C oven for 20 minutes to allow bonding of the tissue to the glass. Following this, the slides were stored upright in a slide rack and allowed to dry overnight at 37$^{o}$C.

### 6.5.3 BACTERIAL TRANSFORMATION AND PURIFICATION OF MOUSE FOXA2 PLASMID

#### 6.5.3.1 Bacterial Transformation

The mouse *Foxa2* gene fragment (1567bp) plasmid was kindly provided by www.hdbr.org. The plasmid was transformed into DH5α competent cells using heat shock protocol.

The steps of transformation protocol are described below:

1. 50µl of DH5α competent cells were added to an Eppendorf placed on ice.
2. The *Foxa2* plasmid DNA(2µl) was added, gently swirled and incubated on ice for 20 minutes
3. The tubes were submerged in the 42ºC water bath for 45 seconds. The duration of this step is critical as optimal transformation efficiency is observed when cells are heat-pulsed for 45-50 seconds.
4. Following the heat-pulse, the tubes were immediately incubated on ice for 2 minutes.
5. 500µl of LB (Lysogeny broth) medium was added to the eppendorf containing the competent cells and the plasmid DNA.
6. The tubes were then incubated at 37ºC for 1 hour with shaking at 225-250 rpm
7. The transformation mixture(100µL) was plated on LB-ampicillin agar plates.
8. The plates were incubated overnight at 37ºC.

#### 6.5.3.2 Starter Cultures and Midiprep

Four colonies were picked up from the transformation mixture plated on agar plate with sterile pipette tips. Each colony was transferred to a flask containing 100 mL of LB-broth and 100 µL of ampicillin with a concentration of 10mg/mL. These starter cultures were incubated at 37ºC overnight with shaking at 225-250 rpm. The next morning, using QIAGEN Hispeed Plasmid Midiprep kit, the plasmid DNA was purified by following the manufacturer's instructions. This procedure is based on alkaline lysis of bacterial cells followed by adsorption of DNA onto silica in the presence of high salt. Bacteria are lysed under alkaline conditions, and the lysate is subsequently neutralized and adjusted to high-salt binding conditions, ready for purification on the QIAprep silica-gel membrane. The optimized buffers in the lysis procedure combined with the unique silica-gel membrane ensure that only DNA will be adsorbed, while RNA, cellular proteins, and metabolites are not retained on the membrane but are found in the flow-through. Salts are efficiently removed by a brief wash step with Buffer PE. High-quality plasmid DNA is then eluted from the QIAprep column.

The purified plasmids are quantified using NanoDrop. The plasmid concentrations obtained from each colony were as follows (Figure 4.7):

Colony 1 104.7 ng/µL

Colony 2 89 ng/ µL

Colony 3 120.2 ng/ µL

Colony 4 108.9 ng/ µL

**Figure 6.5:** Agarose gel electrophoresis depicting the four bacterial colonies (double linear band representing a colony)

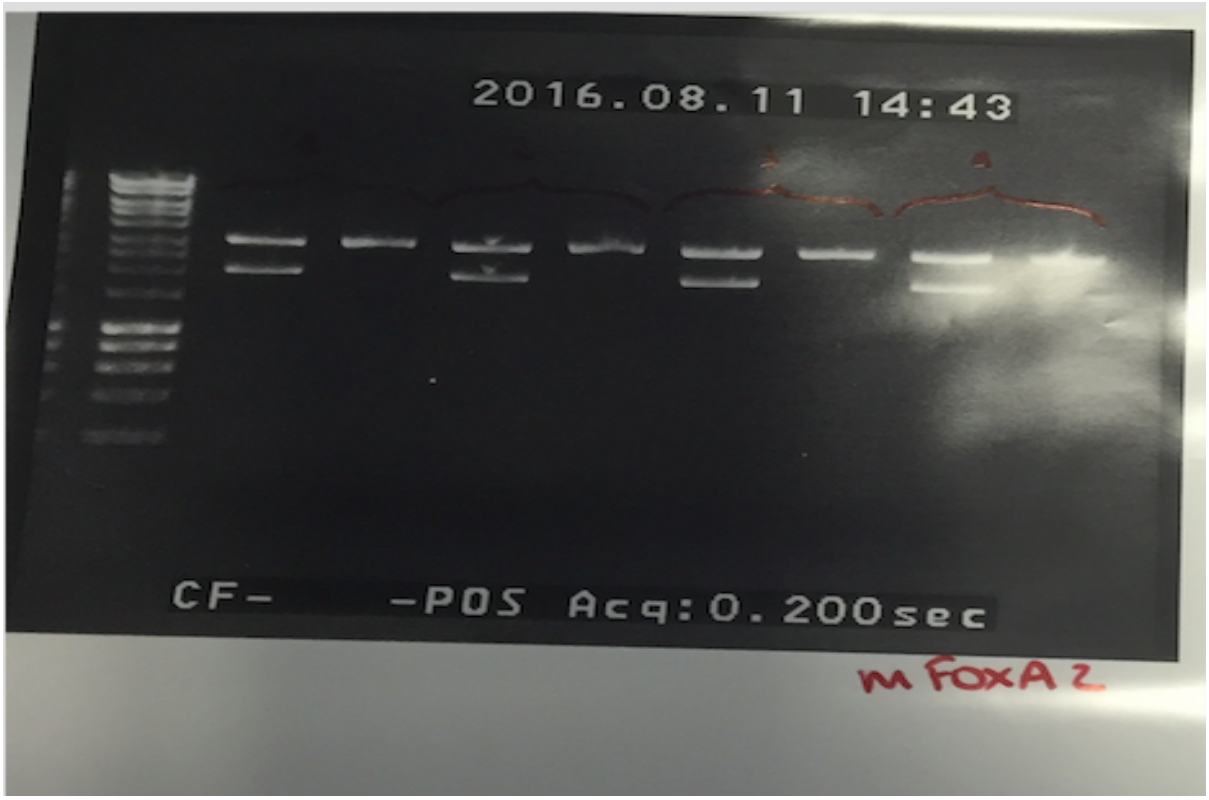

### 6.5.4 PREPARATION OF FOXA2 mRNA PROBE AND LABELLING

#### 6.5.4.1 Linearization of Plasmid (Digestion with BamHI enzymes)

Following isolation of *Foxa2* plasmid DNA, a diagnostic restriction digest was performed with endonuclease BamHI (from Bacillus amyloliquefaciens to confirm the cloning of *Foxa2* into the plasmid. The gel image of the diagnostic restriction digest is shown in figure 4.8. The concentration of the linearized plasmid was quantified using NanoDrop and the final concentration obtained was 174ng/μL.

**Figure 6.6: mouse *Foxa2* linearized plasmid (the single band represents mFoxa2 shown along with standard DNA ladder)**

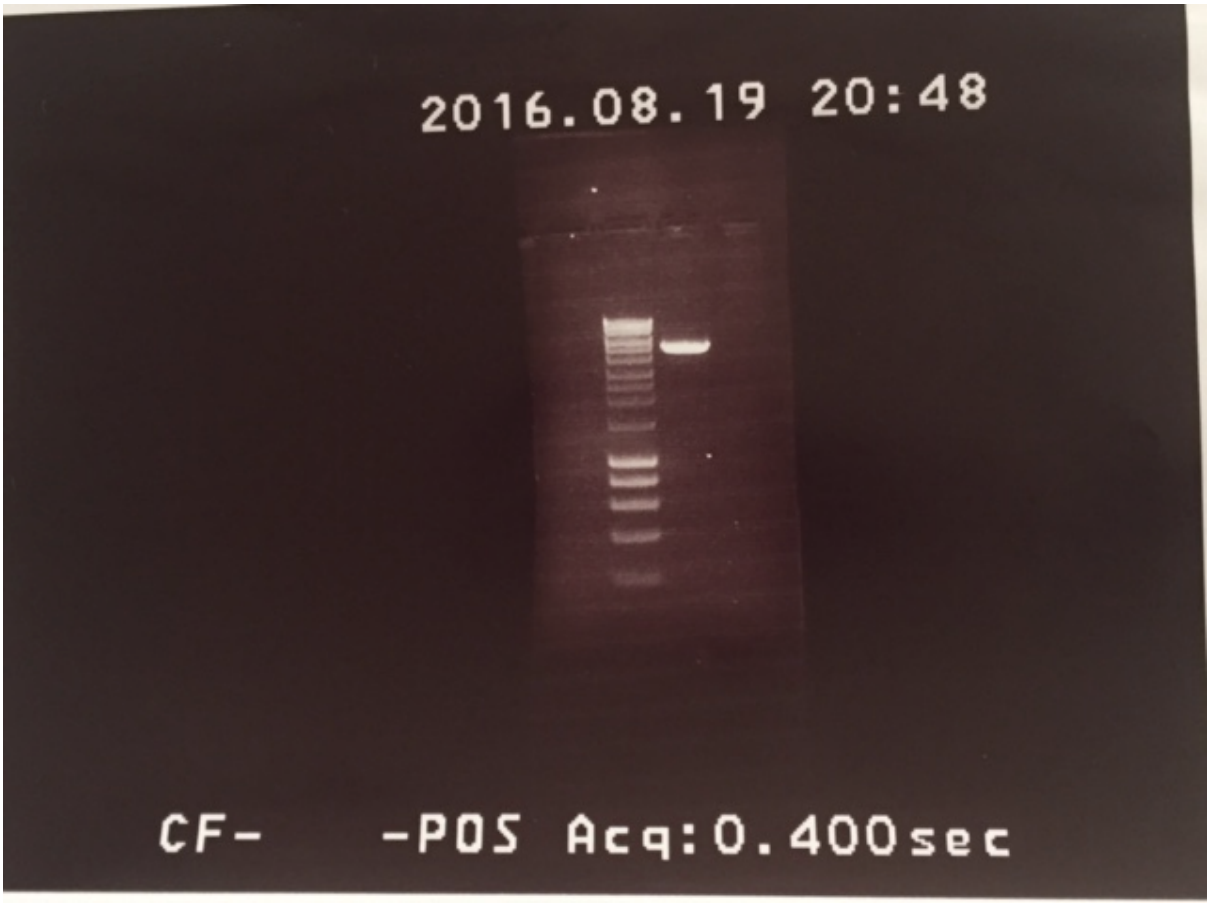

### 6.5.4.2 Digoxigenein (DIG) Labelled RNA Antisense Probe Transcription

DIG labeled RNA antisense probes are widely used for *in situ* hybridization due to their high sensitivity and specificity. These probes are highly stable and used for long-term studies.

The following reagents were used during the labelling:

| | |
|---|---|
| Linearized *Foxa2* plasmid | 5.75µL |
| DNA labeling mix(Digoxigenein) | 2µL |
| Transcription buffer | 2µL |
| RNAase inhibitor | 0.5µL |
| T3 RNA polymerase | 1µL |
| RNase and DNase free water | 8.25µL(added to make up the total volume to 20 µL |

The above reagents were added to an Eppendorf and incubated for 2-4 hours at 37$^{o}$C.The efficiency of transcription was assessed by running 0.5 µL on 1% agarose gel with 1 Kb ladder (Figure 4.9)

**Figure 6.7:**Agarose gel showing the probe after transcription(from left to right:the first band represents the standard DNA ladder,the second single band is the linearized plasmid and the right most band is the probe).

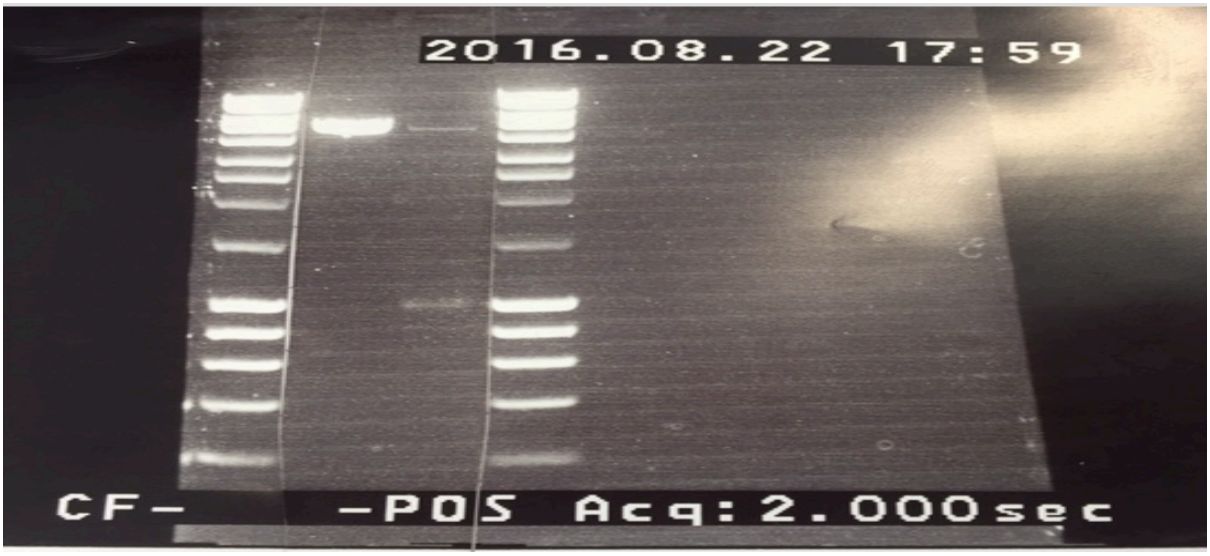


#### 4.6.4.3 Probe Purification

To the 20µL of the transcription reaction(probe), 40µL DEPC water was added to increase the total volume to 60µL.The probe was cleaned by passing through a spin column (CHROMA SPIN-1000 DEPC-H20 columns, BD Biosciences) and inverting the column up and down. The column is then placed in a 15 ml falcon tube and centrifuged at 700g for 5 minutes at 4 $^{o}$C to dry the columns.

### 6.5.5 *IN SITU* HYBRIDIZATION

#### 6.5.5.1 Pre-Hybridization Treatment

**Reagents used:**

| |
|---|
| 4% paraformaldehyde(PFA)-made by adding 16g of PFA, 40 ml 10*PBS, 200µL NaOH, made up to 300ml with DEPC water) |
| Histoclear |
| Ethanol at various concentrations:100%, 90%, 70%, 50%, 25% |
| Proteinase K(20 µg/ml) |
| Triethanolamine(0.1M) |
| Acetic anhydride |

The paraffin slides with mouse embryos (E11.5, E12.5, E.13.5 and E15.5) were subjected to deparrafinisation and hydration by washing with the following reagents as follows:

- Histoclear twice for 10 minutes
- 100% ethanol twice for 2 minutes
- 90% ethanol twice for I minute
- 50% ethanol twice for 1 minute
- 25% ethanol twice for 1 minute
- 1% PBS for 2 minutes

Sections were deparaffinised, rehydrated through decreasing ethanol dilutions, fixed with 4% PFA, incubated with proteinase K, fixed again with 4% PFA and finally incubated with 0.1 M triethanolamine, 0.1% acetic anhydride.

### 6.5.5.2 Hybridization

**Reagents used:**

| | |
|---|---|
| Hybmix (50% formamide, 0.3M sodium chloride, 0.02M Tris HCl, 0.005M EDTA, 10% Dextran sulphate, 1*Denhardt's solution): | 500µL(100 µL/slide) |
| RNAase inhibitor: | 0.5 µL (1 µL/ml) |
| tRNA: | 25 µL(0.5mg/ml) |
| SSC(saline sodium citrate) solution(175.3 g sodium chloride, 88.2 sodium citrate) | |

RNAase inhibitor, tRNA and anti-sense probe at 2:100 dilutions were added to the slides and mixed briefly. Hybmix was added to the slides followed by addition of formamide and SSC. The slides were incubated overnight at 55-65 $^{o}$C.

### 6.5.5.3 Post Hybridization Washing

The slides were further washed with SSC, formamide at hybridization temperature in a glass staining trough in a water bath. The slide rack was first washed in 2XSSC for 10 minutes. After removing the cover slips from each slide, they were washed with formamide twice for 10 minutes each. The slides were washed again in SSC at hybridization temperature and then were allowed to cool to room temperature.

#### 6.5.5.4 Antibody Detection

The following steps were followed for antibody detection:

1. The slides were washed with buffer consisting of 0.1M Tris-HCl Ph 7.5 and 0.15M sodium chloride.
2. Following this, 10% fetal calf serum, 1ml per slide was added and then left to stand for 1 hour (blocking antibody).
3. The slides were then drained and 0.5 ml of anti-Dig antibody (Sigma-Aldrich) was added to each slide and incubated in humid chamber at 4 $^{o}$C overnight.
4. The next day, the slides were washed with 0.1 M Tris-HCl Buffer (pH = 7.5, 0.15 M Sodium chloride) followed by 0.1 M Tris-HCl Buffer (pH = 9.5, 0.1 M Sodium chloride and 0.05M magnesium chloride)
5. PVA (Polyvinyl alcohol)-0.5ml/slide was added to 0.1 M Tris-HCl Buffer (pH = 9.5, 0.1 M Sodium chloride and 0.05M magnesium chloride) to form buffer-PVA mix. PVA helps to concentrate and enhance the development process.
6. 4-Nitro blue tetrazolium chloride solution (NBT, Sigma-Aldrich), 4.5µl/ml and 5-Bromo-4-chloro-3-indolyl phosphate disodium salt (BCIP, Sigma-Aldrich), 3.5 µl/ml were added to the buffer-PVA mix.
7. 0.5ml of the above solution was added to each slide and incubated at room temperature.
8. Once the slides were developed sufficiently, they were washed in running tap water and placed at 50 $^{o}$C for 15 minutes to remove residual PVA.

9. The slides are then dehydrated by separate alcohol series as below:
    - Ethanol 25% for 1 minute
    - Ethanol 50% for 1 minute
    - Ethanol 75% for 30 seconds
    - Ethanol 100% for 30 seconds
    - Histoclear for 10 minutes
10. Following alcohol dehydration, the slides were mounted in vector mount and images were acquired using a Leica microscope.

### 6.5.6 IMMUNOHISTOCHEMISTRY

Paraffin-embedded human tissue samples at 6, 8 and 13 weeks of gestation were obtained from the Human Developmental Biology Resource (Institute of Genetic Medicine, Newcastle, and Institute of Child Health, London; www.hdbr.org).

The main steps involved in immunohistochemistry are:

- Deparrafinisation and rehydration
- Heat induced antigen retrieval
- Addition of primary antibody
- Addition of secondary antibody

#### 6.5.6.1 Deparrafinisation and Rehydration

The slides were washed consecutively with the following reagents:

- Histoclear for 5 minutes
- 100% ethanol for 2 minutes
- 75% ethanol for 2 minutes
- 50% ethanol for 2 minutes
- 25% ethanol for 2 minutes
- Water for 5 minutes

#### 6.5.6.2 Heat Induced Antigen Retrieval

1. The slides were incubated with citric buffer (Citric acid 10Mm, Ph 6.0- prepared by adding 1.2 g of citric acid in 500 ml of water. NaOH 10M was added until the Ph was 6.0).
2. The slides are then placed in a microwave, heated under the following settings and cooling down in each step to avoid over-boiling:

   Power 70 for 3 minutes

   Power 90 for 3 minutes

   Power 90 for 3 minutes

   Power HI for 3 minutes
3. Following this, the slides were removed from the microwave and allowed to stand in the citric acid buffer at room temperature for 1 hour.

#### 6.5.6.3 Addition of Primary Antibody

1. The slides were rinsed with PBT (1XPBS, 1ml of 0.1% Triton X-100) for 5 minutes.
2. To each slide, 200µl of blocking buffer (5% normal goat serum) was added.
3. The slide was covered with a parafilm and allowed to stand for an hour at room temperature.
4. To each slide, 200µL of primary antibody (primary rabbit monoclonal antibody against hFOXA2 (Thermo Fisher Scientific; 701698; 1:250) was added, covered with a parafilm and incubated overnight at 4$^{o}$C.

#### 6.5.6.4 Addition of Secondary Antibody

1. The slides were rinsed with PBT by gentle agitation.
2. To each slide, 200µL of secondary biotinylated goat anti-rabbit antibody (Vector Laboratories; BA-1000; 1:300) was added
3. The slides were incubated for 1 hour at room temperature
4. Following this, the slides were washed with PBT and mounted
5. Images were acquired using a Leica microscope

### 6.5.7 HUMAN *FOXA2* PLASMID

Full length cDNA of human FOXA2 (GENE Bank RefSeq NM 021784.4) was cloned in ORF mammalian expression vector pCMV3 (pCMV3-hFOXA2, Sino Biological Inc). The physical map of the plasmid is shown in figure 4.10. The plasmid information is shown in table 4.3

**Table 6.1:** Human *FOXA2* insert in pCMV3

| | |
|---|---|
| **Gene** | Forkhead box A2, FOXA2 |
| **cDNA size** | 1392bp |
| **RefSeq** | NM 021784.4 |
| **Vector name** | pCMV3-untagged |
| **Vector size** | 6223 bp |
| **Promoter** | CMV |
| **Antibiotic resistance** | Ampicillin |
| **Restriction site** | KpnI + XbaI (6.1kb + 1.39kb) |

**Figure 6.8:** Physical map of plasmid(pCMV3) with *FOXA2* insert cloned into the open reading frame(ORF).

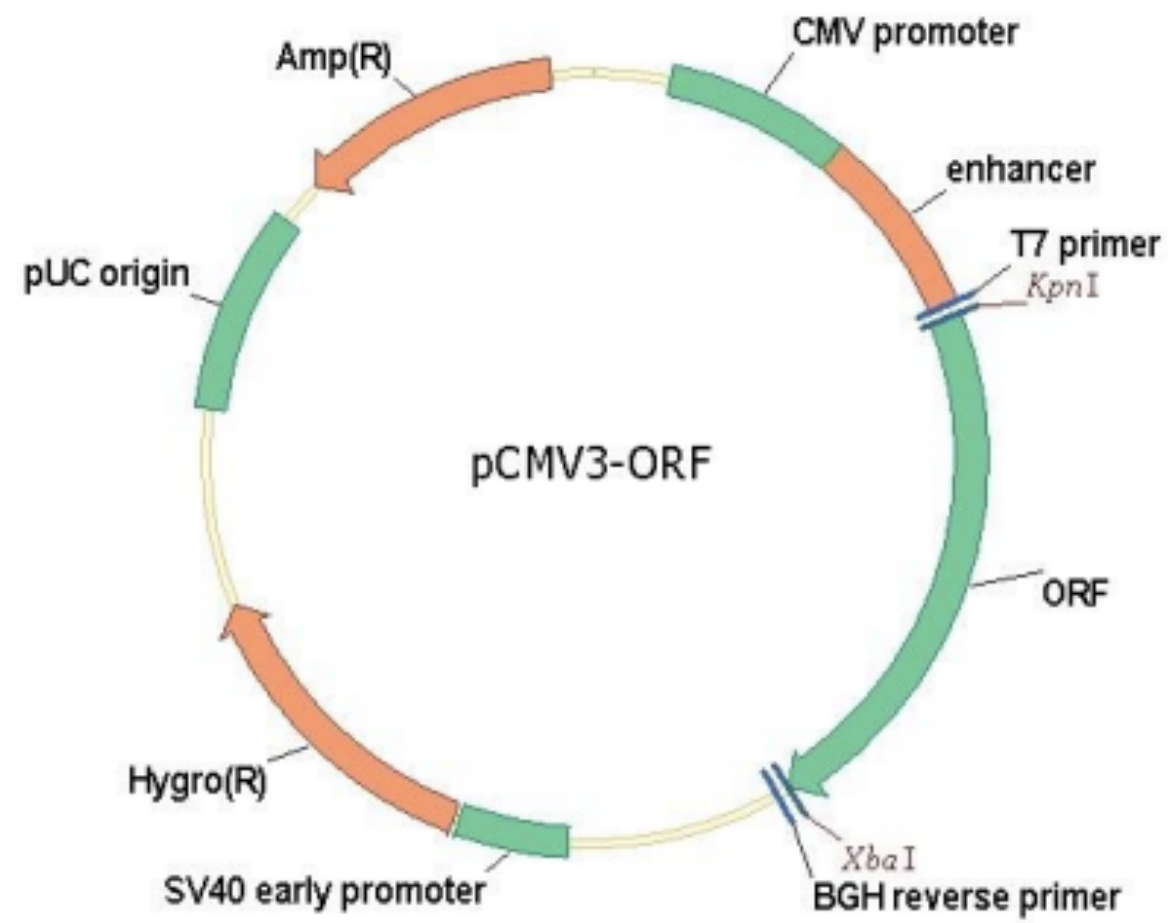

#### 6.5.7.1 Verification of Plasmid by Sequencing

As PCR based cloning carries the risk of insertion of mutations depending on the fidelity of DNA polymerase used, the entire *FOXA2* insert in the vector pCMV3 was sequenced to confirm no mutations have been inserted by error.

The primer sequences of the oligonucleotides used to sequence *FOXA2* insert in pCMV3 vector the insert are shown below:

| **Oligonucleotide** | **Sequence** |
|---|---|
| T7 Promoter | TAATACGACTCACTATAGGG |
| FOXA2_F | CCCTACGCCAACATGAACTCC |
| FOXA2_R | GTCGTTGAAGGAGAGCGAGTG |
| BGH Reverse | TAGAAGGCACAGTCGAGG |

### 6.5.8 MUTAGENIC PRIMER DESIGNING

The mutagenic primers were designed according to the following guidelines from the QuikChange II XL Site-Directed Mutagenesis Kit (Agilent Technologies).

1. Both of the mutagenic primers must contained the desired mutation and anneal to the same sequence on opposite strands of the plasmid.
2. Primers should be between 25 and 45 bases in length.
3. Melting temperature (Tm) of the primers as estimated by the following formula should be ≥78ºC.

   $$Tm = 81.5 + 0.41(\%GC) - \frac{675}{N} - \%\ \text{mismatch}$$

   N is the primer length in bases

   % GC and % mismatch must be whole numbers
4. For primers designed to introduce insertions or deletions, the following formula should be used

   $$Tm = 81.5 + 0.41(\%GC) - 675/N$$

   N does not include the bases, which are being inserted or deleted.

5. The desired mutation should be in the middle of the primer with ~10-15 bases of correct sequence on both sides
6. Optimally, the primers should have a minimum GC content of 40% and should terminate in one or more C or G bases.

**Table 6.2:** Mutagenic Primers used to insert mutations in the *FOXA2* gene carried in the vector

| | |
|---|---|
| **Forward primer** | CAAAGCCGCCCTACCCGTACATCTCGCTC |
| **Reverse Primer** | GAGCGAGATGTACGGGTAGGGCGGCTTTG |

### 6.5.9 SITE-DIRECTED MUTAGENESIS(SDM)

The SDM reaction was prepared on ice in thin-walled PCR tubes utilizing the designed mutagenic primers and the double-stranded DNA vector containing the wild-type gene as shown in the table.

#### 6.5.9.1 SDM reaction

**Table 6.3:** SDM reaction preparation

| **Reagent** | **Amount** |
|---|---|
| **10 X Reaction Buffer** | 5 µL |
| **dNTP mix** | 1 µL |
| **Forward mutagenic primer** | 125 ng |
| **Reverse mutagenic primer** | 125 ng |
| **Quickchange solution** | 1 µL |
| **Vector** | 94 ng |
| **dd$H_2O$** | To a final volume of 50 µL |
| **PfuTurbo DNA Polymerase (2.5 U/ µL)** | 1 µL |

The SDM reaction was put on to the PCR machine on the program “MARK SDM” for 12 cycles according to the settings shown below

**Table 6.4:** PCR settings for the SDM reaction

| Stage | Cycles | Temperature | Time |
|---|---|---|---|
| **1** | 1 | 95 $^{o}$C | 1 minute |
| **2** | 12 | 95 $^{o}$C<br>60 $^{o}$C<br>68 $^{o}$C | 50 seconds<br>50 seconds<br>1 minute/kb of plasmid length |
| **3** | 1 | 68 $^{o}$C | 7 minutes |

After the PCR cycles, the PCR product was cooled on ice and assessed by running 10µL on 1% agarose gel with HyperLadder(BIOLINE). The image is shown as below (figure 4.11).

**Figure 6.9:** PCR product verified on 1% agarose gel (from left to right: standard DNA HyperLadder and the single linear band on the right side of the image represents hFOXA2 plasmid).

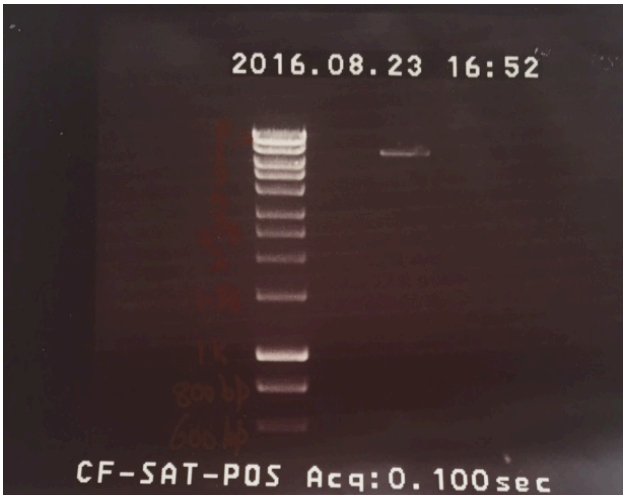

#### 6.5.9.2 Digestion

After the PCR cycles, the product from the SDM reaction was cooled by placing on ice for 2 minute and Dpn I restriction enzyme (1 µL; 10 u/µL) was added to the reaction mixture. It was mixed thoroughly first by pipetting and then spinning the mixture in a microcentrifuge for 1 minute. The reactions were then incubated at 37ºC for 1 hour. Dpn I is a restriction enzyme that recognises and cuts the methylated plasmid DNA and digests them leaving behind the mutation-containing synthesized DNA.

#### 6.5.9.3 Transformation

'Pure Gold' ultra-competent cells at -80 ºC were taken out and thawed gently on ice. 45 µL of the ultra-competent cells were added to new tubes and labelled. Following this, 2 µL of ß-mecaptoethanol was added to each tube, put on ice for 10 minutes. To this, 2 µL of PCR product from the SDM reaction were added to the tubes and stirred using pipette. The mixture was left to stand on ice for 30 minutes. After 30 minutes, the transformation reactions were heat-pulsed for 30 seconds in 42ºC water bath. The reactions were then placed on ice for 2 minutes and 500 µL of pre-warmed LB medium (42ºC) was added. Following this, the reaction mixtures were put on a shaker at 37ºC for 1 hour.

#### 6.5.9.4 Inoculating Agar Plates

250 µL of the transformed cells were added to the middle of agar plates at 37ºC. The transformed cells were spread uniformly across the plate using a sterile spreader. The plates were incubated overnight at 37ºC.

#### 6.5.9.5 Starter Cultures, Midiprep and Double Digestion

One individual colony picked up from the transformation mixture plated on agar plate with sterile pipette tips. Each colony was transferred to a flask containing 100 mL of LB-broth and 100 µL of ampicillin with a concentration of 10mg/mL. These starter cultures were incubated at 37ºC overnight with shaking at 225-250 rpm. The next morning, using QIAGEN Hispeed Plasmid Midiprep kit, the plasmid DNA was purified by following the manufacturer's instructions. This procedure is based on alkaline lysis of bacterial cells followed by adsorption of DNA onto silica in the presence of high salt. Bacteria are lysed under alkaline conditions, and the lysate is subsequently neutralized and adjusted to high-salt binding conditions, ready for purification on the QIAprep silica-gel membrane. The optimized buffers in the lysis procedure combined with the unique silica-gel membrane ensure that only DNA will be adsorbed, while RNA, cellular proteins, and metabolites are not retained on the membrane but are found in the flow-through. Salts are efficiently removed by a brief wash step with Buffer PE. High-quality plasmid DNA is then eluted from the QIAprep column.

The purified plasmids are quantified using NanoDrop. The concentration of the mutant plasmid hFOXA2 was 314 ng/ µL. The restriction enzymes KpnI and XbaI, 1 µL each, were added to 1 µg or 3.2 µL of the plasmid along with 3 µL of buffer and dd$H_2O$ to make up the total volume of the mixture to 30 µL. The restriction enzymes cleave the plasmid at the respective sites resulting in its linearization. The point mutation in the mutant plasmid was confirmed by sanger sequencing.

### 6.5.10 DUAL LUCIFERASE REPORTER(DLR) ASSAY

**Principle**

Luciferases are a class of oxidative enzymes found in several species that enable the organisms to produce bioluminescence or emit light. Under experimental conditions, by transfecting mammalian cells with a genetic construct containing the luciferase gene under the control of a promoter gene of interest, the transcriptional activity of the gene of interest can be measured and quantified by the luciferase reporter activity(257).

Dual reporter assay is a genetic reporter system that is used to study the effect of gene expression and transcriptional activity in eukaryotes. The dual reporter refers to the simultaneous expression and measurement of two individual reporter enzymes (experimental reported and control reporter) within a single system. While the experimental reporter correlates with the effect of the specific experiment, the control reporter serves as a baseline and provides as an internal control.

The Dual-Luciferase Reporter (DLR$^{TM}$) Assay allows the measurement of activities of two enzymes-firefly (Photinus pyralis) luciferase and Renilla (Renilla reniformis) luciferase from a single sample.

Firefly luciferase is a 61kDA monomeric protein that functions as a genetic reporter immediately upon translation. The bioluminescent reaction from firefly luciferase is shown below (Figure 4.12):

**Figure 6.10:** Bioluminescent Reaction-Firefly luciferase (Photinus pyralis) [ Adapted from Dual-Luciferase® Reporter Assay System Technical Manual TM040]

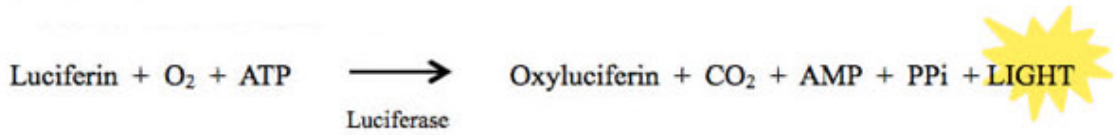


Renilla luciferase is a 36kDA monomeric protein that catalyses the conversion of coelenterazine to coelenteramide with the help of oxygen. The bioluminescent reaction is shown below (Figure 4.13):

**Figure 6.11: Bioluminescent reaction-Renilla luciferase (Renilla reniformis)**

[Adapted from Dual-Luciferase® Reporter Assay System Technical Manual TM040]

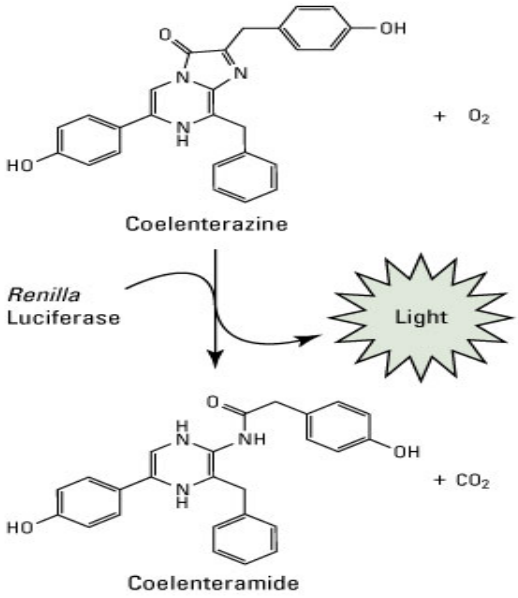

In the DLR™ Assay, Luciferase Assay Reagent (LAR II) is added first to measure and quantify the firefly luciferase reporter luminescence. The reaction is quenched and is followed by addition of Stop & Glo reagent to the same tube that simultaneously initiates the Renilla luciferase luminescent reaction which then decays over the course of the measurement. This integrated assay format provides a rapid quantification of both the reporters in transfected cells

The luminescent signals generated in the Dual-Luciferase Reporter (DLR™) Assay by firefly and Renilla luciferases are shown below (figure 4.14):

**Figure 6.12:** Comparison of luminescent signals generated by firefly and Renilla luciferases

[Adapted from Dual-Luciferase® Reporter Assay System Technical Manual TM040]

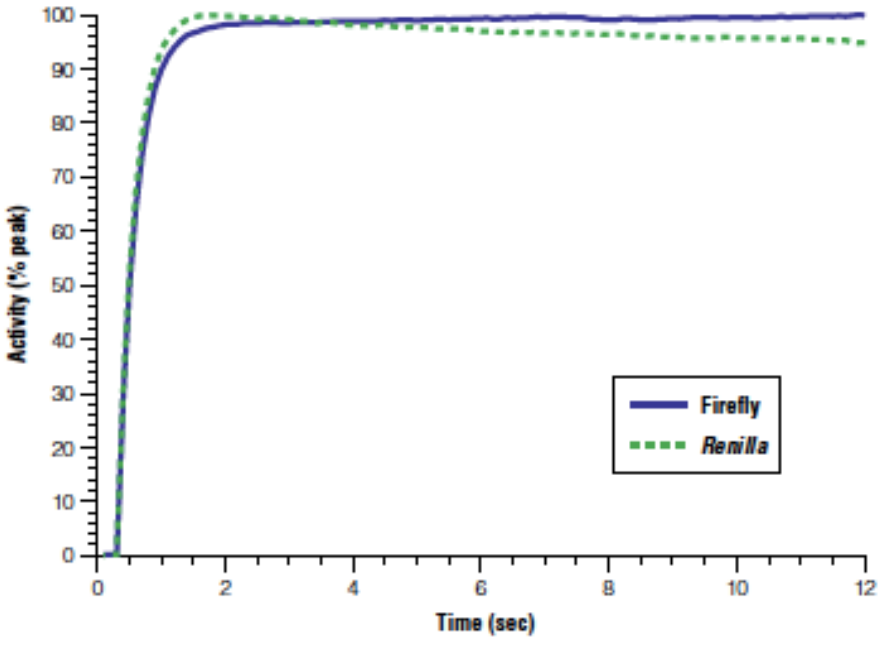

The transcriptional assay experiment using DLR assay consists of the following steps

1. Culture of HEK293T cells and seeding in 24-well plates
2. Addition of reagents containing the wild type and mutant protein with promoter to the cells in the well plate
3. Transfection the cells with Opti-Mem and Lipofectamine
4. Obtaining the cell lysate and measurement of luciferase activity in luminometer

#### 6.5.10.1 Cell culture and Transfection

**Reagents used:**

| |
|---|
| phGT2-294-promoter-luc reporter |
| Renilla SV-40(pRL-SV40 (Promega)) |
| hFOXA2(Wt) |
| hFOXA2(mutant) |
| pBluescript |
| Opti-MEM |
| Lipofectamine 2000 Reagent |

#### 6.5.10.1.1 Cell culture

HEK293T cells were grown in Dulbecco modified Eagle medium (DMEM) supplemented with 10% FBS. 2.5 x $10^5$ cells/well were seeded in 24-well plates.

**Table 6.5:** Quantity of reagents added to each well plate is shown

| | **1** | **2** | **3** | **4** | **5** | **6** | **7** | **8** |
|---|---|---|---|---|---|---|---|---|
| **Renilla SV-40** | 100ng | 100ng | 100ng | 100ng | 100ng | 100ng | 100ng | 100ng |
| **pGL2(empty)** | 200 ng | | | | | | | |
| **hFOXA2(Wt)** | | | 25 ng | 50 ng | 75 ng | 150ng | | |
| **hFOXA2(mutant)** | | | | | | | 25 ng | 50 ng |
| | | | | | | | | |
| **pBluescript** | 200ng | 200ng | 175ng | 150ng | 125ng | 50ng | 175ng | 150ng |
| | | | | | | | | |

| | **9** | **10** | **11** | **12** | **13** | **14** | **15** | **16** |
|---|---|---|---|---|---|---|---|---|
| **Renilla SV-40** | 100ng | 100ng | 100ng | 100ng | 100ng | 100ng | 100ng | 100ng |
| **phGT2-294** | | | 100ng | 100ng | 100ng | 100ng | 100ng | 100ng |
| **hFOXA2(Wt)** | | | | 25 ng | 50 ng | 75 ng | 150ng | |
| **hFOXA2(mutant)** | 75ng | 150ng | | | | | 25ng | 50ng |
| | | | | | | | | |
| **pBluescript** | 125ng | 50ng | 300ng | 275ng | 250ng | 225ng | 150ng | 250ng |

| | **17** | **18** | **19** | **20** | **21** | **22** | **23** | **24** |
|---|---|---|---|---|---|---|---|---|
| **Renilla SV-40** | 100ng | 100ng | 100ng | 100ng | | | | |
| **phGT2-294** | | | 100ng | 100ng | | | | |
| **hFOXA2(Wt)** | | | | | | | | |
| **hFOXA2(mutant)** | 25 ng | 50 ng | 75 ng | 150ng | | | | |
| | | | | | | | | |
| **pBluescript** | 275ng | 250ng | 225ng | 150ng | | | | |
| | | | | | | | | |

#### 6.5.10.1.2 Transfection

1. Opti-Mem medium 150 µL was added to each well.
2. Lipofectamine (2.5 µL) was diluted with 50 µL of Opti-MEM medium and mixed for 5 minutes and added to each well to allow transfection.
3. The transfected HEK293T cells and the cells are incubated at 37ºC for 24 hours.

#### 6.5.10.1.3 Preparation of Cell Lysates

1. Passive Lysis Buffer 1X working solution was prepared by adding 1 volume of 5X Passive Lysis Buffer to 4 volumes of distilled water and mixing well.
2. The growth medium was removed from the cultured cells and sufficient amount of phosphate buffered saline(PBS) was added to wash the surface of the culture vessel.
3. 100 µL of 1X Passive Lysis Buffer was added to each well and the culture plates were placed on a rocking platform at room temperature for 15 minutes.

#### 6.5.10.1.4 Preparation of Luciferase Assay Reagent II (LAR II)

LAR II was prepared as per the manufacturer's instructions by re-suspending the lyophilized Luciferase Assay Substrate in 10 ml of Luciferase Assay Buffer II

#### 6.5.10.1.5 Preparation of Stop & Glo Reagent

Stop & Glo is supplied at 50X concentration. 1 volume of 50X stop & Glo substrate was added to 50 volumes of Stop & Glo buffer.

The steps followed to record the luciferase activities from the luminometer are described below and represented in figure 4.15:

1. The luminometer was set to dispense 100µL of luciferase and the injector was primed initially with 100 µL LAR II.
2. 20 µL of the cell lysate was added to the wells of the multiwell plate.
3. The samples were then placed in the luminometer which will cause the LAR II solution to be injected into the reaction vessel.
4. The measurement of the luciferase activity was recorded by the attached computer.
5. Following this, the luminometer was formatted to dispense 100 µL of Stop & Glo reagent.
6. As before, 20 µL of the cell lysate was added to the wells of the multiwell plate and the Renilla luciferase activity was recorded.

**Figure 6.13:** Sequential steps inside the luminometer

[Adapted from Dual-Luciferase® Reporter Assay System Technical Manual TM040]

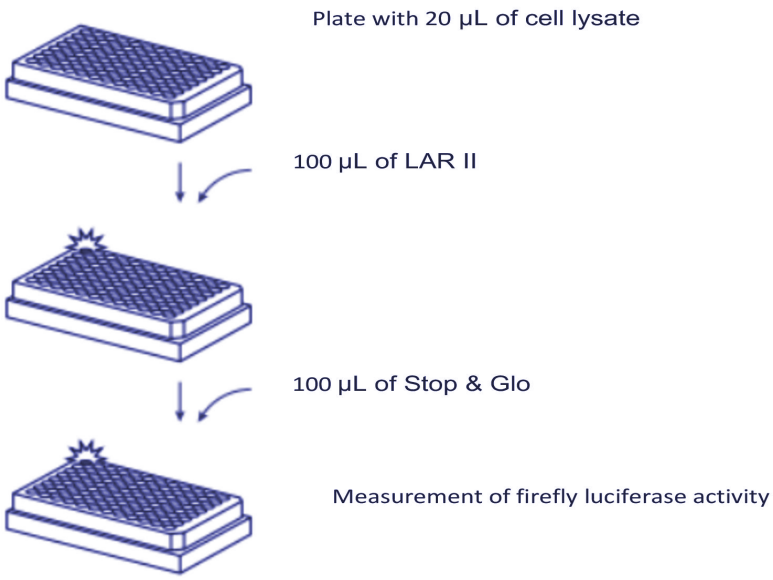

## 6.6 BRIEF DESCRIPTION OF SPECIFIC METHODS

### 6.6.1 *In situ* hybridization

Wild type mouse embryos at different embryonic stages of development (e.11.5, e12.5, e13.5, e15.5 and e18.5) were collected, fixed with 4% paraformaldehyde (PFA) and washed in PBS before proceeding with paraffin embedding. Following this, the paraffin-embedded embryos were sectioned at 7 µm thickness for histochemical evaluation. Using decreasing ethanol dilutions, the sections were deparaffinised, rehydrated and fixed with 4% PFA and incubated with triethanolamine and acetic anhydride. The digoxigenin-labeled anti-sense probe for mFoxa2 was generated by in vitro transcription using T3 RNA polymerase and hybridization was carried out overnight at 65°C. The sections were washed in 0.1 M Tris-HCl Buffer followed by 1 hour blocking at room temperature and overnight incubation at 4°C with anti-Dig antibody. Detection of mFoxa2 was achieved by colorimetric reaction using 4-Nitro blue tetrazolium chloride solution and 5-Bromo-4-chloro-3-indolyl phosphate disodium salt Images were acquired using a Leica microscope.

### 6.6.2 Immunohistochemistry

Paraffin-embedded human embryonic tissue samples at 6, 8 and 13 weeks of gestation were obtained from the Human Developmental Biology Resource (Institute of Genetic Medicine, Newcastle, and Institute of Child Health, London; www.hdbr.org). The sections were deparaffinised and rehydrated through decreasing ethanol dilutions. This was followed by heat-induced antigen retrieval with a microwave in 10 mM sodium citrate buffer (pH 6). The sections were incubated for 1hr in blocking buffer [1XPBS, 0.1% Triton X-100, 5% Normal Goat Serum (Vector Laboratories)]. Endogenous hFOXA2 was detected with a primary rabbit monoclonal antibody against hFOXA2 (Thermo Fisher Scientific; 701698; 1:250) followed by a secondary biotinylated goat anti-rabbit antibody (Vector Laboratories; BA-1000; 1:300). Staining was achieved using DAB Peroxidase Substrate Kit (Vector Laboratories; SK-4100). The colorimetric reaction was stopped with washes in water and the sections were counterstained using Haematoxylin (Sigma-Aldrich). Images were acquired using a Leica microscope.

### 6.6.3 Plasmids and Site-Directed Mutagenesis

Full length cDNA of human *FOXA2* (GENE Bank RefSeq NM 021784.4) was cloned in ORF mammalian expression vector pCMV3 (pCMV3-hFOXA2, Sino Biological Inc). E.coli DH5$\alpha$ competent cells were transformed with hFOXA2 (cDNA size: 1392 bp). The detected mutation was introduced by site-directed mutagenesis using QuikChange II XL Site-Directed Mutagenesis Kit (Agilent Technologies) according to the manufacturer`s instructions (primers used, Forward strand: 5'-CAAAGCCGCCCTACCCGTACATCTCGCTC-3'. Reverse strand: 5'-GAGCGAGATGTACGGGTAGGGCGGCTTTG-3'). Sanger sequencing confirmed the point mutation.

### 6.6.4 Cell Culture and Luciferase Assays

HEK293T cells were grown in Dulbecco modified Eagle medium (DMEM) supplemented with 10% FBS. 2.5 x $10^5$ cells/well were seeded in 24-well plates. phGT2-294-promoter-luc reporter (kindly provided by Professor Yong-Ho Ahn), 200ng and Renilla SV-40, 100ng were transiently co-transfected with either i) equal amounts (50 ng and 75 ng) of Wt or mutant p.S169P hFOXA2 expression plasmids or ii) both Wt and mutant p.S169P hFOXA2 expression plasmid (25 ng or 37.5 ng of each plasmid) using Lipofectamine 2000 (Life Technologies) according to the manufacturer's instructions. 500 ng of pBluescript plasmid was added to keep the total amount of transfected DNA constant. The cells were harvested 24h after transfection and the luciferase activity was measured using the Dual-Luciferase Reporter Assay System (Promega) in a BMG LABTECH Microplate reader (Omega, Germany) according to manufacturer's instructions. Firefly luciferase activity was normalised to the Renilla luciferase expression from pRL-SV40 (Promega). The experiments were independently repeated four times in triplicates and statistical analysis was performed using one-way ANOVA.

### 6.6.5 Western Blotting

Equal amounts (200 ng) of Wt or mutant p.S169P hFOXA2 expression plasmids were transiently transfected in HEK293T cells in 24-well plates using Lipofectamine 2000 and harvested 24 hours after the transfection in a lysis buffer. 300 ng of pBluescript plasmid were added to each transfection mix to maintain the total amount of DNA constant at 500 ng. The samples were than loaded on 12% polyacrylamide gel and transferred on a nitrocellulose membrane. Using 5% dried skimmed milk in PBS-T, the nonspecific binding sites were blocked for 1h. This was followed by the incubation of membrane overnight at 4°C with the primary antibody, rabbit anti-FOXA2 followed by

one-hour incubation with IRDye 800CW Donkey anti-rabbit antibody. Anti-GAPDH (Santa Cruz; 1:5000, rabbit polyclonal) levels were used to normalise the total level of protein. Blots were analysed using Odyssey 2.1 Imaging System (LI-COR Biosciences). The experiments were independently repeated six times and the statistical analysis was performed using one-way ANOVA.

### 6.6.6 Immunocytofluorescence

1 x $10^5$ cells/well were seeded in 4-well cell culture slide (Millipore, Fisher Scientific) and transiently transfected with 200 ng of Wt or mutant p.S169P hFOXA2 expression plasmids and 300 ng of pBluescript plasmid using Lipofectamine 2000 according to the manufacturer's instructions. 24h after transfection, the cells were fixed in 2% PFA in 1X PBS for 10 min and washed with 1X PBS three times. Samples were permeabilised with 0.1% Triton X-100 in 1X PBS for 30 min and blocked with blocking buffer (5% Normal Goat Serum in 1X PBS) for 30 min. The staining was performed by incubating the samples with α-FOXA2 antibody (Thermo Fisher Scientific; 701698, 2ug/ml) in blocking buffer for 1h, followed by a 30 min incubation with goat α-rabbit Alexa fluor 594 (ThermoFisher Scientific; 1:250) and α-PHALLOIDIN Alexa fluor 488 (Molecular Probes; 1:1000) antibodies. The cell nuclei were stained with DAPI (4',6-diamidino-2-phenylindole).

# 6.7 RESULTS FROM THE *IN VITRO* EXPERIMENTS

### 6.7.1 *Foxa2* mRNA expression during Murine Embryonic Development

The mRNA expression panels are shown in figure 6.5.

At embryonic day e11.5 (A) *Foxa2* mRNA transcripts were expressed within the midbrain(MB) and ventral hindbrain(HB). The mRNA was also localised to a few cells localised in the forebrain (FB) (A, asterisk). At this stage of development, no transcripts were detected in the primordium of the anterior pituitary gland, the Rathke's pouch(RP) (dotted line in A and A'), or in the infundibulum(Inf).

At e12.5 (B and B') *Foxa2* mRNA transcripts were detected in the epithelial structures lining the main bronchus (MBr) (B, arrowhead) and in the epithelium lining the lung and oesophagus (B', arrowheads). By e13.5, expression of *Foxa2* appears localised in the ventral side of the anterior lobe(AL) of the developing pituitary gland (C, arrow) with transcripts localised in the ventral marginal zone (C', arrowhead). *Foxa2* mRNA expression was stronger at e15.5 (D) with robust expression in the ventral diencephalon (VD) (asterisk), posterior lobe (PL) and anterior lobe (AL) (arrowheads in D') of the pituitary gland. At embryonic day e18.5 (E), expression was found wide spread in the central nervous system, with strong expression in the lumen surrounding the lateral ventricles (LV) (E, arrowheads) and the third ventricle (TV) (E, asterisks). The mRNA expression was also localised in in the hypothalamic area (Hyp) (E', arrowheads) at e18.5 with distinct pattern in the luminal area where the hypothalamic precursors tanycytes reside (arrowheads in E'). mRNA transcripts were also localised in both the posterior and anterior lobes of the pituitary gland (arrows in E').

**Figure 6.14:** mRNA expression of *Foxa2* during mouse embryonic development

A-D represent sagittal sections, with anterior to the left side, and E is a coronal section. A', C', D', E' show higher-magnification views of the boxed areas in A, C, D, E, respectively. Abbreviations: midbrain, MB; hindbrain, HB; forebrain, FB; Rathke's pouch, RP; infundibulum, Inf; main bronchus, MBr; lung, Lu; oesophagus, OE; ventral diencephalon, VD; pituitary gland posterior lobe, PL; pituitary gland anterior lobe, AL; lateral ventricles, LV; third ventricle, TV; hypothalamus, Hyp. Scale bars represent: 50 µm (A', B, C', D'); 100 µm (B'), 250 µm (A, C, D, E'); 500 µm (E).

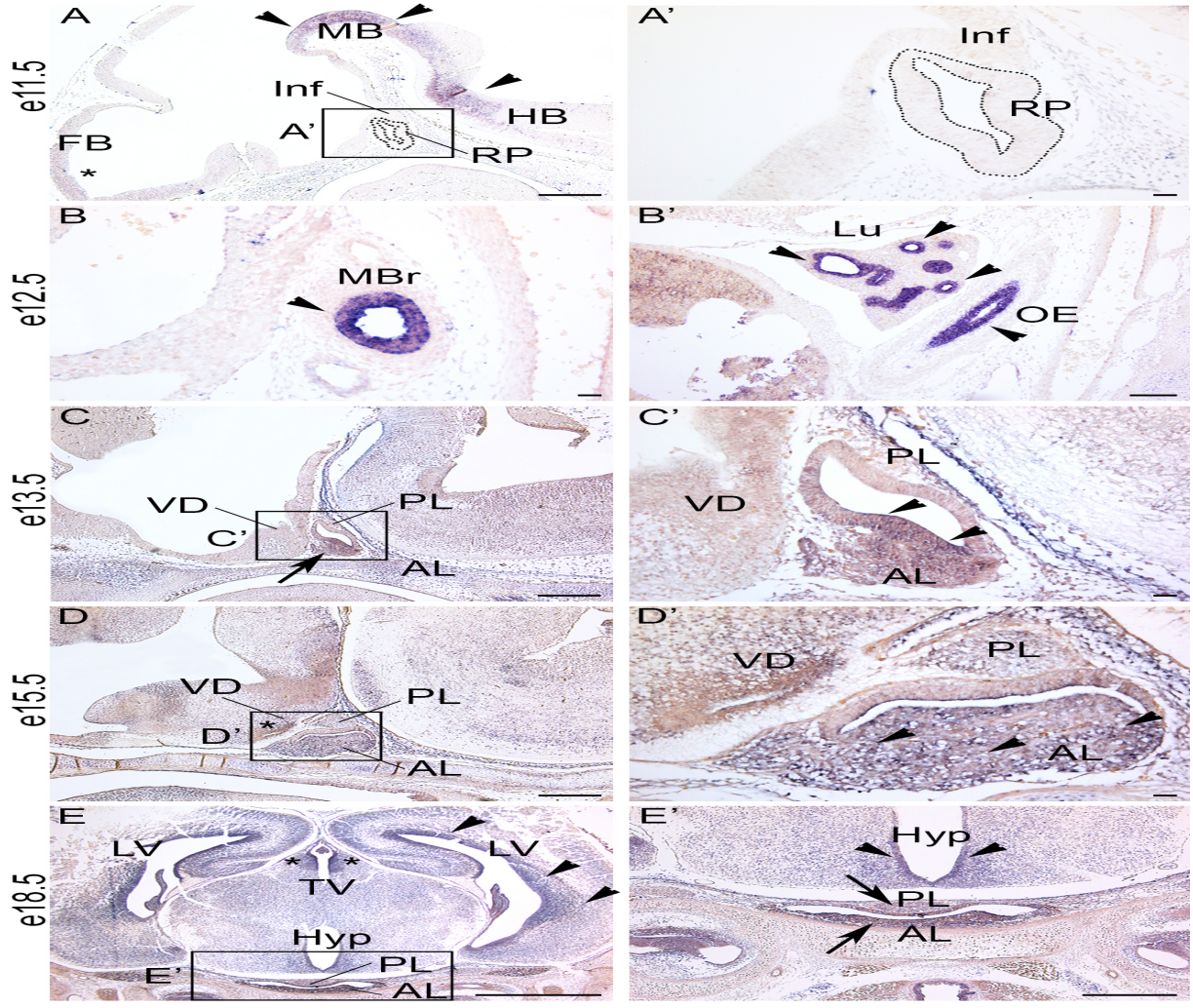

### 6.7.2 *FOXA2* Expression during Human Embryonic Development

The hFOXA2 expression panels are shown in figure 6.6.

The immunohistochemical analysis in human embryos at various developmental stages showed FOXA2 expression at 6 weeks of gestation (Carnegie stage 16) (A, figure 6.6) and in the developing neural tube (NT) (A') and diencephalon (Dc) (arrowheads in A''). The expression is localised in the epithelium surrounding the third ventricle (TV) (B') and in the cells lining the diencephalon (Dc) from 8 weeks of gestation (arrowheads in B''). (Carnegie stage 23) No expression of Foxa2 was detected in the primordium of the pituitary gland (Rathke's pouch, RP) at CS16 (A''') nor in the developing pituitary gland at CS23 (B'''). In the pancreas at 13 weeks of gestation (C) Foxa2 was specifically localised in the cytoplasm of cells scattered in the pancreatic parenchyma (cells pointed by arrowheads in C' and C'').

**Figure 6.15:** FOXA2 expression during human embryonic development

A-C represent coronal sections of human embryos at 6 weeks (Carnegie stage 16), 8 weeks (Carnegie stage 23) and 13 weeks of gestation, respectively. A'-C'' show higher-magnification views of the boxed areas in A, B, C, respectively. Abbreviations: neural tube, NT; diencephalon, Dc; Rathke's pouch, RP; pituitary gland, P; third ventricle, TV. Scale bars represent: 50 µm (A', A'', A''', B', C''); 100 µm (B'', B'''), 250 µm (C').

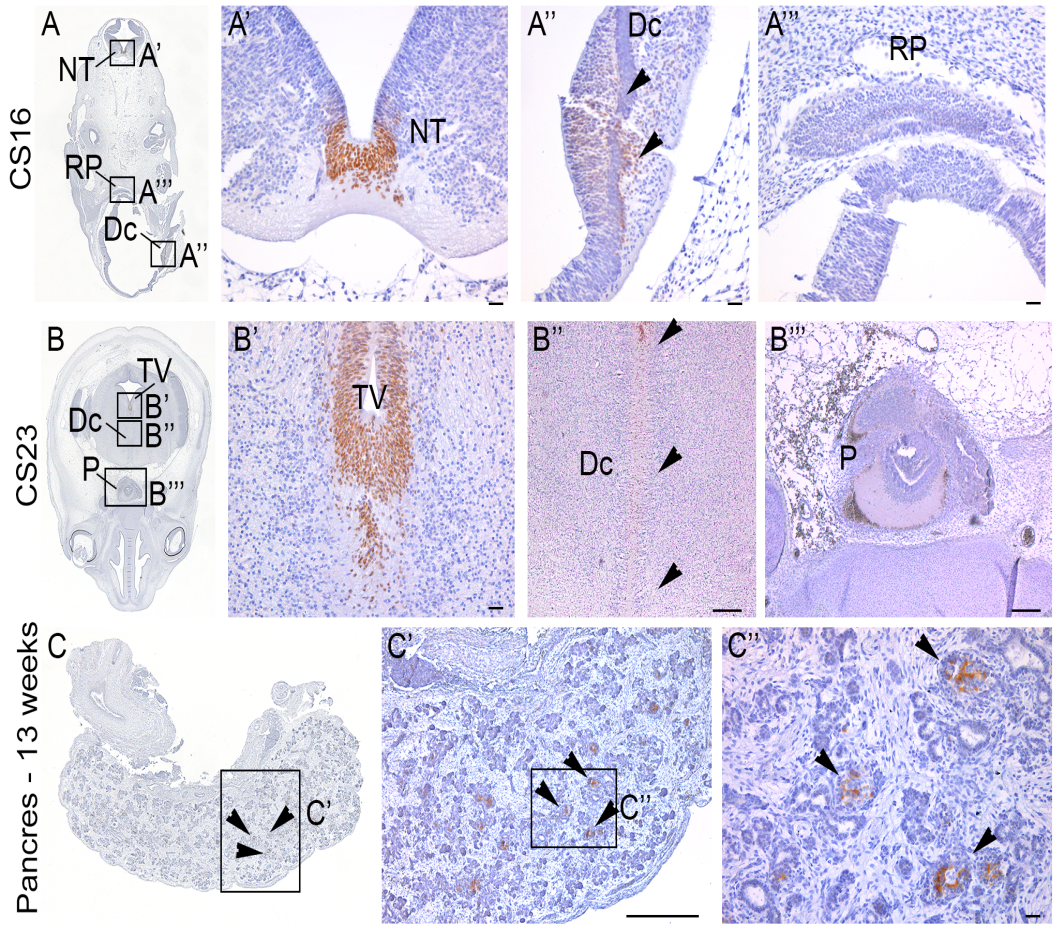

### 6.7.3 Immunocytofluorescence

Using double immunofluorescence on transiently transfected HEK293T cells, it was demonstrated that both the Wt hFOXA2 and mutant hFOXA2 are expressed in the nucleus and the mutation did not result in changes to cellular localization

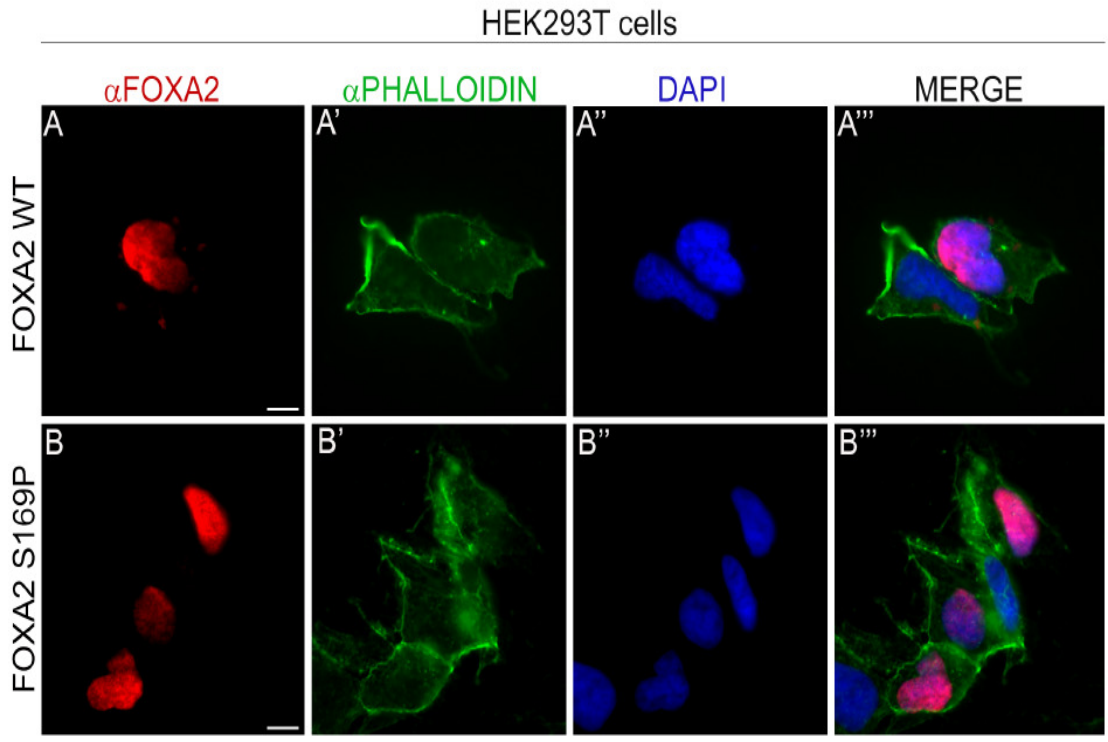


**Figure 6.16:** Double-immunofluorescence using anti-FOXA2 antibody (red A,B) and anti-PHALLOIDIN (green A',B') performed in HEK293 cells transiently transfected with either 200 ng of Wt hFOXA2 (A-A''') or mutant hFOXA2 p.S169P (B-B''') shows nuclear expression of both Wt and mutant FOXA2 (A,B) which overlaps with the nuclear DNA marker DAPI staining (A'', B'') but not with the cytoskeletal marker phalloidin. Abbreviation: DAPI, 4',6-diamidino-2-phenylindole. Scale bars in A and B represent 10 µm.

### 6.7.4 Dual Luciferase Transcriptional Assay

Transcriptional activation assay was performed using the *GLUT2* promoter coupled to luciferase (phGT2-294-promoter-luc) and using HEK293T cells. HEK293T cells were transiently co-transfected with equal quantities of Wt hFOXA2 or mutant hFOXA2 p.S169P and it was demonstrated that the hFOXA2 p.S169P significantly impaired the transcriptional activation of the *GLUT2* luciferase reporter (Figure 6.8).

**Figure 6.17: Dual luciferase transcriptional assay** (graph represents 4 independent experiments performed in triplicate, * p<0.05, one-way ANOVA).

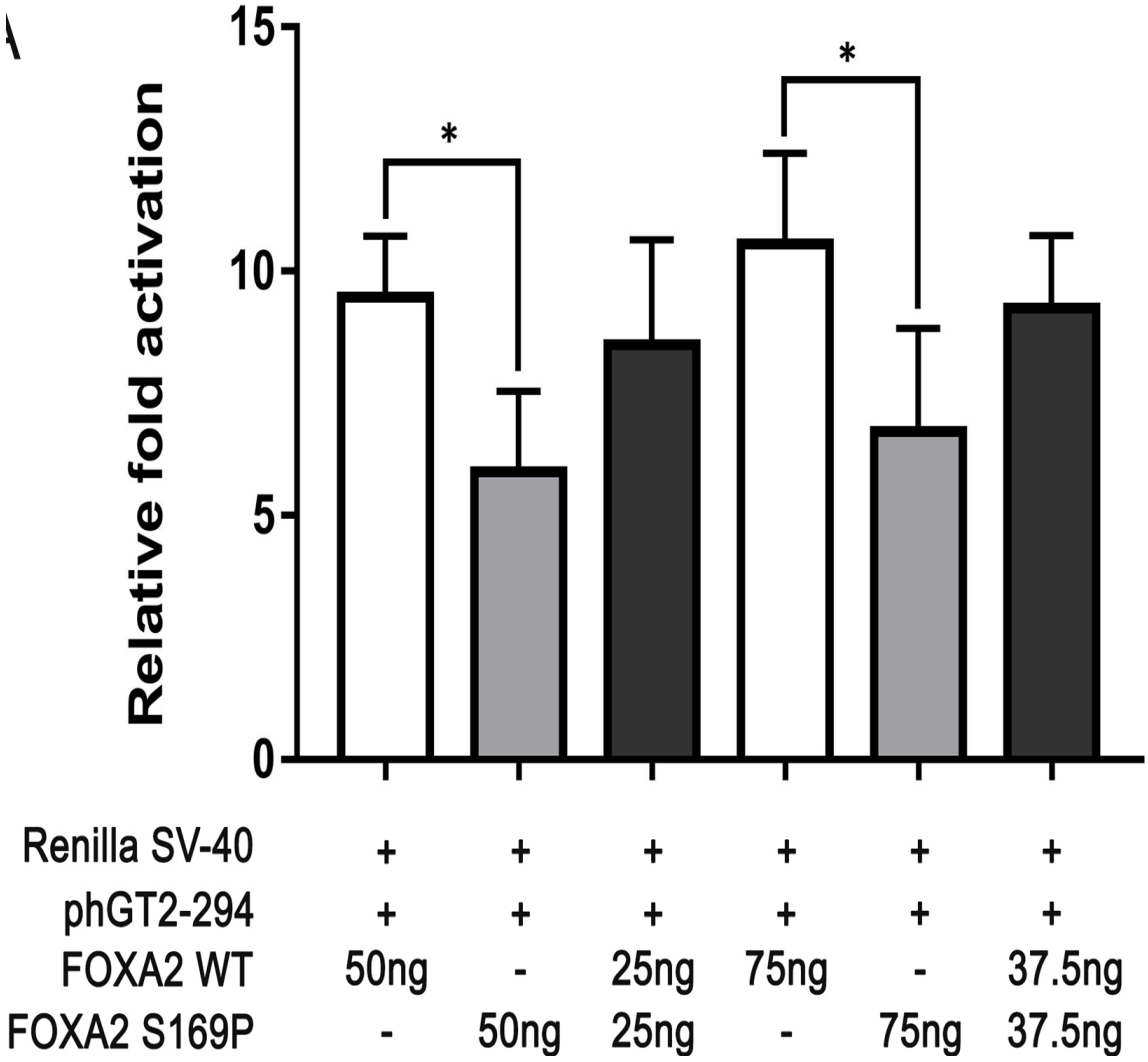


The serine to proline change in position 169 of hFOXA2 results in decreased protein expression levels leading to impairment of transcriptional activation of the human GT2 promoter. Dual luciferase assay in HEK293T cells transiently transfected with 50 ng or 75 ng of Wt hFOXA2 or mutant hFOXA2 p.S169P indicates that Wt hFOXA2 is able to transactivate the human GT2 reporter, whilst the hFOXA2 p.S169P transcriptional activation is impaired.

### 6.7.5 Western Blot Assay

The quantification of protein expression using western blot showed that mutant hFOXA2 p.S169P resulted in significantly reduced protein expression levels compared to the Wt hFOXA2 (figure 6.9). Three independent western blots showed that the levels of the variant hFOXA2 p.S169P protein were reduced compared to the Wt hFOXA2, indicating that the mutation is functional and affects protein levels.

**Figure 6.18:** Western blot assay

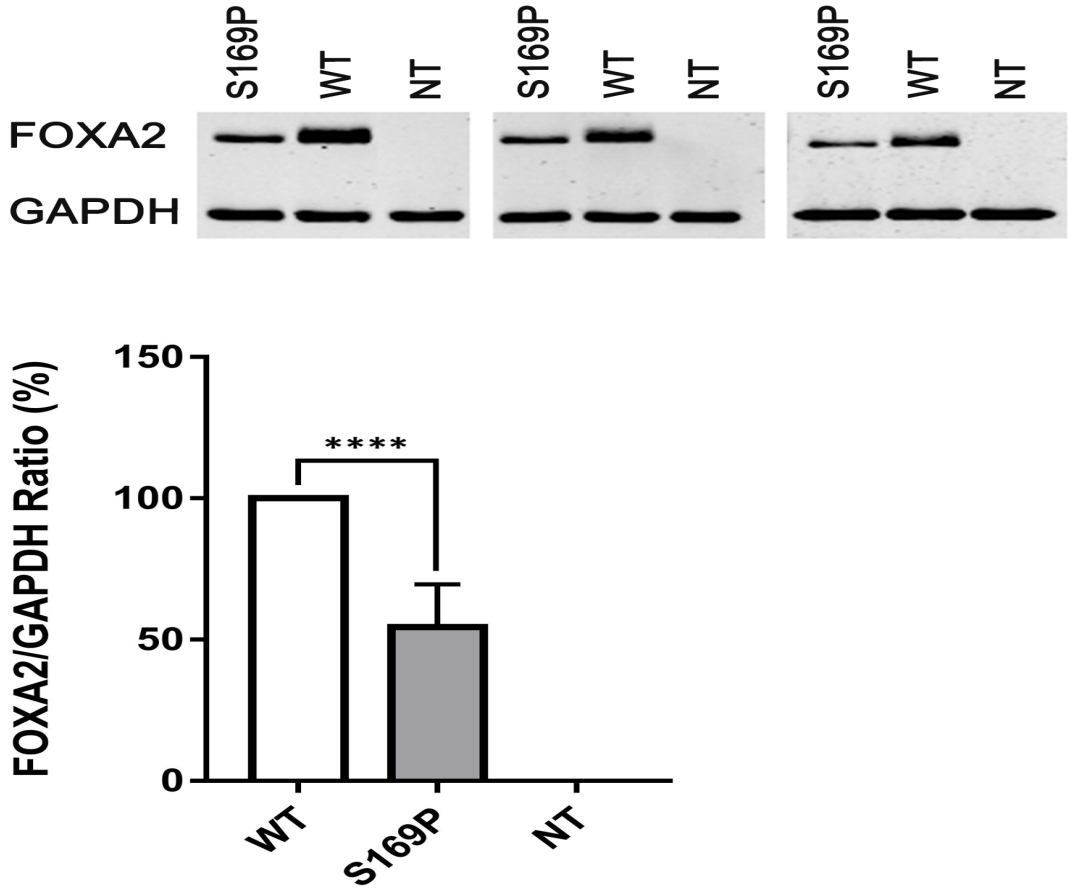


Graph of the quantification of the western blots as percentage of Wt hFOXA2 and hFOXA2 p.S169P normalised to GAPDH indicates that hFOXA2 p.S169P variant results in half of the protein expression levels compared to Wt hFOXA2 (results from 6 independent experiments; **** $p < 0.0001$, one-way ANOVA). Abbreviation: NT, non-transfected; Wt, wild-type

## 6.8 DISCUSSION

Deletions within the cytogenetic location 20p11.2 which contains *FOXA2* as one of the genes have been noted to be associated with clinical phenotype that include hypopituitarism, central nervous system (CNS) defects, hypoglycaemia, facial dysmorphic features and congenital abnormalities of the heart, liver and gastrointestinal tract (258-262). The minimal critical region in this region of 20p11.2 has been mapped to contain 20 genes including *FOXA2* (261) (258). All the patients reported to have the 20p11.2 chromosomal deletion have hypopituitarism, CNS abnormalities and facial dysmorphic features as shared features, strongly indicating that a gene or multiple genes within this chromosome region have a key role in CNS, pituitary and facial development.

Proband A with the rare clinical phenotype of hypopituitarism, CHI, dysmorphic features, liver, pancreas, heart and gastrointestinal abnormalities was found to have a *de novo* heterozygous mutation in the developmental transcription factor *FOXA2* thus identifying the gene responsible for the clinical phenotype of hypopituitarism and hypoglycaemia at the 20p11.2 region. The c.505T>C, p.S169P genetic variant occurring at the conserved forkhead DNA binding domain may provide tissue-specific gene regulation important for the development of multiple organs. The biochemical data demonstrate that the mutation impairs the transcriptional activation of *FOXA2* resulting in lower activation of the glucose transporter type 2 gene (*GLUT2*).

Furthermore, the clinical phenotype of proband A: hypopituitarism, CHI and facial dysmorphic features overlaps with the clinical data published in patients with 20p11.2 deletions (258-262). The impaired transcriptional activation of the phGT2-294-promoter-luc reporter and significant reduction in the protein expression by hFOXA2 p.S169P compared to wild type hFOXA2 demonstrates the pathogenicity of the mutation.

The key signalling pathways important in ventral midline, pituitary and CNS development such as Shh signalling have been shown to be regulated by *FOXA2*. Data from *in vivo* studies using *Wnt1:Cre;Foxa2*$^{flox/flox}$ embryos showed that *Foxa2* has an early role in the initiation of Shh expression (244). Hence it is potentially possible that hFOXA2 mediates the development of pituitary by regulating the expression of Shh. Furthermore, the expression of intracellular transducers and downstream targets of Shh signalling such as Ptch1,Gli1 and Gli2, which regulate the patterning of the ventral midbrain (246) have been shown to be downregulated by *Foxa2* in combination with *Foxa1*.

The midline defects encountered in proband A such as single median maxillary central incisor (SMMC), congenital nasal pyriform aperture stenosis (CNPAS) are often associated with pituitary abnormalities, as described in an extensive literature review by Lo et al. (263). The authors described that hypopituitarism or growth hormone deficiency were present in 43-48% of patients with CNPAS or SMMC. This is consistent with the clinical presentation of proband A, who has hypopituitarism along with hypoplastic pituitary, thin corpus callosum and thin pituitary stalk on the MRI.

The potential role of *FOXA2* in the pituitary development is suggested by the detection of *Foxa2* mRNA transcripts from the early stages of mouse pituitary and brain embryonic development Furthermore, the detection of hFOXA2 by immunohistochemistry in human embryos at various developmental stages, along with the biochemical experiments demonstrating that the variant p.S169P mutation in *FOXA2* impairs transcriptional activation and protein expression levels, strongly indicate that *FOXA2* has a pivotal role in hypothalamic-pituitary axis formation in humans.

Hypoglycaemia in CHI is caused by unregulated insulin secretion while in hypopituitarism it is due to the lack of counter-regulatory hormonal response due to the deficiency of ACTH and GH. Diagnosis can often be challenging, as the hallmark of CHI is detectable insulin in the presence of hypoketotic hypoglycaemia while hypopituitarism causes ketotic hypoglycaemia. The co-existence of hypopituitarism along with a persistent form of hyperinsulinism, as encountered in proband A, is extremely uncommon. Almost half of the patients with persistent CHI do not have mutations in the already recognized genes known to cause CHI. Genetic diagnosis is important as it will inform the prognosis, recurrence risk and guide the medical management besides providing valuable insight into β-cell physiology. The negative mutations in the known CHI genes in proband A together with strong biochemical evidence of CHI makes it highly likely that the CHI is due to a novel genetic aetiology (*FOXA2*). The immunohistochemistry data from this study supports this as there is a good expression of hFOXA2 in the developing human pancreas and a functional role of the hFOXA2 p.S169P mutation.

The closure of ATP dependent potassium channels situated on the β-cell membrane with the resultant depolarization of the membrane results in glucose-stimulated insulin secretion by the exocytosis of the insulin granules (264, 265). The most common form of genetic CHI is due to the mutations in genes encoding the KATP channels (*ABCC8* and *KCNJ11)* (264, 265). Lantz et al. demonstrated that when SUR1 or Kir6.2 promoter/luciferase reporter was transfected with *Foxa2* expression plasmids, *Foxa2*-Sur1 promoter constructs showed 6-fold activation and 4-fold activation was demonstrated on *Foxa2*-kir6.2 constructs implying a vital role of *Foxa2* in the transcriptional activation of the KATP subunits (252). Mutations in *HADH* cause CHI in humans. *HADH* encodes L-3-Hydroxyacyl-CoA-dehydrogenase (HADH), an enzyme involved in the penultimate step of the beta-oxidation pathway (266). *Foxa2* has also been shown to directly target *HADH* causing its transcriptional activation (252, 267) in mice experiments. Pancreatic β-cell specific knock out of *Foxa2* in mice has been shown to have a 3-fold downregulation of *Hadh* mRNA resulting in severe hyperinsulinaemic hypoglycaemia (251, 268). Wang et al. demonstrated that mRNA levels of glucokinase(*GCK*) is decreased upon induction with *Foxa2* in rat insulinoma cell line (INS-1) while loss of Foxa2 function causes *GCK* upregulation (196).

The regulation of genes involved in insulin secretion by *FOXA2* is represented in the figure 6.10.

**Figure 6.19:** Regulation of genes involved in insulin secretion by *FOXA2. FOXA2* upregulates *KCNJ11, ABCC8, HADH* and downregulates *GCK.*

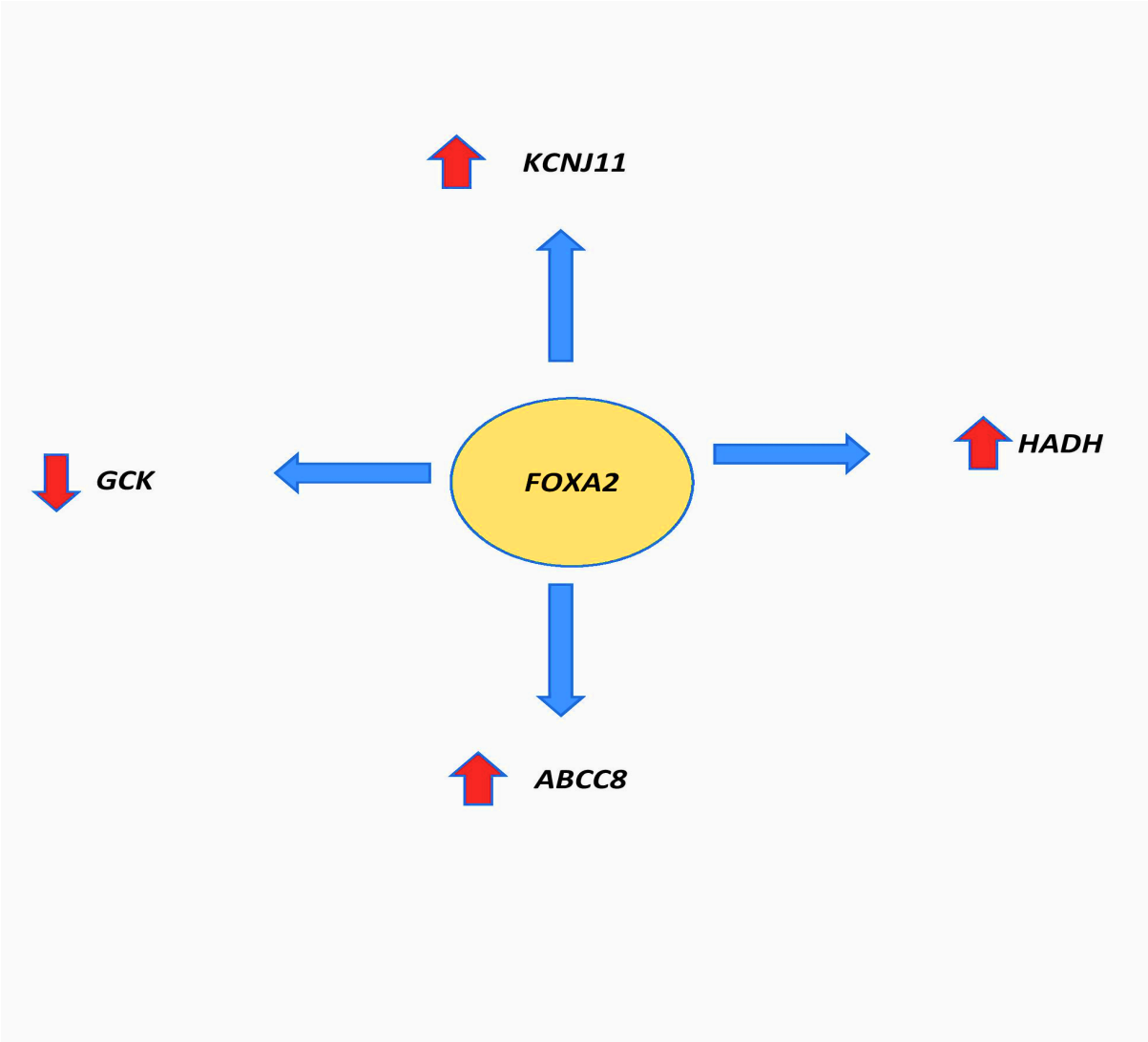

The main role of *GLUT2,* located in the plasma membrane of the pancreatic β-cells, liver, kidney, intestine and its main role is to facilitate the transport of glucose across the membrane and the secretion of insulin (197).The mRNA level of *GLUT2* is influenced by the plasma concentrations of glucose and insulin(269). Cha *et. al* demonstrated *GLUT2* has binding sites for *FOXA2* and showed that the promoter activity of *GLUT2* is synergistically activated by *HNF1* and *HNF3*β *(268)*. The reduction in the transcriptional activation of the *GLUT2* reporter (phGT2-294-promoter-luc) by the mutant hFOXA2 (p.S169P) shown in the transcriptional luciferase assay experiment, could imply that the *GLUT2* tissue expression is reduced in the pancreatic β-cells contributing to CHI in proband A.

Furthermore, data from Lantz et al., demonstrate that *FOXA2* potentially affects the activation of other genes involved in the insulin secretion, and thus a potential candidate gen for CHI. It is also plausible that *Foxa2* could play a role in the development of the pancreas as well as β-cells. *Foxa2* has not only been shown to regulate *Pdx1*, a homeobox gene essential for pancreatic development (267) but has also been linked to regulating the mRNA levels of pancreatic transcription factors such as *Hnf4a* and *Hnf1a*, mutations of which can cause monogenic forms of diabetes. However, some studies contradict that *Foxa2* is an upstream regulator of Pdx1,Hnf4a and Hnf1a (269) . While it has been shown that β-cell-specific deletion of *Foxa2* in mice causes a phenotype of hypoglycaemia (251), it also has been demonstrated it can cause downregulation of *Pdx1* mRNA causing the reduction of PDX-1 protein levels in the pancreatic islets (270) and a targeted β-cell-specific deletion of Pdx1 results in diabetes in transgenic mice (271). Thus, *FOXA2* is a crucial transcription factor that controls the expression of multiple genes involved both in glucose sensing

and glucose homeostasis and therefore has a potential role in diseases involving insulin secretion and glucose homeostasis.

Diazoxide is used as an effective treatment in majority of patients with CHI except in those situations where the CHI is due to mutations abolishing the KATP channel activity (*ABCC8* or *KCNJ11*) or activating mutations in *GCK*. Proband A's response to the treatment with diazoxide could potentially imply that the KATP channel activity has not completely abolished by the variant p.S169P.

*FOXA2* (p.S169P) is the first disease-causing mutation in proband A with an extremely rare complex phenotype of CHI, cranio-facial dysmorphic features, CH, cardiac, liver and gastrointestinal abnormalities. Identification of the genetic cause contributing to such a unique clinical phenotype will help medical management and provide valuable insights into molecular mechanisms underlying pituitary development and β-cell physiology.

# CHAPTER 7

# CLINICAL PHENOTYPE AND WHOLE EXOME SEQUENCING RESULTS (FAMILY B)

## 7.1 SUMMARY OF CHAPTER 7

Chapter 7 begins with the detailed description of the phenotype of proband B from Family B, results from whole exome sequencing followed by a detailed discussion of compound heterozygous *ASXL3* mutations (c.2965C>G, p.R989G and c.3078G>C, p.K1026N).

The manuscript of this chapter is now published. The pdf of the published version is attached in the appendix.

## 7.2 CLINICAL INFORMATION (PROBAND B)

Proband B is a 16-year-old Caucasian British boy born at full term following an induction of labour by ventouse delivery to non-consanguineous Caucasian British parents. The antenatal scans were normal and the birth weight was 4.1 kg (1.84 SDS). He was admitted to the neonatal unit as he was noted to be grunting soon after birth. Whilst in the special care, he had feeding difficulties and required tube feeding. At 4 months of age he required surgical fixation for scaphocephaly. He had bilateral undescended testes and required orchidopexy. From 5 weeks of age he had persistent severe constipation and required daily bowel washouts from 18 months of age followed by colostomy at 3 years. He also has global developmental delay and complex learning difficulties requiring additional support at school. He also has been diagnosed with autism. He was referred to endocrinology assessment of his severe short stature at 7 years of age (-4.11 SDS, Mid Parental Height: -1.1 SDS). He was found to have a normal growth hormone (GH) response (peak GH 11.7µg/l) (Normal:>6.7 µg/l) to an arginine stimulation test. He had a bone age delay of 3 years and the IGF1 was persistently low at 4.9nmol/l (-3.2 SDS). The other baseline pituitary hormones including thyroid function, ACTH, prolactin and cortisol concentrations were all within the normal range. A trial of hGH (50µg/kg/day) was ineffective in improving height velocity (Figure 7.1). An IGF1 generation test after 33 µg/kg of hGH did not produce any response. Subsequently, recombinant IGF1 therapy (mecasermin) was commenced which resulted in improvement of height velocity to -3SDS (Figure 7.1). He has dysmorphic features such as strabismus, prominent forehead and nasal bridge, thin lips, small lower jaw, low set cupped ears, short fifth fingers on both hands, short stature, thickened toenails on his little toes of his feet. He has a normal muscle tone and normal deep tendon reflexes. His cranial MRI scan of brain and spine were

normal. The hearing has been normal. The echocardiogram and renal ultrasound did not identify any abnormalities. The plasma amino acids, urine organic acids, pyruvic acid analysis were within the normal limits. CGH microarray did not reveal any copy number changes. Targeted sequencing of *IGF1, IGF1R* and *GHR* did not reveal any mutations. Currently, the patient continues to require rIGF1 therapy to improve his height. The weight gain continues to be suboptimal (Figure 7.1).

**Figure 7.1:** Growth chart showing height and weight. Improvement in height velocity was noted after commencement of rIGF1

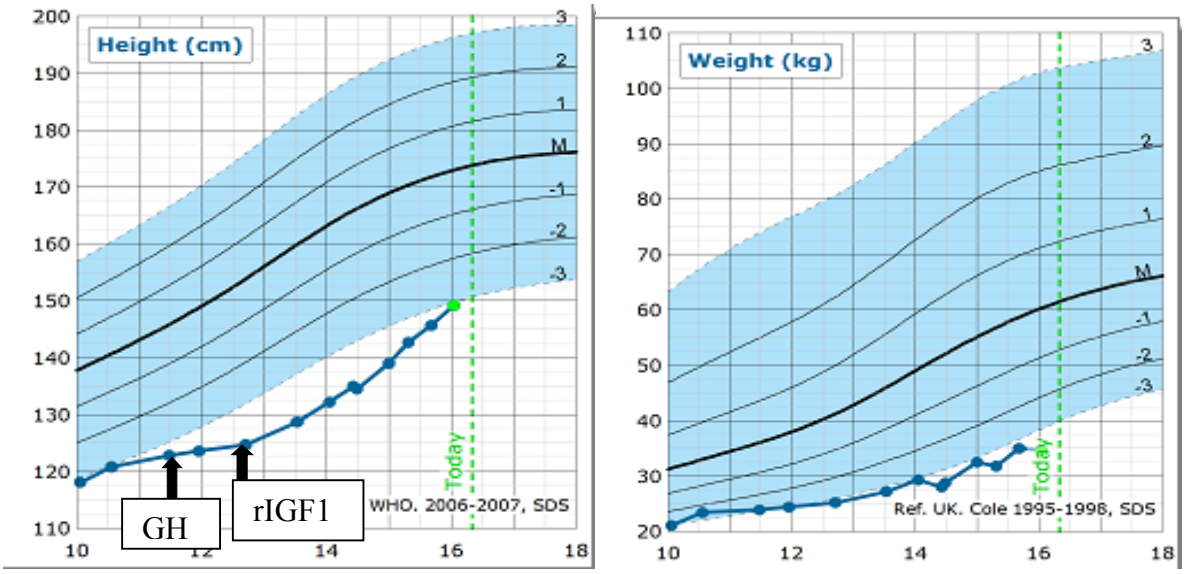


**Figure 7.2:** Pedigree of Family B

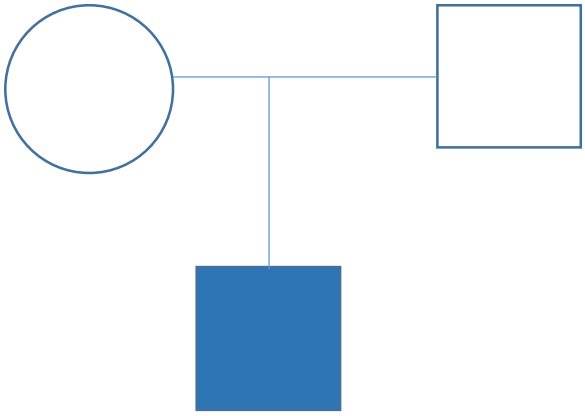

### 7.3 WHOLE EXOME SEQUENCING RESULTS FROM FAMILY B

In this family, whole-exome sequencing was performed on the both the parents(unaffected) and the affected child. Assuming a *de novo* inheritance pattern, filters were applied to whole-exome data as shown in the figure 7.3. The potential candidate variants are listed in the table 7.1.

**Figure 7.3:***De Novo* variant analysis of proband B

De Novo Variant Analysis of Proband B (* Novel variants include variants present in at least 5% minor allele frequency in 1000 Genomes Project, ExAC and NHLBI ESP exomes excluded; ** Predicted deleterious variants included nonsynonymous coding, splice site, frameshift, stop gain variants; *** Variants present in heterozygous state in the child and not present in both the parents)

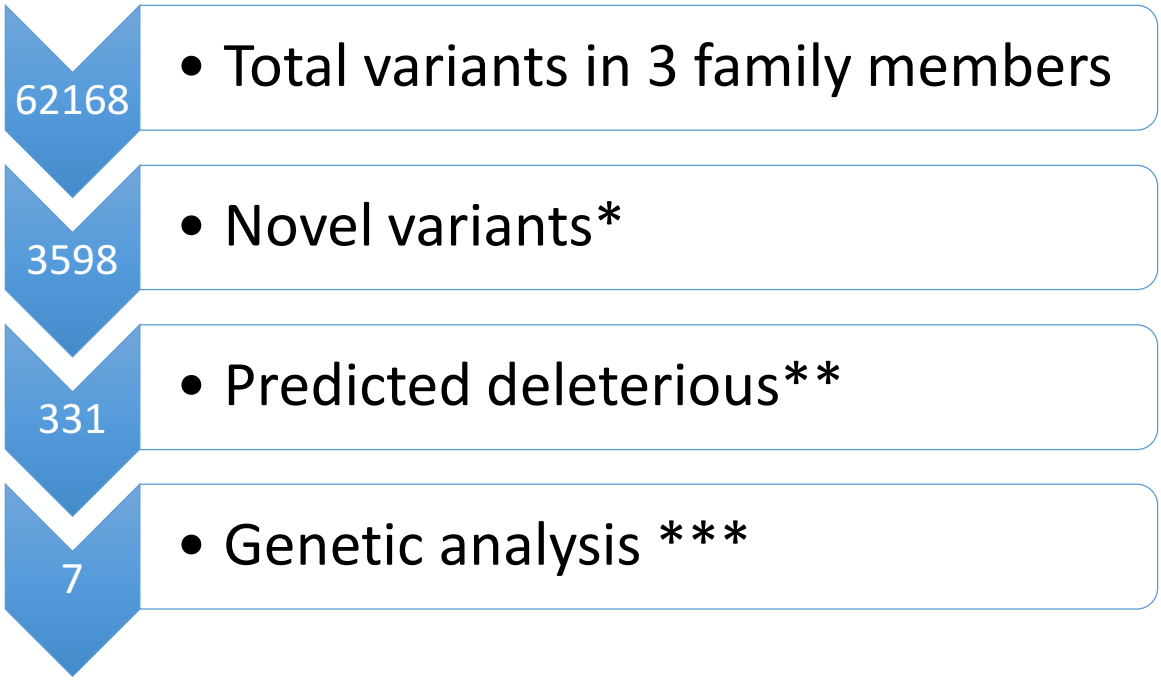

The list of *de novo* variants in proband B are shown below in the table 7.1:

**Table 7.1:** List of *de novo* variants in Proband B

| Chromosome | Gene | Gene region | Protein variant |
|---|---|---|---|
| 2 | PEL1 | Splice site | |
| | | | |
| 3 | ZBTB11 | Splice site | |
| | | | |
| 4 | CORIN | Splice site | |
| | | | |
| 9 | EHMT1 | Exonic | p.A275V |
| | | | |
| 11 | DPF2 | Exonic | p.W369R |
| | | | |
| 17 | KSR1 | Exonic | p.T137P |
| | | | |
| 19 | POP4 | Exonic | p.I177F |

A brief description of these genes is presented next. From the available biological information about these genes, the phenotype of proband B could not be explained with variations in these genes.

**Description of *de novo* variants from proband B**

***PEL1***

From the current literature, the biological information on this gene function is limited.

***ZBTB11*** (Zinc Finger and BTB Domain Containing 11)

From the current literature, the biological information on this gene function is limited.

***CORIN*** (corin, Serine Peptidase)

This belongs to the member of the type II transmembrane serine protease class of the trypsin superfamily that converts pro-atrial natriuretic peptide to biologically active atrial natriuretic peptide (272).Missense mutations of this gene have been associated with pre-eclampsia (273).

***EHMT1*** (Euchromatic Histone Lysine Methyltransferase 1)

The protein encoded by this gene is a histone methyltransferase that is part of the E2F6 complex, which represses transcription. Mutations in this gene are associated with 9q subtelomeric deletion syndrome, Kleefstra syndrome (274).

***DPF2*** *(*Double PHD Fingers 2, also called as Requiem)

This protein functions as a transcription factor which is necessary for the apoptotic response (275).

***KSR1*** (Kinase Suppressor of Ras 1)

This gene promotes phosphorylation of Raf family members and activation of *MAPK1* and/or *MAPK3* (276).

***POP4*** (Processing of Precursor 4)

This gene encodes one of the protein subunits of the small nucleolar ribonucleoprotein complexes: and is involved in processing of precursor RNAs (277).

Assuming a recessive inheritance, the filtering strategy applied to whole-exome sequencing data.

**Figure 7.4: Recessive Inheritance Analysis**

Recessive Variant Analysis of Proband B (* Novel variants include variants present in at least 3% minor allele frequency in 1000 Genomes Project, ExAC and NHLBI ESP exomes excluded; ** Predicted deleterious variants included nonsynonymous coding, splice site, frameshift, stop gain variants; *** Variants present in homozygous/compound heterozygous state in the child)

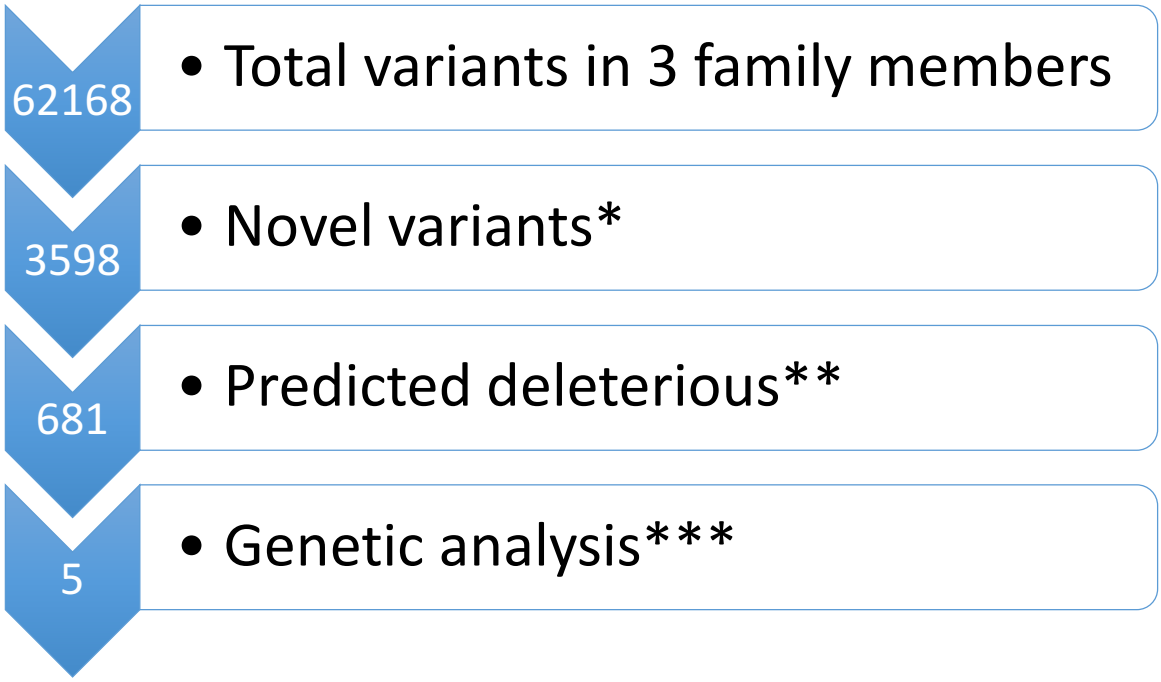

The list of compound heterozygous/homozygous variants from proband B are shown below in table 7.2

**Table 7.2:** List of compound heterozygous/homozygous variants in Proband B

| Chromosome | Gene | Gene region | Protein variant |
|---|---|---|---|
| | | | |
| 1 | MST1L | Exonic | p.H81D/p.G300fs*89 |
| | | | |
| 12 | KLRF2 | Exonic | p.T98R |
| | | | |
| 13 | PABPC3 | Exonic | p.R272del/p.Q292* |
| | | | |
| 14 | WDR89 | Exonic | p.D98E/p.C89Y |
| | | | |
| 18 | ASXL3 | Exonic | p.R989G/p.K1026N |

**Description of Homozygous and Compound Heterozygous variants from proband B**

***MST1L*** (Macrophage Stimulating 1 Like)

This is a protein coding gene with limited information on its biological function from the current literature.

***KLRF2*** (Killer Cell Lectin Like Receptor F2)

This gene comprises of an activating homodimeric C-type lectin-like receptor (CTLR), expressed on natural killer cells and stimulates their cytoxicity and cytokine release (278).

***PABPC3*** (Poly(A) Binding Protein Cytoplasmic 3)

*PABPC3* is an important component of the 3-prime poly(A) tail of eukaryotic mRNA and required for the shortening of poly(A) and initiation of translation (279).

***WDR89*** (WD Repeat-Containing Protein 89)

There is no biological information on the function of this gene from the current literature.

***ASXL3*** (Additional Sex Combs Like 3, Transcriptional Regulator)

This gene encodes a protein containing a plant homeodomain (PHD) zinc finger domain that plays a role in the regulation of gene transcription. Nonsense and frameshift mutations in this gene have been associated with Bainbridge Roper's syndrome(BRPS). *ASXL3* and BRPS have been described in detail in the next section.

## 7.4 BAINBRIDGE-ROPERS SYNDROME(BRPS)

Bainbridge-Roper's syndrome (BRPS: OMIM: 615485) was described for the first time by Bainbridge and his colleagues in the year 2013 (280). *De novo* truncating mutations in the additional sex combs-like 3 (*ASXL3)* gene are implicated in BRPS characterised by severe intellectual deficit, feeding difficulties, failure to thrive and cranio-facial features (280-283). BRPS has been reported only in a few patients in the literature (280-283) Majority of the patients had either frameshift or truncating mutations in *ASXL3*. Splicing mutation in *ASXL3* resulting in BRPS has been reported in one patient (282).BRPS has overlapping clinical phenotype with Bohring-Opitz syndrome (BOS:OMIM:605039), a developmental syndrome characterised by a severe intellectual deficit, distinct posture and cranio-facial abnormalities, feeding problems and failure to thrive [Bohring et al., 2006;]. *De novo* truncating mutations in *ASXL1*, belonging to the same family as *ASXL3* have been implicated to cause BOS (284).

### 7.5 *ASXL3*: GENE DESCRIPTION

*ASXL3* belongs to the ASXL gene family, the mammalian homologues of Drosophila Asx. *ASXL1*, *ASXL2* and *ASXL3* are the three orthologues of ASXL. They encode the Putative Polycomb group (PcG) protein that has a role in regulating the homeotic genes (Hox)(285). PcG proteins have a role in regulating the Hox genes by either as transcriptional repressors or activators (285).ASXL group of genes share a common domain architecture consisting of ASXN, ASXM1, ASXM2(HARE-HTH associated) domains, ASXH and a PHD finger (Figure 7.5), and have a tendency to form complexes with other proteins via methylation of histones (283, 285, 286).

The deubiquitination of histone H2A lysine 119(H2AK119Ub1), a component of the Polycomb repressive deubiquitination (PR-DUB) complex is dependent on *ASXL3* (283).The formation of PR-DUB complex is critical for normal function. The mono-ubiquitin (Ub1) from the H2AK119Ub1 is removed by the interaction of *ASXL3* with BAP1 a ubiquitin terminal hydroxylase (287).Srivastava et al. demonstrated a significant increase in the H2AK119Ub1 due to impaired deubiquitination in the fibroblasts of patients with BRPS (283).

The expression of *ASXL3* in human tissues have been studied and it was found that in the human brain, *ASXL3* expression was found in the white matter, insula, cingulate gyrus and amygdala (288). The expression of *ASXL3* and *ASXL1* follow a similar pattern, however the *ASXL3* expression is relatively less compared to *ASXL1*, which may explain the overlap of some phenotypic features seen in BRPS and BOS (289). The spinal cord, kidney, bone marrow and liver also express *ASXL3*, but at a lower level when compared to *ASXL1* (289).

**Figure 7.5:** *ASXL3* gene with domains

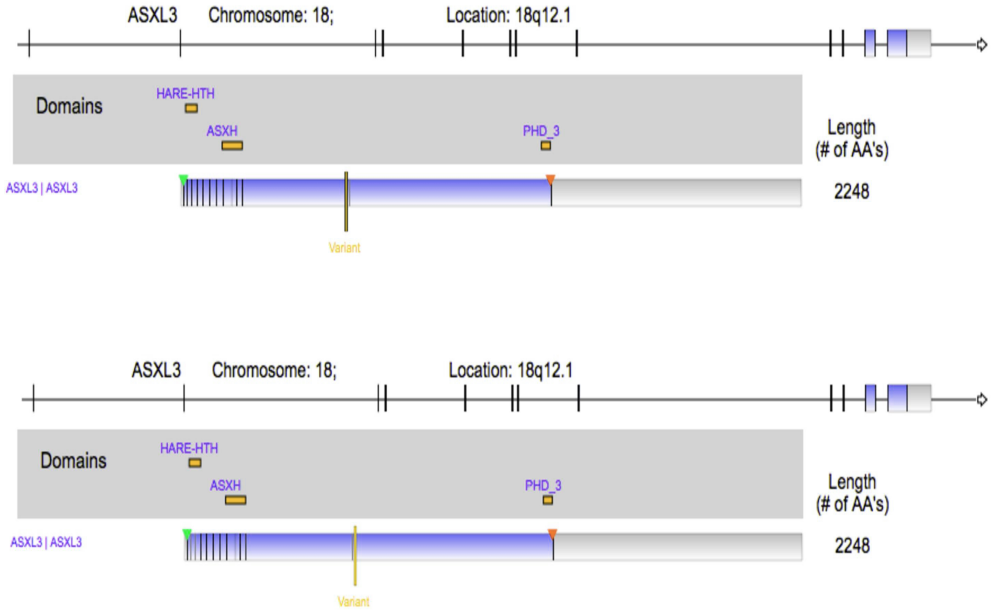

In this study, by WES, a novel compound heterozygous mutation in *ASXL3* was identified in proband B with severe short stature secondary to IGF1 (Insulin Growth Factor 1) deficiency, developmental delay, intellectual deficit, cranio-facial abnormalities. This gene has been explored in detail as the phenotype of proband B segregates with that of BRPS. However, this is the first time, a compound heterozygous mutation in *ASXL3* contributing to BRPS with primary IGF1 deficiency has been described.

### 7.6 EXOME SEQUENCING

A detailed description of the exome sequencing workflow is described in chapter 4.

DNA extracted from blood samples of the child and both the biological parents (trio) using the QIAmp DNA blood Midi Kit (Qiagen, Hilden, Germany) as per the manufacturer's instructions The samples (3 µg/sample) were sheared with the Picoruptor to a size approximately 150-200 bp. The samples were cleaned with 1.8x AMPure beads (Agencourt) and end repaired at 20°C for 30 minutes. The products were A tailed by incubation at 37°C for 30 minutes, cleaned with AMPure beads again and ligated to index adapters at 30°C for 10 minutes to make a pre-capture library using the Agilent Sureselect XT target enrichment system for Illumina. Exons were captured using SureSelect XT Human All Exon V5 capture library and DNA sequencing was carried out using the Illumina HiSeq4000 at 2x150 bp paired-end sequencer.

## 7.7 BIOINFORMATICS

The sequence data were aligned to the reference genome (GRCh37/hg19). Reads were mapped to the reference sequences using BWA mem version 0.7.5a with default parameters (290). The mapped reads were locally re-aligned to improve the alignments around small insertions/deletions (indels) using the Genome Analysis Tool Kit (GATK) version 2.1.13 (291). The read duplicates were identified and filtered to retain only a single representative, using the Picard “MarkDuplicates” tool, version 1.85. Base quality scores were recalibrated using GATK BaseQualityScoreRecalibrator(BQSR). BQSR is a module of GATK to create more accurate base qualities, which in turn improves the accuracy of our variant calls. Functional consequences of the variants identified were annotated using SnpEff. The variants present in at least 5 % minor allele frequency in 1000 Genomes Project, dbSNP142, and NHLBI ESP exomes were excluded. The predicted deleterious variants included non-synonymous coding, splice site, frameshift, stop gain variants.

The conservation of the positions of the two mutations in proband B, R989G and K1026N, was assessed using the UCSC Genome Browser (292). General, sequence-based assessment of the potentially deleterious nature of the mutations was carried out with PolyPhen-2 (293) and SIFT (293). Bespoke interpretation considered predictions of intrinsic disorder made with IUPred (294). Matches to known protein linear motifs were sought in the ELM database (295) and the general likelihood of regions to harbour such motifs – known or novel – was assessed with SLiMPred (296) and ANCHOR (297).

## 7.8 *ASXL3* MUTATIONS IN PROBAND B

Two novel heterozygous mutations in *ASXL3* [NM_030632.1]: c.2965C>G, p. R989G inherited from the mother and c.3078G>C, p. K1026N, inherited from the father were found in the proband B. The mutations were subsequently confirmed by Sanger sequencing (Figure 7.6).

**Figure 7.6:** Compound heterozygous mutations, confirmed by sanger sequencing

**C.2695 C>G**

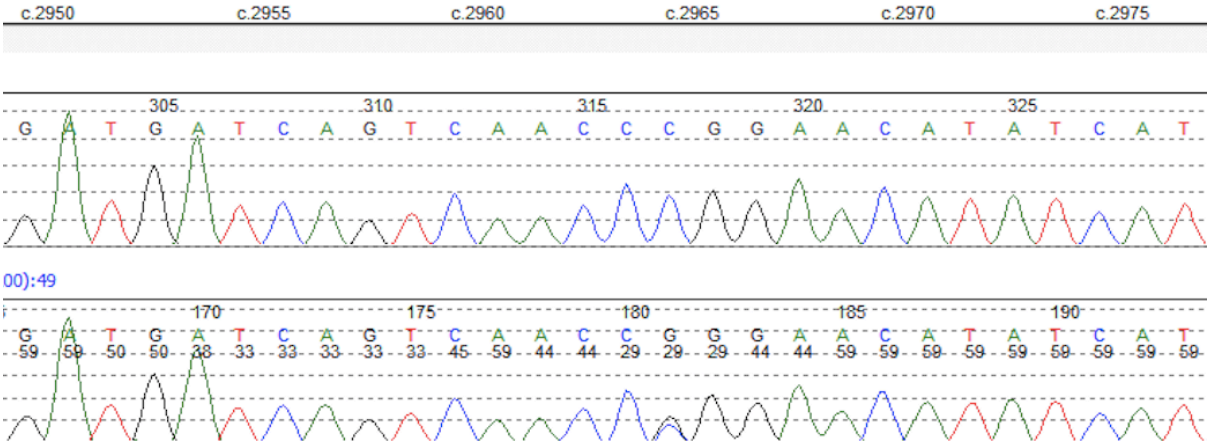


**C.3078 G>C**

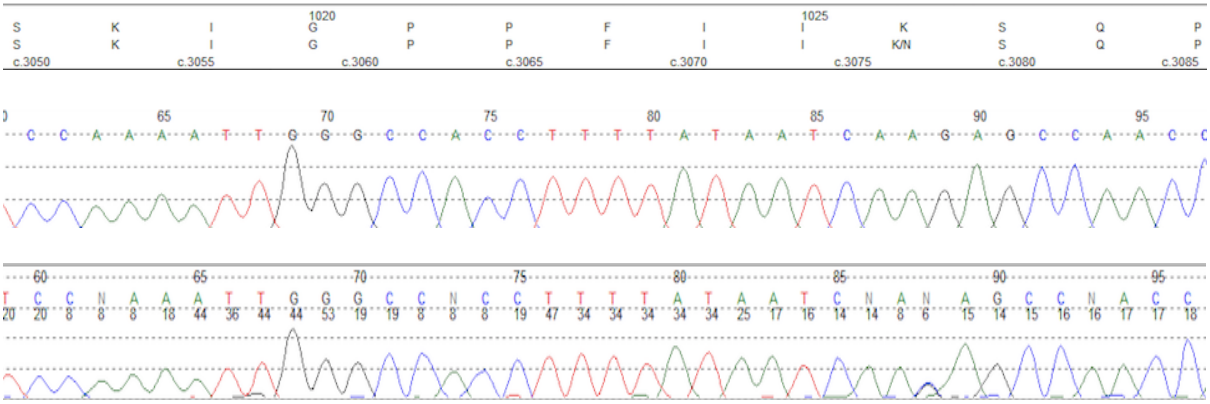

### 7.8.1 Description of *ASXL3* Compound Heterozygous Mutations

The mutations occur in exon 11 and proximal part of exon 12 (Figure 7.6). Both the mutated positions are strongly conserved at the protein level as visualised using the UCSC Genome browser. The conservation is across vertebrates as diverse as lemur, bat, fish and frog, implying that mutation could potentially affect the protein structure or function. Besides, *in silico* analyses using PolyPhen-2 and SIFT predict the amino acid substitutions to be potentially deleterious to the protein function.

Exon 11 and proximal part of exon 12 harbour most of the pathogenic mutations in *ASXL3*. The reported mutations in *ASXL3* retain the ASXN and ASXH domains. In proband B, both the compound heterozygous mutations lie on exon 11 and proximal exon 12, and retain the ASXN and ASXH domains similar to previously described mutations (Figure 7.7). Both these mutations occur on the conserved *ASXM1* domain in *ASXL3* (Figure 7.7) and hence could potentially contribute to the loss of function of the protein contributing to the BRPS like phenotype.

**Figure 7.7**: *ASXL3* gene with domains.1-12 represent the exon numbers. Some of the previously reported frameshift, truncating and splice site mutations have been shown. Compound heterozygous mutations in proband B are highlighted in bold.

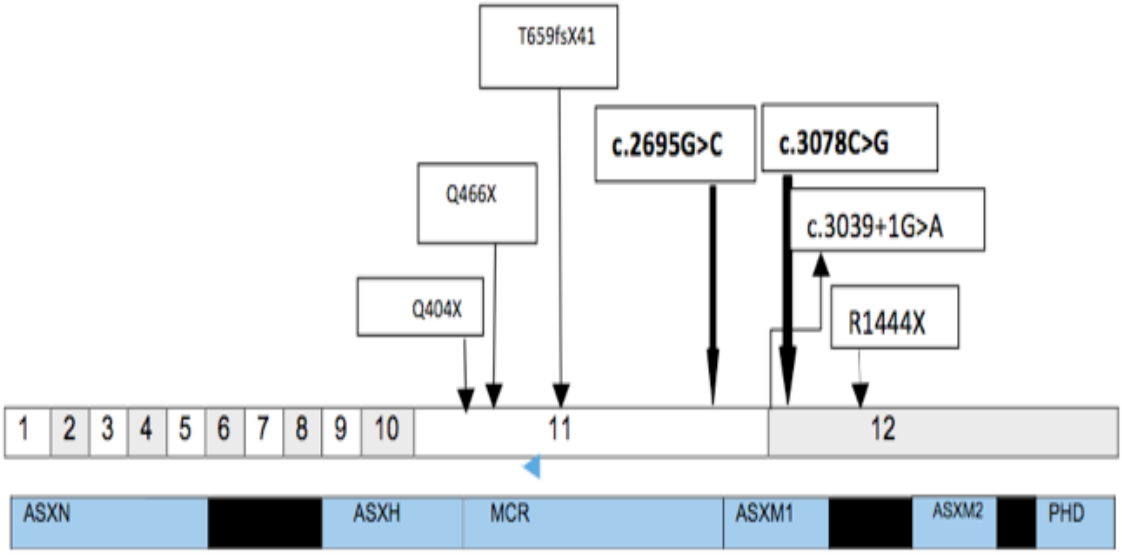

Proband B has features that overlap with those described in previous reported cases of BRPS (Table 7.3)

**Table 7.3:** Comparison of phenotypic features of proband B with patients with BRPS reported in the literature

| Phenotype | Proband B | Bainbridge et al.(4 patients) | Dinwiddie et al. (1 patient) | Srivastava et al (3 patients) | Hori et al. (1 patient) | Balasubramanian et al (12 patients) | Kuechler et al. (6 patients) |
|---|---|---|---|---|---|---|---|
| **Clinical** | | | | | | | |
| **Feeding problems** | + | + | + | + | + | 9/12 | 6/6 |
| **Failure to thrive** | + | + | + | + | + | | |
| **Short stature** | + | + | | ND | + | 2/12 | 2/6 |
| **IUGR** | - | 3/4 | + | 2/3 | + | | |
| **Craniofacial** | | | | | | | |
| **Trigonocephaly** | - | 1/4 | + | 1/3 | + | | |
| **Microcephaly** | - | 2/4 | + | - | + | + | |
| **Scaphocephaly** | + | - | - | - | - | + | |
| **Palate** | High arched | 1/4 | ND | ND | ND | High arched(9/12) | High arched(5/6) |
| **Prominent forehead** | + | 2/4 | ND | 1/3 | ND | + | 5/6 |
| **Prominent eyes** | - | - | + | - | ND | ND | ND |
| **Palpebral fissures** | downslanting | | upslanting | downslanting(2/3) | - | Downslanting-10/12 Upslanting-2/12 | downslanting |
| **Nasal bridge** | long | - | depressed | Broad(1/3) | depressed | Long,prominent | 6/6(prominent columella) |
| **Low set ears** | + | 1/4 | ND | 1/3 | - | + | ND |
| **Posteriorly rotated ears** | Cupped ears | 2/4 | + | + | - | + | |
| **Anteverted nares** | - | + | + | 1/3 | - | ND | 5/6 |
| **Small chin** | + | ND | ND | 2/3 | + | + | ND |
| **Ophthalmic** | | | | | | | |
| **Strabismus** | + | ND | ND | 1/3 | + | 7/12 | 5/6 |
| **Astgmatism** | myopia | ND | Myopia(1/3) | Hyperopia(1/3) | myopia | ND | |
| **Neurological** | | | | | | | |
| **Developmental delay** | + | + | + | + | + | | 6/6 |
| **Intellectual deficit** | + | + | + | 2/3 | + | 12/12 | 5/6 |
| **Seizures** | - | - | + | 1/3 | | 3/12 | 2/6 |
| **Autism** | + | ND | ND | ND | + | 9/12 | Not formally diagnosed |
| **Other Features** | | | | | | | |
| **large fontanelle** | + | 1/4 | ND | ND | ND | ND | ND |
| **Undescended testes** | + | 1/4 | ND | ND | ND | | |
| **Chronic constipation** | + | ND | ND | 1/3 | ND | ND | ND |

+: present -:not present; ND: not described

### 7.8.2 Bioinformatic Analysis of the ASXL3 Compound Heterozygous Mutations, c.2965C>G, p.R989G and c.3078G>C, p.K1026N

A possible molecular mechanism by which the first of the mutations R989G might lead to a functional defect is suggested by a detailed bioinformatics analysis. An analysis of ELM (Eukaryotic Linear Motif) database shows a stretch of amino-acid residues from the position 989 to 997 within the wild-type *ASXL3* that matches with an interaction motif (LIG_14-3-3_CanoR_1; Accession ELME000417) that describes canonical phosphopeptide binding motif of 14-3-3 group of proteins.

14-3-3 proteins are important cell regulators (298), and are best known for their role in cell cycle control. The main determinant of interaction with 14-3-3 proteins is the mutated arginine at position 989 together with a phosphorylated serine residue, 3-5 residues downstream. Besides, the 14-3-3 proteins also have been implicated as histone modification readers (299). This links suggestively to the recently determined role of *ASXL3* in histone deubiquitination (283).According to this hypothesis, mutation of R989 to glycine would prevent the interaction of *ASXL3* with an as-yet unidentified 14-3-3 protein, thereby damaging function through the impairment of its ability to scaffold epigenetic protein complexes (300).Although appealing, it should be pointed at that there is currently no evidence of phosphorylation of any of the relevant Serine residues in the PhosphoSite database (301).However, the content of this database is obviously restricted to cell types and experimental conditions already sampled so the absence does not disprove the hypothesis.

The presence of the R989G mutation in the mother implies that the additional presence of the K1026N is required for pathogenesis. The molecular mechanism for this remains unclear at this point but at least three possibilities can be proposed - 1) the second mutation perturbs the functionality of an additional phosphorylation-dependent 14-3-3 binding motif covering nearby residues 1036-1043; 2) although not lying at one of currently defined key positions, the K1026N mutation affects phosphorylation of *ASXL3* through its location within recognition motifs for kinases (PIKK group, motif from 1024-1030 or GSK3, motif from 1024-1031); or 3) the mutation destroys or creates an interaction motif not currently in the ELM database: the list of such motifs continues to grow (295).The molecular defects caused by the two mutations would specify the disorder additively or synergistically by simultaneously impacting on two points of the molecular interaction network of *ASXL3*.

## 7.9 ASSOCIATION WITH PRIMARY IGF1 DEFICIENCY

The association of primary IGF1 deficiency in BRPS has not been described before. In normal individuals, IGF-1 circulates as part of a ternary complex with a molecular weight of 150 kDa. IGF-1, acid-labile subunit (ALS), and a protein that binds IGF-1 (IGFBP-3) combine and constitute the ternary complex. IGF-1 is a 70-amino acid peptide hormone and growth factor that is structurally homologous to proinsulin (302). A low basal IGF-1 $\leq$ -3 SDS with a height of $\leq$ -3 SDS with normal or elevated levels of GH is indicative of primary IGF-1 deficiency (302). The insulin-like growth factor 1 receptor (IGF1R), is the specific receptor for IGF-1, the binding of which mediates the action. The binding of IGF1 to IGF1R initiates intracellular signalling and IGF-1 is one of the most potent natural activators of the Akt signalling pathway, which stimulates cellular growth and proliferation (303).

In patients with BRPS, the transcriptome analysis of *ASXL3* fibroblasts examining the differentially expressed genes (DEGs) showed that the genes regulating the cellular proliferation are downregulated (283). Since IGF1 plays a vital role in activating the Akt signalling pathway, a potent stimulator for cell proliferation and growth (304) it is possible that *ASXL3* potentially has a role in transcriptional activation of *IGF1* involved in this pathway potentially via epigenetic mechanisms which could be contributing to short stature encountered in these patients (305).

## 7.10 CONCLUSION

The compound heterozygous mutations thus potentially contribute to the loss of function in *ASXL3,* causing a phenotype similar to BRPS. Although with our current knowledge, the molecular interaction between *ASXL3* and IGF1 is unclear, it may be important to look for IGF1 deficiency in patients with *ASXL3* mutation.

# CHAPTER 8

# CLINICAL PHENOTYPE AND WHOLE EXOME SEQUENCING RESULTS (FAMILY C)

## 8.1 SUMMARY OF CHAPTER 8

Chapter 8 begins with the detailed description of the phenotype of proband C from family C and describes the results from whole exome sequencing followed by a detailed discussion of *de novo* frameshift mutation, p.Gly539fs*4 (c.1611_1614dupAAAA) in *CaMKK2*

## 8.2 CLINICAL INFORMATION (PROBAND C)

Proband C is a male infant born to non-consanguineous healthy British parents at 33 weeks gestation by normal vaginal delivery with a birth weight of 1.85 kg. He presented at 7 months of age with a hypoglycaemic seizure (true blood glucose:1.9mmol/L). There had been a history of irritability settling with feeds, 6 weeks prior to the presentation. The investigations showed an elevated plasma insulin of 37pmol/L at the time of hypoglycaemia(1.2mmol/L) with inappropriately supressed free fatty acids(<100umol/L) and beta hydroxyl butyrate(<100umol/L), suggestive of a diagnosis of CHI.

The 18F-DOPA PET CT scan was suggestive of a diffuse disease. The hypoglycaemia responded to diazoxide therapy (10mg/kg/day). He has developmental and speech delay. Genetic testing performed at the University of Exeter Medical School, Exeter was negative for mutations in *KCNJ11, ABCC8, GLUD1, GCK, HADH, HNF4A, INSR, SLC16A1, TRMT10A* and *HNF1A.*

**Figure 8.1** Pedigree of Family C

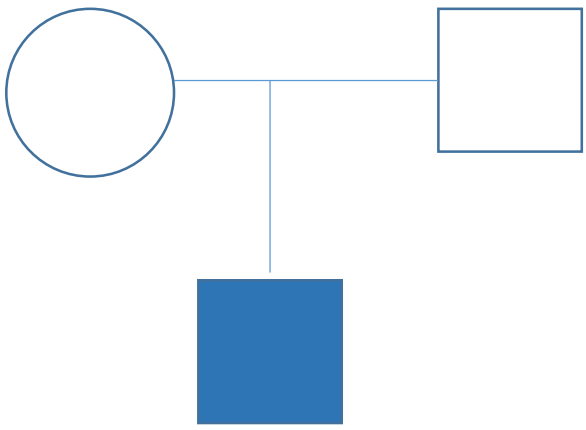

### 8.3 WHOLE EXOME SEQUENCING RESULTS OF FAMILY C

In this family, whole-exome sequencing was performed on the both the parents(unaffected) and the affected child. Assuming a *de novo* inheritance pattern, filters were applied to whole-exome data as shown in the figure 8.2. The potential candidate variants are listed in the table 8.1.

**Figure 8.2:** *De Novo* variant analysis of Family C

De Novo Variant Analysis of Family C (* Novel variants include variants present in at least 5% minor allele frequency in 1000 Genomes Project, ExAC and NHLBI ESP exomes excluded; ** Predicted deleterious variants included nonsynonymous coding, splice site, frameshift, stop gain variants; *** Variants present in heterozygous state in the child and not present in both the parents)

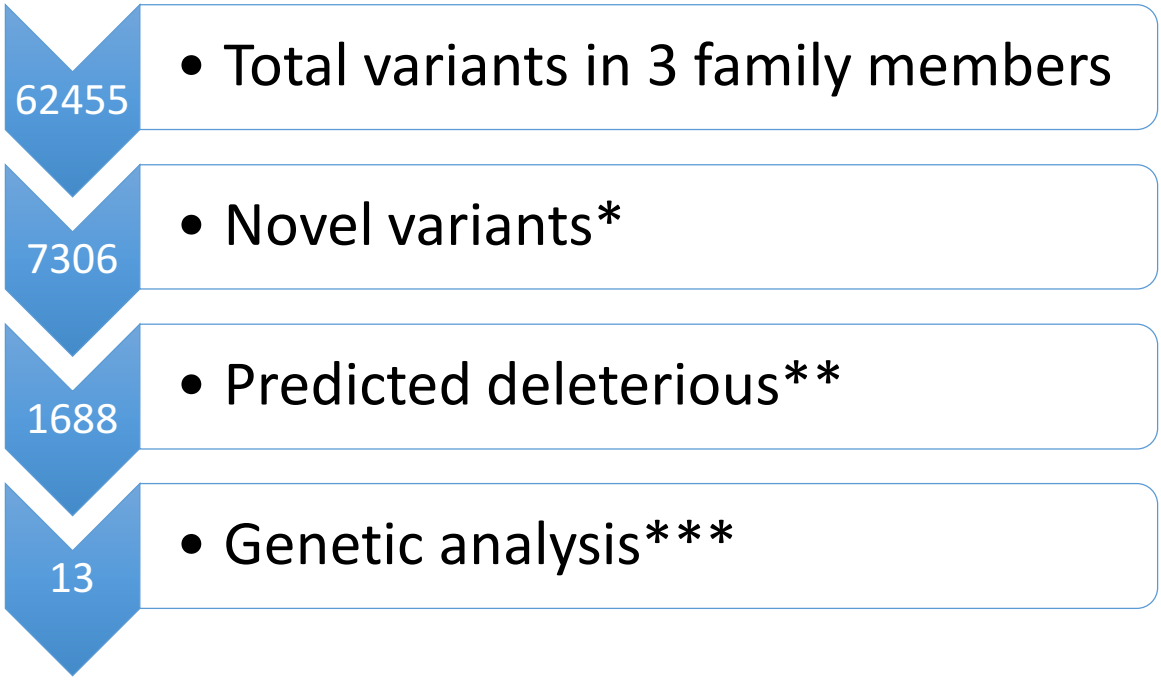

**Table 8.1:** List of *de novo* variants from Proband C

| Chromosome | Gene | Gene region | Protein variant |
|---|---|---|---|
| | | | |
| 1 | IGFN1 | Exonic | p.S1583G |
| | | | |
| 4 | CNOT6L | Exonic | p.Q510fs*4 |
| | | | |
| 4 | ABCE1 | Splice site | |
| | | | |
| 4 | STOX2 | Exonic | p.V108F |
| | | | |
| 6 | NUP153 | Splice site | |
| | | | |
| 6 | PEX7 | Splice site | |
| | | | |
| 7 | KMT2C | Exonic | p.N279D |
| | | | |
| 8 | VPS13B | Splice site | |
| | | | |
| 8 | SPATC1 | Exonic | p.V332del |
| | | | |
| 9 | ORM2 | Exonic | p.Y96S |
| | | | |
| 12 | KMT2D | Exonic | p.S4919fs*13 |
| | | | |
| 12 | CAMKK2 | Exonic | p.G539fs*4 |
| | | | |
| 17 | EFNB3 | Exonic | p.G280fs*7 |
| | | | |

**Brief Description of *de novo* Variants**

***IGFN1*** (Immunoglobulin-Like and Fibronectin Type III Domain Containing 1)

Mansilla et al. showed that *IGFN1* is expressed in skeletal muscle and plays a role in ribosomal protein synthesis (306).

**CNOT6L** (CCR4-NOT Transcription Complex Subunit 6 Like)

*CNOT6* was characterized by Chen et al. following expression in a yeast strain lacking the endogenous yeast *Ccr4* gene and was found to show poly(A) exonuclease activity against a substrate containing five 3-prime adenines (307).

***ABCE1*** (ATP Binding Cassette Subfamily E Member 1)

The protein encoded by this gene is a member of the superfamily of ATP-binding cassette (ABC) transporters. ABC proteins transport various molecules across extra- and intra-cellular membranes.

***STOX2*** **(**Storkhead Box 2)

Nagase et al. by RT-PCR ELISA detected highest expression of *STOX2* in whole adult brain and heart, followed by fetal brain and adult spleen and ovary (308).

***NUP153*** (Nucleoporin 153)

Nuclear pore complexes regulate the transport of macromolecules between the nucleus and cytoplasm.Walther et al. localized Xenopus NUP153 to the nuclear ring of the nuclear pore complex (309).

***PEX7*** (Peroxisomal Biogenesis Factor 7)

Disease associated with *PEX1* mutation include Rhizomelic chondrodysplasia punctata, type 1(310).

***KMT2C*** (Lysine Methyltransferase 2C)

This gene is a member of the myeloid/lymphoid or mixed-lineage leukaemia (MLL) family and ubiquitously expressed in testis and ovary, followed by brain and liver (311).

***VPS13B*** (Vacuolar Protein Sorting 13 Homolog B)

This gene encodes a potential transmembrane protein that may function in vesicle-mediated transport and sorting of proteins within the cell. This protein may play a role in the development and the function of the eye, hematological system, and central nervous system.

***SPATC1*** (Spermatogenesis And Centriole Associated 1)

Using immunohistochemical analysis *Spatc1* expression was found in exclusively in mouse testis, in the cytoplasm of spermatocytes, spermatocytes undergoing meiotic division, round spermatids, and condensed spermatids (312).

***ORM2*** **(Orosomucoid 2)**

*ORM2* is key acute phase plasma protein and is increased in acute inflammation, and thus classified as an acute-phase reactant.

***KMT2D*** **(Lysine Methyltransferase 2D)**

The protein encoded by this gene is a histone methyltransferase that methylates the Lys-4 position of histone H3 and mutations associated with this gene is associated with Kabuki syndrome (8).Although Kabuki syndrome can he associated with hyperinsulinaemic hypoglycaemia, this gene was excluded as proband C did not have any dysmorphic features that may suggest Kabuki syndrome.

***EFNB3*** (Ephrin B3)

*EFNB3* is expressed in the midterm fetus, the highest EFNB3 mRNA level in brain, followed by heart, kidney, and lung; In adults the expression is restricted to brain and is particularly high in forebrain subregions, suggesting that *EFNB3* is important in both brain development and maintenance (313).

***CaMKK2*** ($Ca^{2+}$/calmodulin-dependent protein kinase 2)

$Ca^{2+}$/calmodulin-dependent protein kinase 2 (*CaMKK2*) belongs to the Serine/Threonine protein kinase family and alternative splicing results in multiple transcripts encoding distinct isoforms.

In mice, lacking *CaMKK2* in their islets ($CaMKK2^{-/-}$), the insulin levels were significantly high when compared to their wild-type littermates($CaMKK2^{+/+}$), suggesting that *CaMKK2* and calcium signalling play an important role in the regulation of insulin production from the pancreatic ß cells (314).

As *CaMKK2* segregates with the clinical phenotype of proband C, this gene has been explored in detail and the *CaMKK2* mutation (p.Gly539fs*) is characterized by functional studies, explained in the next section 8.4.

## 8.4 *CAMKK2* ($Ca^{2+}$/CALMODULIN-DEPENDENT PROTEIN KINASE 2) AND EFFECT OF MUTATION *CAMKK2* (p. Gly539fs*4)

This section begins with a brief introduction on *CaMKK2*, its role in insulin secretion. This is followed by a detailed description of the *de novo* heterozygous *CaMKK2* mutation (p. Gly539fs*4) from proband C and functional studies to demonstrate the pathogenicity of the mutations.

### 8.4.1 Calcium/Calmodulin dependent protein kinase 2(CaMKK2)

Human *CaMKK2* maps to chromosome 12q24.2 and spans over 40kb pairs. The major full length isoform of CaMKK2 is isoform 1, however alternative splicing of exons 14 and/or 16 gives rise to multiple transcripts (isoforms 2, 3 ,4, 5, 6 and 7) (315).

### 8.4.2 Role of *CaMKK2* in Insulin Secretion

The secretion of insulin from the β-cells of the pancreas is a tightly co-ordinated process and is closely linked to glucose metabolism by pancreatic β-cell ATP-sensitive potassium channels. Increased blood glucose concentration drives glucose uptake into pancreatic β-cells via the glucose transporter 2, encoded by *GLUT2*, which increases ATP production and raises the cytosolic ATP/ADP ratio resulting in closure of ATP-sensitive potassium channels ($K_{ATP}$) (130). Glucose-dependent closure of $K_{ATP}$ channels facilitates cell membrane depolarization, which stimulates $Ca^{2+}$ influx into the pancreatic β-cell via opening of voltage-gated $Ca^{2+}$ channels. The increase in the intracellular $Ca^{2+}$ triggers exocytosis and release of insulin (141); however, the

molecular mechanisms that control $Ca^{2+}$-triggered insulin release in response to glucose stimulation in β-cells is poorly understood (130).

The intracellular effects of calcium($Ca^{2+}$) in the pancreatic β-cells are largely transduced via CaM (Calmodulin), and $Ca^{2+}$-CaM complex through the activation of tightly regulated set of protein kinases such as the $Ca^{2+}$-CaM-dependent protein kinases 1 and 4 (CaMK1 and CaMK4), and the AMP activated protein kinase (AMPK) (314). These kinases are activated by increasing intracellular $Ca^{2+}$ and belong to a diverse group of enzymes with a role in many cellular responses (314). An important component of this kinase cascade is the $Ca^{2+}$-CaM-dependent protein kinase kinase-2 (*CaMKK2*), which is activated by increased intracellular $Ca^{2+}$ and directs the downstream actions of CaMK1 and CaMK4, the AMP activated protein kinase (AMPK)(316, 317), and the histone deacetylase Sirtuin-1 (Sirt1) (318, 319). Thus *CaMKK2* is important and acts as a $Ca^{2+}$-sensor with a potential key role in glucose-stimulated insulin secretion and therefore a potential candidate gene in disorders relating to glucose homeostasis.

The mechanism of insulin secretion from the pancreatic ß-cell via the $Ca^{2+}$-CaM dependent pathway is shown in the figure 8.3.

**Figure 8.3:** Mechanism of insulin release from ß-cell via the kinase cascade regulated by $Ca^{2+}$-CaM-dependent protein kinase kinase-2 (*CaMKK2*), activated by increased intracellular $Ca^{2+}$ and directs the downstream actions of CaMK1 and CaMK4.

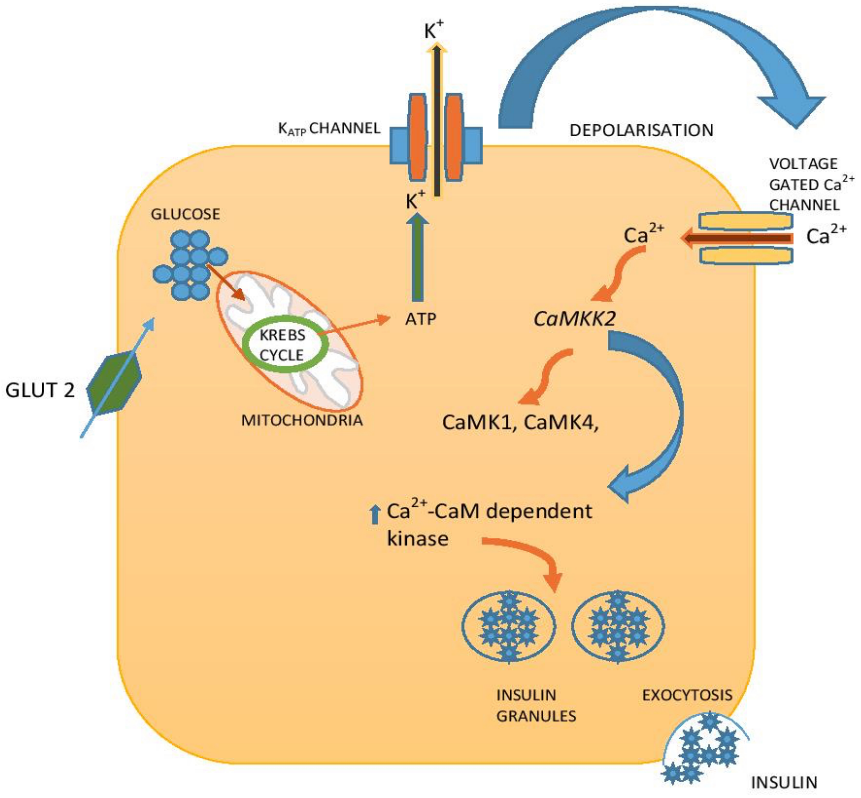

## 8.5 METHODS

DNA extraction, exome sequencing and bioinformatics have been described in detail in chapter 4.

A brief description of the specific methodologies used for functional analysis of the *CaMKK2* isoform 7 pG539fs*4 variant is described below. All the functional work was done in close collaboration with Dr John Scott, University of Melbourne, Australia.

### 8.5.1 Plasmid

Plasmid constructs for full length N-terminal Flag-tagged human *CaMKK2* isoform-1, isoform-7 and isoform-7 pG539fs*4 mutant were generated by custom gene synthesis (General Biosystems), and cloned into the pcDNA3(-) mammalian expression vector using XhoI/HindIII restrictions sites. All constructs were verified by sequencing the entire open reading frame. Plasmid DNA for COS7 cell transfection was prepared using Wizard Plus SV Miniprep DNA Purification Kits (Promega).

### 8.5.2 Expression of human *CaMKK2* isoforms and pGly539fs*4 mutant

COS7 cells were grown in DMEM (Sigma) media with 10% fetal calf serum at 37 °C with 5% $CO_2$. Cells were transfected at 60% confluency with 2 μg of pcDNA3 containing N-terminal Flag-tagged human *CaMKK2* isoform-1, isoform-7 and Gly539fs*4 mutant using FuGene HD (Roche). Transfected cells were harvested after 48 hr by washing with ice-cold phosphate-buffered saline (PBS) followed by rapid lysis *in situ* using 1 ml of lysis buffer (50 mM Tris.HCl [pH 7.4], 150 mM NaCl, 50 mM NaF, 1 mM NaPPi, 1 mM EDTA, 1 mM EGTA, 1 mM DTT, 1% [v/v] Triton X-100) containing Complete protease inhibitor cocktail (Roche). Cellular debris was removed by centrifugation and total protein in the cell lysate was determined using the Bradford

protein assay (Pierce). Recombinant *CaMKK2* was purified from 10 μg of cell lysate using 10 μl of anti-Flag M2 agarose (50% v/v) (Sigma) pre-equilibrated in lysis buffer, followed by successive washes in lysis buffer containing 1 M NaCl, and finally into 50 mM HEPES [pH 7.4]. The immobilized *CaMKK2* was then sedimented by centrifugation and used for kinase assays.

### 8.5.3 *CaMKK2* Assay

CaMKK2 activity was measured using a synthetic peptide substrate (CaMKKtide) (318). Briefly, 10 μl of recombinant CaMKK2 immobilized on anti-Flag M2 agarose beads (50% v/v) was incubated in assay buffer (50 mM HEPES [pH 7.4], 1 mM DTT, 0.02% [v/v] Brij-35) containing 200 μM CaMKKtide, 50 μM $CaCl_2$, 1 μM CaM (Sigma), 200 μM [$\gamma$-$^{32}$P]-ATP (Perkin Elmer) and 5 mM $MgCl_2$ in a standard 30 μl assay for 10 min at 30 °C. Reactions were terminated by spotting 15 μl onto P81 phosphocellulose paper and washing extensively in 1% phosphoric acid. Radioactivity was quantified by liquid scintillation counting, and CaMKK2 activity was corrected for minor differences in expression as determined by immunoblotting using an anti-Flag antibody and Odyssey Infrared Imager.

Kinase activity of CaMKK2 isoforms and pGly539*fs4 mutant was measured over a range of CaM concentrations (0-1000 nM) in the presence of 50 μM $Ca^{2+}$. CaMKK2 activity was express in nmol.min$^{-1}$.mg$^{-1}$ of cell lysate.

### 8.5.4 Immunoblotting

50 μg of total COS7 cell lysate containing recombinant CaMKK2 was denatured in SDS sample buffer, resolved on a 4-15% Mini-Protean Gradient gel (Bio-Rad), before transferring onto Immobilon PVDF membrane (Millipore). The membrane was blocked for 30 min in PBS/1% Tween-20 (PBS-T) supplemented with 2% non-fat milk, and then incubated with rabbit anti-Flag antibody (Cell Signalling; Cat No 2368S; Lot No 6; 100 ng/ml) for a further 30 min. The membrane was then briefly washed in PBS-T, followed by incubation with goat anti-rabbit IgG IRDye680 (Li-Cor) for 30 min. After successive washing with PBS-T, the membrane was scanned with an Odyssey CLx Infrared Imager (Li-Cor).

### 8.5.5 *CaMKK2* isoform-7 (c.1611_1614dupAAAA) (pG539fs*4) mutation

Exome sequencing of family C (proband and the unaffected parents) identified a total of 13 *de novo* variants (*IGFN1, CNOT6L, ABCE1, STOX2, NUP153, PEX7, KMT2C, VPS13B, SPATC1, ORM2, KMT2D, EFNB3, CaMKK2*). A review of literature suggested a potential role *of CaMKK2* in insulin secretion from pancreatic ß-cells and thus segregating with the phenotype of CHI in proband C. The *de novo* heterozygous mutation (c.1611_1614dupAAAA) in CaMKK2 isoform-7 (NM_001270486.1) that results in a frameshift at glycine-539 (pG539fs*4), producing CaMKK2 isoform-7 with a short alternate C-terminal sequence (Figure 8.4 A). None of the other variants segregated with the patient's phenotype and thus were not studied further.

By immunoblotting, it was demonstrated that the pG539fs*4 mutant can be readily expressed in COS7 cells to a similar level as WT CaMKK2(isoform 7) and CaMKK2(isoform 1) (Figure 8.4 B).

The measurement of $Ca^{2+}$-CaM dependent kinase activities showed that pG539fs*4 mutant had significantly higher basal and maximal $Ca^{2+}$-CaM dependent kinase activities (2.86 and 1.38-fold, respectively) relative to WT CaMKK2 isoform 7 (Figure 8.4 C). Furthermore, both WT CaMKK2(isoform 7) and the pG539fs*4 mutant have considerably higher basal activities compared with WT CaMKK2(isoform 1), the most abundant isoform in the majority of tissues. Although the pG539fs*4 mutant has increased kinase activity relative to the other isoforms, the concentration of CaM required for half-maximal stimulation of the pG539fs*4 mutant is similar to WT CaMKK2.7 and WT CaMKK2.1, indicating that CaM sensitivity is unaffected (Table 8.2).

**Table 8.2:** $Ca^{2+}$-CaM stimulated activities of CaMKK2.1 (isoform 1), CaMKK2.7 (isoform 7) and pG539*fs4 mutant measured over a range of CaM concentrations (0-1000 nM) in the presence of a fixed concentration of $Ca^{2+}$ (50 nM), expressed relative to activity in the absence of CaM. Data are presented as mean ± SEM; n=4.

| **CaMKK2 Isoform** | **Concentration of CaM required for half-maximal stimulation (nM)** |
|---|---|
| CaMKK2.1 | 62.1 ± 5.93 |
| CaMKK2.7 | 51.3 ± 7.99 |
| CaMKK2.7 pG539*fs4 | 63.8 ± 10.2 |

**Figure 8.4 A:** Linear domain structure of the CaMKK2 isoforms showing the kinase domain, autoinhibitory sequence (AIS), calmodulin-binding (CaMBS) sequence, and divergent C-terminal sequences (CTS).

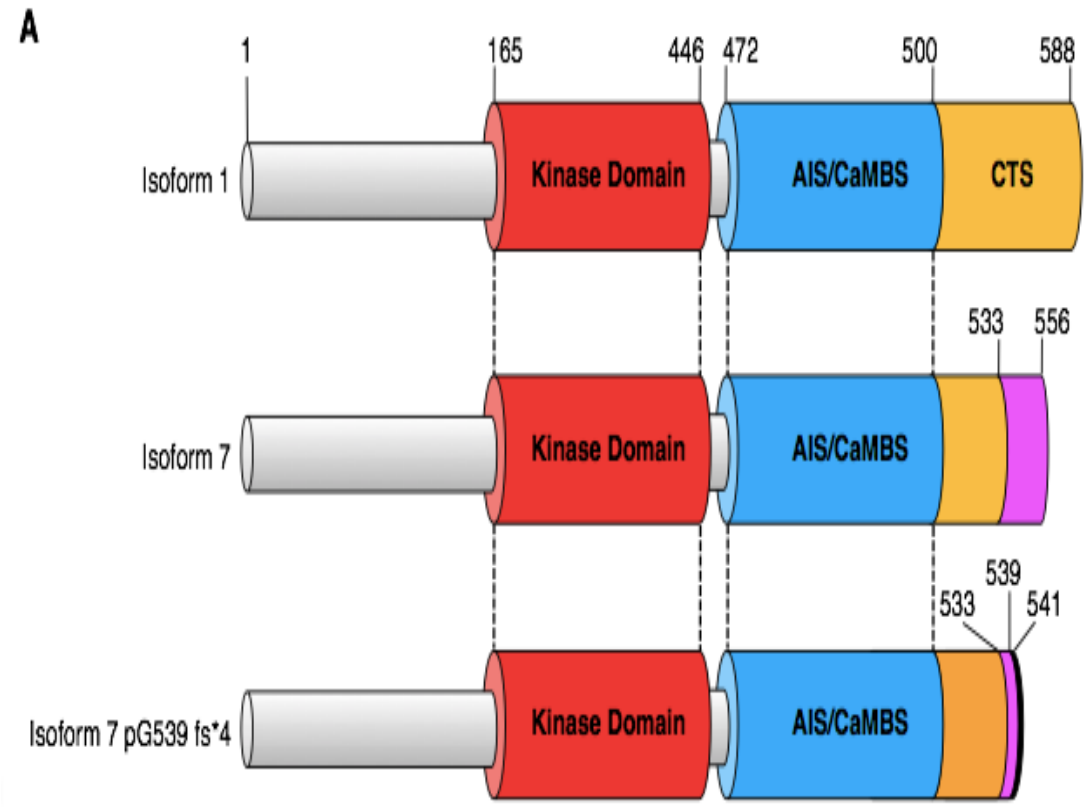

**Figure 8.4 B:** Immunoblotting with rabbit anti-Flag antibody demonstrating the expression of pG539fs*4 mutant at a similar level as wild-type(Wt) isoform-7 in COS7 cells

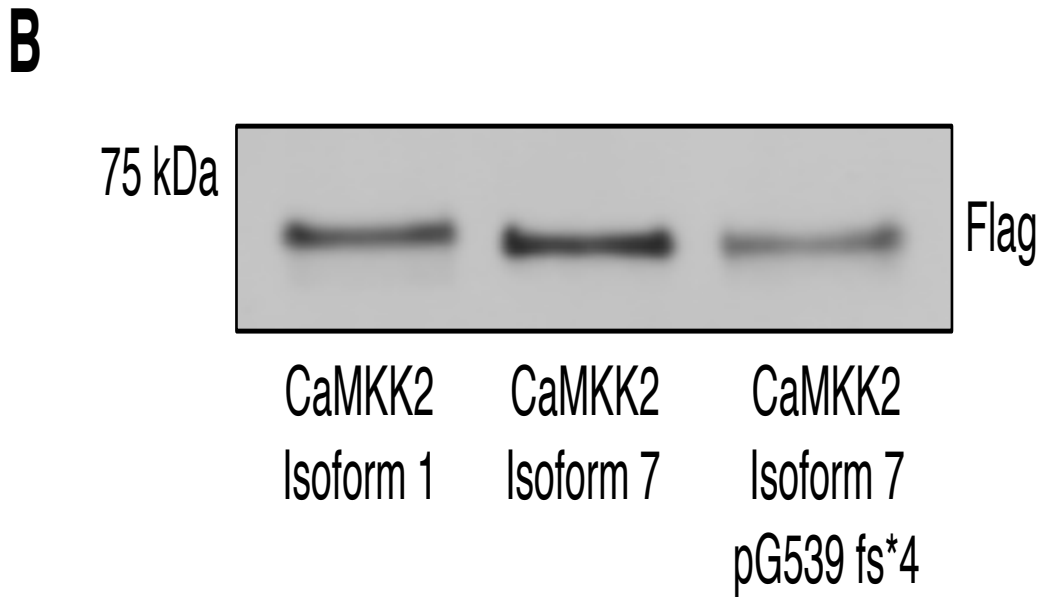

**Figure 8.4 C:** pG539fs*4 mutant showing a significantly higher baseline and $Ca^{2+}$-CaM dependent kinase activity compared with Wt isoform-7. Both isoform-7(CaMKK2.7) and the pG539fs*4 mutant have elevated baseline activity compared with isoform-1(CaMKK2.1)

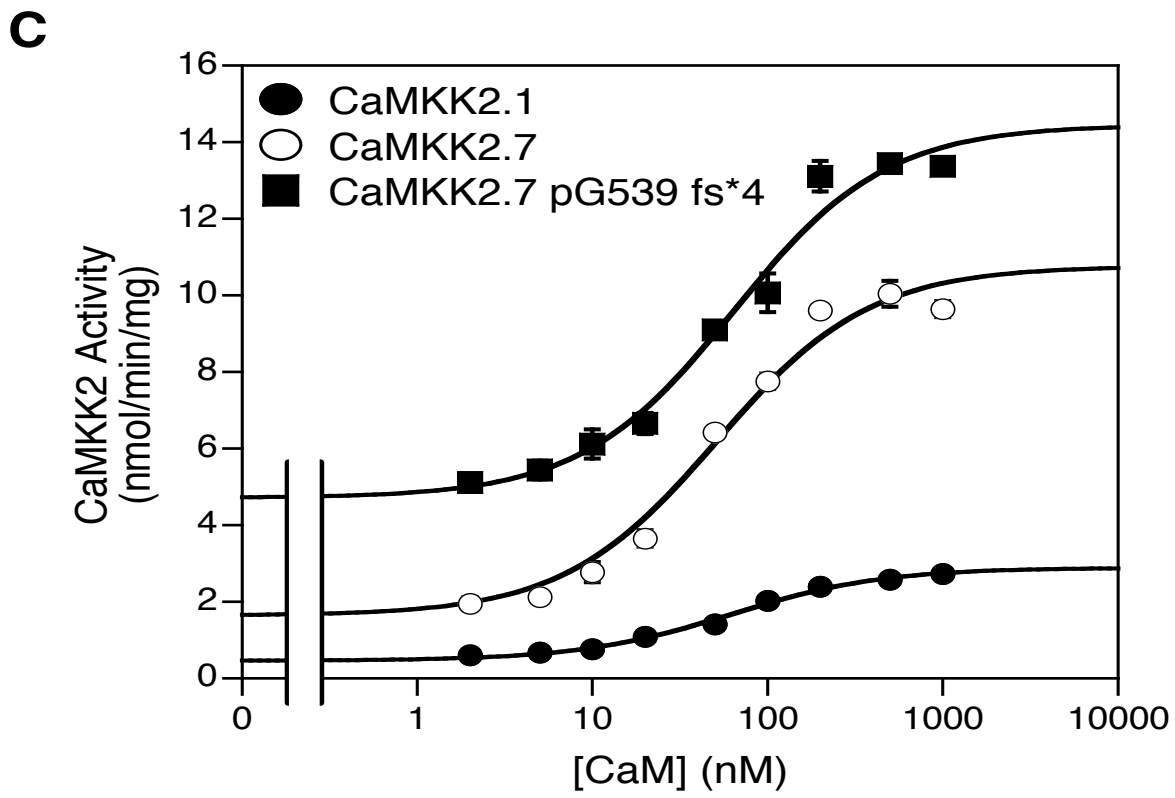

## 8.6 DISCUSSION

WES in proband C identified a frameshift mutation (c.1611_1614dupAAAA) found in our study occurs within the last exon (exon 16) of *CaMKK2* isoform 7. Isoform 1 is the most characterized of the *CaMKK2* isoforms. A little is known about isoform 7 which has 16 exons. The occurrence of the frame-shift mutation in the last exon results in a shorter C-terminal sequence.

Nonsense mediated decay (NMD) is a post-transcriptional surveillance mechanism that degrades transcripts with nonsense mutations (320).As a result of NMD the synthesis of the C-terminally truncated protein is limited. However, the synthesis of the truncated protein depends on the position of the nonsense mutation. The mutations that occur in the beginning of mRNA or residing at least 50 nucleotide 5′ to an exon junction direct the affected mRNA to rapid decay (320).Mutations that occur within the last exon do not activate NMD and yield a stable mRNA that directs the synthesis of C-terminally truncated polypeptides. These aberrant translated protein can act in a dominant negative fashion (321, 322).

The frameshift mutation (c.1611_1614dupAAAA) found in proband C occurs within the last exon (exon 16) of *CaMKK2*.7, and thus may potentially escape NMD mRNA decay and be translated into protein. Consistent with this view, the data from this study demonstrate that the *CaMKK2*.7 pG539fs*4 mutant can be readily expressed in mammalian cells to similar levels as WT *CaMKK2*.7 (Figure 8.4 B), therefore it is reasonable to consider that the pG539fs*4 mutant would be stably translated and functional in the pancreatic β-cells.

Intracellular $Ca^{2+}$ plays a key role in mediating glucose-stimulated insulin secretion, insulin biosynthesis and acts as the key mediator for glucose-stimulated insulin secretion (323-325). Calcium also plays an important role in the transcription of insulin gene and there is evidence this is mediated in part by CaMKs, as treatment of islets or insulin-secreting HIT cells with the CaM antagonist KN-62 blocks $Ca^{2+}$-dependent stimulation of insulin gene transcription (326, 327). The cAMP responsive elements of the human insulin gene is regulated by a transcription factor called activating transcription factor-2(ATF), the activation of which is enhanced by Ca2/CaM-KIV (328). Thus there is increasing body of evidence from the literature that Calcium dependent Calmodulin Kinases (CaMKs) have a potentially important role in the insulin secretion from the pancreatic β-cells.

CaMK1 and CaMK4 are activated by *CaMKK2* through phosphorylation of a conserved threonine residue within the activation loop of the protein (329). In mice lacking *CaMKK2* in their islets, insulin levels were significantly higher when compared to their wild-type littermates, suggesting that *CaMKK2* and $Ca^{2+}$-signalling play an important role in the regulation of insulin production from the pancreatic β-cells (330).Yu et al demonstrated the role of CaM dependent protein kinase cascade in glucose up-regulation of insulin secretion by exposing INS-1 cells to glucose (11.2 mmol/L) (319). This caused an increase in insulin promoter activity and stimulation of CaMKK1 and CaMK4 activity, indicating a role for the CaM-KK/CaM-KIV cascade in the transcriptional activation of the insulin gene (319).

*CaMKK2* isoform 1 is the most abundantly expressed isoform in many tissues. There is only limited information available in the literature about isoform-7. Studies in murine pancreatic islet cells and in the insulin-secreting cell line, INS-1 have demonstrated expression of mRNA encoding CaMK4 and its upstream kinase, CaMKK (319). The mutation found in proband C, occurs in isoform-7. Therefore, comparison of Wt isoform 7, Wt isoform 1 and the mutant pG539fs*4 in COS7 cells using immunoblot demonstrated that the pG539fs*4 mutant can be readily expressed in COS7 cells to a similar level as wild-type(Wt) isoform-7 (Figure 8.4 B).

*CaMKK2* requires $Ca^{2+}$ and CaM for maximal activity and in the case of CaMKK2.7, the activity rises from 1.8 nmol.min.mg to 10 in the presence of $Ca^{2+}$-CaM (Figure 8.4 C). The basal activity of the pG539fs*4 mutant is approximately 40% of the WT CaMKK2.7 maximum activity (Figure 8.4 C), indicating that the regulatory pathways downstream of *CaMKK2* would be substantially switched on in the presence of the pG539fs*4 mutant. *CaMKK2* is an upstream activator of CaMK4, which has been reported to play a role in enhancing insulin gene expression in response to glucose stimulation in pancreatic β-cells. Expression of a constitutively active CaMK4 mutant in the pancreatic cell line *INS-1* was shown to stimulate the insulin gene promoter, whereas this effect was completely blunted by expression of a dominant negative CaMK4 mutant (319). One possibility is that insulin gene expression is increased by this CaMKK2-CaMK4 pathway in proband C carrying the pG539fs*4 frameshift mutant. Since the frame-shift mutation results in a significant increase in the kinase activity when compared with the wild type, it is hypothesised that the increase in *CaMKK2* activity as a result of the pG539fs*4 mutation, to be increasing the insulin secretion (Figure 8.5), probably via the up-regulated transcription of *INS-1* gene.

*In vivo* experiments, examining the effect pancreatic β-cell specific inhibition of CaMKII activity in transgenic mice demonstrated that CaMKII inhibition significantly impaired the glucose tolerance by reducing L-type $Ca^{2+}$ facilitation, $Ca^{2+}$ entry and insulin secretion(331). Whilst the inhibition of CaMKII has been shown to reduce the insulin secretion from in vivo studies, it is plausible that an increased activity of *CaMKK2* as a result of the mutation pG539fs*4 demonstrated in our study is contributing to high insulin secretion seen in the proband C. Furthermore, Dadi et.al also demonstrated that CaMKII inhibition did not have any detectable effect on the $K^+$ channel activities in β cells implying that CaMKII modulates glucose stimulated insulin secretion downstream of $K_{ATP}$ channels(331).

Diazoxide is the first line medication used in the treatment of CHI that acts as an agonist of $K_{ATP}$ channel, thus reducing the insulin secretion. Proband C is currently responding to high dose of diazoxide (10 mg/kg/day). Calcium channel antagonists (such as nifedipine) could be potentially considered in patients with *CaMKK2* mutation if they do not respond or tolerate diazoxide.

**Figure 8.5:** Schematic representation of the mechanism of excess insulin release from ß-cell via increased activation of the kinase cascade by *CaMKK2* (pG539fs*4).

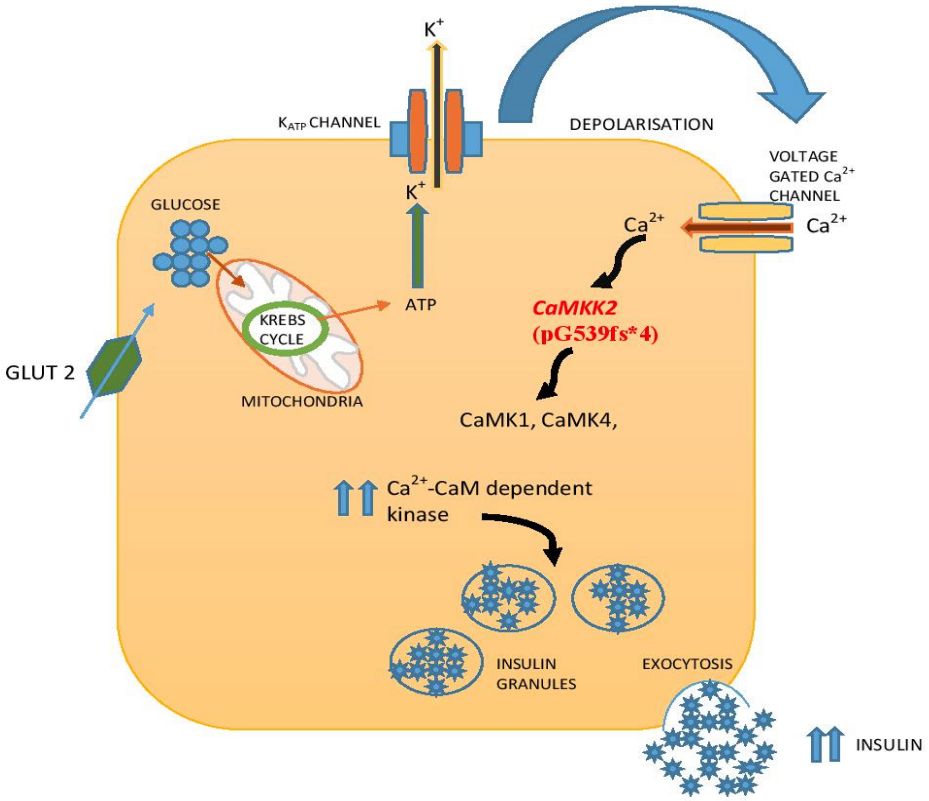

Thus *CaMKK2* is a potential candidate gene for CHI. Screening for more patients with CHI for mutations in *CaMKK2* will help in more understanding of the genotype-phenotype correlation. *CaMKK2* isoform 1 is the predominant isoform and much less is known on *CaMKK2* isoform 7. Developing *CaMKK2* isoform-7 specific antibody and studying the expression in pancreatic islets will be useful to understand the specific role of *CaMKK2* isoform 7 in modulating the insulin secretion. In this study, the direct relationship between the increased kinase activity and insulin secretion has not been explored. Development of mouse model and with the application of gene editing technologies such as CRISPR/CAS9 (Clustered Regularly Interspaced Short Palindromic Repeats/CRISPR-associated system) (380), it is now potentially possible to study the direct effect of the frame-shift mutation and examine the relationship between the increased kinase activity and insulin secretion.

# CHAPTER 9

# CLINICAL PHENOTYPE AND WHOLE EXOME SEQUENCING RESULTS (FAMILIES D, E, F)

## 9.1 SUMMARY OF CHAPTER 9

Chapter 9 begins with the detailed description of the phenotypes of proband D, E, and F from families D, E, F followed by the results from whole exome sequencing.

# FAMILY D

## 9.2 CLINICAL INFORMATION (PROBAND D)

Proband D, a female infant was born at 34 weeks gestation with a birth weight of 1.9 kg to non-consanguineous Caucasian parents. The antenatal history was unremarkable. She was noted to have a cloacal anomaly with a posterior cloaca which was subsequently corrected by urogenital mobilisation reconstructive surgery at 2 years of age. She also has congenital sensorineural deafness, ventricular septal defect and pulmonary stenosis requiring surgical correction. Her renal ultrasound was normal. At 4 years of age, she was diagnosed with growth hormone(GH) deficiency because of her short stature(<2.5SD) and poor linear growth velocity and suboptimal response to glucagon stimulation test (peak GH 3.7 ug/L). She was subsequently commenced on GH with a good response (figure 9.2). The MRI of the pituitary gland showed small anterior pituitary. The other pituitary hormones were within the normal range. She was investigated for recurrent hypoglycaemic episodes and the results of the investigations following a prolonged control fasting were consistent with ketotic hypoglycaemia. The investigations of prolonged fast are summarised in the table below (Table 9.1). She had multiple dysmorphic features such as anteverted nares, small upturned nose, hypertelorism, slight frontal bossing, short proximal bones, femur, humerus, hypermobile joints and down slanting palpebral fissures. There was a history of short stature and dysmorphism in father's side and learning difficulty in mother. There was also a history of still-born previous sibling with midline cleft palate, absent uvula, small jaw, depressed nasal bridge, abnormalities on MRI brain with absence of the inferior cerebellar vermis, partial agenesis of corpus callosum, congenital heart defects and short bones.

Due to persistent hypoglycaemia, a targeted exome sequencing of genes associated with disorders of ketogenesis, ketolysis, carbohydrate metabolism, fatty acid oxidation defects and hyperammonaemia performed at the University of Manchester molecular genetics department did not identify any pathogenic mutations. The genes that were sequenced for the above disorders are as follows:

*ABAT, ACAD9, ACADM, ACADS, ACADVL, ACAT1, ACAT2, AHCY, ARG1, ASL, ASS1, CPS1, CPT1A, CPT2, DECR1, ETFA, ETFB, ETFDH, GLUD1, HADHA, HADHB, HMGCL, HMGCS2, IVD, MMAA, MMAB, MMACHC, MMADHC, MUT, NAGS, OTC, OXCT1, PCCA, PCCB, SLC22A5, SLC25A13, SLC25A15, SLC25A20 AGL, ALDOA, ENO3, EPM2A, FBP1, G6PC, G6PC3, GALE, GALK1, GALT, GBE1, GYS1, LAMP2, LDHA, NHLRC1, PFKM, PGAM2, PGK1, PGM1, PHKA1, PHKA2, PHKB, PHKG1, PHKG2, PRKAG2, PYGL, PYGM, SLC2A1, SLC2A2, SLC37A4.*

**Table 9.1:** Results of investigations following a 19 hour fast:

| | |
|---|---|
| True blood glucose | 2.3mmol/L |
| Insulin | <14pmol/L |
| C-peptide | <33pmol/L |
| Plasma Free fatty acids | 2673umol/L |
| 3 hydroxy butyrate | 1205umol/L |
| Plasma free carnitine | 13.2umol/L |
| 17 OHP | <1nmol/L |
| Plasma amino acids | Normal |
| Urinary organic acids | Normal |

**Figure 9.1** Pedigree of Family D

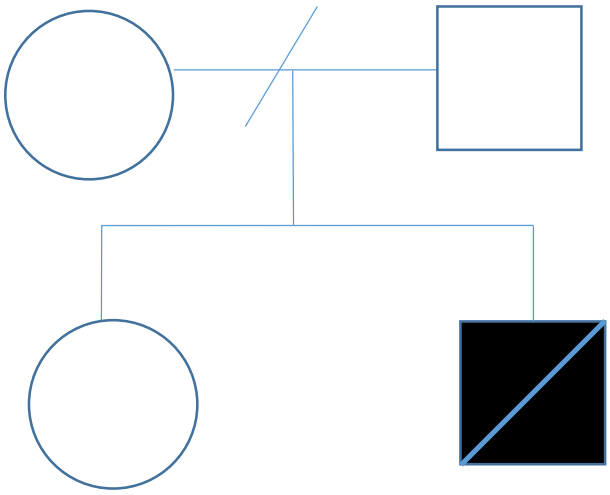

**Figure 9.2:** Growth chart of Proband D showing a good response to GH

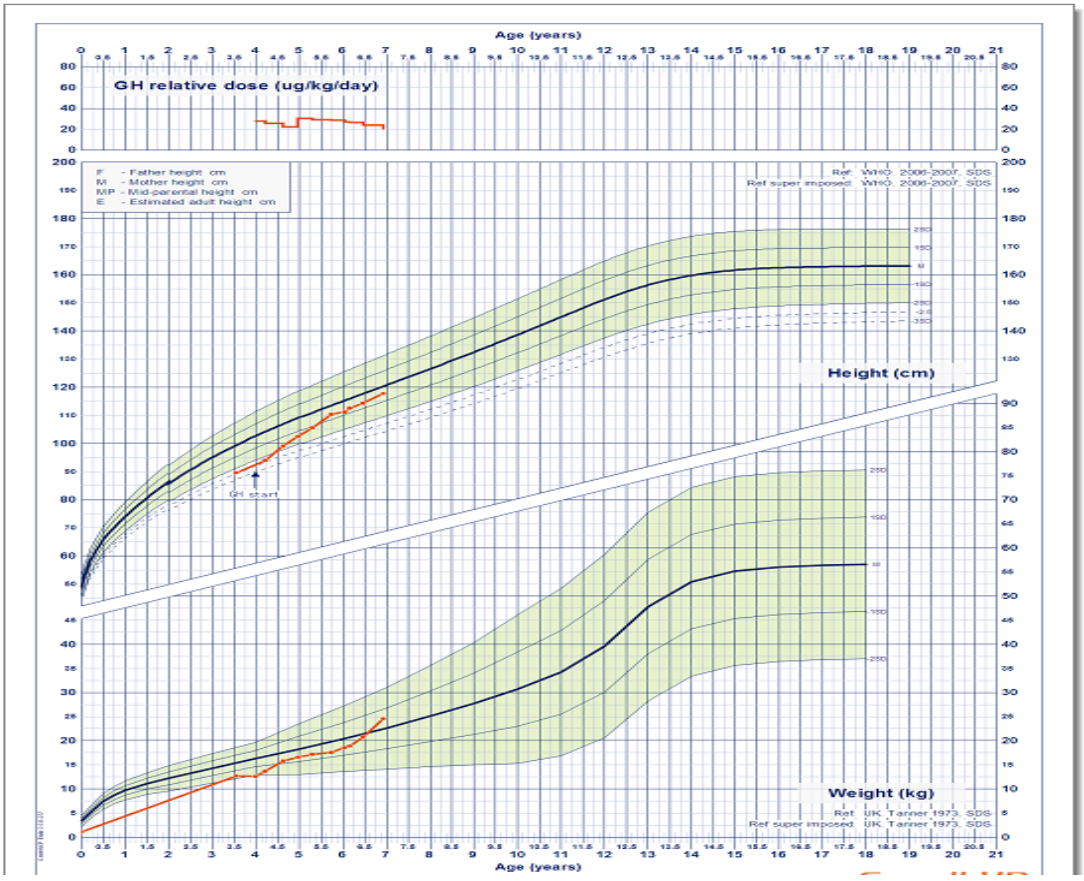

### 9.3 WHOLE EXOME SEQUENCING RESULTS FROM FAMILY D

In this family, whole-exome sequencing was performed on the affected child and biological mother as biological father was unavailable. Filters were applied to whole-exome data as shown in the figure 9.3. The potential candidate variants are listed in the table 9.2.

**Figure 9.3: Variant analysis of Family D**

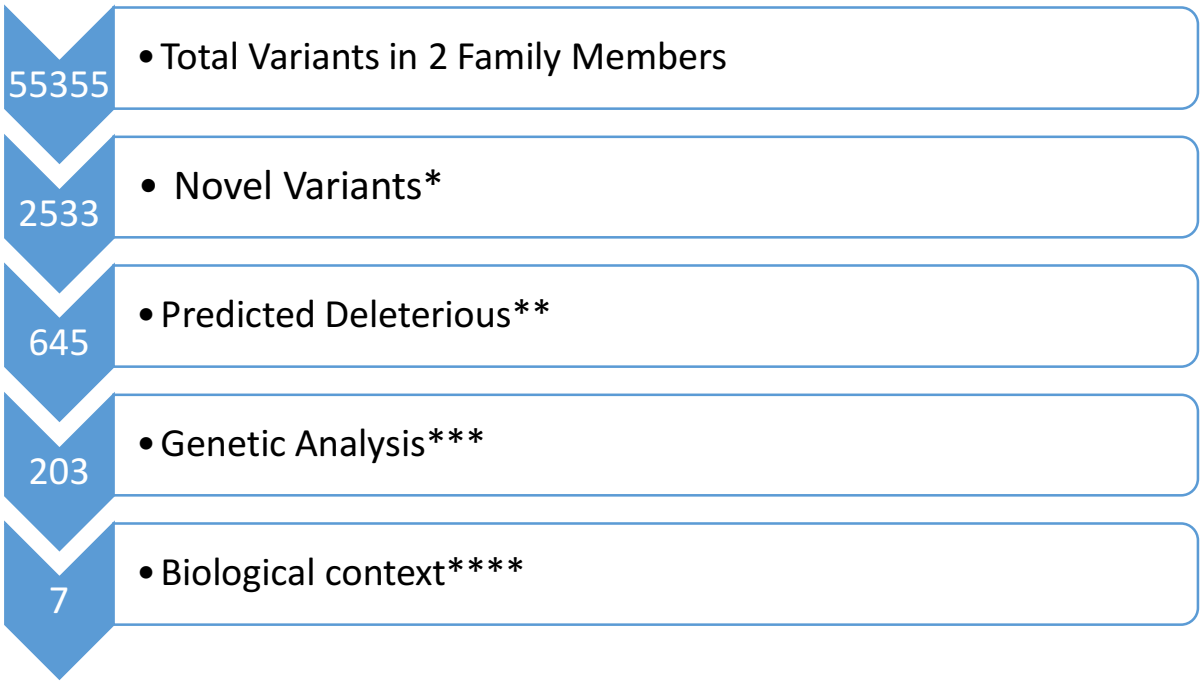


Variant Analysis of Proband D (* Novel variants include variants present in at least 5% minor allele frequency in 1000 Genomes Project, ExAC and NHLBI ESP exomes excluded; ** Predicted deleterious variants included nonsynonymous coding, splice site, frameshift, stop gain variants; *** Variants present in heterozygous state in the child; **** Variants with biological role related to the clinical phenotype of short stature, facial dysmorphia, skeletal abnormalities and congenital heart defects ).

**Table 9.2** List of variants from proband D

| Chromosome | Gene | Gene region | Protein variant |
|---|---|---|---|
| **1** | COL24A1 | Exonic | p.R635W |
| | | | |
| **3** | PLXND1 | Splice site | |
| | | | |
| **4** | TECRL | Exonic | p.E11D |
| | | | |
| **8** | EBF2 | Exonic | p.N477H |
| | | | |
| **10** | ABLIM1 | Exonic | p.D169H |
| | | | |
| **11** | B3GAT3 | Splice site | |

A brief description of the genes is given below

***COL24A1***

This gene is a member of the collagen gene family, encoding Collagen Type XXIV Alpha 1 Chain. This protein has a specific regulatory role in type I collagen fibrillogenesis during foetal development. The gene is associated with a disease such as Miller-Dieker Lissencephaly which consists of muscular dystrophic symptoms

*COL24A1* is associated with osteoblast differentiation through interacting with a transmembrane integrin β3, whilst silencing expression of Smad7 and inhibiting the phosphorylation of the Smad2/3 (332).

***PLXND1***

*PLXND1* contributes towards the development of the cardiovascular, nervous and immune systems. It is suggested that Plexin D1 interacts with Sema through paracrine signalling to guide axonal and other tissues patterning (333). Throughout embryogenesis *PLXND1* is dynamically activated to ensure this patterning structure.

***TECRL***

This gene encodes Trans-2,3-Enoyl-CoA Reductase Like protein. Symptoms associated with this gene include ventricular tachycardia, catecholaminergic polymorphic 3 and catecholaminergic polymorphic ventricular tachycardia. *TECRL* has been quoted as a 'new sudden death gene' (334)

***EBF2***

This gene encodes Early B-Cell Factor 2, as part of the Collier/Olf/EBF (COE) family of genes to produce helix-loop-helix transcription factors. Kieslinger et al. demonstrated that *EBF2* regulates osteoblast and osteoclasts through activation of the RANK decoy receptor (335).

***ABLIM1***

This gene encodes Actin Binding LIM Protein 1, playing a key role in regulation of developmental pathways through its LIM domain. Abnormal splicing of *ABLIM1* has been reported in cases of myotonic dystrophy type 1 (336).

**9.4 *B3GAT3***

*B3GAT3*, encoding β-1,3-glucuronyltransferase 3, has an important role in proteoglycan biosynthesis. Homozygous *B3GAT3* mutations have been associated with short stature, skeletal deformities and congenital heart defects. As this gene appears to segregate with the clinical phenotype of proband D, it has been described in detail along with the splice site mutation (c.888+262T>G) in the sections below.

### 9.4.1 *B3GAT3* mutation (c.888+262T>G)

A heterozygous *B3GAT3* mutation (c.888+262T>G) in the invariant "GT" splice donor site was identified in proband D. This variant is considered to be pathogenic as it decreases the splicing efficiency in the mRNA as predicted by a MaxEntScan score decrease of 100% (from 11.01 to -0.14) thereby creating an alternative splice site resulting in a frame shift and truncation of the protein through misfolding.

### 9.4.2 Biological Function of *B3GAT3*

*B3GAT3* is involved in glycosaminoglycan (GAG) biosynthesis, which provides structural support within the extracellular matrix surrounding the cells(337). Genetic defects can thus lead to multi-system disorders. Several papers have classified a homozygous mutation in *B3GAT3* as the reason for their patients' congenital heart defects, short stature, and mild dysmorphic features (337-340).

A comparison of the phenotype of proband D with that of patients with *B3GAT3* mutations reported in the literature is shown below in the table 9.3.

**Table 9.3:** Comparison of clinical features between proband D and patients with *B3GAT3* mutations reported in the literature

| Phenotype | Our Patient | Baasanjav, S., et al. (2011) | | Job, F. et al. (2016) | v. Oettingen, J.E. et al. | Jones, K.L. et al (2015) |
|---|---|---|---|---|---|---|
| Number of Patients | 1 | 5 | | 1 | 1 | 1 |
| **Skeletal Malformations** | | | | | | |
| Short Stature | ✓ | ✓ | (5/5) | ✗ | ✓ | ✓ |
| Fractures | ✗ | | | ✓ | ✗ | ✓ |
| Anteverted Nares | ✓ | ✓ | (4/5) | ✗ | ✓ | ✓ |
| Small Upturned Nose | ✓ | | | ✓ | ✓ | ✓ |
| Hypertelorism | ✓ | | | | | ✓ |
| Frontal Bossing | ✓ | | | | ✓ | |
| Short Proximal Bones | ✓ | | | ✓ | ✓ | |
| Hypermobile Joints | ✓ | | | | | |
| Dislocating Joints | ✗ | ✓ | | ✓ | ✓ | |
| Joint Laxity | ✗ | | | ✓ | ✓ | |
| Diffuse Demineralisation | ✗ | ✓ | | ✓ | ✗ | ✓ |
| Down Slanting Palperbral Fissures | ✓ | ✓ | (3/5) | ✓ | | |
| **Congenital Heart Defects** | | | | | | |
| Ventricular Septal Defect | ✓ | ✓ | (2/5) | | ✗ | ✓ |
| Pulmonary Stenosis | ✓ | | | | ✗ | |
| Bicuspid Aortic Valve | ✗ | ✓ | (3/5) | ✓ | ✗ | |
| Aortic Root Dilation | ✗ | ✓ | (3/5) | | ✓ | |
| Mitral Valve Prolapse | ✗ | ✓ | (4/5) | | ✗ | |
| **Neurological** | | | | | | |
| Small Anterior Pituitary | ✓ | ✗ | | ✗ | ✗ | |
| Partially Empty Sella | | | | | ✓ | |
| **Other Features** | | | | | | |
| TSH Abnormality | ✗ | | | ✓ | | |
| Cognitive Delay | ✗ | | | ✗ | ✓ | |
| Still-Born Sibiling | ✓ | | | | | |
| GH Deficiency | ✓ | | | | | |
| Congenital Sensorineural Deafness | ✓ | | | | | ✓ |
| Ketotic Hypoglycaemia | ✓ | | | | | |

Proteoglycans are an influential component of the extracellular matrix, orchestrating the cell-cell and cell-matrix interactions (337). Without a functional *B3GAT3* gene, the loss of β-1,3-glucuronlytransferase 3 causes incomplete proteoglycan production due to the final glucuronic acid linkage stage being absent (339). Cell signalling pathways, most notably developmental pathways, may become disrupted and processes such as skeletal development and cardiovascular maturation will halt before they are fully complete (339). Proteoglycans are produced through the secretory pathway in the endoplasmic reticulum followed by the construction of the glycosaminoglycan (GAG) side chain within the Golgi complex (341). Multiple post-translational modifications occur in the Golgi complex; including the addition of disaccharides as well as epimerisation and sulfation of saccharide units, all performed by various glycosyltransferases, epimerases and sulfotransferases (341).

β-1,3-glucuronyltransferase 3 (GlcAT-I), encoded by *B3GAT3* is located on chromosome 11q12.3 and consists of 335 amino acids with one N-linked glycan chain GlcAT-I is a glucuronyltransferase involved in the biosynthesises of GAG-protein linkers for proteoglycans. Specifically, GlcAT-I contributes to the addition of the terminal four saccharides –xylose-galactose-galactose-glucuronic acid, hence its presence in the *cis*-Golgi(342). The addition of this tetra saccharide provides an external face for binding by extracellular signals.

Homozygous mutations in *B3GAT3* have previously been reported throughout the literature with Larsen-like syndrome symptoms. Larsen syndrome is defined as a development disorder of the bones throughout the body, individuals frequently express symptoms such as skeletal dislocations, hearing loss and facial dysmorphism (depressed nasal bridge, frontal bossing and telecanthus) (338).

## 9.5 DISCUSSION

*B3GAT3* transcribes the 335 amino acid glucuronyltransferase I (GlcAT-I) protein which catalyses the final step in proteoglycan biosynthesis through the addition of a xylose-galactose-galactose-glucuronic acid tetra saccharide linkage molecule(340). Homozygous missense mutations in *B3GAT3* have previously been described as 'linkeropathies'. Glycosaminoglycan linkeropathies are characterised by their enzymatic inability to synthesise the common linker region which joins the core protein with its respective glycosaminoglycan side chain(343). Proteoglycans are crucial for effective communication between cells. Disruption of the linkage region caused by mutations in *B3GAT3* have been reported to cause severe developmental defects.

A novel heterozygous splice site mutation in *B3GAT3* (c.888+262T>G) in the invariant "GT" splice donor site was found in proband D. *In silico* modelling of this variant categorised the variant as pathogenic. This variant decreases the splicing efficiency of the mRNA; as predicted by a MaxEntScan score decrease of 100 % (from 11.01 to -0.14). MaxEntScan is a *in silico* splicing defect prediction tool used to analyse the affinity of an intronic sequence to the splicing machinery (344). A decrease of 100 % suggests that the splice site is completely lost, thus incurring a frameshift. Subsequent truncation of the protein would lead to incomplete biosynthesis of the xylose-galactose-galactose-glucuronic acid terminus of the glycosaminoglycan side chain of the proteoglycan

After extensive reviewing of current literature (332-334, 336, 345, 346) it was found that the biological function of the filtered genes such as *COL24A1, PLXND1, TECRL, EBF2, ABLIM1,* and *POSTN* did not segregate with the clinical phenotype whereas *B3GAT3* showed notable traits.

The phenotype of proband D aligns with several other phenotypic features described to be associated with *B3GAT3* mutation (table 9.3). All reported cases of *B3GAT3* have short stature, anteverted nares, down slanting palpebral fissures and ventricular septal defects. However, these have all been associated with homozygous missense mutations such as c.671 T>A (p.Leu224Gln) [2], c.830 G>A (p.Arg277Gln) [1] and c. 667 G>A (p.Gly223Ser) (338). Splice site mutations contributing to *B3GAT3* phenotype as encountered in proband D has not been described in the literature.

In addition to some similarities in phenotypic features shown in table 9.3, proband D also has growth hormone deficiency and recurrent ketotic hypoglycaemia. An initial targeted exome sequencing experiment was conducted to discover any mutated genes involved in ketogenesis, ketolysis, carbohydrate metabolism, fatty acid oxidation defects and hyperammonaemia; no pathogenic mutations were identified.

It is noteworthy to mention that the patient's biological father was also short with facial dysmorphism and short bones. Besides, a history of stillborn elder sibling with facial dysmorphism, short bones and heart defects suggests a likely strong penetrance of a monogenic genetic aetiology in the family. The genetic analysis in the biological father and the elder sibling would have convincingly established the underlying monogenic aetiology. However, this has not been possible due to the non-availability of the DNA samples. After filtering the WES data from proband D, the splice site mutation in *B3GAT3* segregated with many of the phenotypic features. Further functional studies are required to fully characterise the role of this splice site variant in *B3GAT3.*

# FAMILY E

### 9.6 CLINICAL INFORMATION (FAMILY E)

Proband E is a 7-year-old boy who was referred for an endocrinology consultation for severe shore stature (height: -3.5 SDS). He was born at 39 weeks gestation to non-consanguineous, healthy British parents with a birth weight of 2.5 kg. There were no neonatal concerns. There was no evidence of dysmorphism or skeletal dysplasia. The investigations to look into the cause for the short stature revealed a persistently low IGF1 of 5-8nmol/L (12-62). An IGF-1 regeneration test following 33ug/kg of GH did not result in the improvement of serum IGF1 concentration. A growth hormone stimulation test, using glucagon showed a good GH response of 11.2ug/L. A trial of high dose rGH treatment(40ug/kg/day) was commenced with a reasonable response (height: -2.5SDS) (figure 9.5). CGH microarray did not reveal any copy number changes. Targeted sequencing of IGF1, IGF1R and GHR performed at Barts, London, did not reveal any mutations.

**Figure 9.4:** Pedigree of Family E

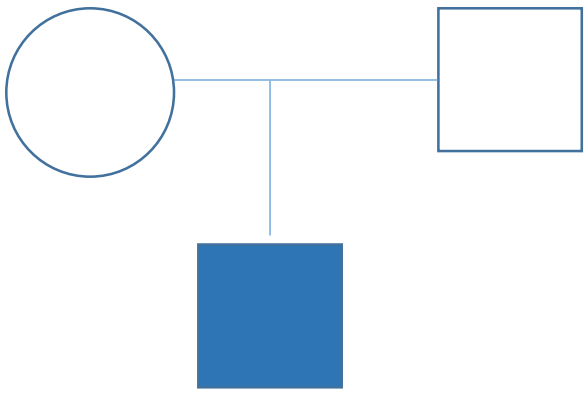

**Figure 9.5:** Growth chart of proband E showing reasonable response to GH therapy

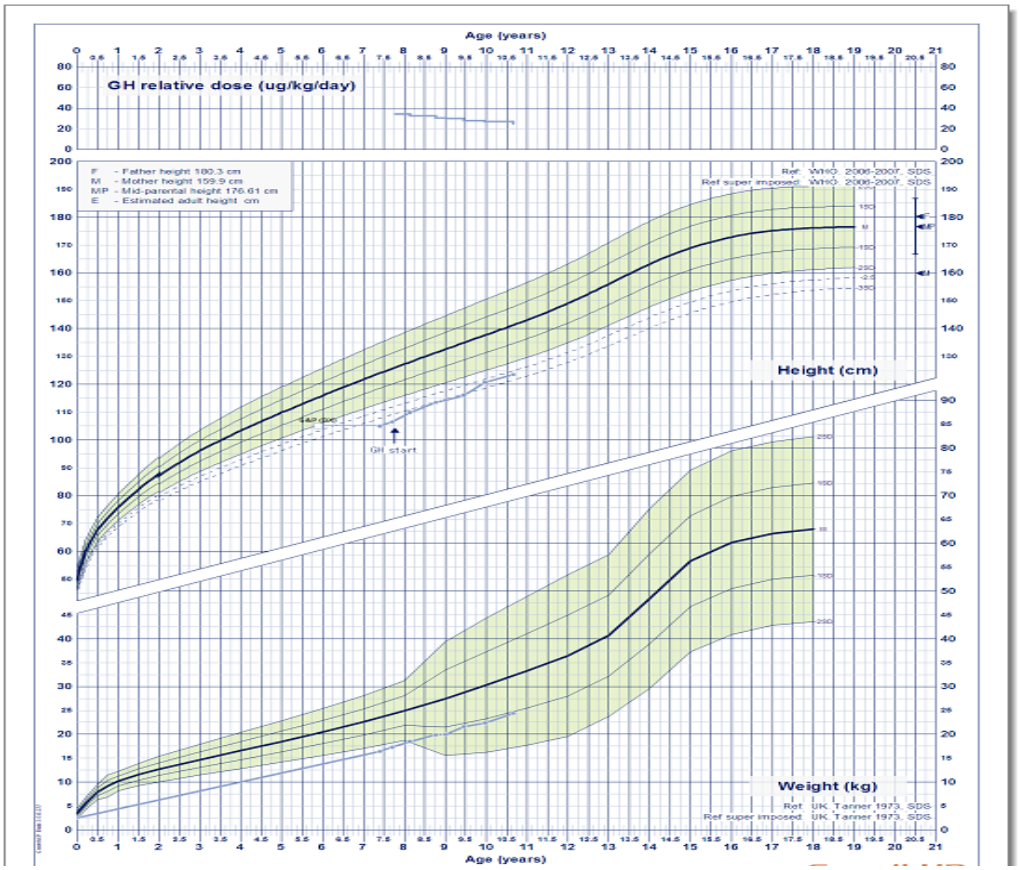


## 9.7 WHOLE EXOME SEQUENCING RESULTS FROM FAMILY E

In this family, whole-exome sequencing was performed on the both the parents(unaffected) and the affected child. Assuming a *de novo* inheritance pattern, filters were applied to whole-exome data as shown in the figure 9.6. The potential candidate variants are listed in the table 9.4.

**Figure 9.6:** *De Novo* variant analysis of Family E

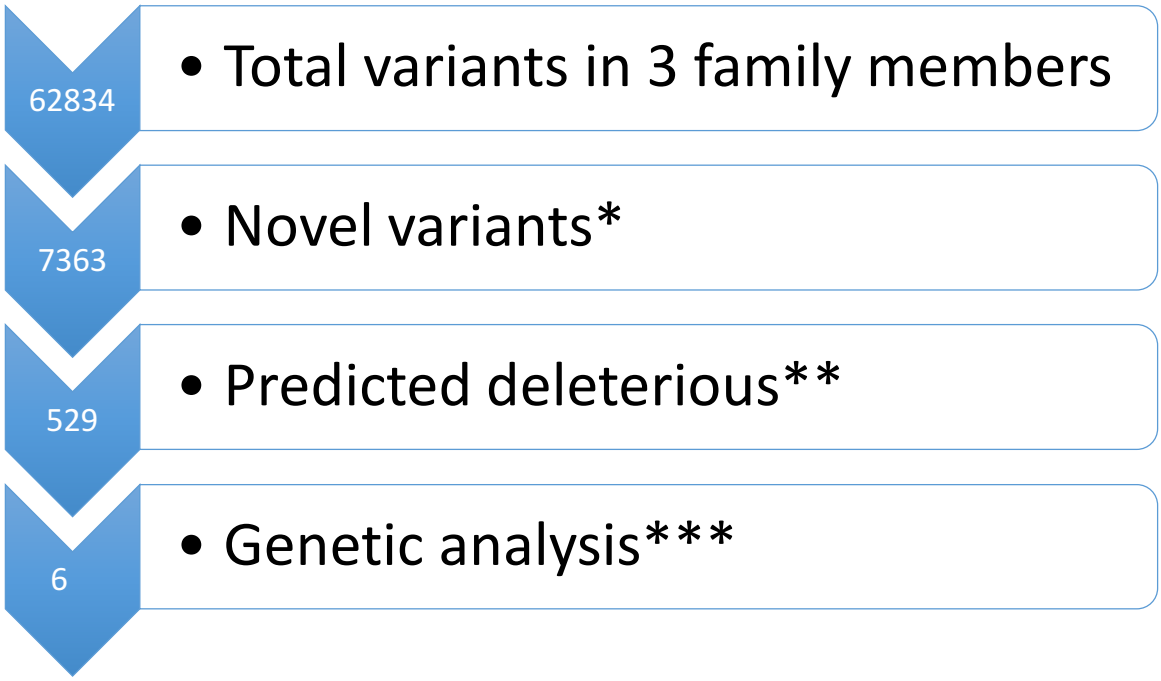


De Novo Variant Analysis of proband E (* Novel variants include variants present in at least 5% minor allele frequency in 1000 Genomes Project, ExAC and NHLBI ESP exomes excluded; ** Predicted deleterious variants included nonsynonymous coding, splice site, frameshift, stop gain variants; *** Variants present in heterozygous state in the child and not present in both the parents)

The potential candidate gene variants and their locations in proband E are shown in table 9.4

**Table 9.4**: List of Genes with Novel, Predicted Deleterious Variants Not Present in both the parents

| Chromosome | Gene | Gene region | Protein variant |
|---|---|---|---|
| 2 | TSGA10 | Splice site | |
| | | | |
| 5 | YTHDC2 | Splice site | |
| | | | |
| 5 | SAR1B | Splice site | |
| | | | |
| 5 | NOTCH4 | Exonic | p.L16del |
| | | | |
| 8 | VPS13B | Splice site | |
| | | | |
| 13 | SKA3 | Splice site | |

A brief description of these genes is presented next. From the available biological information about these genes, the phenotype of proband E could not be explained with variations in these genes.

***TSGA10*** (Testis specific protein 10)

Northern blot analysis detected the expression of this gene in testis and may play a role in the formation of sperm tail fibrous sheath (347).

***YTHDC2*** (YTH Domain Containing 2)

Members of this family function in RNA processing and metabolism, including transcription, alternative splicing, and degradation (348).

***SAR1B*** (Secretion Associated Ras Related GTPase 1B)

Recessive SAR1B mutations have been reported to cause chylomicron retention disease (349).

***NOTCH4*** (Neurogenic Locus Notch Homolog Protein 4)

The *NOTCH4* gene encodes a member of Notch family. The members of this family are transmembrane proteins with an extracellular domain consisting of multiple epidermal growth factor-like (EGF) repeats, and an intracellular domain of various different types (350).In Drosophilia, the members of Notch family interacts with its cell-bound ligands (delta, serrate) and this interaction plays a key role in development. In humans, *Notch4* functions as a receptor for membrane bound ligands Jagged 1, Jagged 2 and Delta 1(351).By studying the *Notch-4* deficient mouse, Krebs et al. concluded that *Notch4* and *Notch1* genes have partially overlapping roles during embryogenesis (352). Mutants mice with constitutive overexpression of *Notch4* developed brain arteriovenous malformations, suggesting Notch pathway to be an inhibitor of vessel sprouting (353).

***VPS13B*** (Vacuolar Protein Sorting 13 Homolog B)

Homozygous mutations in this gene causes autosomal recessive condition, Cohen syndrome (354)

***SKA3*** (Spindle And Kinetochore Associated Complex Subunit 3)

This gene encodes a component of the spindle and kinetochore-associated protein complex that regulates microtubule attachment to the kinetochores during mitosis. The encoded protein localizes to the outer kinetechore and may be required for normal chromosome segregation and cell division (355).

Assuming a recessive inheritance, the filtering strategy applied to whole-exome sequencing data

**Figure 9.7:** Recessive Inheritance Analysis

Recessive Variant Analysis of Proband E (* Novel variants include variants present in at least 3% minor allele frequency in 1000 Genomes Project, ExAC and NHLBI ESP exomes excluded; ** Predicted deleterious variants included nonsynonymous coding, splice site, frameshift, stop gain variants; *** Variants present in homozygous/compound heterozygous state in the child).

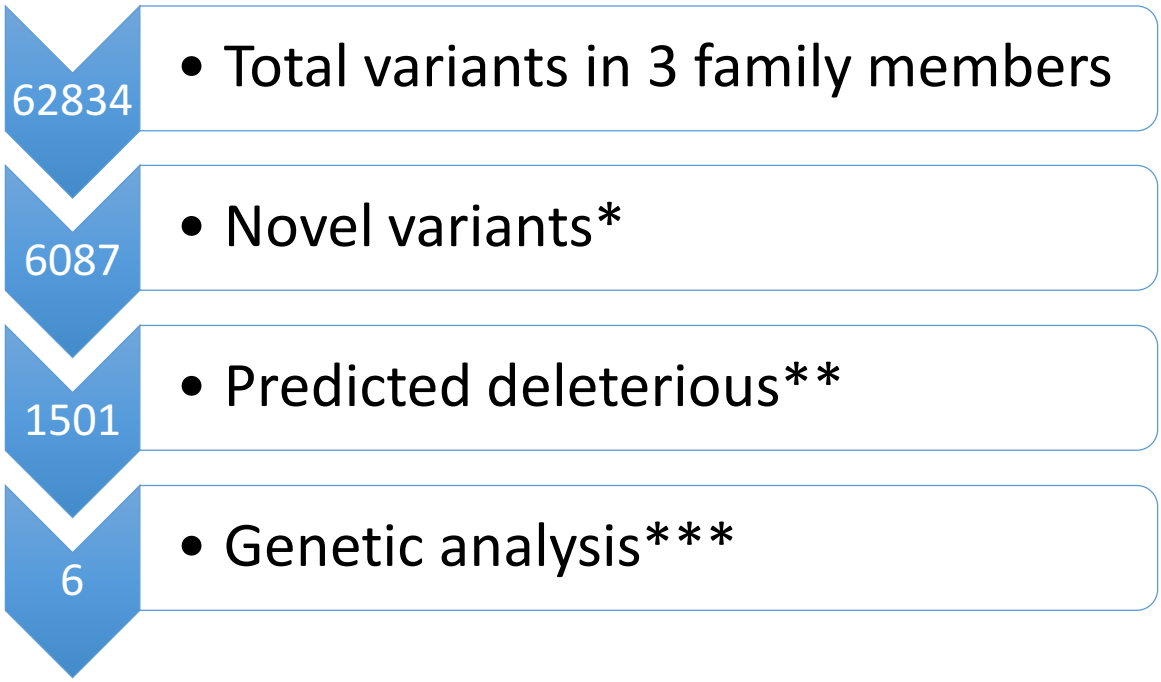

**Table 9.5:** List of Genes with Novel, recessive predicted deleterious variants (Family E)

| Chromosome | Gene | Gene region | Protein variant |
|---|---|---|---|
| | | | |
| 1 | MST1L | Exonic | p.G300fs*89 |
| | | | |
| 4 | ZNF141 | Exonic | p.L70fs*34/p.K69fs*4 |
| | | | |
| 10 | CFAP46 | Exonic | p.G1162R/p.D1126G |
| | | | |
| 12 | CAPZA3 | Exonic | p.R39C/p.R39H |
| | | | |
| 13 | SACS | Exonic | p.R2844H/p.P2651Q |
| | | | |
| 17 | GH1 | Promoter | c.-93delG |

A brief description of these genes is presented next.

***MST1L*** (Macrophage Stimulating 1 Like)

There is only a limited biological information available in the literature.

***ZNF141*** (Zinc Finger Protein 141)

Defects in this gene have been associated with autosomal recessive postaxial polydactyly type A (356).

***CFAP46*** (Cilia And Flagella Associated Protein 46)

This gene is thought to play an important role in ciliary movement

***CAPZA3*** (Capping Actin Protein of Muscle Z-Line Alpha Subunit 3)

The gene encodes a protein that is localized to the neck and tail region of the spermatozoa and may play a role in male fertility (357).

***SACS*** (Sacsin Molecular Chaperone)

This protein is thought to integrate the ubiquitin-proteasome system and Hsp70 chaperone machinery and implicated in the processing of ataxin-1(358).Homozygous mutations are implicated in Spastic ataxia, Charlevoix-Saguenay type (359).

### 9.8 *GH1*(Growth Hormone 1)

Growth hormone (GH), encoded by *GH1*, is a member of the somatotropin family of hormones (360) which stimulates growth during early postnatal somatic development (361). GH regulates glucose, protein and fat metabolism in the body and is essential for tissue maintenance and repair throughout the duration of an individual's life(362). GH consists of 191 amino acids, weighing 22 kDa, arranged in four α-helices connected by two cysteine bridges; forming two distinct domains which have different affinities for binding to growth hormone receptor (GHR) (363).

Binding of GH to GHR induces receptor dimerization leading to transphosphorylation of the intracellular domains of the receptors. Phosphate groups for SH2/SH3 domains of intracellular second messengers to bind are then present on the intracellular side of the plasma membrane. Janus kinase 2 (Jak2) interacts through its SH2 domain and activates a downstream effector, signal transducer and activator of transcription (STAT5) (364). Phosphorylation of STAT5 causes its dissociation from GHR and the phosphorylated STAT5 translocates to the nucleus to activate transcription (365).

Short stature is frequently characterised by a deficiency in growth hormone, known as isolated growth hormone deficiency (IGHD) (366). IGHD is caused by genetic mutations in the promoter region of the *GH1* gene.

Since the biological function of *GH1* segregates with the clinical phenotype of proband E, a detailed description of the mutation *GH1*(c.-93delG) is given in the next section.

### 9.8.1 GH1 promoter variant(c.-93delG)

Proband E has a homozygous promoter region variant (c.-93delG) in the *GH1* gene that could be potentially contributing to the impaired transcription of the *GH1* leading to short stature. An impairment of transcription due to promoter mutation usually causes GHD. Although proband E had a normal GH response to glucagon stimulation test, he responded well to exogenous rGH with subsequent normalisation of IGF1. It is therefore hypothesised that the promoter mutation in proband E to be contributing to the production of biologically inactive GH.

Bioinactive GH was first reported by Kowarski *et al*. when they noted two children who expressed: normal-high immunoassayable GH levels, low basal IGF-1 levels and an increase in IGF-1 circulating concentrations as well as improved somatic growth following exogenous GH administration (367). Bioinactive GH is a rare condition in which there is significant difference between physiological concentrations of GH and the activity that is generated due to them. Bioinactive GH is associated with low insulin-like growth factor-1 (IGF-1), short stature and a response to exogenous GH treatment (368).

Homozygous point mutation in the promoter region of GH1(c.-233C>T) has been shown to reduce the GH1 expression, leading to isolated GH deficiency(366). Beeson et.al identified a homozygous missense *GH1* mutation in *a* patient with severe short stature(height:-3.6SDS), persistent low basal IGF1,normal GH response on provocation test and a good improvement in height velocity after administration of rGH(111). The authors proposed that the mutation led to the disruption of the disulphide bridge Cys-53 to Cys-165 in the GH peptide leading to the production of biologically inactive GH. By *in vitro* experiments it was demonstrated that GHR binding

and Jak2/Stat5 signalling pathway was significantly reduced in the mutant *GH1* when compared to the wild type *GH1*(111).

Proband E has similar phenotypic features as the patient described by Beeson et.al. It is therefore possible that the improvement in height velocity to rGH with normal endogenous GH peak on provocation test is probably because of biologically inactive endogenous GH. The pathogenic effect of the homozygous promoter variant(c.-93delG**)** identified in proband E on *GH1* is currently unclear. Future functional work such as GH binding assay may be needed to study the pathogenicity of the variant.

# FAMILY F

## 9.9 CLINICAL INFORMATION (FAMILY F)

Proband F, a 15-year-old boy presented with a long standing history of tiredness and lethargy. He was born to non-consanguineous British parents and does not have any significant past medical history. His height and weight were appropriate for his age and the systemic examinations were normal, apart from high blood pressure (150/90mm Hg). His elder sibling passed away due to Hurler's disease.

Further investigations revealed a high serum calcium and parathyroid hormone(PTH) concentration, low vitamin D, low albumin and a low urinary calcium creatinine ratio. The investigations are charted in detail in the table below (Table 9.6). The serum calcium profile and PTH from both the parents were within the normal range. The hypercalcemia persisted in the range between 2.82-2.93mmol/L with an unsuppressed PTH and proband F continued to exhibit symptoms of persistent tiredness and lethargy. The vitamin D concentration was persistently low despite the administration of 300,000 IU of ergocalciferol injection. The urinary calcium creatinine ratio was consistently low (<0.01). A differential diagnosis of familial hypoclaciuric hypercalcemia and primary hyperparathyroidism was considered. Microarray did not identify any copy number variants. Genetic testing for familial hypocalciuric hypercalcemia did not identify any pathogenic mutations in *CASR*, *GNA11* and *AP2S1*. Targeted sequencing for genes associated with familial isolated hyperparathyroidism did not detect any mutation in *MEN1, RET, CDC73, CDKN1A, CDK1B, CDK2B* and *CDKN2C*. Sestamibi parathyroid scan to localise parathyroid adenoma was negative. Subsequently the patient was recruited into the study for WES to identify a potential monogenic etiology for hypercalcemia.

Further investigations for persistent hypalbuminaemia included a renal biopsy which showed a slight increase in the mesangial cell matrix and mild increase in the mesangial cell numbers with no evidence of endocapillary crescents. The electron microscopy of the basement membrane showed a variable thickness of the basement membrane with electron-dense deposits. This was consistent with a form of nephrotic syndrome and currently being managed by losartan.

**Table 9.6:** Summary of investigations in proband F

| | |
|---|---|
| Serum calcium | 2.82 mmol/L to 2.93 mmol/L(2.15-2.74) |
| PTH | 11.6-14.6 pmol/L(1.1-6.9) |
| Vitamin D | 6-10 nmol/L(>50) |
| Urine calcium creatinine ratio | <0.01 |
| Albumin | 23-25 g/L(40-60) |
| Phosphate | Normal |
| Magnesium | 0.66 mmol/L(0.78-1.02) |
| Thyroid Function | Normal |
| Urine dipstick | 2+ blood, 3+ protein |
| Ultrasound renal tract | Normal |
| Liver function test | Normal |
| Renal functions(Urea, creatinine) | Normal |

**Figure 9.8** Pedigree of Family F

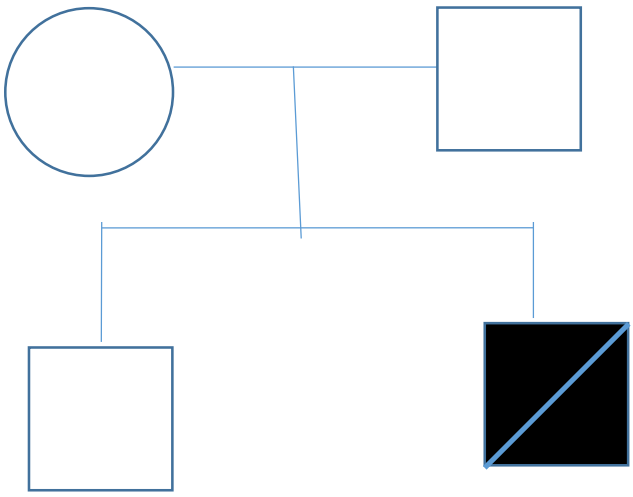

## 9.10 WHOLE EXOME SEQUENCING RESULTS FROM FAMILY F

In this family, whole-exome sequencing was performed on the both the parents(unaffected) and the affected child. Assuming a *de novo* inheritance pattern, filters were applied to whole-exome data as shown in the figure 9.9.

**Figure 9.9** *De Novo* variant analysis of Family F

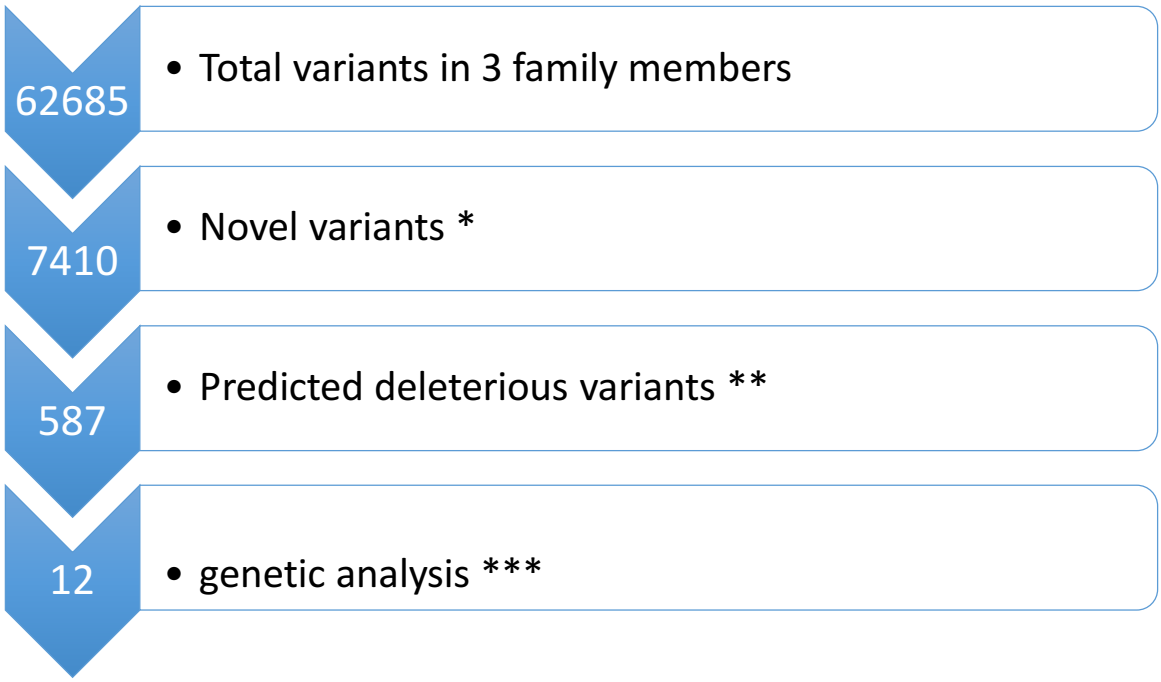


De Novo Variant Analysis of Proband F (* Novel variants include variants present in at least 5% minor allele frequency in 1000 Genomes Project, ExAC and NHLBI ESP exomes excluded; ** Predicted deleterious variants included nonsynonymous coding, splice site, frameshift, stop gain variants; *** Variants present in heterozygous state in the child and not present in both the parents)

The potential candidate gene variants and their locations in family F are shown in table 9.7

**Table 9.7:** List of Genes with Novel, Predicted Deleterious Variants Not Present in both the parents (Family F)

| Chromosome | Gene | Gene region | Protein variant |
|---|---|---|---|
| 2 | AGPS | Splice site | |
| | | | |
| 4 | ABCE1 | Splice site | |
| | | | |
| 7 | MGAM2 | Splice site | |
| | | | |
| 14 | SYT16 | Splice site | |
| | | | |
| 14 | TTLL5 | Exonic | p.D219V |
| | | | |
| 20 | SLC4A11 | Splice site | |
| | | | |
| 1 | CPSF3L | Exonic | p.A13G |
| | | | |
| 6 | FAM8A1 | Exonic | p.L135P |
| | | | |
| 7 | AUTS2 | Exonic | p.Q449H |
| | | | |
| 13 | PABPC3 | Exonic | p.E372G |
| | | | |
| 17 | MPDU1 | Exonic | p.R169fs*44 |
| | | | |
| 17 | SRCIN1 | Exonic | p.R1011P |

A brief description of these genes is presented next. From the available biological information about these genes, the phenotype of proband F could not be explained with variations in these genes.

***AGPS*** (Alkylglycerone-phosphate synthase)

AGPS catalyzes the second step of ether lipid biosynthesis Mutations in this gene have been associated with rhizomelic chondrodysplasia punctata, type 3 and Zellweger syndrome (369).

***ABCE1***(ATP Binding Cassette Subfamily E Member 1)

*ABCE1* belongs to the superfamily of ATP binding cassette proteins and plays an important role in protein translation initiation, elongation, termination, and ribosome recycling in eukaryotes (370).

***MGAM2*** (Maltase-Glucoamylase 2 (Putative))

No information is currently available on the biological function of this gene.

***SYT16*** (Synaptotagmin 16)

SYT16 may have a role in the trafficking and exocytosis of secretory vesicles in non-neuronal tissues. Is Ca(2+)-independent. RT-PCR detected highest SYT16 expression in mouse heart and testis, with weaker expression in kidney and lung (371).

***TTLL5*** (Tubulin Tyrosine Ligase Like 5)

TTLL5 may act as a co-regulator of glucocorticoid receptor mediated gene induction and repression. Recessive mutations in TTL5 have been associated with cone-rod dystrophy (372).

***SLC4A11*** (Solute Carrier Family 4 Member 11)

This gene encodes a voltage-regulated, electrogenic sodium-coupled borate cotransporter that is essential for borate homeostasis, cell growth and cell proliferation. Recessive mutations have been associated with corneal endothelial dystrophy and perceptive deafness (373).

***CPSF3L*** (Cleavage and Polyadenylation-Specific Factor 3-Like Protein)

It is a part of integrator complex and involved in the processing of small nuclear RNAs U1 and U2.(374)

***FAM8A1*** (Family with Sequence Similarity 8 Member A1)

It is a protein coding gene with limited information on its biological function.

***AUTS2*** (Autism Susceptibility Candidate 2)

*AUTS2* has been implicated in neurodevelopment and as a candidate gene for numerous neurological disorders, including autism spectrum disorders and autosomal dominant intellectual disability (375).

***PABPC3*** (Poly(A) Binding Protein Cytoplasmic 3)

Poly(A)-binding proteins (PABP) are involved in messenger RNA stability and initiation of translation. By Northern blot analysis of multiple tissues, it was found to have weak but distinct testis-specific expression (376)

***MPDU1*** (**Mannose-P-Dolichol Utilization Defect 1)**

MPDU1 encodes an endoplasmic reticulum membrane protein and plays a role in the synthesis of lipid-linked oligosaccharides and glycosylphosphatidylinositols. Mutations in this gene result in congenital disorder of glycosylation type If (377)

***SRCIN1*** (SRC Kinase Signaling Inhibitor 1)

SRC kinase signalling inhibitor 1 acts as a negative regulator of SRC and downstream signalling, leading to impaired cell spreading and migration (378).

Assuming a recessive inheritance, the filtering strategy applied to whole-exome sequencing data

**Figure 9.10:** Recessive Inheritance Analysis

Recessive Variant Analysis of Proband F (* Novel variants include variants present in at least 3% minor allele frequency in 1000 Genomes Project, ExAC and NHLBI ESP exomes excluded; ** Predicted deleterious variants included nonsynonymous coding, splice site, frameshift, stop gain variants; *** Variants present in homozygous/compound heterozygous state in the child).

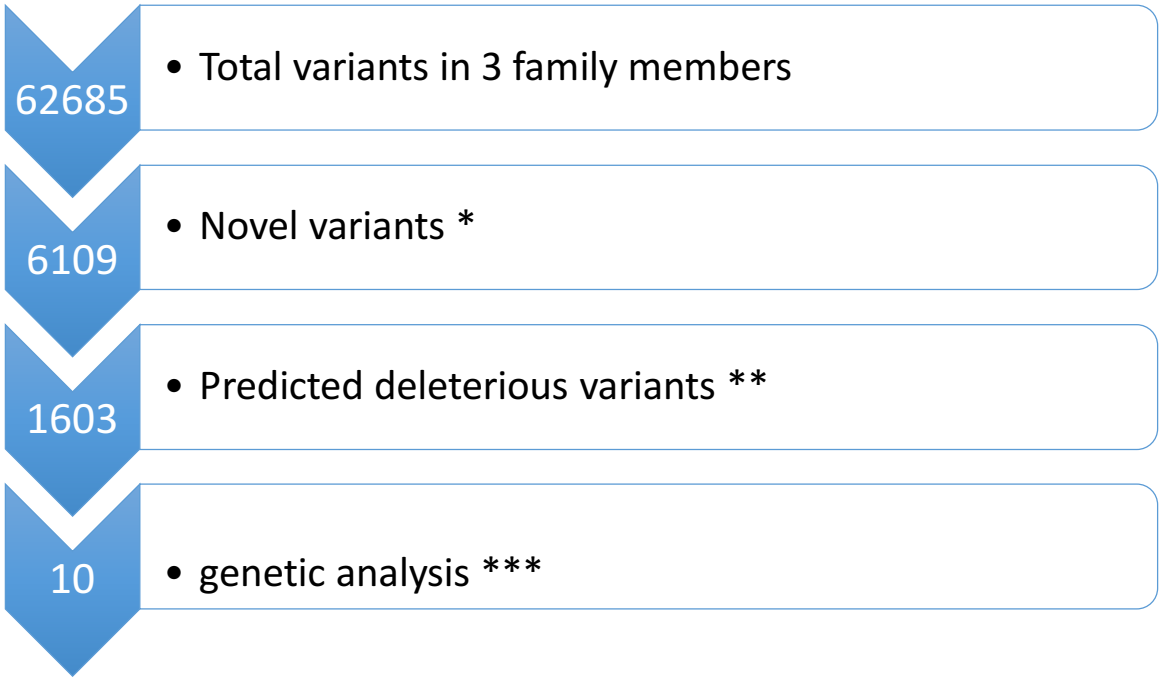

**Table 9.8:** List of Genes with novel, recessive Predicted Deleterious Variants (Family F)

| Chromosome | Gene | Gene region | Protein variant |
|---|---|---|---|
| 1 | INTS11 | Splice site | |
| | | | |
| 2 | CFAP65 | Promoter | |
| | | | |
| 2 | ABCB6 | Exonic | p.A446T,p492T |
| | | | |
| 5 | PDZD2 | Exonic | p.A1649V |
| | | | |
| 9 | BRINP1 | Exonic | p.R358H |
| | | | |
| 11 | DRD4 | Promoter | |
| | | | |
| 11 | MRPL16 | Exonic | p.R199Q |
| | | | |
| 16 | HAS3 | Exonic | p.R173H |
| | | | |
| 13 | SKA3 | Splice site | |
| | | | |
| 13 | PABPC3 | Splice site | |

A brief description of the above genes is given as below

***INTS11*** (Integrator Complex Subunit 11)

This gene associates with the C-terminal domain of RNA polymerase II large subunit and mediates the 3-prime end processing of small nuclear RNAs U1 and U2 (374).

***CFAP65***(Cilia and Flagella associated protein)

Tang et al. (2017) identified homozygous nonsense mutation, in CFAP65, in man with morphological abnormalities of the flagella in spermatozoa (379).

***ABCB6***(ATP binding cassette subfamily B, member 6)

This gene has a role in the transport of porphyrins into the mitochondria(380).

***PDZD2***(PDZ domain containing 2)

This gene interacts with the PKP4 PDZ domain and Ma et al. (2006) localized rat PDZD2 specifically to pancreatic beta cells, with no expression detected in alpha cells(381).

***BRINP1*** (Bone Morphogenetic Protein/Retinoic Acid Inducible Neural-Specific 1)

Diseases associated with this gene mutation include transitional cell carcinoma and bladder carcinoma. The 5' CpG island in the gene is a frequent target for hypermethylation, and it may undergo hypermethylation-based silencing in some bladder cancers(382).

***DRD4***(Dopamine receptor D4)

This gene is localised at 11p15.5 and is associated with dominantly inherited attention deficit hyperactivity disorder(383)

***MRPL16***(Mitochondrial ribosomal protein L-16)

This gene has an essential role in the oxidative phosphorylation in the mitochondria(384).

***HAS3***(Hyaluronon synthase 3)

This gene has been implicated to have an important role in the biosynthesis of hyaluronon (385).

Based on the known biological functions of these genes, the phenotype of proband F could not be explained with variations in these genes.

# CHAPTER 10

# GENERAL DISCUSSION, CONCLUSIONS AND FUTURE DIRECTIONS

## 10.1 GENERAL DISCUSSION

The use of next generation sequencing in children with undiagnosed or unidentified syndromic disorders is becoming more popular in the recent years and increasing the ability to discover novel genes and mutations contributing to novel clinical phenotypes. WES is a cost effective technique in comparison to whole genome sequencing and has the ability to target the coding regions of the genome and thus has an increased chance of uncovering a potential underlying genetic etiology especially in rare undiagnosed diseases. WES has been used increasingly in the field of paediatric endocrinology over the last decade contributing to the discovery of novel genes and genetic pathways. In this study a cohort of patients with varied phenotypes such as persistent CHI, congenital hypopituitarism, dysmorphic short stature with primary IGF1 deficiency, short stature with cardiac and other dysmorphic features, severe short stature with persistent low IGF1 and disorder of calcium metabolism was recruited for WES to identify the underlying genetic etiology. The results from the study have revealed the following:

1. A novel mutation in the transcription factor *FOXA2* that has been shown to cause hypopituitarism and CHI by further functional studies.
2. A novel compound heterozygous mutation in *ASXL3* contributing to Bainbridge Ropers like syndrome in association with primary IGF1 deficiency.
3. A novel frame-shift mutation in *CaMKK2* contributing to increased insulin secretion in a patient with CHI.
4. A novel splice site mutation in *B3GAT3* potentially contributing to severe short stature, facial dysmorphism and skeletal abnormalities.
5. A homozygous mutation in the promoter region of *GH1* possibly causing severe short stature.

The pituitary gland is a master regulator of vital physiological functions such as growth, puberty, lactation, metabolism, stress response and reproduction. The development of the pituitary gland is tightly controlled by signalling molecules and transcription factors that dictate pituitary cell lineage specification, cell proliferation and terminal differentiation into hormone-producing cell (56, 386). Abnormal pituitary development can lead to congenital hypopituitarism (CH) resulting in deficiency in one of more pituitary hormones. CH comprises of a spectrum of disorders with variable phenotypes that can range in severity, from isolated hormone deficiency [isolated growth hormone deficiency being the most common] to combined pituitary hormone deficiency (CPHD) when two or more pituitary hormones are deficient. Hypopituitarism may present as part of a syndrome with abnormalities in structures that share a common embryological origin with the pituitary gland, such as the forebrain and eyes, leading to septo-optic dysplasia (SOD) or holoprosencephaly (HPE) (386). SOD is a rare condition with a prevalence of 1:10,000 (387) live births and comprises the following features: optic nerve hypoplasia, midline forebrain defects and hypopituitarism (388, 389). Mutations in transcription factors such as *HESX1* (68), *PROP1* (390), *POU1F1* (266), *LHX3* (84), *LHX4* (391), *PITX1*, *PITX2* (392), *OTX2* (393), *SOX2* (394) and *SOX3* (395, 396) have been associated with CH in mouse and humans. However, these mutations account only for a small proportion of CH patients with the majority of patients having an unknown genetic cause for their symptoms.

CHI is a rare condition with an estimated prevalence of 1 in 50,000 live births, characterized by an inappropriate secretion of insulin from the β-cells of the pancreas during hypoglycaemia (264). CHI is the most common cause of severe and persistent hypoglycaemia in the neonatal period. The identification and appropriate

management of this condition is very important to avoid hypoglycaemic episodes and prevent the consequent neurological impairment. Mutations in genes *ABCC8* (150, 253-256), *KCNJ11* (150, 253-256), *GLUD1* (397), *GCK* (398), *HADH (171)*, *UCP2* (399), *HNF4A* (400), *HNF1A* (400), *MCT1* (189), *HK1* (194)and *PGM1* (197) have been associated with genetic forms of CHI (265). However, the genetic cause for many CHI patients remains elusive.

The combination of CHI and CHI in a single patient is extremely rare and the underlying genetic etiology causing this complex phenotype is unknown. In this study, a *de novo* heterozygous mutation in the developmental transcription factor, Forkhead box A2, *FOXA2* (c.505T>C, p. S169P) was identified in proband A who presented with CHI, CH, craniofacial dysmorphic features, choroidal coloboma and endoderm-derived organ malformations in liver, lung and gastrointestinal tract. The mutation is at a highly conserved residue within the DNA binding domain. A strong expression of *Foxa2* mRNA was demonstrated in the developing hypothalamus, pituitary, pancreas, lungs and oesophagus of mouse embryos using *in situ* hybridization. Expression profiling on human embryos by immunohistochemistry showed strong expression of hFOXA2 in the neural tube, third ventricle, diencephalon and in the pancreas. Transient transfection of HEK293T cells with Wt (Wild type) hFOXA2 or mutant hFOXA2 showed impairment in transcriptional reporter activity by the mutant hFOXA2. Further analyses using western blot assays showed that the *FOXA2* p.(S169P) variant is pathogenic resulting in lower expression levels when compared with Wt hFOXA2.

The results thus demonstrate, the causative role of *FOXA2* in a complex congenital syndrome with CH, CHI and endoderm-derived organ abnormalities.

As discussed before, in around 50% of the patients with persistent CHI, the underlying molecular genetic etiology is unknown (217). Due to the heterogeneity of CHI, WES studies have been less successful in identifying novel genes involved in the secretion of insulin from the pancreatic ß-cell, the mutation of which might result in CHI. The downstream signalling pathway that follows the entry of calcium into ß-cell, triggered by membrane depolarisation is not fully understood. In this study, a *de novo* heterozygous frameshift mutation (p.G539fs*4) was found at the terminal exon (exon 16) of *CaMKK2* (NM_001270486.1) (isoform-7) in proband C with persistent CHI with no known genetic etiology. $Ca^{2+}$/calmodulin-dependent protein kinase 2 (*CaMKK2*) belongs to the Serine/Threonine protein kinase family and alternative splicing results in multiple transcripts encoding distinct isoforms.

Calcium has been found to have a key role in mediating glucose stimulated insulin secretion via the action of multifunctional kinases (CaM-KI and CaM-KIV), activated by *CaMKK2,* an upstream kinase (329). The entry of calcium into the ß-cell via the voltage gated calcium channel triggers the cascade of kinases, regulated by an upstream kinase, encoded by *CaMKK2*. The frameshift mutation in *CaMKK2* (p.G539fs*4) causes an excess insulin secretion by increasing the $Ca^{2+}$/calmodulin-dependent protein kinase activity. This was shown by expressing *CaMKK2* isoform-7 (WT) and the pG539fs*4 mutant in COS7 cells and it was found that pG539fs*4 mutant was noted to have significantly higher basal and $Ca^{2+}$-CaM dependent kinase activity compared with WT isoform-7. Furthermore, the isoform-7 and the pG539fs*4 mutant have elevated basal activity compared with isoform-1, the major *CaMKK2* isoform expressed in most tissues. It is therefore hypothesised that the increase in the $Ca^{2+}$-CaM dependent kinase activity as a result of the mutation, to be increasing the insulin secretion, probably via upregulated transcription of *INS-1*.

*De novo* truncating and splicing mutations in the additional sex combs-like 3 (*ASXL3*) gene have been implicated in the development of Bainbridge-Ropers syndrome (BRPS) characterised by severe developmental delay, feeding problems, short stature and characteristic facial features (280). In this study, a novel compound heterozygous mutation in *ASXL3* was found in proband B with severe short stature, learning difficulties, feeding difficulties and dysmorphic features with. Additionally, the patient also has primary insulin like growth factor-1 (IGF1) deficiency. The mutations occur in exon 11 and proximal part of exon 12 and are strongly conserved at the protein level across various species. *In silico* analyses using PolyPhen-2 and SIFT predict the amino acid substitutions to be potentially deleterious to the protein function. Detailed bioinformatics analysis show that the molecular defects caused by the two compound heterozygous mutations synergistically impact on two points of the molecular interaction network of *ASXL3.*

Homozygous missense mutations in *B3GAT3* have previously been described as 'linkeropathies' characterized by short stature, skeletal deformities and congenital heart defects (340) and also been described in patients with Larsen-like syndrome, defined as a development disorder of the bones throughout the body; individuals frequently express symptoms such as skeletal dislocations, hearing loss and facial dysmorphism(338). In this study, a novel heterozygous splice site mutation in *B3GAT3* was identified in proband D with severe short stature, growth hormone (GH) deficiency, facial dysmorphism and congenital heart defects amongst other symptoms. The heterozygous mutation in *B3GAT3* (c.888+262T>G) in the invariant "GT" splice donor is predicted to be pathogenic as it decreases the splicing efficiency in the mRNA that might result in the formation of truncated protein.

Homozygous mutation in the promoter region of *GH1* has been described in the literature before to be causing an isolated growth hormone deficiency(366). In this study, a homozygous *GH1* promoter mutation was identified in a child with severe short stature and persistent low IGF1. Although there was no evidence of GH deficiency on dynamic stimulation test, the child demonstrated a good response to a trial of recombinant GH. This may suggest the possibility of bio-inactive GH which has been previously reported in children with short stature(111). However, the mechanism of the promoter mutation leading to the production of biologically in-active GH peptide is currently unclear and requires further functional studies.

## 10.2 CONCLUSIONS

WES is a useful and powerful technique in identifying novel genetic etiologies and pathways in rare endocrine disorders in children.

In this study, a novel genetic etiology(*FOXA2*) is characterised for the first time as a cause for an extremely rare phenotype of CHI and CH. *In vitro* studies demonstrated a strong expression of pattern of *FOXA2* not only during the various stages of murine pituitary development but also during human pituitary development and pancreas.

A novel type of mutation contributing to BRPS was demonstrated in this study and characterized by detailed bioinformatics methods. Only *de novo* truncating and splice site mutation have been described so far in BRPS. This study identified a compound heterozygous mutation in *ASXL3*, contributing to BRPS with an expanding clinical spectrum of primary IGF1 deficiency.

A novel frameshift mutation in *CaMKK2* contributing to increased insulin secretion in a patient with persistent CHI was characterised in this study by demonstrating an increase in the kinase activity induced by the frameshift variant when compared to the wild type.

This study also identified a novel splice site invariant in *B3GAT3* contributing to short stature, facial dysmorphism, congenital heart defects segregating with phenotypic features previously defined in patients with homozygous mutation in *B3GAT3*.

A homozygous mutation in the promoter region of *GH1* possibly contributing to short stature with the production of biologically inactive GH was identified in a patient with severe short stature and low IGF1.

## 10.3 FUTURE DIRECTIONS

The identification of *FOXA2* mutation in an individual with an extremely rare complex phenotype of CHI, cranio-facial dysmorphic features and CH will certainly provide valuable insights into the molecular mechanisms underlying pituitary development β-cell physiology. Screening more patients with similar phenotype will give further insight into the role of this transcription factor in the insulin secretion and in related diseases like neonatal diabetes mellitus and maturity onset diabetes of the young (MODY). Furthermore, this will provide more information on genotype-phenotype correlations in patients with *FOXA2* mutations.

*CaMKK2* has various isoforms generated by alternative splicing of the mRNA. The frameshift mutation pG539fs*4 leading to an increased insulin secretion is at the terminal C-sequence of *CaMKK2* isoform 7. However, a very little is known about *CaMKK2* isoform 7. Screening for mutations in *CaMKK2* in patients with persistent CHI without known genetic etiology will help in understanding the precise role of *CaMKK2* in governing the insulin secretion thereby establishing the precise function of isoform 7. Furthermore, clinical trials will help to establish the efficacy of nifedipine (calcium channel antagonist) in patients with persistent CHI and *CAMKK2* mutation especially when patients do not respond to diazoxide or develop significant side effects.

Advances in CRISPR/Cas9 gene editing technology has enabled the induction of target modifications in a variety of model organisms (381, 401). CRISPR/Cas9 system can potentially be used as a genetic tool in studying the specific molecular mechanisms of the *FOXA2* mutation in regulating the insulin secretion and its role in pituitary development.

In addition, the blood or skin cells from the patients with *CaMKK2* pG539fs*4 mutation can be used to generate induced pluripotent stem cells *in vitro* that can differentiate into insulin secreting cells. The insulin secretion can be measured from these cells under basal and glucose stimulated conditions. Using CRISPR technology, the pG539fs*4 can be repaired back to wild-type sequence to examine if the insulin secretion returns back to normal.

The biological role of the splice site invariant (c.888+262T>G) in *B3GAT3* causing the typical phenotypic features in proband D is not well understood. Further functional studies are required needed to fully characterise the role of this splice site variant mutation in *B3GAT3*. Similarly, the role of *GH1* promoter variant (c.-93delG), causing severe short stature in proband E with persistent low IGF1, normal endogenous GH secretion on stimulation test but a good response to exogenous recombinant GH is not entirely clear. Further *in vitro* experiments involving GHR binding and Janus kinase (Jak)2/signal transducer and activator of transcription (Stat)5 activation will be required to study the impact of the promoter mutation (111).

# CHAPTER 11

# REFERENCES

1. Lander ES, Linton LM, Birren B, Nusbaum C, Zody MC, Baldwin J, et al. Initial sequencing and analysis of the human genome. Nature. 2001;409(6822):860-921.
2. de Bruin C, Dauber A. Insights from exome sequencing for endocrine disorders. Nat Rev Endocrinol. 2015;11(8):455-64.
3. Bamshad MJ, Ng SB, Bigham AW, Tabor HK, Emond MJ, Nickerson DA, et al. Exome sequencing as a tool for Mendelian disease gene discovery. Nature reviews Genetics. 2011;12(11):745-55.
4. Biesecker LG, Green RC. Diagnostic clinical genome and exome sequencing. N Engl J Med. 2014;371(12):1170.
5. Rabbani B, Tekin M, Mahdieh N. The promise of whole-exome sequencing in medical genetics. J Hum Genet. 2014;59(1):5-15.
6. Biesecker LG, Shianna KV, Mullikin JC. Exome sequencing: the expert view. Genome Biol. 2011;12(9):128.
7. Ng SB, Turner EH, Robertson PD, Flygare SD, Bigham AW, Lee C, et al. Targeted capture and massively parallel sequencing of 12 human exomes. Nature. 2009;461(7261):272-6.
8. Ng SB, Bigham AW, Buckingham KJ, Hannibal MC, McMillin MJ, Gildersleeve HI, et al. Exome sequencing identifies MLL2 mutations as a cause of Kabuki syndrome. Nat Genet. 2010;42(9):790-3.
9. Chiu RW, Chan KC, Gao Y, Lau VY, Zheng W, Leung TY, et al. Noninvasive prenatal diagnosis of fetal chromosomal aneuploidy by massively parallel genomic sequencing of DNA in maternal plasma. Proc Natl Acad Sci U S A. 2008;105(51):20458-63.
10. Chen EZ, Chiu RW, Sun H, Akolekar R, Chan KC, Leung TY, et al. Noninvasive prenatal diagnosis of fetal trisomy 18 and trisomy 13 by maternal plasma DNA sequencing. PLoS One. 2011;6(7):e21791.
11. Sehnert AJ, Rhees B, Comstock D, de Feo E, Heilek G, Burke J, et al. Optimal detection of fetal chromosomal abnormalities by massively parallel DNA sequencing of cell-free fetal DNA from maternal blood. Clin Chem. 2011;57(7):1042-9.
12. Rabbani B, Mahdieh N, Hosomichi K, Nakaoka H, Inoue I. Next-generation sequencing: impact of exome sequencing in characterizing Mendelian disorders. J Hum Genet. 2012;57(10):621-32.
13. Schork NJ, Murray SS, Frazer KA, Topol EJ. Common vs. rare allele hypotheses for complex diseases. Curr Opin Genet Dev. 2009;19(3):212-9.

14. Marian AJ. Molecular genetic studies of complex phenotypes. Transl Res. 2012;159(2):64-79.

15. Hoischen A, Gilissen C, Arts P, Wieskamp N, van der Vliet W, Vermeer S, et al. Massively parallel sequencing of ataxia genes after array-based enrichment. Hum Mutat. 2010;31(4):494-9.

16. Chan Y, Holmen OL, Dauber A, Vatten L, Havulinna AS, Skorpen F, et al. Common variants show predicted polygenic effects on height in the tails of the distribution, except in extremely short individuals. PLoS Genet. 2011;7(12):e1002439.

17. Wood AR, Esko T, Yang J, Vedantam S, Pers TH, Gustafsson S, et al. Defining the role of common variation in the genomic and biological architecture of adult human height. Nat Genet. 2014;46(11):1173-86.

18. Nilsson O, Guo MH, Dunbar N, Popovic J, Flynn D, Jacobsen C, et al. Short stature, accelerated bone maturation, and early growth cessation due to heterozygous aggrecan mutations. J Clin Endocrinol Metab. 2014;99(8):E1510-8.

19. Dunkel L, Quinton R. Transition in endocrinology: induction of puberty. Eur J Endocrinol. 2014;170(6):R229-39.

20. Abreu AP, Dauber A, Macedo DB, Noel SD, Brito VN, Gill JC, et al. Central precocious puberty caused by mutations in the imprinted gene MKRN3. N Engl J Med. 2013;368(26):2467-75.

21. Macedo DB, Abreu AP, Reis AC, Montenegro LR, Dauber A, Beneduzzi D, et al. Central precocious puberty that appears to be sporadic caused by paternally inherited mutations in the imprinted gene makorin ring finger 3. J Clin Endocrinol Metab. 2014;99(6):E1097-103.

22. Eckler MJ, McKenna WL, Taghvaei S, McConnell SK, Chen B. Fezf1 and Fezf2 are required for olfactory development and sensory neuron identity. J Comp Neurol. 2011;519(10):1829-46.

23. Kotan LD, Hutchins BI, Ozkan Y, Demirel F, Stoner H, Cheng PJ, et al. Mutations in FEZF1 cause Kallmann syndrome. Am J Hum Genet. 2014;95(3):326-31.

24. Margolin DH, Kousi M, Chan YM, Lim ET, Schmahmann JD, Hadjivassiliou M, et al. Ataxia, dementia, and hypogonadotropism caused by disordered ubiquitination. N Engl J Med. 2013;368(21):1992-2003.

25. Shi CH, Schisler JC, Rubel CE, Tan S, Song B, McDonough H, et al. Ataxia and hypogonadism caused by the loss of ubiquitin ligase activity of the U box protein CHIP. Hum Mol Genet. 2014;23(4):1013-24.

26. Caburet S, Arboleda VA, Llano E, Overbeek PA, Barbero JL, Oka K, et al. Mutant cohesin in premature ovarian failure. N Engl J Med. 2014;370(10):943-9.
27. de Vries L, Behar DM, Smirin-Yosef P, Lagovsky I, Tzur S, Basel-Vanagaite L. Exome sequencing reveals SYCE1 mutation associated with autosomal recessive primary ovarian insufficiency. J Clin Endocrinol Metab. 2014;99(10):E2129-32.
28. Kasippillai T, MacArthur DG, Kirby A, Thomas B, Lambalk CB, Daly MJ, et al. Mutations in eIF4ENIF1 are associated with primary ovarian insufficiency. J Clin Endocrinol Metab. 2013;98(9):E1534-9.
29. Zangen D, Kaufman Y, Zeligson S, Perlberg S, Fridman H, Kanaan M, et al. XX ovarian dysgenesis is caused by a PSMC3IP/HOP2 mutation that abolishes coactivation of estrogen-driven transcription. Am J Hum Genet. 2011;89(4):572-9.
30. Beuschlein F, Fassnacht M, Assie G, Calebiro D, Stratakis CA, Osswald A, et al. Constitutive activation of PKA catalytic subunit in adrenal Cushing's syndrome. N Engl J Med. 2014;370(11):1019-28.
31. Cao Y, He M, Gao Z, Peng Y, Li Y, Li L, et al. Activating hotspot L205R mutation in PRKACA and adrenal Cushing's syndrome. Science. 2014;344(6186):913-7.
32. Goh G, Scholl UI, Healy JM, Choi M, Prasad ML, Nelson-Williams C, et al. Recurrent activating mutation in PRKACA in cortisol-producing adrenal tumors. Nat Genet. 2014;46(6):613-7.
33. Sato Y, Maekawa S, Ishii R, Sanada M, Morikawa T, Shiraishi Y, et al. Recurrent somatic mutations underlie corticotropin-independent Cushing's syndrome. Science. 2014;344(6186):917-20.
34. Assie G, Libe R, Espiard S, Rizk-Rabin M, Guimier A, Luscap W, et al. ARMC5 mutations in macronodular adrenal hyperplasia with Cushing's syndrome. N Engl J Med. 2013;369(22):2105-14.
35. Gagliardi L, Schreiber AW, Hahn CN, Feng J, Cranston T, Boon H, et al. ARMC5 mutations are common in familial bilateral macronodular adrenal hyperplasia. J Clin Endocrinol Metab. 2014;99(9):E1784-92.
36. Sahakitrungruang T, Srichomthong C, Pornkunwilai S, Amornfa J, Shuangshoti S, Kulawonganunchai S, et al. Germline and somatic DICER1 mutations in a pituitary blastoma causing infantile-onset Cushing's disease. J Clin Endocrinol Metab. 2014;99(8):E1487-92.
37. Chan LF, Clark AJ, Metherell LA. Familial glucocorticoid deficiency: advances in the molecular understanding of ACTH action. Horm Res. 2008;69(2):75-82.

38. Meimaridou E, Hughes CR, Kowalczyk J, Guasti L, Chapple JP, King PJ, et al. Familial glucocorticoid deficiency: New genes and mechanisms. Mol Cell Endocrinol. 2013;371(1-2):195-200.

39. Prasad R, Chan LF, Hughes CR, Kaski JP, Kowalczyk JC, Savage MO, et al. Thioredoxin Reductase 2 (TXNRD2) mutation associated with familial glucocorticoid deficiency (FGD). J Clin Endocrinol Metab. 2014;99(8):E1556-63.

40. Meimaridou E, Kowalczyk J, Guasti L, Hughes CR, Wagner F, Frommolt P, et al. Mutations in NNT encoding nicotinamide nucleotide transhydrogenase cause familial glucocorticoid deficiency. Nat Genet. 2012;44(7):740-2.

41. Hughes CR, Guasti L, Meimaridou E, Chuang CH, Schimenti JC, King PJ, et al. MCM4 mutation causes adrenal failure, short stature, and natural killer cell deficiency in humans. J Clin Invest. 2012;122(3):814-20.

42. Sun Y, Bak B, Schoenmakers N, van Trotsenburg AS, Oostdijk W, Voshol P, et al. Loss-of-function mutations in IGSF1 cause an X-linked syndrome of central hypothyroidism and testicular enlargement. Nat Genet. 2012;44(12):1375-81.

43. Mazzarella R, Pengue G, Jones J, Jones C, Schlessinger D. Cloning and expression of an immunoglobulin superfamily gene (IGSF1) in Xq25. Genomics. 1998;48(2):157-62.

44. Kuhnen P, Turan S, Frohler S, Guran T, Abali S, Biebermann H, et al. Identification of PENDRIN (SLC26A4) mutations in patients with congenital hypothyroidism and "apparent" thyroid dysgenesis. J Clin Endocrinol Metab. 2014;99(1):E169-76.

45. van Dijk FS, Zillikens MC, Micha D, Riessland M, Marcelis CL, de Die-Smulders CE, et al. PLS3 mutations in X-linked osteoporosis with fractures. N Engl J Med. 2013;369(16):1529-36.

46. Baxter RM, Arboleda VA, Lee H, Barseghyan H, Adam MP, Fechner PY, et al. Exome sequencing for the diagnosis of 46,XY disorders of sex development. J Clin Endocrinol Metab. 2015;100(2):E333-44.

47. Hughes IA, Houk C, Ahmed SF, Lee PA, Lawson Wilkins Pediatric Endocrine Society/European Society for Paediatric Endocrinology Consensus G. Consensus statement on management of intersex disorders. J Pediatr Urol. 2006;2(3):148-62.

48. Achermann JC, Ito M, Ito M, Hindmarsh PC, Jameson JL. A mutation in the gene encoding steroidogenic factor-1 causes XY sex reversal and adrenal failure in humans. Nat Genet. 1999;22(2):125-6.

49. Sinclair AH, Berta P, Palmer MS, Hawkins JR, Griffiths BL, Smith MJ, et al. A gene from the human sex-determining region encodes a protein with homology to a conserved DNA-binding motif. Nature. 1990;346(6281):240-4.

50. Hughes IA, Davies JD, Bunch TI, Pasterski V, Mastroyannopoulou K, MacDougall J. Androgen insensitivity syndrome. Lancet (London, England). 2012;380(9851):1419-28.

51. Yang Y, Muzny DM, Reid JG, Bainbridge MN, Willis A, Ward PA, et al. Clinical whole-exome sequencing for the diagnosis of mendelian disorders. N Engl J Med. 2013;369(16):1502-11.

52. Lee H, Deignan JL, Dorrani N, Strom SP, Kantarci S, Quintero-Rivera F, et al. Clinical exome sequencing for genetic identification of rare Mendelian disorders. JAMA. 2014;312(18):1880-7.

53. Guo MH, Shen Y, Walvoord EC, Miller TC, Moon JE, Hirschhorn JN, et al. Whole exome sequencing to identify genetic causes of short stature. Horm Res Paediatr. 2014;82(1):44-52.

54. Green RC, Berg JS, Grody WW, Kalia SS, Korf BR, Martin CL, et al. ACMG recommendations for reporting of incidental findings in clinical exome and genome sequencing. Genet Med. 2013;15(7):565-74.

55. Alatzoglou KS, Dattani MT. Genetic forms of hypopituitarism and their manifestation in the neonatal period. Early Hum Dev. 2009;85(11):705-12.

56. Mehta A, Dattani MT. Developmental disorders of the hypothalamus and pituitary gland associated with congenital hypopituitarism. Best Pract Res Clin Endocrinol Metab. 2008;22(1):191-206.

57. Kelberman D, Dattani MT. The role of transcription factors implicated in anterior pituitary development in the aetiology of congenital hypopituitarism. Ann Med. 2006;38(8):560-77.

58. Sheng HZ, Moriyama K, Yamashita T, Li H, Potter SS, Mahon KA, et al. Multistep control of pituitary organogenesis. Science. 1997;278(5344):1809-12.

59. Rizzoti K, Lovell-Badge R. Early development of the pituitary gland: induction and shaping of Rathke's pouch. Rev Endocr Metab Disord. 2005;6(3):161-72.

60. Dasen JS, Rosenfeld MG. Signaling and transcriptional mechanisms in pituitary development. Annu Rev Neurosci. 2001;24:327-55.

61. Zhu X, Gleiberman AS, Rosenfeld MG. Molecular physiology of pituitary development: signaling and transcriptional networks. Physiol Rev. 2007;87(3):933-63.

62. Scully KM, Rosenfeld MG. Pituitary development: regulatory codes in mammalian organogenesis. Science. 2002;295(5563):2231-5.
63. Romero CJ, Nesi-Franca S, Radovick S. The molecular basis of hypopituitarism. Trends Endocrinol Metab. 2009;20(10):506-16.
64. Webb EA, Dattani MT. Septo-optic dysplasia. Eur J Hum Genet. 2010;18(4):393-7.
65. Kelberman D, Dattani MT. Genetics of septo-optic dysplasia. Pituitary. 2007;10(4):393-407.
66. Kelberman D, Dattani MT. Septo-optic dysplasia - novel insights into the aetiology. Horm Res. 2008;69(5):257-65.
67. Haddad NG, Eugster EA. Hypopituitarism and neurodevelopmental abnormalities in relation to central nervous system structural defects in children with optic nerve hypoplasia. J Pediatr Endocrinol Metab. 2005;18(9):853-8.
68. Dattani MT, Martinez-Barbera JP, Thomas PQ, Brickman JM, Gupta R, Martensson IL, et al. Mutations in the homeobox gene HESX1/Hesx1 associated with septo-optic dysplasia in human and mouse. Nat Genet. 1998;19(2):125-33.
69. Thomas PQ, Dattani MT, Brickman JM, McNay D, Warne G, Zacharin M, et al. Heterozygous HESX1 mutations associated with isolated congenital pituitary hypoplasia and septo-optic dysplasia. Hum Mol Genet. 2001;10(1):39-45.
70. McNay DE, Turton JP, Kelberman D, Woods KS, Brauner R, Papadimitriou A, et al. HESX1 mutations are an uncommon cause of septooptic dysplasia and hypopituitarism. J Clin Endocrinol Metab. 2007;92(2):691-7.
71. Pevny L, Placzek M. SOX genes and neural progenitor identity. Curr Opin Neurobiol. 2005;15(1):7-13.
72. Rizzoti K, Brunelli S, Carmignac D, Thomas PQ, Robinson IC, Lovell-Badge R. SOX3 is required during the formation of the hypothalamo-pituitary axis. Nat Genet. 2004;36(3):247-55.
73. Hagstrom SA, Pauer GJ, Reid J, Simpson E, Crowe S, Maumenee IH, et al. SOX2 mutation causes anophthalmia, hearing loss, and brain anomalies. Am J Med Genet A. 2005;138A(2):95-8.
74. Williamson KA, Hever AM, Rainger J, Rogers RC, Magee A, Fiedler Z, et al. Mutations in SOX2 cause anophthalmia-esophageal-genital (AEG) syndrome. Hum Mol Genet. 2006;15(9):1413-22.

75. Solomon NM, Nouri S, Warne GL, Lagerstrom-Fermer M, Forrest SM, Thomas PQ. Increased gene dosage at Xq26-q27 is associated with X-linked hypopituitarism. Genomics. 2002;79(4):553-9.

76. Woods KS, Cundall M, Turton J, Rizotti K, Mehta A, Palmer R, et al. Over- and underdosage of SOX3 is associated with infundibular hypoplasia and hypopituitarism. Am J Hum Genet. 2005;76(5):833-49.

77. Laumonnier F, Ronce N, Hamel BC, Thomas P, Lespinasse J, Raynaud M, et al. Transcription factor SOX3 is involved in X-linked mental retardation with growth hormone deficiency. Am J Hum Genet. 2002;71(6):1450-5.

78. Fernandes M, Hebert JM. The ups and downs of holoprosencephaly: dorsal versus ventral patterning forces. Clin Genet. 2008;73(5):413-23.

79. Roessler E, Du YZ, Mullor JL, Casas E, Allen WP, Gillessen-Kaesbach G, et al. Loss-of-function mutations in the human GLI2 gene are associated with pituitary anomalies and holoprosencephaly-like features. Proc Natl Acad Sci U S A. 2003;100(23):13424-9.

80. Ellsworth BS, Butts DL, Camper SA. Mechanisms underlying pituitary hypoplasia and failed cell specification in Lhx3-deficient mice. Dev Biol. 2008;313(1):118-29.

81. Sheng HZ, Zhadanov AB, Mosinger B, Jr., Fujii T, Bertuzzi S, Grinberg A, et al. Specification of pituitary cell lineages by the LIM homeobox gene Lhx3. Science. 1996;272(5264):1004-7.

82. Bhangoo AP, Hunter CS, Savage JJ, Anhalt H, Pavlakis S, Walvoord EC, et al. Clinical case seminar: a novel LHX3 mutation presenting as combined pituitary hormonal deficiency. J Clin Endocrinol Metab. 2006;91(3):747-53.

83. Rajab A, Kelberman D, de Castro SC, Biebermann H, Shaikh H, Pearce K, et al. Novel mutations in LHX3 are associated with hypopituitarism and sensorineural hearing loss. Hum Mol Genet. 2008;17(14):2150-9.

84. Netchine I, Sobrier ML, Krude H, Schnabel D, Maghnie M, Marcos E, et al. Mutations in LHX3 result in a new syndrome revealed by combined pituitary hormone deficiency. Nat Genet. 2000;25(2):182-6.

85. Pfaeffle RW, Savage JJ, Hunter CS, Palme C, Ahlmann M, Kumar P, et al. Four novel mutations of the LHX3 gene cause combined pituitary hormone deficiencies with or without limited neck rotation. J Clin Endocrinol Metab. 2007;92(5):1909-19.

86. Mullen RD, Colvin SC, Hunter CS, Savage JJ, Walvoord EC, Bhangoo AP, et al. Roles of the LHX3 and LHX4 LIM-homeodomain factors in pituitary development. Mol Cell Endocrinol. 2007;265-266:190-5.

87. Machinis K, Pantel J, Netchine I, Leger J, Camand OJ, Sobrier ML, et al. Syndromic short stature in patients with a germline mutation in the LIM homeobox LHX4. Am J Hum Genet. 2001;69(5):961-8.

88. Tajima T, Hattori T, Nakajima T, Okuhara K, Tsubaki J, Fujieda K. A novel missense mutation (P366T) of the LHX4 gene causes severe combined pituitary hormone deficiency with pituitary hypoplasia, ectopic posterior lobe and a poorly developed sella turcica. Endocr J. 2007;54(4):637-41.

89. Machinis K, Amselem S. Functional relationship between LHX4 and POU1F1 in light of the LHX4 mutation identified in patients with pituitary defects. J Clin Endocrinol Metab. 2005;90(9):5456-62.

90. Boncinelli E, Morgan R. Downstream of Otx2, or how to get a head. Trends Genet. 2001;17(11):633-6.

91. Kurokawa D, Kiyonari H, Nakayama R, Kimura-Yoshida C, Matsuo I, Aizawa S. Regulation of Otx2 expression and its functions in mouse forebrain and midbrain. Development. 2004;131(14):3319-31.

92. Tajima T, Ohtake A, Hoshino M, Amemiya S, Sasaki N, Ishizu K, et al. OTX2 loss of function mutation causes anophthalmia and combined pituitary hormone deficiency with a small anterior and ectopic posterior pituitary. J Clin Endocrinol Metab. 2009;94(1):314-9.

93. Ragge NK, Brown AG, Poloschek CM, Lorenz B, Henderson RA, Clarke MP, et al. Heterozygous mutations of OTX2 cause severe ocular malformations. Am J Hum Genet. 2005;76(6):1008-22.

94. Wyatt A, Bakrania P, Bunyan DJ, Osborne RJ, Crolla JA, Salt A, et al. Novel heterozygous OTX2 mutations and whole gene deletions in anophthalmia, microphthalmia and coloboma. Hum Mutat. 2008;29(11):E278-83.

95. Suh H, Gage PJ, Drouin J, Camper SA. Pitx2 is required at multiple stages of pituitary organogenesis: pituitary primordium formation and cell specification. Development. 2002;129(2):329-37.

96. Meyer-Marcotty P, Weisschuh N, Dressler P, Hartmann J, Stellzig-Eisenhauer A. Morphology of the sella turcica in Axenfeld-Rieger syndrome with PITX2 mutation. J Oral Pathol Med. 2008;37(8):504-10.

97. Vieira V, David G, Roche O, de la Houssaye G, Boutboul S, Arbogast L, et al. Identification of four new PITX2 gene mutations in patients with Axenfeld-Rieger syndrome. Mol Vis. 2006;12:1448-60.

98. Olson LE, Dasen JS, Ju BG, Tollkuhn J, Rosenfeld MG. Paired-like repression/activation in pituitary development. Recent Prog Horm Res. 2003;58:249-61.

99. Olson LE, Tollkuhn J, Scafoglio C, Krones A, Zhang J, Ohgi KA, et al. Homeodomain-mediated beta-catenin-dependent switching events dictate cell-lineage determination. Cell. 2006;125(3):593-605.

100. Vesper AH, Raetzman LT, Camper SA. Role of prophet of Pit1 (PROP1) in gonadotrope differentiation and puberty. Endocrinology. 2006;147(4):1654-63.

101. Turton JP, Mehta A, Raza J, Woods KS, Tiulpakov A, Cassar J, et al. Mutations within the transcription factor PROP1 are rare in a cohort of patients with sporadic combined pituitary hormone deficiency (CPHD). Clin Endocrinol (Oxf). 2005;63(1):10-8.

102. Bottner A, Keller E, Kratzsch J, Stobbe H, Weigel JF, Keller A, et al. PROP1 mutations cause progressive deterioration of anterior pituitary function including adrenal insufficiency: a longitudinal analysis. J Clin Endocrinol Metab. 2004;89(10):5256-65.

103. Cohen LE, Wondisford FE, Salvatoni A, Maghnie M, Brucker-Davis F, Weintraub BD, et al. A "hot spot" in the Pit-1 gene responsible for combined pituitary hormone deficiency: clinical and molecular correlates. J Clin Endocrinol Metab. 1995;80(2):679-84.

104. Turton JP, Reynaud R, Mehta A, Torpiano J, Saveanu A, Woods KS, et al. Novel mutations within the POU1F1 gene associated with variable combined pituitary hormone deficiency. J Clin Endocrinol Metab. 2005;90(8):4762-70.

105. Lamolet B, Pulichino AM, Lamonerie T, Gauthier Y, Brue T, Enjalbert A, et al. A pituitary cell-restricted T box factor, Tpit, activates POMC transcription in cooperation with Pitx homeoproteins. Cell. 2001;104(6):849-59.

106. Pulichino AM, Vallette-Kasic S, Tsai JP, Couture C, Gauthier Y, Drouin J. Tpit determines alternate fates during pituitary cell differentiation. Genes Dev. 2003;17(6):738-47.

107. Vallette-Kasic S, Brue T, Pulichino AM, Gueydan M, Barlier A, David M, et al. Congenital isolated adrenocorticotropin deficiency: an underestimated cause of neonatal death, explained by TPIT gene mutations. J Clin Endocrinol Metab. 2005;90(3):1323-31.

108. Vallette-Kasic S, Pulichino AM, Gueydan M, Barlier A, David M, Malpuech G, et al. A neonatal form of isolated ACTH deficiency frequently associated with Tpit gene mutations. Endocr Res. 2004;30(4):943-4.

109. Wagner JK, Eble A, Hindmarsh PC, Mullis PE. Prevalence of human GH-1 gene alterations in patients with isolated growth hormone deficiency. Pediatr Res. 1998;43(1):105-10.

110. Hernandez LM, Lee PD, Camacho-Hubner C. Isolated growth hormone deficiency. Pituitary. 2007;10(4):351-7.

111. Besson A, Salemi S, Deladoey J, Vuissoz JM, Eble A, Bidlingmaier M, et al. Short stature caused by a biologically inactive mutant growth hormone (GH-C53S). J Clin Endocrinol Metab. 2005;90(5):2493-9.

112. Maheshwari HG, Silverman BL, Dupuis J, Baumann G. Phenotype and genetic analysis of a syndrome caused by an inactivating mutation in the growth hormone-releasing hormone receptor: Dwarfism of Sindh. J Clin Endocrinol Metab. 1998;83(11):4065-74.

113. Miyai K. Congenital thyrotropin deficiency--from discovery to molecular biology, postgenome and preventive medicine. Endocr J. 2007;54(2):191-203.

114. Trarbach EB, Silveira LG, Latronico AC. Genetic insights into human isolated gonadotropin deficiency. Pituitary. 2007;10(4):381-91.

115. Scommegna S, Galeazzi D, Picone S, Farinelli E, Agostino R, Bozzao A, et al. Neonatal identification of pituitary aplasia: a life-saving diagnosis. Review of five cases. Horm Res. 2004;62(1):10-6.

116. Ahmad T, Borchert M, Geffner M. Optic nerve hypoplasia and hypopituitarism. Pediatr Endocrinol Rev. 2008;5(3):772-7.

117. Mehta A, Hindmarsh PC, Dattani MT. An update on the biochemical diagnosis of congenital ACTH insufficiency. Clin Endocrinol (Oxf). 2005;62(3):307-14.

118. Mehta A, Hindmarsh PC, Stanhope RG, Turton JP, Cole TJ, Preece MA, et al. The role of growth hormone in determining birth size and early postnatal growth, using congenital growth hormone deficiency (GHD) as a model. Clin Endocrinol (Oxf). 2005;63(2):223-31.

119. de Weerth C, Zijl RH, Buitelaar JK. Development of cortisol circadian rhythm in infancy. Early Hum Dev. 2003;73(1-2):39-52.

120. van Tijn DA, de Vijlder JJ, Vulsma T. Role of corticotropin-releasing hormone testing in assessment of hypothalamic-pituitary-adrenal axis function in infants with congenital central hypothyroidism. J Clin Endocrinol Metab. 2008;93(10):3794-803.

121. van Tijn DA, de Vijlder JJ, Vulsma T. Role of the thyrotropin-releasing hormone stimulation test in diagnosis of congenital central hypothyroidism in infants. J Clin Endocrinol Metab. 2008;93(2):410-9.

122. Hussain K, Hindmarsh P, Aynsley-Green A. Spontaneous hypoglycemia in childhood is accompanied by paradoxically low serum growth hormone and appropriate cortisol counterregulatory hormonal responses. J Clin Endocrinol Metab. 2003;88(8):3715-23.
123. Grumbach MM. A window of opportunity: the diagnosis of gonadotropin deficiency in the male infant. J Clin Endocrinol Metab. 2005;90(5):3122-7.
124. van Tijn DA, Schroor EJ, Delemarre-van de Waal HA, de Vijlder JJ, Vulsma T. Early assessment of hypothalamic-pituitary-gonadal function in patients with congenital hypothyroidism of central origin. J Clin Endocrinol Metab. 2007;92(1):104-9.
125. Garel C, Leger J. Contribution of magnetic resonance imaging in non-tumoral hypopituitarism in children. Horm Res. 2007;67(4):194-202.
126. Mehta A, Hindmarsh PC, Mehta H, Turton JP, Russell-Eggitt I, Taylor D, et al. Congenital hypopituitarism: clinical, molecular and neuroradiological correlates. Clin Endocrinol (Oxf). 2009;71(3):376-82.
127. Senniappan S, Arya VB, Hussain K. The molecular mechanisms, diagnosis and management of congenital hyperinsulinism. Indian J Endocrinol Metab. 2013;17(1):19-30.
128. Hussain K, Blankenstein O, De Lonlay P, Christesen HT. Hyperinsulinaemic hypoglycaemia: biochemical basis and the importance of maintaining normoglycaemia during management. Arch Dis Child. 2007;92(7):568-70.
129. Aynsley-Green A, Hussain K, Hall J, Saudubray JM, Nihoul-Fekete C, De Lonlay-Debeney P, et al. Practical management of hyperinsulinism in infancy. Arch Dis Child Fetal Neonatal Ed. 2000;82(2):F98-F107.
130. Dunne MJ, Cosgrove KE, Shepherd RM, Aynsley-Green A, Lindley KJ. Hyperinsulinism in infancy: from basic science to clinical disease. Physiol Rev. 2004;84(1):239-75.
131. Johnson JH, Newgard CB, Milburn JL, Lodish HF, Thorens B. The high Km glucose transporter of islets of Langerhans is functionally similar to the low affinity transporter of liver and has an identical primary sequence. J Biol Chem. 1990;265(12):6548-51.
132. Matschinsky FM. Banting Lecture 1995. A lesson in metabolic regulation inspired by the glucokinase glucose sensor paradigm. Diabetes. 1996;45(2):223-41.
133. Ashcroft FM, Harrison DE, Ashcroft SJ. Glucose induces closure of single potassium channels in isolated rat pancreatic beta-cells. Nature. 1984;312(5993):446-8.

134. Inagaki N, Gonoi T, Clement JPt, Namba N, Inazawa J, Gonzalez G, et al. Reconstitution of IKATP: an inward rectifier subunit plus the sulfonylurea receptor. Science. 1995;270(5239):1166-70.

135. Lopatin AN, Makhina EN, Nichols CG. Potassium channel block by cytoplasmic polyamines as the mechanism of intrinsic rectification. Nature. 1994;372(6504):366-9.

136. Zerangue N, Schwappach B, Jan YN, Jan LY. A new ER trafficking signal regulates the subunit stoichiometry of plasma membrane K(ATP) channels. Neuron. 1999;22(3):537-48.

137. Martin GM, Chen PC, Devaraneni P, Shyng SL. Pharmacological rescue of trafficking-impaired ATP-sensitive potassium channels. Front Physiol. 2013;4:386.

138. Hung LW, Wang IX, Nikaido K, Liu PQ, Ames GF, Kim SH. Crystal structure of the ATP-binding subunit of an ABC transporter. Nature. 1998;396(6712):703-7.

139. Matsuo M, Kioka N, Amachi T, Ueda K. ATP binding properties of the nucleotide-binding folds of SUR1. J Biol Chem. 1999;274(52):37479-82.

140. Tucker SJ, Gribble FM, Proks P, Trapp S, Ryder TJ, Haug T, et al. Molecular determinants of KATP channel inhibition by ATP. EMBO J. 1998;17(12):3290-6.

141. Dunne MJ, Petersen OH. Potassium selective ion channels in insulin-secreting cells: physiology, pharmacology and their role in stimulus-secretion coupling. Biochim Biophys Acta. 1991;1071(1):67-82.

142. Aizawa T, Sato Y, Ishihara F, Taguchi N, Komatsu M, Suzuki N, et al. ATP-sensitive K+ channel-independent glucose action in rat pancreatic beta-cell. Am J Physiol. 1994;266(3 Pt 1):C622-7.

143. Gembal M, Detimary P, Gilon P, Gao ZY, Henquin JC. Mechanisms by which glucose can control insulin release independently from its action on adenosine triphosphate-sensitive K+ channels in mouse B cells. J Clin Invest. 1993;91(3):871-80.

144. Straub SG, Cosgrove KE, Ammala C, Shepherd RM, O'Brien RE, Barnes PD, et al. Hyperinsulinism of infancy: the regulated release of insulin by KATP channel-independent pathways. Diabetes. 2001;50(2):329-39.

145. Komatsu M, Schermerhorn T, Aizawa T, Sharp GW. Glucose stimulation of insulin release in the absence of extracellular Ca2+ and in the absence of any increase in intracellular Ca2+ in rat pancreatic islets. Proc Natl Acad Sci U S A. 1995;92(23):10728-32.

146. Senniappan S, Shanti B, James C, Hussain K. Hyperinsulinaemic hypoglycaemia: genetic mechanisms, diagnosis and management. J Inherit Metab Dis. 2012;35(4):589-601.

147. Stanley CA. Perspective on the Genetics and Diagnosis of Congenital Hyperinsulinism Disorders. J Clin Endocrinol Metab. 2016;101(3):815-26.
148. Glaser B, Chiu KC, Anker R, Nestorowicz A, Landau H, Ben-Bassat H, et al. Familial hyperinsulinism maps to chromosome 11p14-15.1, 30 cM centromeric to the insulin gene. Nat Genet. 1994;7(2):185-8.
149. Thomas PM, Cote GJ, Wohllk N, Haddad B, Mathew PM, Rabl W, et al. Mutations in the sulfonylurea receptor gene in familial persistent hyperinsulinemic hypoglycemia of infancy. Science. 1995;268(5209):426-9.
150. Thomas P, Ye Y, Lightner E. Mutation of the pancreatic islet inward rectifier Kir6.2 also leads to familial persistent hyperinsulinemic hypoglycemia of infancy. Hum Mol Genet. 1996;5(11):1809-12.
151. Kane C, Shepherd RM, Squires PE, Johnson PR, James RF, Milla PJ, et al. Loss of functional KATP channels in pancreatic beta-cells causes persistent hyperinsulinemic hypoglycemia of infancy. Nat Med. 1996;2(12):1344-7.
152. Flanagan SE, Clauin S, Bellanne-Chantelot C, de Lonlay P, Harries LW, Gloyn AL, et al. Update of mutations in the genes encoding the pancreatic beta-cell K(ATP) channel subunits Kir6.2 (KCNJ11) and sulfonylurea receptor 1 (ABCC8) in diabetes mellitus and hyperinsulinism. Hum Mutat. 2009;30(2):170-80.
153. Cartier EA, Conti LR, Vandenberg CA, Shyng SL. Defective trafficking and function of KATP channels caused by a sulfonylurea receptor 1 mutation associated with persistent hyperinsulinemic hypoglycemia of infancy. Proc Natl Acad Sci U S A. 2001;98(5):2882-7.
154. Partridge CJ, Beech DJ, Sivaprasadarao A. Identification and pharmacological correction of a membrane trafficking defect associated with a mutation in the sulfonylurea receptor causing familial hyperinsulinism. J Biol Chem. 2001;276(38):35947-52.
155. Shyng SL, Ferrigni T, Shepard JB, Nestorowicz A, Glaser B, Permutt MA, et al. Functional analyses of novel mutations in the sulfonylurea receptor 1 associated with persistent hyperinsulinemic hypoglycemia of infancy. Diabetes. 1998;47(7):1145-51.
156. Dekel B, Lubin D, Modan-Moses D, Quint J, Glaser B, Meyerovitch J. Compound heterozygosity for the common sulfonylurea receptor mutations can cause mild diazoxide-sensitive hyperinsulinism. Clin Pediatr (Phila). 2002;41(3):183-6.
157. Crane A, Aguilar-Bryan L. Assembly, maturation, and turnover of K(ATP) channel subunits. J Biol Chem. 2004;279(10):9080-90.

158. Taschenberger G, Mougey A, Shen S, Lester LB, LaFranchi S, Shyng SL. Identification of a familial hyperinsulinism-causing mutation in the sulfonylurea receptor 1 that prevents normal trafficking and function of KATP channels. J Biol Chem. 2002;277(19):17139-46.
159. Huopio H, Reimann F, Ashfield R, Komulainen J, Lenko HL, Rahier J, et al. Dominantly inherited hyperinsulinism caused by a mutation in the sulfonylurea receptor type 1. J Clin Invest. 2000;106(7):897-906.
160. Pinney SE, MacMullen C, Becker S, Lin YW, Hanna C, Thornton P, et al. Clinical characteristics and biochemical mechanisms of congenital hyperinsulinism associated with dominant KATP channel mutations. J Clin Invest. 2008;118(8):2877-86.
161. Flanagan SE, Kapoor RR, Banerjee I, Hall C, Smith VV, Hussain K, et al. Dominantly acting ABCC8 mutations in patients with medically unresponsive hyperinsulinaemic hypoglycaemia. Clin Genet. 2011;79(6):582-7.
162. Macmullen CM, Zhou Q, Snider KE, Tewson PH, Becker SA, Aziz AR, et al. Diazoxide-unresponsive congenital hyperinsulinism in children with dominant mutations of the beta-cell sulfonylurea receptor SUR1. Diabetes. 2011;60(6):1797-804.
163. Fahien LA, MacDonald MJ, Kmiotek EH, Mertz RJ, Fahien CM. Regulation of insulin release by factors that also modify glutamate dehydrogenase. J Biol Chem. 1988;263(27):13610-4.
164. Stanley CA. Hyperinsulinism/hyperammonemia syndrome: insights into the regulatory role of glutamate dehydrogenase in ammonia metabolism. Mol Genet Metab. 2004;81 Suppl 1:S45-51.
165. Kapoor RR, Flanagan SE, Fulton P, Chakrapani A, Chadefaux B, Ben-Omran T, et al. Hyperinsulinism-hyperammonaemia syndrome: novel mutations in the GLUD1 gene and genotype-phenotype correlations. Eur J Endocrinol. 2009;161(5):731-5.
166. Weinzimer SA, Stanley CA, Berry GT, Yudkoff M, Tuchman M, Thornton PS. A syndrome of congenital hyperinsulinism and hyperammonemia. J Pediatr. 1997;130(4):661-4.
167. Zammarchi E, Filippi L, Novembre E, Donati MA. Biochemical evaluation of a patient with a familial form of leucine-sensitive hypoglycemia and concomitant hyperammonemia. Metabolism. 1996;45(8):957-60.
168. Palladino AA, Stanley CA. The hyperinsulinism/hyperammonemia syndrome. Rev Endocr Metab Disord. 2010;11(3):171-8.

169. Treberg JR, Clow KA, Greene KA, Brosnan ME, Brosnan JT. Systemic activation of glutamate dehydrogenase increases renal ammoniagenesis: implications for the hyperinsulinism/hyperammonemia syndrome. Am J Physiol Endocrinol Metab. 2010;298(6):E1219-25.

170. Bahi-Buisson N, Roze E, Dionisi C, Escande F, Valayannopoulos V, Feillet F, et al. Neurological aspects of hyperinsulinism-hyperammonaemia syndrome. Dev Med Child Neurol. 2008;50(12):945-9.

171. Clayton PT, Eaton S, Aynsley-Green A, Edginton M, Hussain K, Krywawych S, et al. Hyperinsulinism in short-chain L-3-hydroxyacyl-CoA dehydrogenase deficiency reveals the importance of beta-oxidation in insulin secretion. J Clin Invest. 2001;108(3):457-65.

172. Hardy OT, Hohmeier HE, Becker TC, Manduchi E, Doliba NM, Gupta RK, et al. Functional genomics of the beta-cell: short-chain 3-hydroxyacyl-coenzyme A dehydrogenase regulates insulin secretion independent of K+ currents. Mol Endocrinol. 2007;21(3):765-73.

173. Li C, Chen P, Palladino A, Narayan S, Russell LK, Sayed S, et al. Mechanism of hyperinsulinism in short-chain 3-hydroxyacyl-CoA dehydrogenase deficiency involves activation of glutamate dehydrogenase. J Biol Chem. 2010;285(41):31806-18.

174. Kapoor RR, James C, Flanagan SE, Ellard S, Eaton S, Hussain K. 3-Hydroxyacyl-coenzyme A dehydrogenase deficiency and hyperinsulinemic hypoglycemia: characterization of a novel mutation and severe dietary protein sensitivity. J Clin Endocrinol Metab. 2009;94(7):2221-5.

175. Heslegrave AJ, Kapoor RR, Eaton S, Chadefaux B, Akcay T, Simsek E, et al. Leucine-sensitive hyperinsulinaemic hypoglycaemia in patients with loss of function mutations in 3-Hydroxyacyl-CoA Dehydrogenase. Orphanet J Rare Dis. 2012;7:25.

176. Flanagan SE, Patch AM, Locke JM, Akcay T, Simsek E, Alaei M, et al. Genome-wide homozygosity analysis reveals HADH mutations as a common cause of diazoxide-responsive hyperinsulinemic-hypoglycemia in consanguineous pedigrees. J Clin Endocrinol Metab. 2011;96(3):E498-502.

177. Matschinsky FM. Regulation of pancreatic beta-cell glucokinase: from basics to therapeutics. Diabetes. 2002;51 Suppl 3:S394-404.

178. Glaser B, Kesavan P, Heyman M, Davis E, Cuesta A, Buchs A, et al. Familial hyperinsulinism caused by an activating glucokinase mutation. N Engl J Med. 1998;338(4):226-30.

179. Christesen HB, Jacobsen BB, Odili S, Buettger C, Cuesta-Munoz A, Hansen T, et al. The second activating glucokinase mutation (A456V): implications for glucose homeostasis and diabetes therapy. Diabetes. 2002;51(4):1240-6.

180. Cuesta-Munoz AL, Huopio H, Otonkoski T, Gomez-Zumaquero JM, Nanto-Salonen K, Rahier J, et al. Severe persistent hyperinsulinemic hypoglycemia due to a de novo glucokinase mutation. Diabetes. 2004;53(8):2164-8.

181. Gupta RK, Vatamaniuk MZ, Lee CS, Flaschen RC, Fulmer JT, Matschinsky FM, et al. The MODY1 gene HNF-4alpha regulates selected genes involved in insulin secretion. J Clin Invest. 2005;115(4):1006-15.

182. Pearson ER, Boj SF, Steele AM, Barrett T, Stals K, Shield JP, et al. Macrosomia and hyperinsulinaemic hypoglycaemia in patients with heterozygous mutations in the HNF4A gene. PLoS Med. 2007;4(4):e118.

183. Gremlich S, Nolan C, Roduit R, Burcelin R, Peyot ML, Delghingaro-Augusto V, et al. Pancreatic islet adaptation to fasting is dependent on peroxisome proliferator-activated receptor alpha transcriptional up-regulation of fatty acid oxidation. Endocrinology. 2005;146(1):375-82.

184. Prentki M, Joly E, El-Assaad W, Roduit R. Malonyl-CoA signaling, lipid partitioning, and glucolipotoxicity: role in beta-cell adaptation and failure in the etiology of diabetes. Diabetes. 2002;51 Suppl 3:S405-13.

185. Fajans SS, Bell GI. Macrosomia and neonatal hypoglycaemia in RW pedigree subjects with a mutation (Q268X) in the gene encoding hepatocyte nuclear factor 4alpha (HNF4A). Diabetologia. 2007;50(12):2600-1.

186. Pingul MM, Hughes N, Wu A, Stanley CA, Gruppuso PA. Hepatocyte nuclear factor 4alpha gene mutation associated with familial neonatal hyperinsulinism and maturity-onset diabetes of the young. J Pediatr. 2011;158(5):852-4.

187. Flanagan SE, Kapoor RR, Mali G, Cody D, Murphy N, Schwahn B, et al. Diazoxide-responsive hyperinsulinemic hypoglycemia caused by HNF4A gene mutations. Eur J Endocrinol. 2010;162(5):987-92.

188. Stanescu DE, Hughes N, Kaplan B, Stanley CA, De Leon DD. Novel presentations of congenital hyperinsulinism due to mutations in the MODY genes: HNF1A and HNF4A. J Clin Endocrinol Metab. 2012;97(10):E2026-30.

189. Meissner T, Otonkoski T, Feneberg R, Beinbrech B, Apostolidou S, Sipila I, et al. Exercise induced hypoglycaemic hyperinsulinism. Arch Dis Child. 2001;84(3):254-7.

190. Ishihara H, Wang H, Drewes LR, Wollheim CB. Overexpression of monocarboxylate transporter and lactate dehydrogenase alters insulin secretory responses to pyruvate and lactate in beta cells. J Clin Invest. 1999;104(11):1621-9.

191. Otonkoski T, Kaminen N, Ustinov J, Lapatto R, Meissner T, Mayatepek E, et al. Physical exercise-induced hyperinsulinemic hypoglycemia is an autosomal-dominant trait characterized by abnormal pyruvate-induced insulin release. Diabetes. 2003;52(1):199-204.

192. Gonzalez-Barroso MM, Giurgea I, Bouillaud F, Anedda A, Bellanne-Chantelot C, Hubert L, et al. Mutations in UCP2 in congenital hyperinsulinism reveal a role for regulation of insulin secretion. PLoS One. 2008;3(12):e3850.

193. Vozza A, Parisi G, De Leonardis F, Lasorsa FM, Castegna A, Amorese D, et al. UCP2 transports C4 metabolites out of mitochondria, regulating glucose and glutamine oxidation. Proc Natl Acad Sci U S A. 2014;111(3):960-5.

194. Pinney SE, Ganapathy K, Bradfield J, Stokes D, Sasson A, Mackiewicz K, et al. Dominant form of congenital hyperinsulinism maps to HK1 region on 10q. Horm Res Paediatr. 2013;80(1):18-27.

195. Henquin JC, Sempoux C, Marchandise J, Godecharles S, Guiot Y, Nenquin M, et al. Congenital hyperinsulinism caused by hexokinase I expression or glucokinase-activating mutation in a subset of beta-cells. Diabetes. 2013;62(5):1689-96.

196. Wang H, Gauthier BR, Hagenfeldt-Johansson KA, Iezzi M, Wollheim CB. Foxa2 (HNF3beta ) controls multiple genes implicated in metabolism-secretion coupling of glucose-induced insulin release. J Biol Chem. 2002;277(20):17564-70.

197. Tegtmeyer LC, Rust S, van Scherpenzeel M, Ng BG, Losfeld ME, Timal S, et al. Multiple phenotypes in phosphoglucomutase 1 deficiency. N Engl J Med. 2014;370(6):533-42.

198. Rahier J, Guiot Y, Sempoux C. Persistent hyperinsulinaemic hypoglycaemia of infancy: a heterogeneous syndrome unrelated to nesidioblastosis. Arch Dis Child Fetal Neonatal Ed. 2000;82(2):F108-12.

199. Verkarre V, Fournet JC, de Lonlay P, Gross-Morand MS, Devillers M, Rahier J, et al. Paternal mutation of the sulfonylurea receptor (SUR1) gene and maternal loss of 11p15 imprinted genes lead to persistent hyperinsulinism in focal adenomatous hyperplasia. J Clin Invest. 1998;102(7):1286-91.

200. Fournet JC, Mayaud C, de Lonlay P, Verkarre V, Rahier J, Brunelle F, et al. Loss of imprinted genes and paternal SUR1 mutations lead to focal form of congenital hyperinsulinism. Horm Res. 2000;53 Suppl 1:2-6.

201. Otonkoski T, Nanto-Salonen K, Seppanen M, Veijola R, Huopio H, Hussain K, et al. Noninvasive diagnosis of focal hyperinsulinism of infancy with [18F]-DOPA positron emission tomography. Diabetes. 2006;55(1):13-8.

202. Choufani S, Shuman C, Weksberg R. Beckwith-Wiedemann syndrome. Am J Med Genet C Semin Med Genet. 2010;154C(3):343-54.

203. Finegold DN, Stanley CA, Baker L. Glycemic response to glucagon during fasting hypoglycemia: an aid in the diagnosis of hyperinsulinism. J Pediatr. 1980;96(2):257-9.

204. Hussain K, Bryan J, Christesen HT, Brusgaard K, Aguilar-Bryan L. Serum glucagon counterregulatory hormonal response to hypoglycemia is blunted in congenital hyperinsulinism. Diabetes. 2005;54(10):2946-51.

205. Levitt Katz LE, Satin-Smith MS, Collett-Solberg P, Thornton PS, Baker L, Stanley CA, et al. Insulin-like growth factor binding protein-1 levels in the diagnosis of hypoglycemia caused by hyperinsulinism. J Pediatr. 1997;131(2):193-9.

206. Christesen HB, Brusgaard K, Alm J, Sjoblad S, Hussain K, Fenger C, et al. Rapid genetic analysis in congenital hyperinsulinism. Horm Res. 2007;67(4):184-8.

207. Thornton PS, Alter CA, Katz LE, Baker L, Stanley CA. Short- and long-term use of octreotide in the treatment of congenital hyperinsulinism. J Pediatr. 1993;123(4):637-43.

208. Laje P, Halaby L, Adzick NS, Stanley CA. Necrotizing enterocolitis in neonates receiving octreotide for the management of congenital hyperinsulinism. Pediatr Diabetes. 2010;11(2):142-7.

209. Le Quan Sang KH, Arnoux JB, Mamoune A, Saint-Martin C, Bellanne-Chantelot C, Valayannopoulos V, et al. Successful treatment of congenital hyperinsulinism with long-acting release octreotide. Eur J Endocrinol. 2012;166(2):333-9.

210. Modan-Moses D, Koren I, Mazor-Aronovitch K, Pinhas-Hamiel O, Landau H. Treatment of congenital hyperinsulinism with lanreotide acetate (Somatuline Autogel). J Clin Endocrinol Metab. 2011;96(8):2312-7.

211. De Leon DD, Li C, Delson MI, Matschinsky FM, Stanley CA, Stoffers DA. Exendin-(9-39) corrects fasting hypoglycemia in SUR-1-/- mice by lowering cAMP in pancreatic beta-cells and inhibiting insulin secretion. J Biol Chem. 2008;283(38):25786-93.

212. Calabria AC, Li C, Gallagher PR, Stanley CA, De Leon DD. GLP-1 receptor antagonist exendin-(9-39) elevates fasting blood glucose levels in congenital hyperinsulinism owing to inactivating mutations in the ATP-sensitive K+ channel. Diabetes. 2012;61(10):2585-91.

213. Senniappan S, Alexandrescu S, Tatevian N, Shah P, Arya V, Flanagan S, et al. Sirolimus therapy in infants with severe hyperinsulinemic hypoglycemia. N Engl J Med. 2014;370(12):1131-7.

214. Fekete CN, de Lonlay P, Jaubert F, Rahier J, Brunelle F, Saudubray JM. The surgical management of congenital hyperinsulinemic hypoglycemia in infancy. J Pediatr Surg. 2004;39(3):267-9.

215. Mohnike K, Blankenstein O, Minn H, Mohnike W, Fuchtner F, Otonkoski T. [18F]-DOPA positron emission tomography for preoperative localization in congenital hyperinsulinism. Horm Res. 2008;70(2):65-72.

216. Bax KN, van der Zee DC. The laparoscopic approach toward hyperinsulinism in children. Semin Pediatr Surg. 2007;16(4):245-51.

217. Kapoor RR, Flanagan SE, Arya VB, Shield JP, Ellard S, Hussain K. Clinical and molecular characterisation of 300 patients with congenital hyperinsulinism. Eur J Endocrinol. 2013;168(4):557-64.

218. Li H, Durbin R. Fast and accurate long-read alignment with Burrows-Wheeler transform. Bioinformatics. 2010;26(5):589-95.

219. DePristo MA, Banks E, Poplin R, Garimella KV, Maguire JR, Hartl C, et al. A framework for variation discovery and genotyping using next-generation DNA sequencing data. Nat Genet. 2011;43(5):491-8.

220. McKenna A, Hanna M, Banks E, Sivachenko A, Cibulskis K, Kernytsky A, et al. The Genome Analysis Toolkit: A MapReduce framework for analyzing next-generation DNA sequencing data. Genome Research. 2010;20(9):1297-303.

221. Cingolani P, Platts A, Wang le L, Coon M, Nguyen T, Wang L, et al. A program for annotating and predicting the effects of single nucleotide polymorphisms, SnpEff: SNPs in the genome of Drosophila melanogaster strain w1118; iso-2; iso-3. Fly (Austin). 2012;6(2):80-92.

222. Ng PC, Henikoff S. SIFT: Predicting amino acid changes that affect protein function. Nucleic Acids Res. 2003;31(13):3812-4.

223. Ramensky V, Bork P, Sunyaev S. Human non-synonymous SNPs: server and survey. Nucleic Acids Res. 2002;30(17):3894-900.

224. Sunyaev S, Ramensky V, Koch I, Lathe W, 3rd, Kondrashov AS, Bork P. Prediction of deleterious human alleles. Hum Mol Genet. 2001;10(6):591-7.
225. Flanagan SE, Patch AM, Ellard S. Using SIFT and PolyPhen to predict loss-of-function and gain-of-function mutations. Genet Test Mol Biomarkers. 2010;14(4):533-7.
226. Nachman MW, Crowell SL. Estimate of the mutation rate per nucleotide in humans. Genetics. 2000;156(1):297-304.
227. Vissers LE, de Ligt J, Gilissen C, Janssen I, Steehouwer M, de Vries P, et al. A de novo paradigm for mental retardation. Nat Genet. 2010;42(12):1109-12.
228. Gilissen C, Arts HH, Hoischen A, Spruijt L, Mans DA, Arts P, et al. Exome sequencing identifies WDR35 variants involved in Sensenbrenner syndrome. Am J Hum Genet. 2010;87(3):418-23.
229. Hoischen A, van Bon BW, Gilissen C, Arts P, van Lier B, Steehouwer M, et al. De novo mutations of SETBP1 cause Schinzel-Giedion syndrome. Nat Genet. 2010;42(6):483-5.
230. Lalonde E, Albrecht S, Ha KC, Jacob K, Bolduc N, Polychronakos C, et al. Unexpected allelic heterogeneity and spectrum of mutations in Fowler syndrome revealed by next-generation exome sequencing. Hum Mutat. 2010;31(8):918-23.
231. Simpson MA, Irving MD, Asilmaz E, Gray MJ, Dafou D, Elmslie FV, et al. Mutations in NOTCH2 cause Hajdu-Cheney syndrome, a disorder of severe and progressive bone loss. Nat Genet. 2011;43(4):303-5.
232. Mosse YP, Laudenslager M, Longo L, Cole KA, Wood A, Attiyeh EF, et al. Identification of ALK as a major familial neuroblastoma predisposition gene. Nature. 2008;455(7215):930-5.
233. Chang SC, Heacock PN, Clancey CJ, Dowhan W. The PEL1 gene (renamed PGS1) encodes the phosphatidylglycero-phosphate synthase of Saccharomyces cerevisiae. J Biol Chem. 1998;273(16):9829-36.
234. Ohtake S, Ito Y, Fukuta M, Habuchi O. Human N-acetylgalactosamine 4-sulfate 6-O-sulfotransferase cDNA is related to human B cell recombination activating gene-associated gene. J Biol Chem. 2001;276(47):43894-900.
235. Masuda K, Shima H, Watanabe M, Kikuchi K. MKP-7, a novel mitogen-activated protein kinase phosphatase, functions as a shuttle protein. J Biol Chem. 2001;276(42):39002-11.

236. Wei P, Garber ME, Fang SM, Fischer WH, Jones KA. A novel CDK9-associated C-type cyclin interacts directly with HIV-1 Tat and mediates its high-affinity, loop-specific binding to TAR RNA. Cell. 1998;92(4):451-62.

237. Fullgrabe J, Lynch-Day MA, Heldring N, Li W, Struijk RB, Ma Q, et al. The histone H4 lysine 16 acetyltransferase hMOF regulates the outcome of autophagy. Nature. 2013;500(7463):468-71.

238. Katoh M, Katoh M. Identification and characterization of human FMNL1, FMNL2 and FMNL3 genes in silico. Int J Oncol. 2003;22(5):1161-8.

239. Ang SL, Rossant J. HNF-3 beta is essential for node and notochord formation in mouse development. Cell. 1994;78(4):561-74.

240. Weinstein DC, Ruiz i Altaba A, Chen WS, Hoodless P, Prezioso VR, Jessell TM, et al. The winged-helix transcription factor HNF-3β is required for notochord development in the mouse embryo. Cell. 1994;78(4):575-88.

241. Jin O, Harpal K, Ang SL, Rossant J. Otx2 and HNF3beta genetically interact in anterior patterning. Int J Dev Biol. 2001;45(1):357-65.

242. Treier M, O'Connell S, Gleiberman A, Price J, Szeto DP, Burgess R, et al. Hedgehog signaling is required for pituitary gland development. Development. 2001;128(3):377-86.

243. Buscher D, Bosse B, Heymer J, Ruther U. Evidence for genetic control of Sonic hedgehog by Gli3 in mouse limb development. Mech Dev. 1997;62(2):175-82.

244. Dahmane N, Sanchez P, Gitton Y, Palma V, Sun T, Beyna M, et al. The Sonic Hedgehog-Gli pathway regulates dorsal brain growth and tumorigenesis. Development. 2001;128(24):5201-12.

245. Mo R, Freer AM, Zinyk DL, Crackower MA, Michaud J, Heng HH, et al. Specific and redundant functions of Gli2 and Gli3 zinc finger genes in skeletal patterning and development. Development. 1997;124(1):113-23.

246. Mavromatakis YE, Lin W, Metzakopian E, Ferri ALM, Yan CH, Sasaki H, et al. Foxa1 and Foxa2 positively and negatively regulate Shh signalling to specify ventral midbrain progenitor identity. Mechanisms of Development. 2011;128(1-2):90-103.

247. Lee CS, Friedman JR, Fulmer JT, Kaestner KH. The initiation of liver development is dependent on Foxa transcription factors. Nature. 2005;435(7044):944-7.

248. Wan H, Dingle S, Xu Y, Besnard V, Kaestner KH, Ang SL, et al. Compensatory roles of Foxa1 and Foxa2 during lung morphogenesis. J Biol Chem. 2005;280(14):13809-16.

249. Gao N, LeLay J, Vatamaniuk MZ, Rieck S, Friedman JR, Kaestner KH. Dynamic regulation of Pdx1 enhancers by Foxa1 and Foxa2 is essential for pancreas development. Genes Dev. 2008;22(24):3435-48.

250. Friedman JR, Kaestner KH. The Foxa family of transcription factors in development and metabolism. Cell Mol Life Sci. 2006;63(19-20):2317-28.

251. Sund NJ, Vatamaniuk MZ, Casey M, Ang SL, Magnuson MA, Stoffers DA, et al. Tissue-specific deletion of Foxa2 in pancreatic beta cells results in hyperinsulinemic hypoglycemia. Genes Dev. 2001;15(13):1706-15.

252. Lantz KA, Vatamaniuk MZ, Brestelli JE, Friedman JR, Matschinsky FM, Kaestner KH. Foxa2 regulates multiple pathways of insulin secretion. Journal of Clinical Investigation. 2004;114(4):512-20.

253. Aguilar-Bryan L, Nichols C, Wechsler S, Clement J, Boyd A, Gonzalez G, et al. Cloning of the beta cell high-affinity sulfonylurea receptor: a regulator of insulin secretion. Science. 1995;268(5209):423-6.

254. Nestorowicz A, Wilson BA, Schoor KP, Inoue H, Glaser B, Landau H, et al. Mutations in the sulonylurea receptor gene are associated with familial hyperinsulinism in Ashkenazi Jews. Hum Mol Genet. 1996;5(11):1813-22.

255. Nestorowicz A, Inagaki N, Gonoi T, Schoor KP, Wilson BA, Glaser B, et al. A Nonsense Mutation in the Inward Rectifier Potassium Channel Gene, Kir6.2, Is Associated With Familial Hyperinsulinism. Diabetes. 1997;46(11):1743-8.

256. Thomas P, Cote G, Wohllk N, Haddad B, Mathew P, Rabl W, et al. Mutations in the sulfonylurea receptor gene in familial persistent hyperinsulinemic hypoglycemia of infancy. Science. 1995;268(5209):426-9.

257. Thorne N, Inglese J, Auld DS. Illuminating insights into firefly luciferase and other bioluminescent reporters used in chemical biology. Chem Biol. 2010;17(6):646-57.

258. Dayem-Quere M, Giuliano F, Wagner-Mahler K, Massol C, Crouzet-Ozenda L, Lambert J-C, et al. Delineation of a region responsible for panhypopituitarism in 20p11.2. American Journal of Medical Genetics Part A. 2013;161(7):1547-54.

259. Tsai EA, Grochowski CM, Falsey AM, Rajagopalan R, Wendel D, Devoto M, et al. Heterozygous Deletion ofFOXA2Segregates with Disease in a Family with Heterotaxy, Panhypopituitarism, and Biliary Atresia. Human Mutation. 2015;36(6):631-7.

260. Garcia-Heras J, Kilani RA, Martin RA, Lamp S. A deletion of proximal 20p inherited from a normal mosaic carrier mother in a newborn with panhypopituitarism and craniofacial dysmorphism. Clin Dysmorphol. 2005;14(3):137-40.

261. Kamath BM, Thiel BD, Gai X, Conlin LK, Munoz PS, Glessner J, et al. SNP array mapping of chromosome 20p deletions: genotypes, phenotypes, and copy number variation. Hum Mutat. 2009;30(3):371-8.

262. Williams PG, Wetherbee JJ, Rosenfeld JA, Hersh JH. 20p11 deletion in a female child with panhypopituitarism, cleft lip and palate, dysmorphic facial features, global developmental delay and seizure disorder. Am J Med Genet A. 2011;155A(1):186-91.

263. Lo FS, Lee YJ, Lin SP, Shen EY, Huang JK, Lee KS. Solitary maxillary central incisor and congenital nasal pyriform aperture stenosis. European Journal of Pediatrics. 1998;157(1):39-44.

264. Hussain K, Senniappan S, Arya V. The molecular mechanisms, diagnosis and management of congenital hyperinsulinism. Indian Journal of Endocrinology and Metabolism. 2013;17(1):19.

265. Stanley CA. Perspective on the Genetics and Diagnosis of Congenital Hyperinsulinism Disorders. The Journal of Clinical Endocrinology & Metabolism. 2016;101(3):815-26.

266. Tatsumi K-i, Miyai K, Notomi T, Kaibe K, Amino N, Mizuno Y, et al. Cretinism with combined hormone deficiency caused by a mutation in the PIT1 gene. Nature Genetics. 1992;1(1):56-8.

267. Ben-Shushan E, Marshak S, Shoshkes M, Cerasi E, Melloul D. A Pancreatic -Cell-specific Enhancer in the HumanPDX-1 Gene Is Regulated by Hepatocyte Nuclear Factor 3 (HNF-3 ), HNF-1 , and SPs Transcription Factors. Journal of Biological Chemistry. 2001;276(20):17533-40.

268. Cha JY, Kim H, Kim KS, Hur MW, Ahn Y. Identification of transacting factors responsible for the tissue-specific expression of human glucose transporter type 2 isoform gene. Cooperative role of hepatocyte nuclear factors 1alpha and 3beta. J Biol Chem. 2000;275(24):18358-65.

269. Wang H, Gauthier BR, Hagenfeldt-Johansson KA, Iezzi M, Wollheim CB. Foxa2 (HNF3 ) Controls Multiple Genes Implicated in Metabolism-Secretion Coupling of Glucose-induced Insulin Release. Journal of Biological Chemistry. 2002;277(20):17564-70.

270. Lee CS, Sund NJ, Vatamaniuk MZ, Matschinsky FM, Stoffers DA, Kaestner KH. Foxa2 Controls Pdx1 Gene Expression in Pancreatic -Cells In Vivo. Diabetes. 2002;51(8):2546-51.

271. Ahlgren U, Jonsson J, Jonsson L, Simu K, Edlund H. beta -Cell-specific inactivation of the mouse Ipf1/Pdx1 gene results in loss of the beta -cell phenotype and maturity onset diabetes. Genes & Development. 1998;12(12):1763-8.

272. Yan W, Sheng N, Seto M, Morser J, Wu Q. Corin, a mosaic transmembrane serine protease encoded by a novel cDNA from human heart. J Biol Chem. 1999;274(21):14926-35.

273. Cui Y, Wang W, Dong N, Lou J, Srinivasan DK, Cheng W, et al. Role of corin in trophoblast invasion and uterine spiral artery remodelling in pregnancy. Nature. 2012;484(7393):246-50.

274. Kleefstra T, Brunner HG, Amiel J, Oudakker AR, Nillesen WM, Magee A, et al. Loss-of-function mutations in euchromatin histone methyl transferase 1 (EHMT1) cause the 9q34 subtelomeric deletion syndrome. Am J Hum Genet. 2006;79(2):370-7.

275. Gabig TG, Mantel PL, Rosli R, Crean CD. Requiem: a novel zinc finger gene essential for apoptosis in myeloid cells. J Biol Chem. 1994;269(47):29515-9.

276. Nguyen A, Burack WR, Stock JL, Kortum R, Chaika OV, Afkarian M, et al. Kinase suppressor of Ras (KSR) is a scaffold which facilitates mitogen-activated protein kinase activation in vivo. Mol Cell Biol. 2002;22(9):3035-45.

277. van Eenennaam H, Pruijn GJ, van Venrooij WJ. hPop4: a new protein subunit of the human RNase MRP and RNase P ribonucleoprotein complexes. Nucleic Acids Res. 1999;27(12):2465-72.

278. Kuttruff S, Koch S, Kelp A, Pawelec G, Rammensee HG, Steinle A. NKp80 defines and stimulates a reactive subset of CD8 T cells. Blood. 2009;113(2):358-69.

279. Grange T, de Sa CM, Oddos J, Pictet R. Human mRNA polyadenylate binding protein: evolutionary conservation of a nucleic acid binding motif. Nucleic Acids Res. 1987;15(12):4771-87.

280. Bainbridge MN, Hu H, Muzny DM, Musante L, Lupski JR, Graham BH, et al. De novo truncating mutations in ASXL3 are associated with a novel clinical phenotype with similarities to Bohring-Opitz syndrome. Genome Med. 2013;5(2):11.

281. Dinwiddie DL, Soden SE, Saunders CJ, Miller NA, Farrow EG, Smith LD, et al. De novo frameshift mutation in ASXL3 in a patient with global developmental delay, microcephaly, and craniofacial anomalies. BMC Med Genomics. 2013;6:32.

282. Hori I, Miya F, Ohashi K, Negishi Y, Hattori A, Ando N, et al. Novel splicing mutation in the ASXL3 gene causing Bainbridge-Ropers syndrome. Am J Med Genet A. 2016;170(7):1863-7.

283. Srivastava A, Ritesh KC, Tsan YC, Liao R, Su F, Cao X, et al. De novo dominant ASXL3 mutations alter H2A deubiquitination and transcription in Bainbridge-Ropers syndrome. Hum Mol Genet. 2016;25(3):597-608.

284. Bohring A, Oudesluijs GG, Grange DK, Zampino G, Thierry P. New cases of Bohring-Opitz syndrome, update, and critical review of the literature. Am J Med Genet A. 2006;140(12):1257-63.

285. Katoh M. Functional and cancer genomics of ASXL family members. Br J Cancer. 2013;109(2):299-306.

286. Aravind L, Iyer LM. The HARE-HTH and associated domains: novel modules in the coordination of epigenetic DNA and protein modifications. Cell Cycle. 2012;11(1):119-31.

287. Di Croce L, Helin K. Transcriptional regulation by Polycomb group proteins. Nat Struct Mol Biol. 2013;20(10):1147-55.

288. Jones AR, Overly CC, Sunkin SM. The Allen Brain Atlas: 5 years and beyond. Nat Rev Neurosci. 2009;10(11):821-8.

289. Shmueli O, Horn-Saban S, Chalifa-Caspi V, Shmoish M, Ophir R, Benjamin-Rodrig H, et al. GeneNote: whole genome expression profiles in normal human tissues. C R Biol. 2003;326(10-11):1067-72.

290. Li H, Durbin R. Fast and accurate long-read alignment with Burrows-Wheeler transform. Bioinformatics. 2010;26(5):589-95.

291. McKenna A, Hanna M, Banks E, Sivachenko A, Cibulskis K, Kernytsky A, et al. The Genome Analysis Toolkit: a MapReduce framework for analyzing next-generation DNA sequencing data. Genome Res. 2010;20(9):1297-303.

292. Tyner C, Barber GP, Casper J, Clawson H, Diekhans M, Eisenhart C, et al. The UCSC Genome Browser database: 2017 update. Nucleic Acids Res. 2017;45(D1):D626-D34.

293. Kumar P, Henikoff S, Ng PC. Predicting the effects of coding non-synonymous variants on protein function using the SIFT algorithm. Nat Protoc. 2009;4(7):1073-81.

294. Dosztanyi Z, Csizmok V, Tompa P, Simon I. IUPred: web server for the prediction of intrinsically unstructured regions of proteins based on estimated energy content. Bioinformatics. 2005;21(16):3433-4.

295. Dinkel H, Van Roey K, Michael S, Kumar M, Uyar B, Altenberg B, et al. ELM 2016--data update and new functionality of the eukaryotic linear motif resource. Nucleic Acids Res. 2016;44(D1):D294-300.
296. Mooney C, Pollastri G, Shields DC, Haslam NJ. Prediction of short linear protein binding regions. J Mol Biol. 2012;415(1):193-204.
297. Dosztanyi Z, Meszaros B, Simon I. ANCHOR: web server for predicting protein binding regions in disordered proteins. Bioinformatics. 2009;25(20):2745-6.
298. Aghazadeh Y, Papadopoulos V. The role of the 14-3-3 protein family in health, disease, and drug development. Drug Discov Today. 2016;21(2):278-87.
299. Yun M, Wu J, Workman JL, Li B. Readers of histone modifications. Cell Res. 2011;21(4):564-78.
300. Katoh M. Functional proteomics of the epigenetic regulators ASXL1, ASXL2 and ASXL3: a convergence of proteomics and epigenetics for translational medicine. Expert Rev Proteomics. 2015;12(3):317-28.
301. Hornbeck PV, Zhang B, Murray B, Kornhauser JM, Latham V, Skrzypek E. PhosphoSitePlus, 2014: mutations, PTMs and recalibrations. Nucleic Acids Res. 2015;43(Database issue):D512-20.
302. Cohen J, Blethen S, Kuntze J, Smith SL, Lomax KG, Mathew PM. Managing the child with severe primary insulin-like growth factor-1 deficiency (IGFD): IGFD diagnosis and management. Drugs R D. 2014;14(1):25-9.
303. Ashare A, Nymon AB, Doerschug KC, Morrison JM, Monick MM, Hunninghake GW. Insulin-like growth factor-1 improves survival in sepsis via enhanced hepatic bacterial clearance. Am J Respir Crit Care Med. 2008;178(2):149-57.
304. Manning BD, Cantley LC. AKT/PKB signaling: navigating downstream. Cell. 2007;129(7):1261-74.
305. Madonna R, De Caterina R, Geng YJ. Epigenetic regulation of insulin-like growth factor signaling: A novel insight into the pathophysiology of neonatal pulmonary hypertension. Vascul Pharmacol. 2015;73:4-7.
306. Mansilla F, Dominguez CA, Yeadon JE, Corydon TJ, Burden SJ, Knudsen CR. Translation elongation factor eEF1A binds to a novel myosin binding protein-C-like protein. J Cell Biochem. 2008;105(3):847-58.
307. Chen J, Chiang YC, Denis CL. CCR4, a 3'-5' poly(A) RNA and ssDNA exonuclease, is the catalytic component of the cytoplasmic deadenylase. EMBO J. 2002;21(6):1414-26.

308. Nagase T, Kikuno R, Ishikawa KI, Hirosawa M, Ohara O. Prediction of the coding sequences of unidentified human genes. XVI. The complete sequences of 150 new cDNA clones from brain which code for large proteins in vitro. DNA Res. 2000;7(1):65-73.
309. Walther TC, Fornerod M, Pickersgill H, Goldberg M, Allen TD, Mattaj IW. The nucleoporin Nup153 is required for nuclear pore basket formation, nuclear pore complex anchoring and import of a subset of nuclear proteins. EMBO J. 2001;20(20):5703-14.
310. Motley A, Hettema E, Distel B, Tabak H. Differential protein import deficiencies in human peroxisome assembly disorders. J Cell Biol. 1994;125(4):755-67.
311. Nagase T, Kikuno R, Ishikawa K, Hirosawa M, Ohara O. Prediction of the coding sequences of unidentified human genes. XVII. The complete sequences of 100 new cDNA clones from brain which code for large proteins in vitro. DNA Res. 2000;7(2):143-50.
312. Goto M, Eddy EM. Speriolin is a novel spermatogenic cell-specific centrosomal protein associated with the seventh WD motif of Cdc20. J Biol Chem. 2004;279(40):42128-38.
313. Tang XX, Pleasure DE, Ikegaki N. cDNA cloning, chromosomal localization, and expression pattern of EPLG8, a new member of the EPLG gene family encoding ligands of EPH-related protein-tyrosine kinase receptors. Genomics. 1997;41(1):17-24.
314. Marcelo KL, Means AR, York B. The Ca(2+)/Calmodulin/CaMKK2 Axis: Nature's Metabolic CaMshaft. Trends Endocrinol Metab. 2016;27(10):706-18.
315. Hsu LS, Chen GD, Lee LS, Chi CW, Cheng JF, Chen JY. Human Ca2+/calmodulin-dependent protein kinase kinase beta gene encodes multiple isoforms that display distinct kinase activity. J Biol Chem. 2001;276(33):31113-23.
316. Hawley SA, Pan DA, Mustard KJ, Ross L, Bain J, Edelman AM, et al. Calmodulin-dependent protein kinase kinase-beta is an alternative upstream kinase for AMP-activated protein kinase. Cell Metab. 2005;2(1):9-19.
317. Hurley RL, Anderson KA, Franzone JM, Kemp BE, Means AR, Witters LA. The Ca2+/calmodulin-dependent protein kinase kinases are AMP-activated protein kinase kinases. J Biol Chem. 2005;280(32):29060-6.
318. Scott JW, Park E, Rodriguiz RM, Oakhill JS, Issa SM, O'Brien MT, et al. Autophosphorylation of CaMKK2 generates autonomous activity that is disrupted by a T85S mutation linked to anxiety and bipolar disorder. Sci Rep. 2015;5:14436.
319. Yu X, Murao K, Sayo Y, Imachi H, Cao WM, Ohtsuka S, et al. The role of calcium/calmodulin-dependent protein kinase cascade in glucose upregulation of insulin gene expression. Diabetes. 2004;53(6):1475-81.

320. Neu-Yilik G, Amthor B, Gehring NH, Bahri S, Paidassi H, Hentze MW, et al. Mechanism of escape from nonsense-mediated mRNA decay of human beta-globin transcripts with nonsense mutations in the first exon. RNA. 2011;17(5):843-54.

321. Nagy E, Maquat LE. A rule for termination-codon position within intron-containing genes: when nonsense affects RNA abundance. Trends Biochem Sci. 1998;23(6):198-9.

322. Thermann R, Neu-Yilik G, Deters A, Frede U, Wehr K, Hagemeier C, et al. Binary specification of nonsense codons by splicing and cytoplasmic translation. EMBO J. 1998;17(12):3484-94.

323. Wollheim CB, Sharp GW. Regulation of insulin release by calcium. Physiol Rev. 1981;61(4):914-73.

324. Worley JF, 3rd, McIntyre MS, Spencer B, Mertz RJ, Roe MW, Dukes ID. Endoplasmic reticulum calcium store regulates membrane potential in mouse islet beta-cells. J Biol Chem. 1994;269(20):14359-62.

325. Meldolesi J, Pozzan T. The endoplasmic reticulum Ca2+ store: a view from the lumen. Trends Biochem Sci. 1998;23(1):10-4.

326. Leibiger IB, Leibiger B, Moede T, Berggren PO. Exocytosis of insulin promotes insulin gene transcription via the insulin receptor/PI-3 kinase/p70 s6 kinase and CaM kinase pathways. Mol Cell. 1998;1(6):933-8.

327. Enslen H, Soderling TR. Roles of calmodulin-dependent protein kinases and phosphatase in calcium-dependent transcription of immediate early genes. J Biol Chem. 1994;269(33):20872-7.

328. Ban N, Yamada Y, Someya Y, Ihara Y, Adachi T, Kubota A, et al. Activating transcription factor-2 is a positive regulator in CaM kinase IV-induced human insulin gene expression. Diabetes. 2000;49(7):1142-8.

329. Racioppi L, Means AR. Calcium/calmodulin-dependent protein kinase kinase 2: roles in signaling and pathophysiology. J Biol Chem. 2012;287(38):31658-65.

330. Marcelo KL, Ribar T, Means CR, Tsimelzon A, Stevens RD, Ilkayeva O, et al. Research Resource: Roles for Calcium/Calmodulin-Dependent Protein Kinase Kinase 2 (CaMKK2) in Systems Metabolism. Mol Endocrinol. 2016;30(5):557-72.

331. Dadi PK, Vierra NC, Ustione A, Piston DW, Colbran RJ, Jacobson DA. Inhibition of pancreatic beta-cell Ca2+/calmodulin-dependent protein kinase II reduces glucose-stimulated calcium influx and insulin secretion, impairing glucose tolerance. J Biol Chem. 2014;289(18):12435-45.

332. Wang W, Olson D, Liang G, Franceschi RT, Li C, Wang B, et al. Collagen XXIV (Col24alpha1) promotes osteoblastic differentiation and mineralization through TGF-beta/Smads signaling pathway. Int J Biol Sci. 2012;8(10):1310-22.
333. Gay CM, Zygmunt T, Torres-Vazquez J. Diverse functions for the semaphorin receptor PlexinD1 in development and disease. Dev Biol. 2011;349(1):1-19.
334. Perry MD, Vandenberg JI. TECRL: connecting sequence to consequence for a new sudden cardiac death gene. EMBO Mol Med. 2016;8(12):1364-5.
335. Kieslinger M, Folberth S, Dobreva G, Dorn T, Croci L, Erben R, et al. EBF2 regulates osteoblast-dependent differentiation of osteoclasts. Dev Cell. 2005;9(6):757-67.
336. Ohsawa N, Koebis M, Mitsuhashi H, Nishino I, Ishiura S. ABLIM1 splicing is abnormal in skeletal muscle of patients with DM1 and regulated by MBNL, CELF and PTBP1. Genes Cells. 2015;20(2):121-34.
337. von Oettingen JE, Tan WH, Dauber A. Skeletal dysplasia, global developmental delay, and multiple congenital anomalies in a 5-year-old boy-report of the second family with B3GAT3 mutation and expansion of the phenotype. Am J Med Genet A. 2014;164A(6):1580-6.
338. Girisha KM, Bidchol AM, Graul-Neumann L, Gupta A, Hehr U, Lessel D, et al. Phenotype and genotype in patients with Larsen syndrome: clinical homogeneity and allelic heterogeneity in seven patients. BMC Med Genet. 2016;17:27.
339. Job F, Mizumoto S, Smith L, Couser N, Brazil A, Saal H, et al. Functional validation of novel compound heterozygous variants in B3GAT3 resulting in severe osteopenia and fractures: expanding the disease phenotype. BMC Med Genet. 2016;17(1):86.
340. Jones KL, Schwarze U, Adam MP, Byers PH, Mefford HC. A homozygous B3GAT3 mutation causes a severe syndrome with multiple fractures, expanding the phenotype of linkeropathy syndromes. Am J Med Genet A. 2015;167A(11):2691-6.
341. Baasanjav S, Al-Gazali L, Hashiguchi T, Mizumoto S, Fischer B, Horn D, et al. Faulty initiation of proteoglycan synthesis causes cardiac and joint defects. Am J Hum Genet. 2011;89(1):15-27.
342. Budde BS, Mizumoto S, Kogawa R, Becker C, Altmuller J, Thiele H, et al. Skeletal dysplasia in a consanguineous clan from the island of Nias/Indonesia is caused by a novel mutation in B3GAT3. Hum Genet. 2015;134(7):691-704.

343. Mizumoto S, Yamada S, Sugahara K. Mutations in Biosynthetic Enzymes for the Protein Linker Region of Chondroitin/Dermatan/Heparan Sulfate Cause Skeletal and Skin Dysplasias. Biomed Res Int. 2015;2015:861752.

344. Jian X, Boerwinkle E, Liu X. In silico tools for splicing defect prediction: a survey from the viewpoint of end users. Genet Med. 2014;16(7):497-503.

345. Ducy P, Zhang R, Geoffroy V, Ridall AL, Karsenty G. Osf2/Cbfa1: a transcriptional activator of osteoblast differentiation. Cell. 1997;89(5):747-54.

346. Siegel DA, Huang MK, Becker SF. Ectopic dendrite initiation: CNS pathogenesis as a model of CNS development. Int J Dev Neurosci. 2002;20(3-5):373-89.

347. Modarressi MH, Cameron J, Taylor KE, Wolfe J. Identification and characterisation of a novel gene, TSGA10, expressed in testis. Gene. 2001;262(1-2):249-55.

348. Tanabe A, Konno J, Tanikawa K, Sahara H. Transcriptional machinery of TNF-alpha-inducible YTH domain containing 2 (YTHDC2) gene. Gene. 2014;535(1):24-32.

349. Jones B, Jones EL, Bonney SA, Patel HN, Mensenkamp AR, Eichenbaum-Voline S, et al. Mutations in a Sar1 GTPase of COPII vesicles are associated with lipid absorption disorders. Nat Genet. 2003;34(1):29-31.

350. Li L, Huang GM, Banta AB, Deng Y, Smith T, Dong P, et al. Cloning, characterization, and the complete 56.8-kilobase DNA sequence of the human NOTCH4 gene. Genomics. 1998;51(1):45-58.

351. Gray GE, Mann RS, Mitsiadis E, Henrique D, Carcangiu ML, Banks A, et al. Human ligands of the Notch receptor. Am J Pathol. 1999;154(3):785-94.

352. Krebs LT, Xue Y, Norton CR, Shutter JR, Maguire M, Sundberg JP, et al. Notch signaling is essential for vascular morphogenesis in mice. Genes Dev. 2000;14(11):1343-52.

353. Murphy PA, Lam MT, Wu X, Kim TN, Vartanian SM, Bollen AW, et al. Endothelial Notch4 signaling induces hallmarks of brain arteriovenous malformations in mice. Proc Natl Acad Sci U S A. 2008;105(31):10901-6.

354. Kolehmainen J, Black GC, Saarinen A, Chandler K, Clayton-Smith J, Traskelin AL, et al. Cohen syndrome is caused by mutations in a novel gene, COH1, encoding a transmembrane protein with a presumed role in vesicle-mediated sorting and intracellular protein transport. Am J Hum Genet. 2003;72(6):1359-69.

355. Daum JR, Wren JD, Daniel JJ, Sivakumar S, McAvoy JN, Potapova TA, et al. Ska3 is required for spindle checkpoint silencing and the maintenance of chromosome cohesion in mitosis. Curr Biol. 2009;19(17):1467-72.

356. Kalsoom UE, Klopocki E, Wasif N, Tariq M, Khan S, Hecht J, et al. Whole exome sequencing identified a novel zinc-finger gene ZNF141 associated with autosomal recessive postaxial polydactyly type A. J Med Genet. 2013;50(1):47-53.
357. Miyagawa Y, Tanaka H, Iguchi N, Kitamura K, Nakamura Y, Takahashi T, et al. Molecular cloning and characterization of the human orthologue of male germ cell-specific actin capping protein alpha3 (cpalpha3). Mol Hum Reprod. 2002;8(6):531-9.
358. Parfitt DA, Michael GJ, Vermeulen EG, Prodromou NV, Webb TR, Gallo JM, et al. The ataxia protein sacsin is a functional co-chaperone that protects against polyglutamine-expanded ataxin-1. Hum Mol Genet. 2009;18(9):1556-65.
359. Engert JC, Berube P, Mercier J, Dore C, Lepage P, Ge B, et al. ARSACS, a spastic ataxia common in northeastern Quebec, is caused by mutations in a new gene encoding an 11.5-kb ORF. Nat Genet. 2000;24(2):120-5.
360. Rojas-Gil AP, Ziros PG, Kanetsis E, Papathanassopoulou V, Nikolakopoulou NM, He K, et al. Combined effect of mutations of the GH1 gene and its proximal promoter region in a child with growth hormone neurosecretory dysfunction (GHND). J Mol Med (Berl). 2007;85(9):1005-13.
361. Takahashi Y, Chihara K. Short stature by mutant growth hormones. Growth Horm IGF Res. 1999;9 Suppl B:37-40; discussion -1.
362. Petkovic V, Miletta MC, Boot AM, Losekoot M, Fluck CE, Pandey AV, et al. Short stature in two siblings heterozygous for a novel bioinactive GH mutant (GH-P59S) suggesting that the mutant also affects secretion of the wild-type GH. Eur J Endocrinol. 2013;168(3):K35-43.
363. Sakharov DA, Thevis M, Tonevitsky AG. Analysis of major isoforms of human growth hormone before and after intensive physical exercise. Bull Exp Biol Med. 2008;146(4):466-9.
364. Brown RJ, Adams JJ, Pelekanos RA, Wan Y, McKinstry WJ, Palethorpe K, et al. Model for growth hormone receptor activation based on subunit rotation within a receptor dimer. Nat Struct Mol Biol. 2005;12(9):814-21.
365. Nosaka T, Kawashima T, Misawa K, Ikuta K, Mui AL, Kitamura T. STAT5 as a molecular regulator of proliferation, differentiation and apoptosis in hematopoietic cells. EMBO J. 1999;18(17):4754-65.

366. Madeira JL, Jorge AA, Martin RM, Montenegro LR, Franca MM, Costalonga EF, et al. A homozygous point mutation in the GH1 promoter (c.-223C>T) leads to reduced GH1 expression in siblings with isolated GH deficiency (IGHD). Eur J Endocrinol. 2016;175(2):K7-K15.

367. Kowarski AA, Schneider J, Ben-Galim E, Weldon VV, Daughaday WH. Growth failure with normal serum RIA-GH and low somatomedin activity: somatomedin restoration and growth acceleration after exogenous GH. J Clin Endocrinol Metab. 1978;47(2):461-4.

368. Dateki S, Hizukuri K, Tanaka T, Katsumata N, Katavetin P, Ogata T. An immunologically anomalous but considerably bioactive GH produced by a novel GH1 mutation (p.D116E). Eur J Endocrinol. 2009;161(2):301-6.

369. Wanders RJ, Dekker C, Hovarth VA, Schutgens RB, Tager JM, Van Laer P, et al. Human alkyldihydroxyacetonephosphate synthase deficiency: a new peroxisomal disorder. J Inherit Metab Dis. 1994;17(3):315-8.

370. Tian Y, Han X, Tian DL. The biological regulation of ABCE1. IUBMB Life. 2012;64(10):795-800.

371. Fukuda M. Molecular cloning, expression, and characterization of a novel class of synaptotagmin (Syt XIV) conserved from Drosophila to humans. J Biochem. 2003;133(5):641-9.

372. Sergouniotis PI, Chakarova C, Murphy C, Becker M, Lenassi E, Arno G, et al. Biallelic variants in TTLL5, encoding a tubulin glutamylase, cause retinal dystrophy. Am J Hum Genet. 2014;94(5):760-9.

373. Vithana EN, Morgan P, Sundaresan P, Ebenezer ND, Tan DT, Mohamed MD, et al. Mutations in sodium-borate cotransporter SLC4A11 cause recessive congenital hereditary endothelial dystrophy (CHED2). Nat Genet. 2006;38(7):755-7.

374. Baillat D, Hakimi MA, Naar AM, Shilatifard A, Cooch N, Shiekhattar R. Integrator, a multiprotein mediator of small nuclear RNA processing, associates with the C-terminal repeat of RNA polymerase II. Cell. 2005;123(2):265-76.

375. Beunders G, Voorhoeve E, Golzio C, Pardo LM, Rosenfeld JA, Talkowski ME, et al. Exonic deletions in AUTS2 cause a syndromic form of intellectual disability and suggest a critical role for the C terminus. Am J Hum Genet. 2013;92(2):210-20.

376. Feral C, Guellaen G, Pawlak A. Human testis expresses a specific poly(A)-binding protein. Nucleic Acids Res. 2001;29(9):1872-83.

377. Schenk B, Imbach T, Frank CG, Grubenmann CE, Raymond GV, Hurvitz H, et al. MPDU1 mutations underlie a novel human congenital disorder of glycosylation, designated type If. J Clin Invest. 2001;108(11):1687-95.

378. Damiano L, Le Devedec SE, Di Stefano P, Repetto D, Lalai R, Truong H, et al. p140Cap suppresses the invasive properties of highly metastatic MTLn3-EGFR cells via impaired cortactin phosphorylation. Oncogene. 2012;31(5):624-33.

379. Tang S, Wang X, Li W, Yang X, Li Z, Liu W, et al. Biallelic Mutations in CFAP43 and CFAP44 Cause Male Infertility with Multiple Morphological Abnormalities of the Sperm Flagella. Am J Hum Genet. 2017;100(6):854-64.

380. Krishnamurthy PC, Du G, Fukuda Y, Sun D, Sampath J, Mercer KE, et al. Identification of a mammalian mitochondrial porphyrin transporter. Nature. 2006;443(7111):586-9.

381. Ma X, Chen C, Veevers J, Zhou X, Ross RS, Feng W, et al. CRISPR/Cas9-mediated gene manipulation to create single-amino-acid-substituted and floxed mice with a cloning-free method. Sci Rep. 2017;7:42244.

382. Izumi H, Inoue J, Yokoi S, Hosoda H, Shibata T, Sunamori M, et al. Frequent silencing of DBC1 is by genetic or epigenetic mechanisms in non-small cell lung cancers. Hum Mol Genet. 2005;14(8):997-1007.

383. LaHoste GJ, Swanson JM, Wigal SB, Glabe C, Wigal T, King N, et al. Dopamine D4 receptor gene polymorphism is associated with attention deficit hyperactivity disorder. Mol Psychiatry. 1996;1(2):121-4.

384. Kenmochi N, Suzuki T, Uechi T, Magoori M, Kuniba M, Higa S, et al. The human mitochondrial ribosomal protein genes: mapping of 54 genes to the chromosomes and implications for human disorders. Genomics. 2001;77(1-2):65-70.

385. Spicer AP, Nguyen TK. Mammalian hyaluronan synthases: investigation of functional relationships in vivo. Biochem Soc Trans. 1999;27(2):109-15.

386. Kelberman D, Rizzoti K, Lovell-Badge R, Robinson IC, Dattani MT. Genetic regulation of pituitary gland development in human and mouse. Endocr Rev. 2009;30(7):790-829.

387. Patel L, McNally RJ, Harrison E, Lloyd IC, Clayton PE. Geographical distribution of optic nerve hypoplasia and septo-optic dysplasia in Northwest England. J Pediatr. 2006;148(1):85-8.

388. Birkebaek NH, Patel L, Wright NB, Grigg JR, Sinha S, Hall CM, et al. Endocrine status in patients with optic nerve hypoplasia: relationship to midline central nervous system abnormalities and appearance of the hypothalamic-pituitary axis on magnetic resonance imaging. J Clin Endocrinol Metab. 2003;88(11):5281-6.

389. Willnow S, Kiess W, Butenandt O, Dorr HG, Enders A, Strasser-Vogel B, et al. Endocrine disorders in septo-optic dysplasia (De Morsier syndrome)--evaluation and follow up of 18 patients. Eur J Pediatr. 1996;155(3):179-84.

390. Wu W, Cogan JD, Pfäffle RW, Dasen JS, Frisch H, O'Connell SM, et al. Mutations in PROP1 cause familial combined pituitary hormone deficiency. Nature Genetics. 1998;18(2):147-9.

391. Machinis K, Pantel J, Netchine I, Léger J, Camand OJA, Sobrier M-L, et al. Syndromic Short Stature in Patients with a Germline Mutation in the LIM Homeobox LHX4. The American Journal of Human Genetics. 2001;69(5):961-8.

392. Semina EV, Reiter R, Leysens NJ, Alward WLM, Small KW, Datson NA, et al. Cloning and characterization of a novel bicoid-related homeobox transcription factor gene, RIEG, involved in Rieger syndrome. Nature Genetics. 1996;14(4):392-9.

393. Dateki S, Fukami M, Sato N, Muroya K, Adachi M, Ogata T. OTX2Mutation in a Patient with Anophthalmia, Short Stature, and Partial Growth Hormone Deficiency: Functional Studies Using theIRBP,HESX1, andPOU1F1Promoters. The Journal of Clinical Endocrinology & Metabolism. 2008;93(10):3697-702.

394. Kelberman D, Rizzoti K, Avilion A, Bitner-Glindzicz M, Cianfarani S, Collins J, et al. Mutations within Sox2/SOX2 are associated with abnormalities in the hypothalamo-pituitary-gonadal axis in mice and humans. J Clin Invest. 2006;116(9):2442-55.

395. Laumonnier F, Ronce N, Hamel BCJ, Thomas P, Lespinasse J, Raynaud M, et al. Transcription Factor SOX3 Is Involved in X-Linked Mental Retardation with Growth Hormone Deficiency. The American Journal of Human Genetics. 2002;71(6):1450-5.

396. Woods KS, Cundall M, Turton J, Rizotti K, Mehta A, Palmer R, et al. Over- and Underdosage of SOX3 Is Associated with Infundibular Hypoplasia and Hypopituitarism. The American Journal of Human Genetics. 2005;76(5):833-49.

397. Stanley CA, Lieu YK, Hsu BYL, Burlina AB, Greenberg CR, Hopwood NJ, et al. Hyperinsulinism and Hyperammonemia in Infants with Regulatory Mutations of the Glutamate Dehydrogenase Gene. New England Journal of Medicine. 1998;338(19):1352-7.

398. Glaser B, Kesavan P, Heyman M, Davis E, Cuesta A, Buchs A, et al. Familial Hyperinsulinism Caused by an Activating Glucokinase Mutation. New England Journal of Medicine. 1998;338(4):226-30.

399. González-Barroso MM, Giurgea I, Bouillaud F, Anedda A, Bellanné-Chantelot C, Hubert L, et al. Mutations in UCP2 in Congenital Hyperinsulinism Reveal a Role for Regulation of Insulin Secretion. PLoS ONE. 2008;3(12):e3850.

400. Stanescu DE, Hughes N, Kaplan B, Stanley CA, De León DD. Novel Presentations of Congenital Hyperinsulinism due to Mutations in the MODY genes:HNF1AandHNF4A. The Journal of Clinical Endocrinology & Metabolism. 2012;97(10):E2026-E30.

401. Sander JD, Joung JK. CRISPR-Cas systems for editing, regulating and targeting genomes. Nat Biotechnol. 2014;32(4):347-55.

# CHAPTER 12

# APPENDIX

NHS
Health Research Authority

National Research Ethics Service
North West - Liverpool Central Research Ethics Committee
3rd Floor
Barlow House
4 Minshull Street
Manchester
M1 3DZ

Telephone: 0207 104 8020

29 October 2015

Dr Senthil Senniappan
Consultant Paediatric Endocrinologist & Honorary Senior Lecturer
Alder Hey Children's Hospital NHS Foundation Trust
Department of Paediatric Endocrinology
Alder Hey Children's Hospital
Eaton Road
Liverpool
L12 2AP

Dear Dr Senniappan

| | |
|---|---|
| **Study title:** | **Whole Exome Sequencing in Rare Endocrine disorders** |
| **REC reference:** | **15/NW/0758** |
| **IRAS project ID:** | **179435** |

Thank you for responding to the Committee's request for further information on the above research and submitting revised documentation.

The further information has been considered on behalf of the Committee by the Vice-Chair.

We plan to publish your research summary wording for the above study on the HRA website, together with your contact details. Publication will be no earlier than three months from the date of this opinion letter. Should you wish to provide a substitute contact point, require further information, or wish to make a request to postpone publication, please contact the REC Manager, Mrs Carol Ebenezer, nrescommittee.northwest-liverpoolcentral@nhs.net .

**Confirmation of ethical opinion**

On behalf of the Committee, I am pleased to confirm a favourable ethical opinion for the above research on the basis described in the application form, protocol and supporting documentation as revised, subject to the conditions specified below.

**Conditions of the favourable opinion**

The favourable opinion is subject to the following conditions being met prior to the start of the study.

Alder Hey Children's NHS
NHS Foundation Trust

**Clinical Research Business Unit**
**2nd Floor Institute in the Park**
Alder Hey Children's NHS Foundation Trust
Eaton Road, Liverpool
L12 2AP
0151 252 5570
Matthew.Peak@alderhey.nhs.uk
Charlie.Orton@alderhey.nhs.uk
Katherine.Jopson@alderhey.nhs.uk
Lucy.Cooper@alderhey.nhs.uk
www.alderhey.com

Dr Senthil Senniappan
Consultant Paediatric Endocrinologist & Honorary Senior Lecturer
Alder Hey Children's Hospital NHS Foundation Trust
Department of Paediatric Endocrinology
Alder Hey Children's Hospital
Eaton Road
Liverpool
L12 2AP

**RE:** Whole Exome Sequencing in Rare Endocrine disorders
**REC Ref:** 15/NW/0758
**R&D Ref:** 15/25/RE

Dear Dr Senniappan,

Thank you for submitting the above application to the Research & Development Office. It has now been reviewed against the requirements of the Research Governance Framework for Health and Social Care and relevant legislation. I am pleased to confirm that following completion of these checks approval is now granted for the study to commence within the Alder Hey Children's NHS Foundation Trust.

All NHS Trusts are performance managed by the National Institute for Health Research (NIHR) by benchmarks which measure the time taken to recruit the first patient into a research study and the local site's recruitment to time and target. All investigators within the Trust are supported by Data Managers within the Clinical Research Business Unit who can interpret these benchmarks for you and advise you on the timing and format in which data should be submitted to the CRBU. **R&D approval is conditional upon these data being submitted in a timely fashion each month.**

It will be the responsibility of the local Principal Investigator to comply with the responsibilities laid down, in the Research Governance Framework for Health and Social Care, by the Department of Health. Please see the enclosed leaflet for further information.

A full copy of the Research Governance Framework for Health and Social Care can also be obtained from the Department of Health website at www.doh.gov.uk or the R&D Office.

Yours sincerely

pp LM Cooper

Professor Matthew Peak
Director of Research

INVESTOR IN PEOPLE

# Parents of participating children Information Sheet

**Aim of the project**

The aim of this project is to investigate the genetic causes of endocrine problem (hormonal problem) in newborn, infants and children. Previous research has already identified a number of abnormalities in certain genes that can contribute to endocrine disorder(s) but we still don't know the cause in the majority of children. The aim of this study is to unravel further genetic causes that can cause or contribute to endocrine disorders.

**Why has been my child identified to participate in this study?**

Your child has been identified as having an endocrinological (hormonal) problem for which a potential genetic diagnosis is not known. We feel that, by this project we may be able to identify the genetic diagnosis, which may help in the future management of the condition.

**How is the study being done?**

If you agree to participate in this study, your child will have an additional blood sample taken when they are having their routine investigations. We will use this blood sample to extract DNA (genetic material). The DNA will then be used to analyse certain genes by the method of whole exome sequencing. The extra blood sample that we take will do no harm to your child, as the amount of blood that we will take is extremely small. As a part of the study, we might request blood samples from you or other related family members. This blood sample will be used to extract DNA that will be used only for the purpose of establishing a genetic cause for your child's hormonal problem.

**What are the risks and discomfort?**

No risk to the child can be foreseen. Your child might have a cannula inserted for routine medical treatment and we will then take the blood sample from the cannula. There is discomfort from the insertion of the cannula but we would normally numb the skin anyway with a local anaesthetic cream.

For further understanding and information about genes/DNA/whole exome sequencing, please refer to the information below.

1. **What are Genes?**

   The human body is made of cells. The cells contain DNA. The DNA is made of genes. Genes are chemical instructions that tell a cell what job to perform. A gene is like a recipe for making a particular protein. Proteins do important jobs in every cell of the body. Genes are written in code, with four chemicals (represented by the letters A, T, C, and G) that spell out the instructions to make a protein. People generally have two copies of most genes, one copy from each parent.

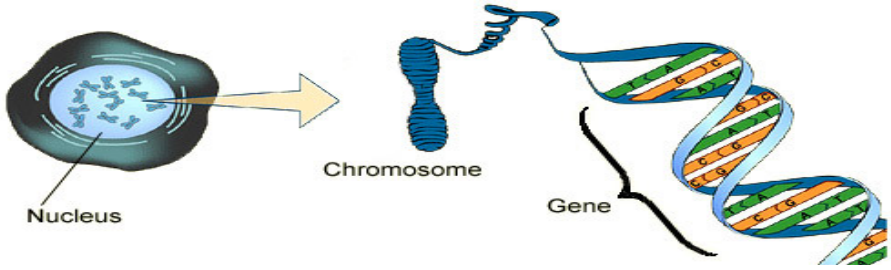

## 2. What is a genome and what is an exome?

Most genes are made up of introns and exons. Exons are the parts of the gene that contain the information used to make a protein. They are the “coding” part of the gene. Introns are regions of DNA in between exons and do not code for proteins.

The genome includes a person’s entire DNA, both the introns and the exons. The exome includes only the exons (the parts used to make proteins). The introns and other non-coding sequences of DNA are not part of the exome.

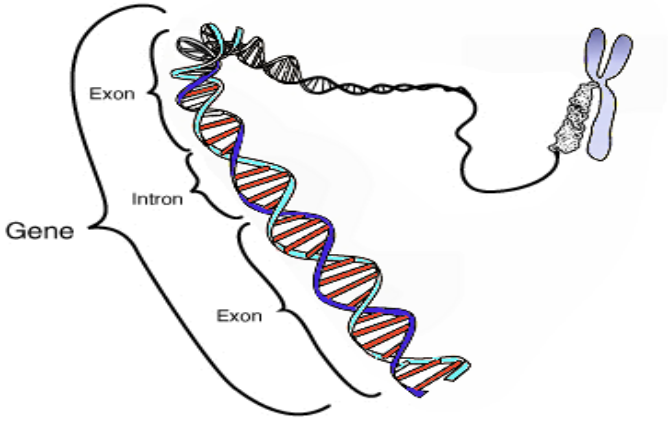


## 3. What is whole exome sequencing (WES)?

Some genetic tests “read” the genetic code of a single gene to see if that gene has any changes. Other genetic tests look for extra or missing pieces of DNA. Whole exome sequencing reads through the exons of most of the genes all at once. The exome is estimated to comprise approximately 1% of the genome, yet contains approximately 85% of disease-causing pathogenic variants.

## 4. What is the purpose of WES?

The purpose of whole exome sequencing is to try to find a genetic cause of your child’s signs and symptoms. Because WES looks at more genes than most genetic tests, it may find a genetic cause for your child’s signs and symptoms even if previous genetic testing did not.

## 5. How is the WES performed?

This test requires 3mls (about 1 teaspoon) of blood from the patient having WES. Sometimes blood samples from parents or other family members are also tested. The laboratory will isolate DNA from the blood sample. The exons (coding parts) of most genes will be examined. This is done for both the person having exome sequencing and for any family members that give DNA for comparison.

## 6. How is WES interpreted?

Your child’s DNA will be compared to a normal “reference” DNA sequence and (if applicable) to family members’ DNA. WES will identify some changes in the DNA that differ from the normal sequence. The researcher will use the clinical information, as well as many different scientific tools in the laboratory, to decide which genetic changes are likely to be responsible for your child’s signs and symptoms.

## 7. What are the benefits of WES?

WES may find a genetic cause for your child’s signs and symptoms. This may help guide medical care. A genetic diagnosis may give your family information about the chance that you could have other children affected with the same condition. This information may also be useful for other family members.

**8. What are the limitations of WES?**

It is possible that this test will not always find a reason for your child's signs and symptoms. WES may reveal information that is unexpected or unwanted. Approximately 85-92% of the exons are sequenced by this test. This test does not sequence every exon well enough to find all mutations in each exon.

**9. What kind of results can I expect from WES?**

The results could either show that there is a change to the usual sequence of the genetic material found in your child's sample (a variant) or there is not. If a variant is found, laboratory scientists will check to see if that specific variant has been found in other people who have a similar condition to your child. We all have some variations in our genetic material; no two people have exactly the same DNA sequence. However, many of the variations are completely normal and have no clinical effect, others enable us to have different characteristics and features. At this stage of our understanding of genetics, we do not always know if a rare variant could be harmful or not. Depending on the answer to this, you may receive one of the following results:

- The variant is thought to be definitely the cause of your child's condition or contributes to it in some way. Usually we know this because it has been found in many others with the same condition. Professionals call this a pathogenic or disease-causing variant.
- There is a variant but it is not certain if this is connected with your child's condition. This is sometimes called a variant of unknown significance and we may have to wait until science has advanced further to find out what it means for your child.
- The variant is thought to be harmless and not the cause of your child's condition. This is called a polymorphism or benign variant.
- If we don't find a variant, it does not necessarily mean there is no genetic cause for your condition. We still do not have enough understanding of genetics to recognise the underlying causes for all conditions.

**10. What are secondary findings?**

A *secondary finding* is a test result that is not expected and is not related to the reason for doing the test. For example, a mutation in a gene that is not related to the patient's condition is considered a secondary finding. Secondary findings may have important implications for your or your child's health.

Some genetic disorders do not have any effective treatment and may lead to death or lifelong disability. These types of results can be incidentally picked up during the research study. In whole exome sequencing the chance of finding an unexpected variant has been estimated to be three in every 100 tests performed.

**11. Can I opt out from receiving the secondary findings?**

Yes. The findings that are related to the disease/condition that is being tested for will be reported. You will have an option to choose not to receive (or receive) the information while signing the consent form about the secondary findings that are not related to the condition that is being tested for.

**12. Could there be results that affect others in my family?**

With any genetic test, there could be results that affect your blood relatives. For example, your condition may be one that could be inherited, and this might then be of importance to your children, brothers and sisters or parents. If this is the case, your health professional will explain this.

**13. Do I have to take part in this study?**

If you decide, now or at a later stage, that you do not wish to participate in this research project, that is entirely your right and will not in any way prejudice any present or future treatment.

**14. Who do I speak to if problems arise?**

If you have any complaints about the way in which this research project has been, or is being conducted, please, in the first instance, discuss them with the research team.

Thank you for your help and cooperation

Dr Dinesh Giri
Clinical Research Fellow in Paediatric Endocrinology
Alder Hey Children's Hospital & Institute of Child Health, University of Liverpool
Eaton Road
Liverpool L12 2AP. Email:Dinesh.Giri@alderhey.nhs.uk

# PATIENT INFORMATION SHEET FOR CHILDREN AGED UPTO 8 YEARS

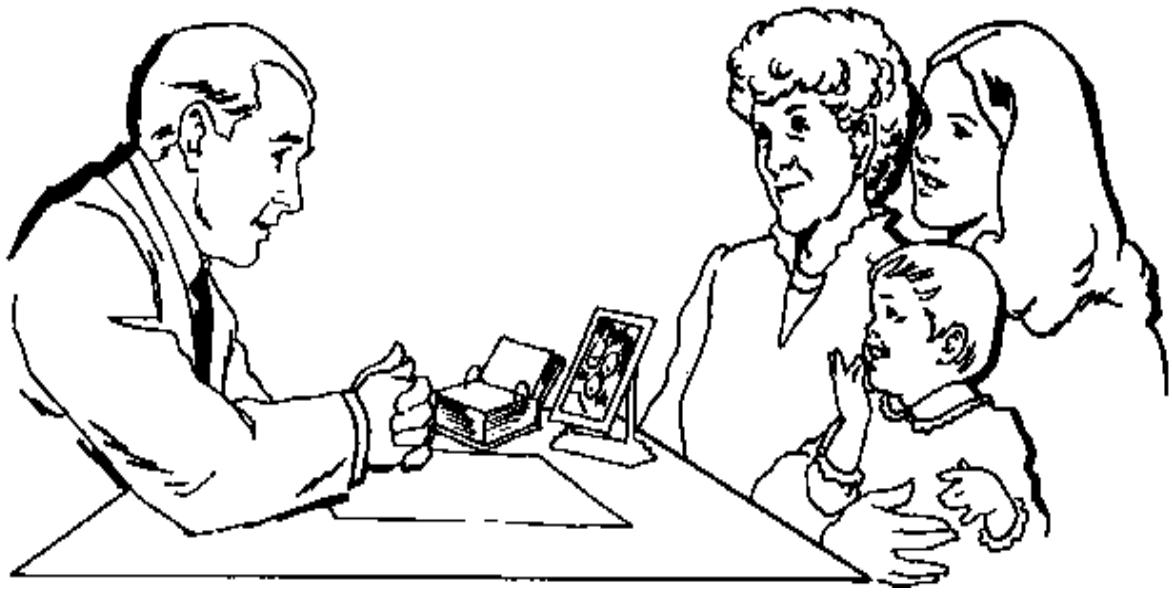

*Version 2.0, 15.10.2015*

***Whole Exome Sequencing in rare Endocrine Disorders***

## We would like you to read this with your mum or dad. The doctors can also help you.

## You are invited to join a research study. Ask your mum and dad or the doctors if you have any questions.

### What is a research study?

Research studies help us learn new things. We can test new ideas. By doing research we try to find an answer to a scientific question.

## Why are we doing this research?

Genes are information passed on by your Mum and Dad. They decide everything about you and how your body works. Genes tell our bodies how to keep us healthy. But sometimes things go wrong and people may develop a problem that can make them become ill. Imagine, you are baking a cake and following the instructions from the recipe book. The genes are like the instructions in the recipe book. If you put the wrong thing in the cake then it doesn't turn out how you expected. Similarly, if there is something wrong in the genes and if the genes do not work properly, then it may cause people to become ill. This research is to try and find out if there is anything wrong in the way the genes work.

This is how the genes look like.

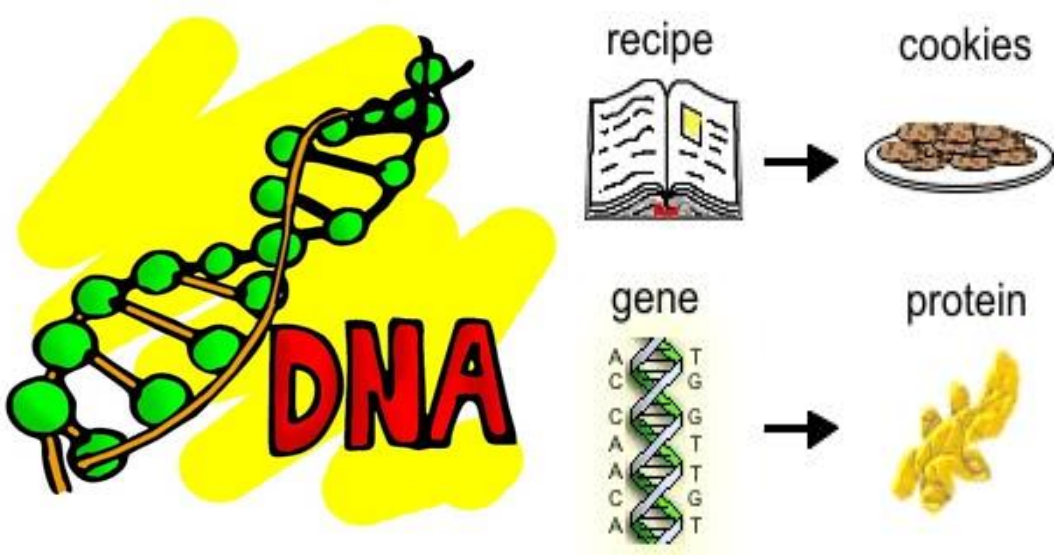


## Why me?

Hormones are special chemicals your body makes to help it do certain things - like growing up. They are important and keep us healthy and strong. We are doing this research to find out more about your hormone problem and to see if it the problem is caused by some of your genes that don't work right.

## What would happen if I join this research?

If you decide to be in the research, we will need to take a small amount of your blood. We will try to get blood at the same time when you are having blood test in the clinic. If we cannot do this we will ask your permission to take a separate blood test, for this we will put special cream on to numb the skin beforehand.
We will look at your past doctor visits and use information about your care.

### What will you do with my blood?

There are very small building blocks in your body called cells. The cells are so small you can't even see them. We will get some of your cells out of your blood. We need to get your body's recipe out of your cells. Then we need to look at what it tells your body to do.

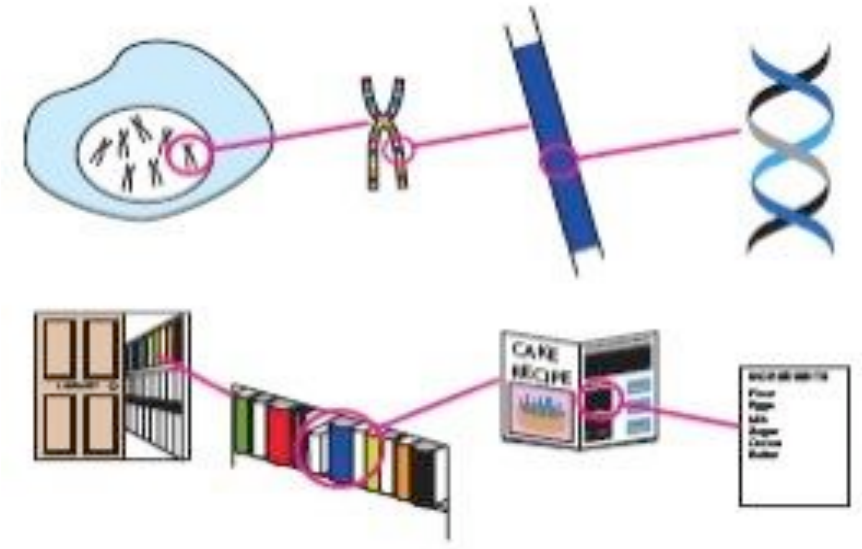

## What other things can happen if i want to join the study?

If we have to take a separate blood test, this will hurt a little, but we will put numbing cream on first. Sometimes the needle can leave a bruise on the skin.

You can say 'no' to what we ask you to do for the research at any time and we will stop.

## Could the research help me?

This research may not help you immediately. We do hope to learn something from this research though. And someday we hope it will help other kids who have similar problems like you do.

## What else should I know about this research?

If you don't want to be in the study, you don't have to be. It is also OK to say yes and change your mind later. You can stop being in the research at any time. If you want to stop, please tell the research doctors. We will still take good care of you no matter what you decide.


# Thank You for reading this. Please ask any questions.

Alder Hey Children's NHS Foundation Trust

UNIVERSITY OF LIVERPOOL

# PATIENT INFORMATION SHEET FOR CHILDREN AGED 9-12 YEARS

## This paper talks about our research. Please ask us any questions that you have.

*Version 2.0, 15.10.2015*

## What is a research study?

Research studies help us learn new things. We can test new ideas. First, we ask a question. Then we try to find the answer.

.

## Why are we doing this research?

Genes are information passed on by your Mum and Dad. They decide everything about you and how your body works. There are over 30,000 genes on each chromosome which act as special carrier for your genes. They are tightly packed inside the cells which are body's building blocks. They are so small that you can only see them under a microscope. The genes give out instructions to the body that tells it to work properly. The instructions are also called as proteins. Sometimes, faulty instructions can cause problems. We are doing this research to find out more about your hormone problem and to see if it the problem is caused by some of your genes that don't work right.

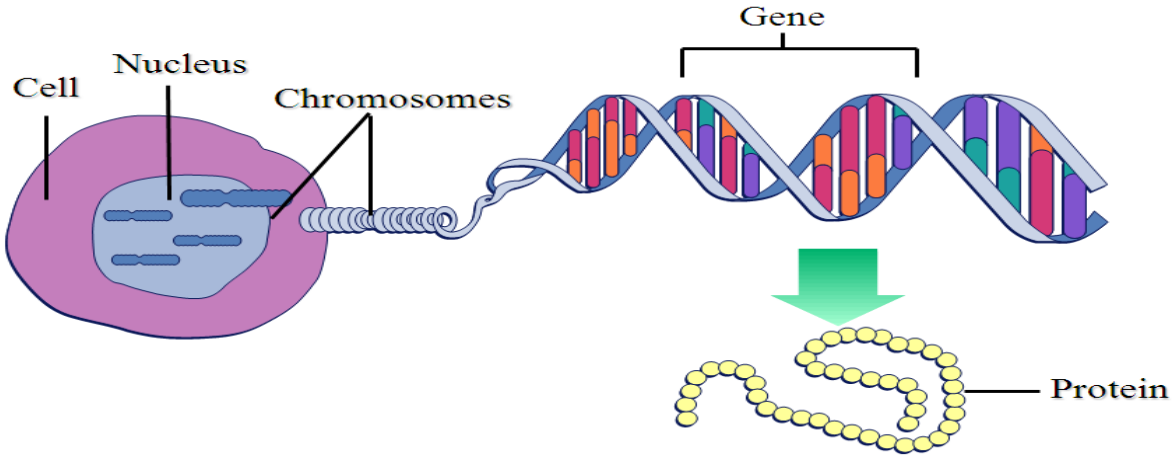

**Why have I been asked to take part?**
As you may know, that you are seeing your Doctor in the hospital because you have hormone problem. Hormones are special chemicals your body makes to help it do certain things - like growing up. They are important and keep us healthy and strong. There are different hormones in our body, each of which has a specific role of action. We are doing this research to find out more about your hormone problem and to see if it the problem is caused by some of your genes that don't work right.

**What would happen if I join this research?**
If you decide to be in the research, we will ask you to do the following:

- Blood test: We will try to get blood at the same time when you are having blood test in the clinic without a new needle. If we cannot do this we will ask your permission to take a separate blood test, for this we will put special cream on to numb the skin beforehand.
- Medical records: We will look at your past doctor visits and use information about your care.

**Are there any risks if join the study?**
No. The needle used to test your blood can hurt. Sometimes the needle can leave a bruise on the skin. We can put a cream on your skin before we take blood. This cream would help so it won't hurt as much.

You can say 'no' to what we ask you to do for the research at any time and we will stop.

**Could the research help me?**

This research may not help you immediately. We do hope to learn something from this research though. And someday we hope it will help other kids who have similar problems like you do.

**What else should I know about this research?**

If you don't want to be in the study, you don't have to be.
It is also OK to say yes and change your mind later. You can stop being in the research at any time. If you want to stop, please tell the research doctors.


**Thank You for reading this. Please ask us if you have any questions.**

.

Alder Hey Children's NHS Foundation Trust

UNIVERSITY OF LIVERPOOL

# PATIENT INFORMATION SHEET FOR YOUNG PEOPLE AGED 13-15 YEARS

## You are invited to join a research project. Ask your mum and dad or the doctors if you have any questions.

### Why have I been asked to take part?

Hormones are special chemicals your body makes to help it do certain things - like growing up. They are important and keep us healthy and strong. There are different hormones in our body, each of which has a specific role of action. We are doing this research to find out more about your hormone problem and to see if it the problem is caused by some of your genes that don't work right.

### Why are we doing this research?

Genes are information passed on by your Mum and Dad. They decide everything about you and how your body works. So, if you have a genetic problem, it might be because certain genes don't work properly. There are over 30,000 genes on each chromosome which act as special carrier for your genes. Genes are made of DNA. DNA contains four chemicals (adenine, thymine, cytosine, and guanine — called A, T, C, and G for short) and different patterns of A, T, G, and C code for the instructions for making things your body needs to function (like the enzymes to digest food or the specific action of a particular hormone).Imagine, if there is a problem in giving a right instruction code(like a spelling mistake in the DNA) then it may result in a particular problem or illness. We are doing this research to find out if there is a genetic reason for the hormonal problem.

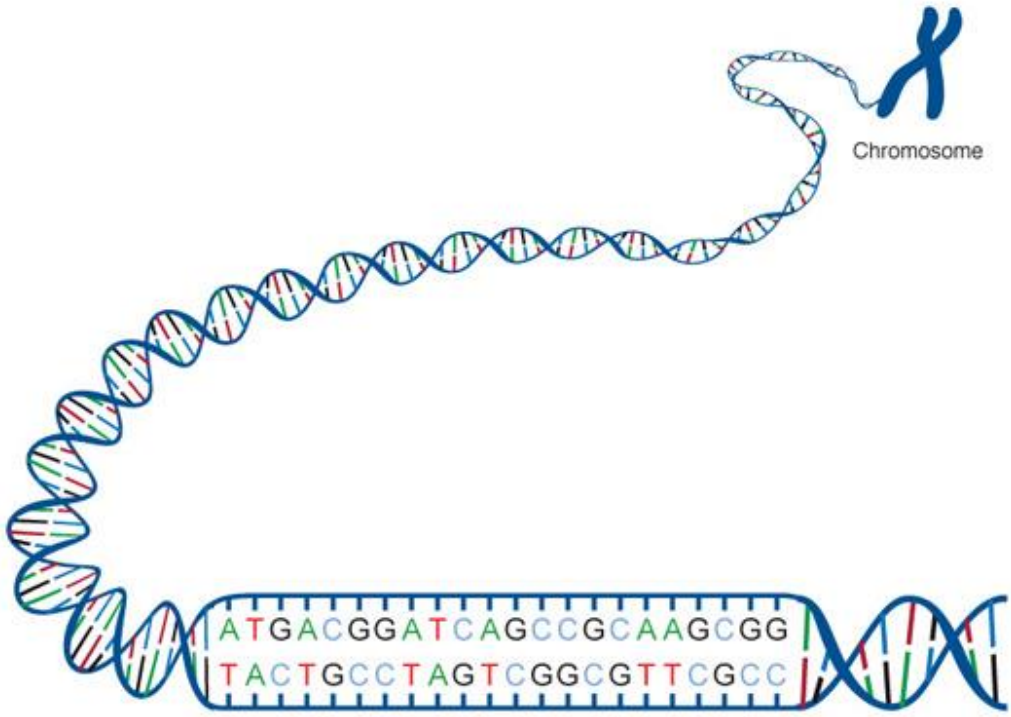


**What would happen if I join this research?**

If you decide to be in the research, we will need to take a small amount of your blood (about one teaspoon). We will try to get blood at the same time when you are having blood test in the clinic
We will look at your health records and use information about your care.

**What will you do with my blood?**

We will use your blood sample to get DNA from your cells and also to run tests to find out if there are any problems in the instructions code(sequence) of the DNA that make up your genes.

**Could the research help me?**

This research may not help you immediately. We do hope to learn something from this research though. And someday we hope it will help other kids who have similar problems like you do.

**Do I have to take part?**

If you and your parents talk about it and together you decide not to take part, that's OK. If there are things that you are worried about it, talk to the research team about how you feel. Tell your parents and the doctors and nurses if you don't want to join. It's OK if you decide to be in the Project and then change your mind.

**Is there any risk involved?**

No risk is involved. The needle used to test your blood can hurt. Sometimes the needle can leave a bruise on the skin. We can put a numbing cream on your skin before we take blood. This cream would help so it won't hurt as much. You can say 'no' to what we ask you to do for the research at any time and we will stop.

**What else should I know about this research?**

If you don't want to be in the study, you don't have to be. It is also OK to say yes and change your mind later. You can stop being in the research at any time. If you want to stop, please tell the research doctors. If you stop taking part, won't be affected.

## Thank You for reading this. Please ask if you have any questions.

**PATIENT/PARTICIPANT CONSENT FORM**

Title of Project: Whole Exome Sequencing in rare Endocrine disorders.
Research Team:
Dr Senthil Senniappan, Consultant Paediatric Endocrinologist & Honorary Senior Lecturer &
Dr Dinesh Giri, Clinical Research Fellow, Paediatric Endocrinology

Please tick the boxes as appropriate

I have read and understood the Information Sheet for parents of participating children dated __ /__ /__ (version__). I have had the opportunity to consider this information, ask questions and I have had these answered satisfactorily. ☐

I understand that my child's participation in this study is my decision and that I am free to withdraw at any time without giving any reason. If I do withdraw consent now or later, I don't need to give any reason and my child's present or future medical care or legal rights will not be affected. ☐

I understand that sections of any of my child's medical notes may be looked at by research team, where it is relevant to my child taking part in research. I give permission for these individuals to have access to the records ☐

I understand information on my child will be stored on a computer database for the purposes of research only. I give permission for information to be stored on the database ☐

I understand that this research project will involve collecting blood sample from my child. I agree for the blood sample to be collected from my child for this purpose. ☐

I understand that it is not possible to guarantee that any genetic results of significance for my child will be found through this project and I also understand that the results may not be able to provide a clinical diagnosis. ☐

I agree for my child's blood samples to be stored at the end of this project for future research after obtaining further informed consent. ☐

Secondary Findings

I choose to receive results about genetic disorders that that are not related to my or my child's current signs and symptoms. ☐

I choose not to receive results about genetic disorders that are not related to my or my child's current signs and symptoms. I understand that I will not have access to these results later ☐

Name of the Child Date of Birth

Name of Patient/Parent Date Signature

Name of Person taking Consent Date Signature

**PARENT CONSENT FORM**

Title of Project: Whole Exome Sequencing in rare Endocrine disorders.
Research Team:
Dr Senthil Senniappan, Consultant Paediatric Endocrinologist & Honorary Senior Lecturer &
Dr Dinesh Giri, Clinical Research Fellow, Paediatric Endocrinology

Please tick the boxes as appropriate

I have read and understood the Information Sheet for parents of participating children dated __ /__ /__ (version__). I have had the opportunity to consider this information, ask questions and I have had these answered satisfactorily. ☐

I understand that my participation in this study is my decision and that I am free to withdraw at any time without giving any reason. If I do withdraw consent now or later, I don't need to give any reason and my present or future medical care or legal rights will not be affected. ☐

I agree to give a sample of blood for the purpose of this research study. ☐

I understand that samples, DNA sequence, and information from my health records from hospital/GP and any other information will be looked into by research team. ☐

I understand that by giving my blood sample, my DNA sequence will be compared to that of my affected child's DNA sequence. ☐

I understand my health information will be stored on a computer database for the purposes of research only. I give permission for information to be stored on the database ☐

Name of Parent Date

Signature

Relationship to the child: Mum/Dad

Name of the Child Date of Birth

Name of Person taking Consent Date

Signature

## LIST OF PUBLICATIONS

- **D.Giri**, M.L.Vignola, A.Gualtieri, V.Scagliotti, P.McNamara, M.Peak, M.Didi, C.Gaston-Massuet, S.Senniappan. Novel *FOXA2* Mutation causes Hyperinsulinism, Hypopituitarism with Craniofacial and Endoderm-Derived Organ Abnormalities. **In Press-Human Molecular Genetics, 2017.**

- **D.Giri**, D.Rigden, M.Didi, M.Peak, P.McNamara, S.Senniappan. Novel compound heterozygous *ASXL3* mutation causing Bainbridge-Ropers like syndrome and primary IGF1 deficiency. Int J Pediatr Endocrinol. 2017; 2017:8.

- **D.Giri**, D.Pintus, G.Burnside, A.Ghatak, F.Mehta, P.Paul, S.Senniappan-Treating Vitamin D deficiency in Children with Type I Diabetes could improve their Glycaemic Control-In Press: BMC Research Notes, 2017

- **D.Giri**, R.Jayaram, S.Senniappan.Hypothyroidism and subcutaneous calcifications-Is there a missing link?.- Arch Dis Child Educ Pract Ed edpract-2016-311834

- D.Dayal, **D.Giri**, S.Senniappan. A Rare Association of Central Hypothyroidism and Adrenal Deficiency in a boy with Williams-Beuren syndrome- Ann Pediatr Endocrinol Metab. 2017; 22(1): 65–67

- **D.Giri**, H.Alsaffar, R.Ramakrishnan. Acanthosis nigricans and its response to metformin. Pediatr Dermatol. 2017 Jul 30. doi: 10.1111/pde.13206. [Epub ahead of print]

- **D.Giri**,J.Blair,P.Dharmaraj,R.Ramakrishnan,U.Das,M.Didi,S.Senniappan.Test osterone improves the first year height velocity in adolescent boys with constitutional delay of growth and puberty. Int J Endocrinol Metab. 2017 ;15(2): e42311.

- **Giri D**, Roncaroli F, A.Sinha, M.Didi, S.Senniappan. Silent Crooke's Cell Corticotroph Adenoma of the Pituitary Gland Presenting as Delayed Puberty. Endocrinology Diabetes Metab Case Rep.2017.pili:16-0153

- **Giri D**, P. Patil, R.Hart, M.Didi, S.Senniappan. Congenital Hyperinsulinism and Poland syndrome in association with gene duplication in 10p13-14. Endocrinology Diabetes Metab Case Rep 03 2017, EDM160125, 10.1530/EDM-16-0125.

- **Giri D**, Price V, Yung Z, Didi M, Senniappan S. Fluoxetine-Induced Hypoglycaemia in a Patient with Congenital Hyperinsulinism on Lanreotide Therapy. J Clin Res Pediatr Endocrinol. 2016;8(3):347-50

- Ozsu E, **Giri D**, Seymen Karabulut G, Senniappan. Successful transition to sulfonylurea therapy in two Iraqi siblings with neonatal diabetes mellitus and iDEND syndrome due to ABCC8 mutation. J Pediatr Endocrinol Metab. 2016 ;29(12):1403-1406

- **D.Giri**, R.Hart, I.Ellis, R.Ramakrishnan. An Unusual case of Hereditary Nephrogenic Diabetes Insipidus (HNDI) affecting mother and daughter J Pediatr Endocrinol Metab. 2016 Jan 1;29(1):93-6.

- **D.Giri**, V.Mckay, A.Weber, J.Blair. Multiple endocrine neoplasia syndromes 1 and 2: manifestations and management in childhood and adolescence. Arch Dis Child 2015; 100:994-999

- **D.Giri**, V.McKay, S.Avula, M.Didi, S.Senniappan. Congenital Hyperinsulinism and cochlear hypoplasia in a rare case of Pallister Hall Syndrome. Int J Clin Pediatr. 2015;4(2-3):154-157

- C.Ponmani, **D.Giri**, K.Hussain, S.Senniappan. 13q deletion in a girl contributing to antenatal stroke, insulin resistance and lymphedema precox: expanding the clinical spectrum. J Med Cases. 2015;6(6):264-267

- **D.Giri**, R.Ramakrishnan, J.Hayden, L.Brook, U.Das, M.Zulf Mughal, P.Selby, P.Dharmaraj, S.Senniappan. Denosumab Therapy for Refractory Hypercalcemia secondary to squamous cell carcinoma of skin in Epidermolysis Bullosa. World J Oncol. 2015;6(2):345-348

- **Giri D**, Rath S, Babarao S. Hypothalamic pituitary axis dysfunction in a neonate with severe Hypoxic-ischemic encephalopathy. J Clin Neonatol 2016;5: 61-3

- Balasubramanian S, Suresh N, Ravichandran C, **Dinesh Chand GH**.Reference values for oxygen saturation by pulse oximetry in healthy children at sea level in Chennai. Ann Trop Paediatr. 2006 Jun;26(2):95-9.

ACCEPTED MANUSCRIPT

# Novel *FOXA2* Mutation Causes Hyperinsulinism, Hypopitutarism with Craniofacial and Endoderm-Derived Organ Abnormalities

Dinesh Giri, Maria Lillina Vignola, Angelica Gualtieri, Valeria Scagliotti, Paul McNamara, Matthew Peak, Mohammed Didi, Carles Gaston-Massuet, Senthil Senniappan ✉

*Human Molecular Genetics*, ddx318, https://doi.org/10.1093/hmg/ddx318
**Published:** 24 August 2017 **Article history** ▾

## Abstract

Congenital hypopituitarism(CH) is characterised by the deficiency of one or more pituitary hormones and can present alone or in association with complex disorders. Congenital hyperinsulinism(CHI) is a disorder of unregulated insulin secretion despite hypoglycemia that can occur in isolation or as part of a wider syndrome. Molecular diagnosis is unknown in many cases of CH and CHI. The underlying genetic etiology causing the complex phenotype of CH and CHI is unknown. In this study, we identified a *de novo* heterozygous mutation in the developmental transcription factor, forkhead box A2, *FOXA2* (c.505T>C,p.S169P) in a child with CHI and CH with craniofacial dysmorphic features, choroidal coloboma and endoderm-derived organ malformations in liver, lung and gastrointestinal tract by whole exome sequencing. The mutation is at a highly conserved residue within the DNA binding domain. We demonstrated strong expression of *Foxa2* mRNA in the developing hypothalamus, pituitary, pancreas, lungs and oesophagus of mouse embryos using *in situ* hybridization. Expression profiling on human embryos by immunohistochemistry showed strong expression of hFOXA2 in the neural tube, third ventricle, diencephalon and pancreas. Transient transfection of HEK293T cells with Wt(Wild type) hFOXA2 or mutant hFOXA2 showed an impairment in transcriptional reporter activity by the mutant hFOXA2. Further analyses using western blot assays showed that the *FOXA2* p.(S169P) variant is pathogenic resulting in lower expression levels when compared with Wt hFOXA2. Our results show, for the first time, the causative role of *FOXA2* in a complex congenital syndrome with hypopituitarism, hyperinsulinism and endoderm-derived organ abnormalities.

10th INTERNATIONAL MEETING OF PEDIATRIC ENDOCRINOLOGY
SEPTEMBER 14-17 2017
WASHINGTON D.C.

**Abstract 933: CALCIUM/CALMODULIN DEPENDENT PROTEIN KINASE 2 (CAMKK2) MUTATION – A NOVEL GENETIC CAUSE OF CONGENITAL HYPERINSULINISM**

**Primary Topic:** Fetal and Neonatal Endocrinology and Metabolism, including Hypoglycemia

## CALCIUM/CALMODULIN DEPENDENT PROTEIN KINASE 2 (CAMKK2) MUTATION – A NOVEL GENETIC CAUSE OF CONGENITAL HYPERINSULINISM

Dinesh Giri, FRCPCH, University of Liverpool & Alder Hey Children's NHS Foundation Trust, Liverpool, United Kingdom; John W Scott, PhD, University of Melbourne, Melbourne, Australia; Bruce E Kemp, PhD, Australian Catholic University, Melbourne, Australia; Anthony R Means, PhD, Baylor College of Medicine, Houston, TX, United States; Senthil Senniappan, PhD, University of Liverpool & Alder Hey Children's NHS Foundation Trust, Liverpool, United Kingdom

### Objectives

$Ca^{2+}$/calmodulin-dependent protein kinase 2 (CaMKK2) belongs to the Serine/Threonine protein kinase family and alternative splicing results in multiple transcripts encoding distinct isoforms. CaMKK2 mRNA has been shown to express in mouse pancreatic islets and loss of CaMKK2 increases the glucose mediated insulin secretion. We report, for the first time, CaMKK2 mutation as a novel genetic cause of congenital hyperinsulinism (CHI).

### Methods

A Caucasian child born to non-consanguineous parents at 33 weeks gestation presented with hypoglycaemic seizures at 7 months of age requiring intravenous glucose load up to 15mg/kg/min. The investigations confirmed CHI [plasma insulin concentration of 37pmol/L and supressed β hydroxy butyrate (<100mmol/L) during hypoglycaemia]. No mutation was identified in ABCC8, KCNJ11 or GCK. The 18-Fluro-DOPA PET CT scan suggested diffuse CHI and the patient responded well to diazoxide therapy. At the age of 5 years, the patient requires 10mg/kg/day of diazoxide and has features of developmental and speech delay.

### Results

Whole exome sequencing was performed on the genomic DNA of the patient and the biological parents. A de novo heterozygous frameshift mutation (p.G539fs*4) was found at the terminal exon (exon 16) of CaMKK2 (NM_001270486.1) (isoform-7). CaMKK2 isoform-7 (WT) and the pG539fs*4 mutant were expressed in COS7 cells and the pG539fs*4 mutant was noted to have significantly higher basal and $Ca^{2+}$-CaM dependent kinase activity compared with WT isoform-7. Both isoform-7 and the pG539fs*4 mutant have elevated basal activity compared with isoform-1, the major CaMKK2 isoform expressed in most tissues.

### Conclusions

We describe for the first time, CaMKK2 mutation as a novel genetic cause of persistent CHI. The potential mechanism is likely to involve alteration in the AMPK (substrate for CaMKK2) regulated insulin secretion driven specifically by isoform 7. This has wider implications in understanding the molecular genetic aetiology of CHI as well as monogenic diabetes mellitus.

10th INTERNATIONAL MEETING OF PEDIATRIC ENDOCRINOLOGY
SEPTEMBER 14-17 2017
WASHINGTON D.C.

**Abstract 879: A NOVEL DENOVO FORKHEAD BOX A2 (FOXA2) MUTATION LEADS TO CONGENITAL HYPERINSULINISM, CRANIOFACIAL DYSMORPHIC FEATURES AND CONGENITAL HYPOPITUITARISM**

**Primary Topic:** Neuroendocrinology including Hypothalmic Pituitary
**Secondary Topic:** Fetal and Neonatal Endocrinology and Metabolism, including Hypoglycemia

## A NOVEL DENOVO FORKHEAD BOX A2 (FOXA2) MUTATION LEADS TO CONGENITAL HYPERINSULINISM, CRANIOFACIAL DYSMORPHIC FEATURES AND CONGENITAL HYPOPITUITARISM

Dinesh Giri, FRCPCH, University of Liverpool & Alder Hey Children's NHS Foundation Trust, Liverpool, United Kingdom; Maria Lillina Vignola, MSc, Queen Mary University of London, London, United Kingdom; Angelica Gualtieri, MSc, Queen Mary University of London, London, United Kingdom; Valeria Scagliotti, MSc, Queen Mary University of London, London, United Kingdom; Mohammed Didi, MRCPCH, Alder Hey Children's NHS Foundation Trust, Liverpool, United Kingdom; Carles Gaston-Massuet, PhD, Barts & The London Medical School,Queen Mary University of London, London, United Kingdom; Senthil Senniappan, PhD, University of Liverpool & Alder Hey Children's NHS Foundation Trust, Liverpool, United Kingdom

**Objectives**

FOXA2, located at the at the cytogenetic location 20p11.21, has been shown to play a role in the pancreatic β-cell development. FOXA2 knockout mouse has been shown to exhibit severe hyperinsulinaemia. Genes at 20p11.21 have been implicated to have a potential role in the pituitary development.We show for the first time that a de novo mutation in the developmanetal transcription factor FOXA2 (formerly HNF3B) is associated with congenital hyperinsulinism (CHI) combined with hypopituitarism in humans.

**Methods**

A female baby born to non-consanguineous Caucasian parents at 42 weeks gestation with a birth weight of 4.185Kg (+1.72SDS) was noted to have high glucose requirement and a hypoglycaemia screen confirmed CHI. She also developed TSH,ACTH and GH deficiencies. Genetic analysis was negative for ABCC8, KCNJ11, HNF4A or GCK mutations. MRI brain showed a hypoplastic anterior pituitary, absent posterior pituitary, thin pituitary stalk and corpus callosum.18F-DOPA PET-CT suggested diffuse pancreatic lesion. She has solitary median maxillary incisor, congenital nasal pyriform aperture stenosis, pulmonary stenosis, choroidal coloboma and hepatic portal bridging fibrosis.

**Results**

Whole exome trio sequencing identified a novel de novo heterozygous mutation in FOXA2 (c.505T>C, p.(S169P) in the child. The identified variant is highly conserved, not present in control databases and predicted to be deleterious to the protein function. We have demonstrated strong expression of FOXA2 mRNA in the pituitary of mouse embryos by in situ hybridisation. Expression profiling on human embryos by immunohistochemistry, showed strong expression in the neural tube, third ventricle, diencephalon and in the pancreas. Transient transfection of HEK293T cells with Wt(Wild type) hFOXA2 or mutant hFOXA2 showed an impairment in transcriptional reporter activity by the mutant hFOXA2. Furhter biochemical analyses demonstrated that the c.505T>C, p.(S169P) variant is pathogenic resulting in lower expression levels when compared with Wt hFOXA2

**Conclusions**

We describe, for the first time, the expression of FOXA2 in human pituitary and pancreatic development and the disruptive effect of the mutation on the protein function thereby demonstrating FOXA2 as a novel candidate gene in humans with pituitary and pancreatic β-cell disorders.

10th INTERNATIONAL MEETING OF PEDIATRIC ENDOCRINOLOGY
SEPTEMBER 14-17 2017
WASHINGTON D.C.

**Abstract 854: NOVEL COMPOUND HETEROZYGOUS ASXL3 MUTATION CAUSING BAINBRIDGE-ROPERS LIKE SYNDROME AND PRIMARY IGF1 DEFICIENCY**

**Primary Topic:** Syndromes
**Secondary Topic:** Growth and GH/IGF Axis

## NOVEL COMPOUND HETEROZYGOUS ASXL3 MUTATION CAUSING BAINBRIDGE-ROPERS LIKE SYNDROME AND PRIMARY IGF1 DEFICIENCY

Dinesh Giri, FRCPCH, University of Liverpool & Alder Hey Children's NHS Foundation Trust, Liverpool, United Kingdom; Daniel Rigden, PhD, University of Liverpool, Liverpool, United Kingdom; Paul Mcnamara, PhD, University of Liverpool, Liverpool, United Kingdom; Matthew Peak, PhD, Alder Hey Children's NHS Foundation Trust, Liverpool, United Kingdom; Mohammed Didi, MRCPCH, Alder Hey Children's NHS Foundation Trust, Liverpool, United Kingdom; Senthil Senniappan, PhD, University of Liverpool & Alder Hey Children's NHS Foundation Trust, Liverpool, United Kingdom

**Objectives**

De novo truncating and splicing mutations in the additional sex combs-like 3 (ASXL3) are implicated in Bainbridge-Ropers syndrome (BRPS) characterised by severe developmental delay, short stature and characteristic facial features. We describe, for the first time, a patient with severe short stature secondary to IGF1 deficiency, learning difficulties, feeding difficulties and dysmorphic features with a novel compound heterozygous mutation in ASXL3.

**Methods**

A 7-year-old boy had severe short stature (-3.5 SDS), dysmorphic features [downward slanting of eyes, low set ears, short neck, hypoplastic toe nails, shortening of metacarpals and ring finger], severe learning difficulties, and speech delay. Peak growth hormone (GH) was 11.7µg/l to arginine stimulation and bone age was delayed by 3 years. The rest of the pituitary function was normal. IGF1 was persistently low at 4.9nmol/l (-3.1 SDS) with no increase on IGF1 generation test. A trial of high dose GH (50µg/kg/day) was ineffective and recombinant IGF1 therapy was commenced. CGH microarray did not reveal any copy number changes.

**Results**

Whole exome sequencing revealed two novel heterozygous ASXL3 mutations [p.(Arg989Gly), p.(Lys1026Asn)] in the patient, inherited from his unaffected mother and his unaffected father respectively. The missense mutations affect highly conserved amino acid residues across several species and in silico analysis predict the changes to be deleterious (SIFT), disease causing and probably damaging (MutationTaster, PolyPhen and SIFT) on protein function. Detailed bioinformatic analysis showed that the molecular defects caused by the mutations affect phosphorylation and interaction of ASXL3 with proteins regulating cell cycle, thus synergistically impacting on two points of the molecular interaction network of ASXL3.

**Conclusions**

ASXL3 is a putative Polycomb group (PcG) protein that is required to maintain the transcriptionally repressive state of homeotic genes throughout development. We hypothesise that ASXL3 potentially has a role in transcriptional activation of IGF1 in signalling pathways that regulate cell proliferation, which could potentially be contributing to short stature encountered in these patients.

**BSPED 2017: Accepted abstract**

# Novel Splicing Mutation in *B3GAT3* associated with Short Stature, GH deficiency, Hypoglycaemia, Developmental delay and Multiple Congenital Anomalies

*Samuel Bloor, Dinesh Giri, Mohammed Didi, Senthil Senniappan*

## Introduction

*B3GAT3*, encoding β-1,3-glucuronyltransferase 3, has an important role in proteoglycan biosynthesis. Homozygous *B3GAT3* mutations have been associated with short stature, skeletal deformities and congenital heart defects. We describe for the first time, a novel heterozygous splice site mutation in *B3GAT3* contributing to severe short stature, growth hormone (GH) deficiency, recurrent ketotic hypoglycaemia, facial dysmorphism and congenital heart defects.

## Patient and Methods

A female infant, born at 34 weeks gestation to non-consanguineous Caucasian parents with a birth weight of 1.9kg was noted to have cloacal abnormality, ventricular septal defect and pulmonary stenosis and congenital sensorineural deafness. She also had recurrent hypoglycaemic episodes and the results were consistent with severe ketotic hypoglycaemia. At 4 years of age, she was diagnosed with GH deficiency due to her short stature (height<2.5SD) and commenced on GH therapy. MRI of the pituitary gland revealed small anterior pituitary. She has multiple dysmorphic features: anteverted nares, small upturned nose, hypertelorism, slight frontal bossing, short proximal bones, hypermobile joints and down slanting palpebral fissures. There is a history of short stature and dysmorphism in father and a stillborn previous sibling with multiple dysmorphic features, congenital heart defects and short bones. Targeted exome sequencing of genes associated with ketogenesis, ketolysis, carbohydrate metabolism and fatty acid oxidation was negative for pathogenic mutations. Whole exome sequencing (WES) was performed on the genomic DNA from the patient but the DNA samples from biological parents were unavailable.

## Results

A heterozygous *B3GAT3* mutation (c.888+262T>G) in the invariant “GT” splice donor site was identified. This variant is considered to be pathogenic as it decreases the splicing efficiency in the mRNA as predicted by a MaxEntScan score decrease of 100% (from 11.01 to -0.14) thereby creating an alternative splice site resulting in a frame shift and truncation of the protein through misfolding.

## Conclusion

*B3GAT3* is involved in glycosaminoglycan (GAG) biosynthesis, which provides structural support within the extracellular matrix surrounding the cells. Genetic defects can thus lead to multi-system disorders. We report a novel splice site mutation in *B3GAT3* associated with short stature, GH deficiency and multiple congenital anomalies.

*Human Molecular Genetics*, 2017, Vol. 0, No. 0 1–12

**doi: 10.1093/hmg/ddx318**
Advance Access Publication Date: 24 August 2017
Original Article

ORIGINAL ARTICLE

# Novel *FOXA2* mutation causes Hyperinsulinism, Hypopituitarism with Craniofacial and Endoderm-derived organ abnormalities

Dinesh Giri[1,2], Maria Lillina Vignola[3], Angelica Gualtieri[3], Valeria Scagliotti[3], Paul McNamara[2], Matthew Peak[4], Mohammed Didi[1], Carles Gaston-Massuet[3] and Senthil Senniappan[1,2,*]

[1]Department of Paediatric Endocrinology, Alder Hey Children's Hospital NHS Foundation Trust, Liverpool, UK, [2]Department of Women and Children's Health, Institute in the Park, University of Liverpool, Liverpool L12 2AP, UK, [3]Centre for Endocrinology, William Harvey Research Institute, Barts & the London School of Medicine, Queen Mary University of London, John Vane Science Centre, Charterhouse Square, London EC1M 6BQ, UK and [4]NIHR Alder Hey Clinical Research Facility for Experimental Medicine, Alder Hey Children's NHS Foundation Trust, Liverpool, L12 2AP, UK

*To whom correspondence should be addressed at: Department of Paediatric Endocrinology, Alder Hey Children's Hospital NHS Trust, Eaton Road, Liverpool, UK. Tel: +441512525281; Fax: +441512824606; Email: senthilkss@yahoo.co.uk

## Abstract

Congenital hypopituitarism (CH) is characterized by the deficiency of one or more pituitary hormones and can present alone or in association with complex disorders. Congenital hyperinsulinism (CHI) is a disorder of unregulated insulin secretion despite hypoglycaemia that can occur in isolation or as part of a wider syndrome. Molecular diagnosis is unknown in many cases of CH and CHI. The underlying genetic etiology causing the complex phenotype of CH and CHI is unknown. In this study, we identified a *de novo* heterozygous mutation in the developmental transcription factor, forkhead box A2, *FOXA2* (c.505T>C, p.S169P) in a child with CHI and CH with craniofacial dysmorphic features, choroidal coloboma and endoderm-derived organ malformations in liver, lung and gastrointestinal tract by whole exome sequencing. The mutation is at a highly conserved residue within the DNA binding domain. We demonstrated strong expression of *Foxa2* mRNA in the developing hypothalamus, pituitary, pancreas, lungs and oesophagus of mouse embryos using *in situ* hybridization. Expression profiling on human embryos by immunohistochemistry showed strong expression of hFOXA2 in the neural tube, third ventricle, diencephalon and pancreas. Transient transfection of HEK293T cells with Wt (Wild type) hFOXA2 or mutant hFOXA2 showed an impairment in transcriptional reporter activity by the mutant hFOXA2. Further analyses using western blot assays showed that the *FOXA2* p.(S169P) variant is pathogenic resulting in lower expression levels when compared with Wt hFOXA2. Our results show, for the first time, the causative role of *FOXA2* in a complex congenital syndrome with hypopituitarism, hyperinsulinism and endoderm-derived organ abnormalities.

**Received:** June 19, 2017. **Revised:** July 31, 2017. **Accepted:** July 31, 2017

## Introduction

The pituitary gland is a master regulator of vital physiological functions such as growth, puberty, lactation, metabolism, stress response and reproduction. The development of the pituitary gland is tightly controlled by signalling molecules and transcription factors that dictate pituitary cell lineage specification, cell proliferation and terminal differentiation into hormone-producing cells (1,2). Abnormal pituitary development can lead to congenital hypopituitarism (CH) resulting in deficiency in one or more pituitary hormones. CH comprises of a spectrum of disorders with variable phenotypes that can range in severity, from isolated hormone deficiency [isolated growth hormone deficiency being the most common] to combined pituitary hormone deficiency (CPHD) when two or more pituitary hormones are deficient. CH may present as part of a syndrome with abnormalities in structures that share a common embryological origin with the pituitary gland, such as the forebrain and eyes, leading to septo-optic dysplasia (SOD) or holoprosencephaly (HPE) (1). SOD is a rare condition with a prevalence of 1:10 000 (3) live births and comprises the following features: optic nerve hypoplasia, midline forebrain defects and hypopituitarism (4,5). Mutations in transcription factors such as *HESX1* (6), *PROP1* (7), *POU1F1* (8), *LHX3* (9), *LHX4* (10), *PITX1, PITX2* (11), *OTX2* (12), *SOX2* (13) and *SOX3* (14,15) have been associated with CH in mouse and humans. However, these mutations account only for a small proportion of CH patients with the majority of patients having an unknown genetic cause for their symptoms.

Congenital hyperinsulinism (CHI) is a rare condition with an estimated prevalence of 1 in 50 000 live births, characterized by an inappropriate secretion of insulin from the β-cells of the pancreas during hypoglycemia (16). CHI is the most common cause of severe and persistent hypoglycaemia in the neonatal period. The identification and appropriate management of this condition is very important to avoid hypoglycaemic episodes and prevent the consequent neurological impairment. Mutations in genes *ABCC8* (17–21), *KCNJ11* (17–21), *GLUD1* (22), *GCK* (23), *HADH* (24), *UCP2* (25), *HNF4A* (26), *HNF1A* (26), *MCT1* (27), *HK1* (28) and *PGM1* (29) have been associated with genetic forms of CHI (30). However, the genetic cause for many CHI patients remains elusive.

*FOXA2* (formerly hepatocyte nuclear factor-3β, *HNF-3β*) belongs to the family of the forkhead class of transcription factors that has an essential role in embryogenesis during the formation of the node, notochord and floorplate (31,32), which are important for the development of the vertebrate body axis. Thus, *Foxa2* null mice embryos die during early gestation, at embryonic day 9.5, and fail to form axial mesoderm (31). Later during organogenesis, *Foxa2* co-operates with *Foxa1* and are required for the formation of endoderm-derived organs such as the liver (33), lung (34), pancreas (35) and gastrointestinal tract (36). *Foxa2* has been shown to be important in the development of anterior forebrain structures, which have the same embryonic origin as the pituitary gland (37). Data from murine genetic studies have shown a genetic interaction between *Foxa2* and Sonic Hedgehog (*Shh*) signalling pathway with overlapping expression pattern of *Foxa2* and *Shh* in the notochord and floor plate at e8.5. *Foxa2* can modulate *Shh* signalling, contributing to the specification of ventral motor neuron progenitor identity (38). The secretion of Shh by the notochord and floor plate is an important morphogenetic signal that is required for the development of central nervous system including the pituitary gland (39). In the islet cells of mature pancreas, *Foxa2* has been shown to activate components of insulin secretion, such as sulfonylurea receptor1 [sur1], (40) and the inward rectifier potassium channel member 6.2 [kir 6.2] (40). In humans, mutations in *ABCC8* [encoding SUR1] and *KCNJ11* [encoding Kir 6.2] (17–21) are the most common causes of genetic forms of CHI. Notably, tissue-specific deletion of *Foxa2* from the pancreatic β-cells (*Foxa2*$^{loxp/loxp}$; Ins:Cre) has been shown to the development of CHI in mouse (41).

Thus, *FOXA2* is an important developmental transcription factor required for the formation of ventral midline structures such as the floorplate and forebrain, as well as endoderm-derived organs including the pancreas, and regulating glucose homeostasis in mature pancreatic β-cells. To date, mutations in *FOXA2* causing disorders of glucose homeostasis, endoderm abnormalities and CH have not been described in humans. In this study, we report for the first time, a '*de novo*' heterozygous mutation in *FOXA2* in a patient with unique clinical phenotype of CH, persistent CHI, craniofacial dysmorphism, abnormalities in the liver, heart, lung and the gastrointestinal tract. This finding brings a new insight into the underlying molecular cause of a complex clinical phenotype that will serve as a tool to elucidate the pathogenesis of these congenital malformations and to better understand the development and function of the pituitary gland and the pancreas.

## Results

### Clinical findings

Our patient, a 5-year-old girl, was born to non-consanguineous Caucasian British parents at 42 weeks' gestation with a birth weight of 4.185 kg (+1.72 SDS). The pregnancy was normal and the 20-week antenatal scan showed polyhydramnios. The delivery was complicated by shoulder dystocia, needing resuscitation. She was found to be persistently hypoglycaemic (blood glucose < 2.5 mmol/l) requiring a total glucose load of 25 mg/kg/min (normal: 4–6 mg/kg/min) to maintain normoglycaemia (blood glucose > 3.5 mmol/l). She had low free thyroxine (FT4) (5.3 pmol/l) and suppressed thyroid-stimulating hormone (TSH) (<0.03 mu/l) that persisted even after the phase of acute severe illness. She also had an undetectable adrenocorticotropic hormone (ACTH) (<1.1 pmol/l) with no cortisol response to synacthen stimulation (peak cortisol to synacthen <50 nmol/l). Hydrocortisone replacement (10 mg/m$^2$/day) was commenced followed by levothyroxine therapy. The MRI scan of the brain showed a hypoplastic anterior pituitary, absent posterior pituitary, interrupted pituitary stalk and a thin corpus callosum (Fig. 1B). The hypoglycaemia persisted and further investigations showed an inappropriately high plasma insulin (200 pmol/l) and c-peptide (1500 pmol/l) with suppressed plasma free fatty acid (<100 μmol/l) and beta hydroxyl butyrate (<100 μmol/l) during hypoglycaemia (blood glucose: 1.2 mmol/l) confirming the diagnosis of CHI. The Growth hormone (GH) was undetectable at the time of hypoglycaemia [<0.05 μg/l]. A trial of diazoxide (5 mg/kg/day) was commenced along with chlorothiazide (7 mg/kg/day). However, the patient suffered from significant fluid retention leading to discontinuation of diazoxide. Commencement of octreotide (10 mcg/kg/day) caused a derangement of liver enzymes and therefore had to be discontinued after which the liver enzymes returned to normal levels. She developed significant feed intolerance due to severe gastroesophageal reflux which persisted despite maximum medical treatment. A gastro-jejonostomy tube was inserted to support feeding. Normoglycaemia was maintained by continuous feed via the gastro-jejonostomy tube. Genetic analysis was negative for *ABCC8*, *KCNJ11*, *HNF4A* and *GCK* mutations. The 18F-DOPA PET-CT scan of the pancreas suggested a diffuse uptake.

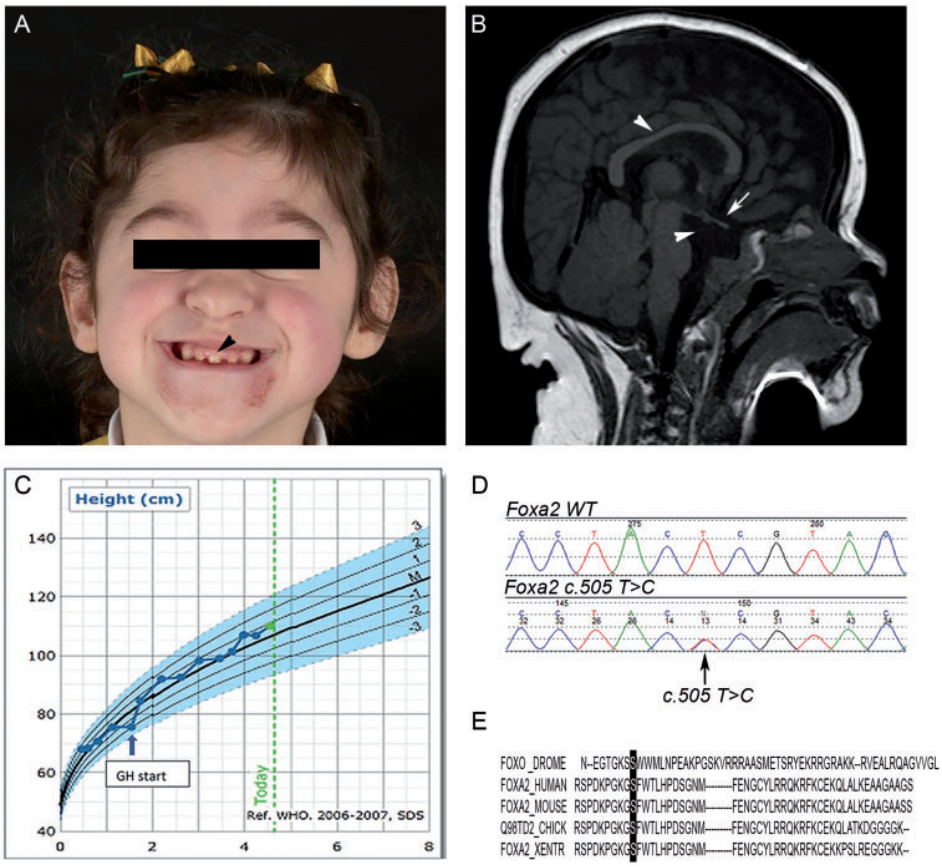


**Figure 1.** Picture of the patient's face showing single central incisor tooth (**A**, arrowhead). (**B**) Sagittal view of the MRI scan of the brain: The normal pituitary gland cannot be identified, the sella turcica is shallow and poorly defined with possibly a very hypoplastic anterior pituitary gland (arrowhead). Also, there is no evidence of the normal high signal of the posterior pituitary. There is a very short and thin pituitary stalk in its superior third (arrow) which is suggestive of an interrupted pituitary stalk. The corpus callosum is also noted to be thin (arrowhead). (**C**) The patient's linear growth curve compared with British contemporary references. Recombinant GH was started at 1.5 years of age when the linear height was -3SDS. A good response to GH treatment is seen subsequently with an improvement in the height SDS. (**D**) Electropherograms show the wild type (Wt FOXA2) and the presence of the missense mutation (thymine to cytosine) in the patient at the nucleotide position 505. (**E**) The evolutionary conservation of the amino acid residue serine at position 169 is shown across different species such as drosophila, human, mouse, chicken and frog. Abbreviations: standard deviation score, SDS; wild-type, Wt; growth hormone, GH; drosophila, DROME; frog, XENTR.

The facial dysmorphic features comprise of a single median maxillary central (SMMC) incisor (Fig. 1A), congenital nasal pyriform aperture stenosis (CNPAS), which was conservatively managed, and a left choroidal coloboma. She does not have any vision abnormalities. The cardiac echocardiogram revealed pulmonary stenosis which required balloon dilatation. She had a persistent oxygen requirement (0.5–1 l via nasal cannulae) of unknown etiology [negative for respiratory infections, normal chest imaging (CT) and bronchoscopy] from birth. At 1.5 years of age she was diagnosed with GH deficiency [height $<$ -3 SDS, IGF1 $<$ 3.3 nmol/l and a peak GH of 1.1 μg/l (normal $>$ 7 μg/l) to arginine stimulation] and was commenced on rGH (recombinant GH) therapy. She demonstrated a good response to treatment with rGH (25 mcg/kg/day) with an improvement in the height velocity (Fig. 1C). She developed persistently elevated liver transaminases when she was 3 years old, with a negative autoimmune hepatitis and infection screen. The liver biopsy showed dense chronic inflammation with portal-portal bridging fibrosis. The clinical features are summarized in Table 1.

She is currently 5 years old, with persistent CHI, motor, speech and developmental delay and continues to be on rGH, levothyroxine and hydrocortisone replacements. There are no symptoms suggestive of diabetes insipidus and the biochemistry has been completely normal. She has shown response to the reintroduction of diazoxide (5 mg/kg/day) and chlorothiazide without any features of fluid retention, which has enabled her to come off continuous feeds for 6 h.

## Mutation analysis

A novel heterozygous *FOXA2* mutation (c.505T>C, p.S169P) was identified in the affected child but not in the parents by whole exome sequencing. To further validate our results, the mutation was confirmed by Sanger sequencing (Fig. 1D). The variant is not present in control databases (ExAc, dbSNP, 1000 genome). Multiple sequence alignment shows that the serine residue at position 169 is highly conserved across different species, from drosophila, human, mouse, chicken to frog (Fig. 1E), suggesting that this residue is functionally important and has been maintained throughout evolution in different species. The *FOXA2* mutation (c.505T>C, p.S169P) lies at the DNA binding domain of the transcription factor. *In silico* analysis using SIFT, PolyPhen, Mutation Taster predict this aminoacid substitution to have deleterious impact on the protein function.

**Table 1.** Summary of clinical features

| | |
|---|---|
| Face | Single median maxillary central incisor, congenital nasal pyriform aperture stenosis |
| Eye | Left choroidal coloboma |
| Heart | Supra-valvular pulmonary stenosis |
| Gastrointestinal | Feed intolerance, severe gastro-esophageal reflux disease requiring gastro-jejonostomy feeding |
| Liver | Portal-portal bridging fibrosis, elevated transaminases |
| Lung | Persistent oxygen requirement of unknown etiology |
| Pancreas | Persistent form of hyperinsulinism |
| Pituitary | ACTH, GH and TSH deficiencies |
| | Thin pituitary stalk, hypoplastic anterior pituitary |
| | Thin corpus callosum |
| Neuro-developmental | Speech and motor developmental delay |

### Functional analysis

To further characterize the possible role of *FOXA2* in the observed clinical phenotype, we studied the expression of *Foxa2* at the mRNA level during mouse embryonic development. *Foxa2* mRNA transcripts were detected in the midbrain, ventral forebrain, ventral hindbrain, epithelial structures lining the main bronchus, lungs and the esophagus from embryonic day (e)11.5 (Fig. 2). Importantly, the expression of *Foxa2* mRNA was detected in the pituitary gland from e13.5 (Fig. 2C–C′) in the anterior lobe. From e15.5, *Foxa2* mRNA expression was stronger with robust expression in the ventral diencephalon, and anterior lobe of the pituitary gland (Fig. 2D–D′). At embryonic day e18.5, *Foxa2* mRNA transcripts were localized in the hypothalamic-pituitary axis, with transcripts strongly expressed in the ventral hypothalamus and anterior pituitary (Fig. 2E–E′). Analysis of hFOXA2 expression in human embryos by immunohistochemistry revealed expression of hFOXA2 in the ventral neural tube (Fig. 3A′) and in the diencephalon (Fig. 3A″) at six weeks (Carnegie stage 16), and around the third ventricle at 8 weeks (Carnegie stage 23) (Fig. 3B′). hFOXA2 was specifically localized in the cytoplasm of cells scattered in the pancreatic parenchyma at 13 weeks of gestation (Fig. 3C–C′–C″). In summary, our expression analysis shows expression of *Foxa2* mRNA in hypothalamic-pituitary axis and lungs during mice embryonic development. hFOXA2 expression was detected in midline neural tube and pancreas.

*FOXA2* has been previously shown to bind and activate the human glucose transporter type 2 (*GLUT2*) (42). To determine the pathogenic effect of *FOXA2* p.S169P variant, we performed transcriptional activation assays using the *GLUT2* promoter coupled to luciferase (phGT2-294-promoter-luc). We used transiently transfected HEK293T cells with equal quantities of Wt hFOXA2 or mutant hFOXA2 p.S169P and demonstrated that the hFOXA2 p.S169P significantly impairs the transcriptional activation of the *GLUT2* luciferase reporter (Fig. 4A). We also performed quantification of protein expression using western blot and showed that the mutant hFOXA2 p.S169P results in significantly reduced protein expression levels compared to the Wt hFOXA2 (Fig. 4B). Using double immunofluorescence on transiently transfected HEK293T cells, we demonstrated that both the Wt hFOXA2 and mutant hFOXA2 are expressed in the nucleus and the mutation did not result in changes to cellular localization (Fig. 5). Together the results indicate that the hFOXA2 p.S169P variant results in lower transcriptional activity due to an effect of the mutation on the FOXA2 protein levels.

## Discussion

We have characterized a '*de novo*' heterozygous mutation in the developmental transcription factor *FOXA2* that causes a rare and unique clinical phenotype of hypopituitarism, CHI, dysmorphic features, liver, pancreas, heart and gastrointestinal abnormalities. The c.505T>C, p.S169P genetic variant occurs at the conserved forkhead DNA binding domain of the *FOXA2*. This region binds to the DNA and may provide tissue-specific gene regulation important for the development of multiple organs. Our data has confirmed that the mutation impairs the transcriptional activation of *FOXA2*. Importantly, *FOXA2* is localized at the cytogenetic location 20p11.2 and some studies have linked chromosomal deletions within this region with the clinical phenotype of hypopituitarism, central nervous system (CNS) defects, hypoglycaemia, facial dysmorphic features and congenital abnormalities of the heart, liver and gastrointestinal tract (43–47). Chromosomal deletions of the 20p11.2 are rare (46) and recent studies have mapped the minimal critical region which contains 20 genes (43), including *FOXA2*. All the patients reported to have the 20p11.2 chromosomal deletion have hypopituitarism, CNS abnormalities and facial dysmorphic features as shared features, strongly indicating that a gene or multiple genes within this chromosome region have a key role in CNS, pituitary and facial development. We have identified the gene responsible for the clinical phenotype of hypopituitarism at the 20p11.2 region as *FOXA2* and confirmed the causative role with functional analysis.

In our study, we show that *FOXA2* mutation causes the clinical phenotype of hypopituitarism, CHI and facial dysmorphic features that overlaps with the clinical data published in patients with 20p11.2 deletions (43–47). The mutation in hFOXA2 p.S169P is pathogenic, as it results in impaired transcriptional activation of the phGT2-294-promoter-luc reporter and significant reduction in the protein expression compared to wild type hFOXA2. Interestingly, *FOXA2* has been shown to regulate key signalling pathways important in ventral midline, pituitary and CNS development such as *Shh* signaling (38). Data from *in vivo* studies using Wnt1:Cre; $Foxa2^{flox/flox}$ embryos showed that *Foxa2* has an early role in the initiation of Shh expression. *Foxa2*, in combination with *Foxa1*, downregulates the expression of intracellular transducers and downstream targets of *shh* signalling such as Ptch1, Gli1 and Gli2, which regulate the patterning of the ventral midbrain (38). Hence, we hypothesize that hFOXA2 could mediate its role in pituitary development by regulating Shh expression. Moreover, the midline anomalies in our patient including SMMC, CNPAS are often associated with pituitary abnormalities, as described in an extensive literature review by Lo *et al.* (48), where hypopituitarism or growth hormone deficiency were identified in 43–48% of patients with CNPAS or SMMC. This is consistent with the clinical presentation of our patient, who has hypopituitarism along with hypoplastic pituitary, thin corpus callosum and thin pituitary stalk on the MRI.

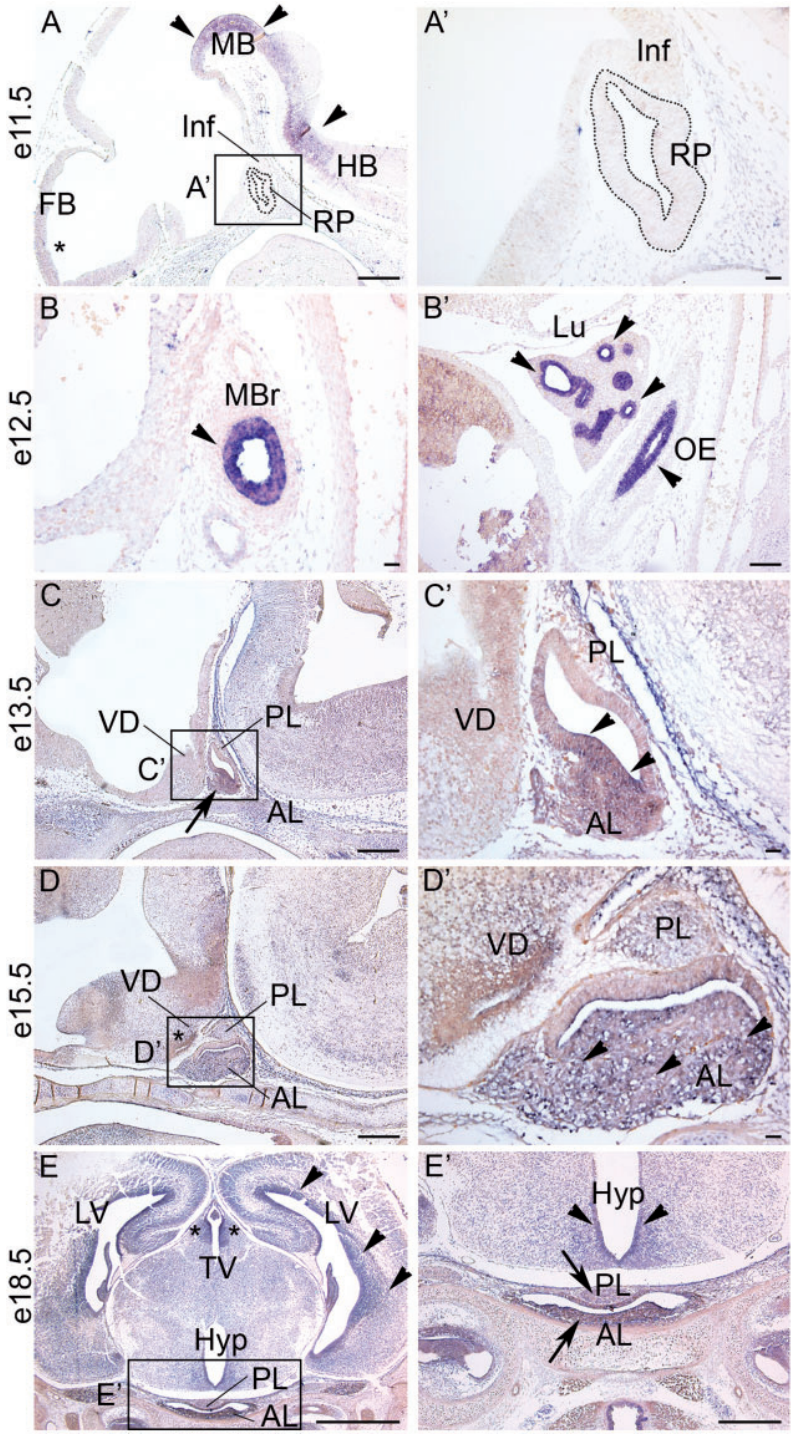


**Figure 2.** mRNA expression of *Foxa2* during mouse embryonic development. **A–D** represent sagittal sections, with anterior to the left side, and E is a coronal section. **A′**, **C′**, **D′**, **E′** show higher-magnification views of the boxed areas in A, C, D, E, respectively. At embryonic day e11.5 (A) *Foxa2* mRNA transcripts were expressed within the midbrain (MB) and ventral hindbrain (HB) (arrowheads) and also in a few cells localized in the forebrain (asterisk) (FB). At this stage of development no transcripts were detected in the primordium of the anterior pituitary gland, the Rathke's pouch (RP dotted line in A and A′), or in the infundibulum (Inf). A′ shows an enlarged image of the squared area in A, confirming undetectable expression of *Foxa2* at this stage in the RP and Inf. At e12.5 (B and **B′**) *Foxa2* mRNA transcripts were detected in the epithelial structures lining the main bronchus (MBr) (B, arrowhead) and in the epithelium lining the lung (Lu) and oesophagus (OE) (B′, arrowheads). By e13.5, expression of *Foxa2* appears localized in the ventral side of the anterior lobe of the developing pituitary gland (AL, arrow) with transcripts localized in the ventral marginal zone (arrowheads in C′). *Foxa2* mRNA expression become stronger at e15.5 (D) with robust expression in the ventral diencephalon (VD, asterisk), posterior lobe (PL) and anterior lobe (AL, arrowheads in D′) of the pituitary gland. At embryonic day e18.5 (**E**), expression was found widely spread in the central nervous system, with strong expression in the lumen surrounding the lateral ventricles (LV, arrowheads) and the third ventricle (TV, asterisks). Enlarged image of the boxed area in E shows mRNA expression localized in the hypothalamic area (Hyp) (E′, arroheads) with distinct pattern in the luminal area where the hypothalamic precursors

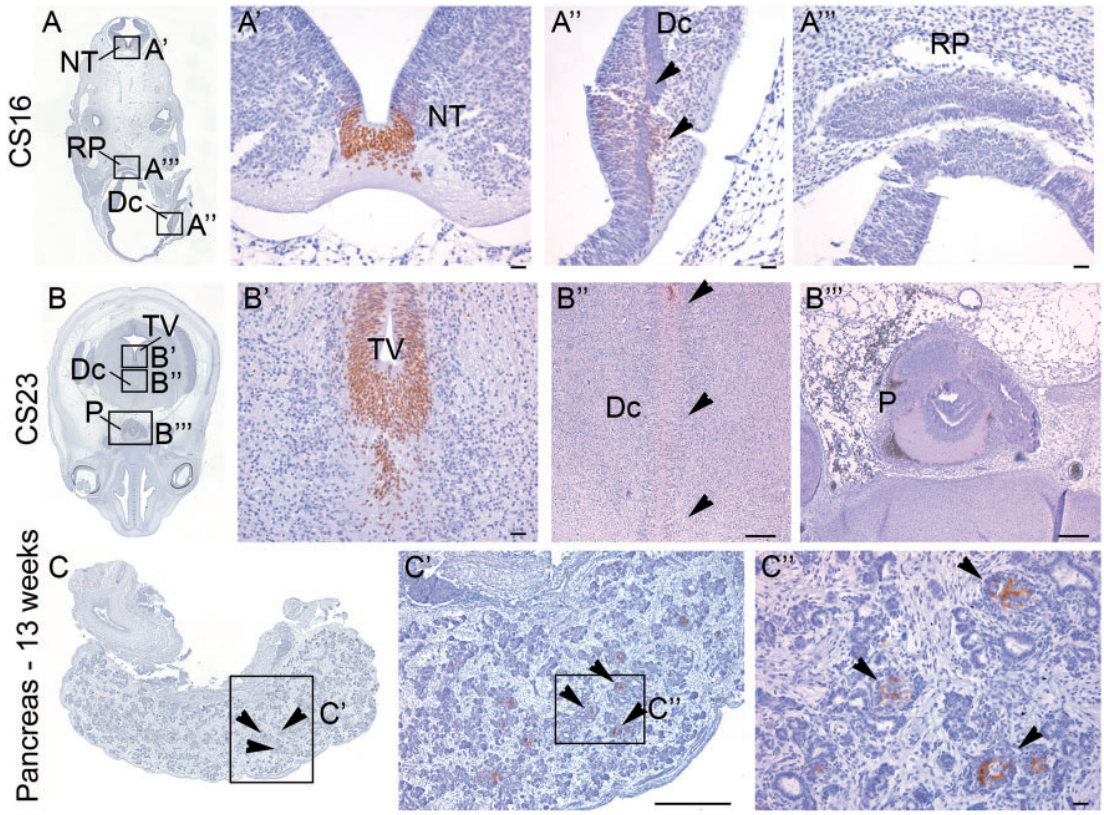


**Figure 3.** Immunohistochemical analysis of human FOXA2 expression during human embryonic development. **A–C** represent coronal sections of human embryos at 6 weeks (Carnegie stage 16), 8 weeks (Carnegie stage 23) and 13 weeks of gestation, respectively. **A′–C″** show higher-magnification views of the boxed areas in A, B, C, respectively. At 6 weeks of gestation (A) Foxa2 expression was observed in the developing neural tube (NT) (A′) and diencephalon (Dc) (arrowheads in A″). At 8 weeks of gestation (B) its expression was localized in the epithelium surrounding the third ventricle (TV) (B′) and in the cells lining the diencephalon (Dc) (arrowheads in B″). No expression of Foxa2 was detected in the primordium of the pituitary gland (Rathke's pouch, RP) at CS16 (A‴) nor in the developing pituitary gland at CS23 (B‴). In the pancreas at 13 weeks of gestation (C) Foxa2 was specifically localized in the cytoplasm of cells scattered in the pancreatic parenchyma (cells pointed by arrowheads in C′ and C″). Abbreviations: neural tube, NT; diencephalon, Dc; Rathke's pouch, RP; pituitary gland, P; third ventricle, TV. Scale bars represent: 50 μm (A′, A″, A‴, B′, C″); 100 μm (B″, B‴), 250 μm (C′).

The detection of *Foxa2* mRNA transcripts from the early stages of mouse pituitary and brain embryonic development suggests a potential role in the development of these structures. Furthermore, the detection of hFOXA2 by immunohistochemistry in human embryos at various developmental stages, along with the biochemical experiments demonstrating that the variant p.S169P mutation in *FOXA2* impairs transcriptional activation and protein expression levels, strongly indicate that *FOXA2* has a pivotal role in hypothalamic-pituitary axis formation in humans.

The co-existence of hypopituitarism along with a persistent form of hyperinsulinism, as encountered in our patient, is extremely uncommon. Hypoglycaemia in CHI is caused by unregulated insulin secretion while in hypopituitarism it is due to the lack of counter-regulatory hormonal response due to the deficiency of ACTH and GH. Diagnosis can often be challenging, as the hallmark of CHI is detectable insulin in the presence of hypoketotic hypoglycaemia while hypopituitarism causes ketotic hypoglycaemia. Almost half of the patients with persistent CHI do not have mutations in the already recognized genes known to cause CHI. Genetic diagnosis is important as it will inform the prognosis, recurrence risk and guide the medical management besides providing valuable insight into β-cell physiology. The negative mutations in the known CHI genes in our patient together with strong biochemical evidence of CHI, makes it highly likely that the CHI in our patient is due to a novel genetic aetiology (*FOXA2*). We have further confirmed this by demonstrating the expression of hFOXA2 in the developing human pancreas.

Glucose-stimulated insulin secretion occurs by the closure of ATP dependent KATP channels situated on the β-cell membrane with the resultant depolarization of the membrane causing the exocytosis of the insulin granules (16,30). KATP channels consist of 2 subunits, SUR1 and Kir6.2, encoded by *ABCC8* and *KCNJ11* respectively, the mutations of which cause defects in the channels resulting in the most common form of genetic CHI (16,30). Lantz *et al.* demonstrated that when SUR1 or Kir6.2 promoter/luciferase reporter was transfected with *Foxa2*

tanycytes reside (arrowheads in E′). mRNA transcripts were also localized in both the posterior (PL) and anterior (AL) lobes of the pituitary gland (arrows in E′). Abbreviations: midbrain, MB; hindbrain, HB; forebrain, FB; Rathke's pouch, RP; infundibulum, Inf; main bronchus, MBr; lung, Lu; oesophagus, OE; ventral diencephalon, VD; pituitary gland posterior lobe, PL; pituitary gland anterior lobe, AL; lateral ventricles, LV; third ventricle, TV; hypothalamus, Hyp. Scale bars represent: 50 μm (A′, B, C′, D′); 100 μm (B′), 250 μm (A, C, D, E′); 500 μm (E).

expression plasmids, *Foxa2*-Sur1 and *Foxa2*-Kir6.2 promoter constructs showed 6-fold and 4-fold activation respectively demonstrating a vital role of *Foxa2* in the transcriptional activation of the KATP subunits (40). Hence, a *FOXA2* mutation could potentially alter the expression of SUR1 and/or Kir6.2 leading to hyperinsulinism although the precise mechanism is yet to be explored. The other possible mechanism could be linked to *HADH* that encodes L-3-Hydroxyacyl-CoA-dehydrogenase (HADH), an enzyme involved in the penultimate step of the beta-oxidation pathway (8). Mutations in *HADH* cause CHI in humans. It has been demonstrated in mice that *Foxa2* directly targets *HADH* causing its transcriptional activation (49). Sund *et al.* demonstrated that *Foxa2* knocked out from the β-cells in mice resulted in a 3-fold downregulation of *Hadh* mRNA leading to severe hyperinsulinaemic hypoglycaemia (41,42). The third possibility could be linked to *GLUT2*, which is expressed in the plasma membrane of the pancreatic β-cells, liver, kidney and intestine to facilitate insulin secretion by transporting the glucose across the cell membrane (29). Wang *et al.* showed that *GLUT2* plays an important role in the insulin secretion from the β-cells as its mRNA level is influenced by the plasma concentrations of glucose and insulin (50). Cha *et al.* demonstrated that *GLUT2* has binding sites for *FOXA2* and showed that the promoter activity of *GLUT2* is synergistically activated by FOXA2 in NIH3T3 cells (42). *FOXA2* also plays a critical role in the tissue specific expression of GLUT2 (42). The reduction in the transcriptional activation of the *GLUT2* reporter (phGT2-294-promoter-luc) activity by the mutant hFOXA2 (p.S169P) shown in our transcriptional assay experiment, could imply that the GLUT2 tissue expression is reduced in the pancreatic β-cells of patients with *FOXA2* mutation. However, the precise mechanism by which this leads to hyperinsulinaemic hypoglycaemia is not yet understood.

It is also plausible that *Foxa2* plays a role in the development of the pancreas. *Foxa2* has been shown to regulate *Pdx1*, a homeobox gene essential for pancreatic development (49). *Foxa2* has also been linked to regulating the mRNA levels of pancreatic transcription factors such as *Hnf4a* and *Hnf1a*, mutations of which can cause monogenic forms of diabetes mellitus. However, some studies contradict that *Foxa2* is an upstream regulator of Pdx1, Hnf4a and Hnf1a (50). While it has been shown that β-cell-specific deletion of *Foxa2* in mice causes a phenotype of hypoglycaemia (41), it also has been demonstrated that it can cause downregulation of *Pdx1* mRNA causing the reduction of PDX-1 protein levels in the pancreatic islets (51) and a targeted β-cell-specific deletion of *Pdx1* results in diabetes in transgenic mice (52). Thus, *FOXA2* is a crucial transcription factor that controls the expression of multiple genes involved both in glucose sensing and glucose homeostasis and therefore has a potential role in diseases involving insulin secretion and glucose homeostasis.

Diazoxide is used as an effective treatment in majority of patients with CHI except in those with mutations abolishing the KATP channel activity (*ABCC8* or *KCNJ11*) or activating mutations in *GCK*. Our patient has shown response to diazoxide treatment which could potentially imply that the variant p.S169P has not completely abolished the KATP channel activity or increased the *GCK* expression.

Whilst it is difficult to speculate the progression of abnormalities in glucose homeostasis in patients with *FOXA2* mutation, screening more patients with similar phenotype will give further insights into the role of this transcription factor in the insulin secretion and in related diseases like neonatal diabetes mellitus and maturity onset diabetes of the young (MODY). The main limitation of our study is the lack of more patients with similar phenotype. As the combination of the phenotype comprising CHI and hypopituitarism is extremely rare, we were unable to recruit more patients for this study. However we are hopeful that the dissemination of the findings from this study will alert the researchers from across the world to screen for *FOXA2* mutations in patients with similar phenotype, thereby enabling a better understanding of genotype-phenotype correlations.

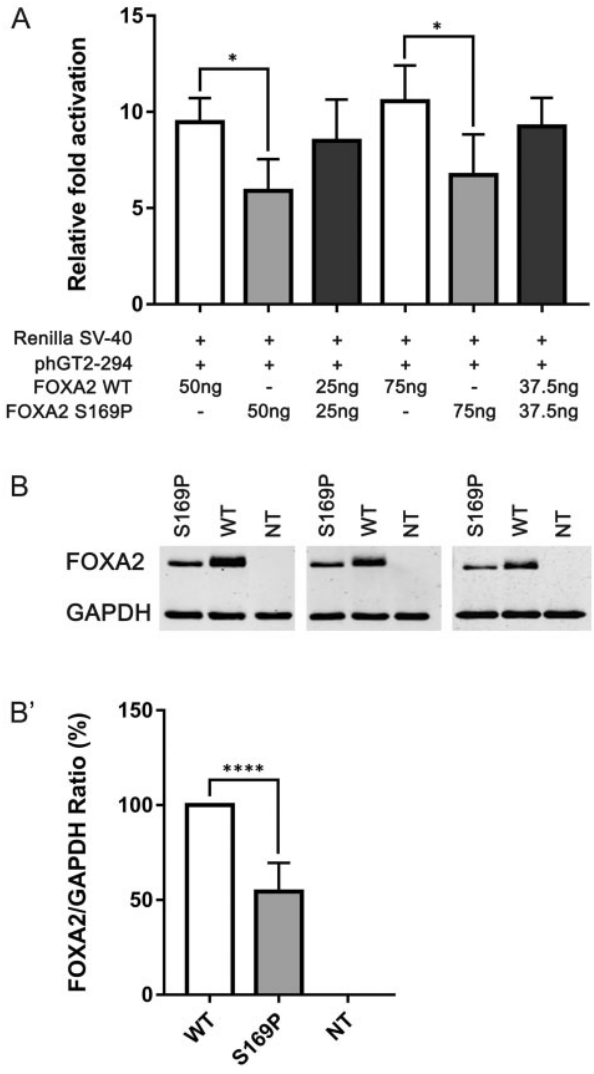


**Figure 4.** The serine to proline change in position 169 of hFOXA2 results in decreased protein expression levels leading to impairment of transcriptional activation of the human GT2 promoter. Dual luciferase assay (**A**) in HEK293T cells transiently transfected with 50 ng or 75 ng of Wt hFOXA2 or mutant hFOXA2 p.S169P indicates that Wt hFOXA2 is able to transactivate the human GT2 reporter, whilst the hFOXA2 p.S169P transcriptional activation is impaired (graph represents 4 independent experiments performed in triplicate, $^{*}P < 0.05$, one-way ANOVA). 3 independent western blots (**B**) show that the levels of the variant hFOXA2 p.S169P protein are reduced compared to the Wt hFOXA2, indicating that the mutation is functional and affects protein levels. Graph of the quantification of the western blots (**B′**) as percentage of Wt hFOXA2 and hFOXA2 p.S169P normalized to GAPDH indicates that hFOXA2 p.S169P variant results in half of the protein expression levels compared to Wt hFOXA2 (results from 6 independent experiments; $^{****}P < 0.0001$, one-way ANOVA). Abbreviation: NT, non-transfected; Wt, wild-type.

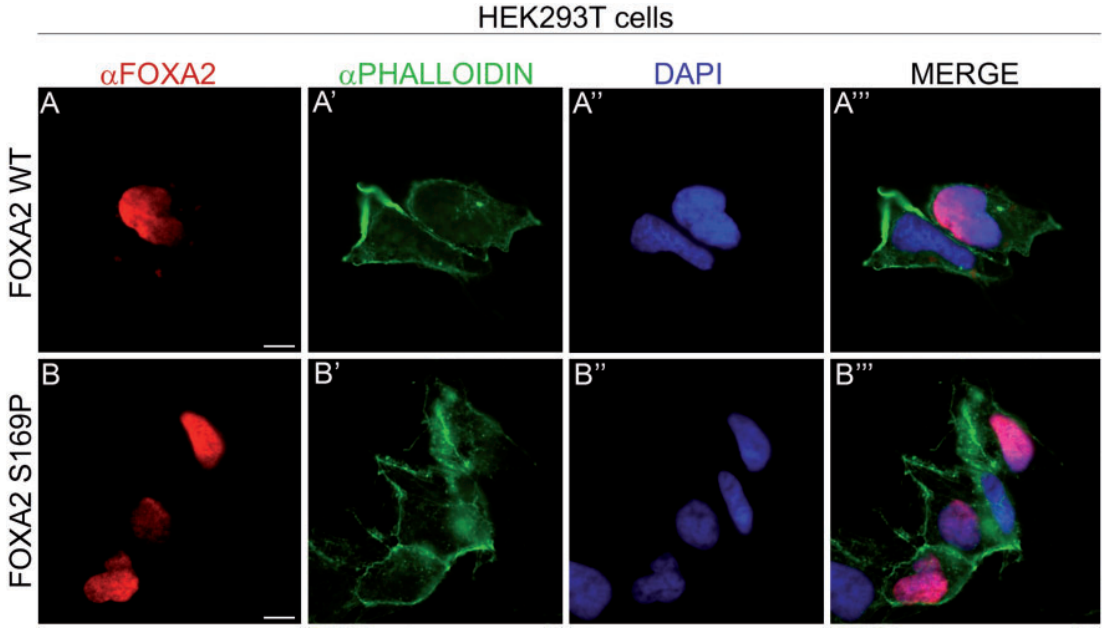


**Figure 5.** The S169P mutation in hFOXA2 does not result in changes in cellular localization of the protein. Double-immunofluorescence using anti-FOXA2 antibody (red **A**, **B**) and anti-PHALLOIDIN (green **A′**, **B′**) performed in HEK293 cells transiently transfected with either 200 ng of Wt hFOXA2 (**A**–**A‴**) or mutant hFOXA2 p.S169P (**B**–**B‴**) shows nuclear expression of both Wt and mutant FOXA2 (A, B) which overlaps with the nuclear DNA marker DAPI staining (**A″**, **B″**) but not with the cytoskeletal marker phalloidin. Abbreviation: DAPI, 4′,6-diamidino-2-phenylindole. Scale bars in A and B represent 10 μm.

In conclusion, we have identified the first disease-causing mutation in *FOXA2* in an individual with an extremely rare complex phenotype of CHI, cranio-facial dysmorphic features, CH, cardiac, liver and gastrointestinal abnormalities. Identification of the genetic cause contributing to such a unique clinical phenotype will help medical management and provide valuable insights into molecular mechanisms underlying pituitary development and β-cell physiology.

## Materials and Methods

### Patient enrolment

The patient was recruited to the 'Whole exome sequencing for rare endocrine disorders' study following written consent from the parents. The study was given favorable ethical opinion by the North West – Liverpool Central Research Ethics Committee (REC Reference: 15/NW/0758) and site study approval was granted by the Clinical Research Business Unit at Alder Hey Children's NHS Foundation Trust, Liverpool, UK.

### DNA extraction

DNA was obtained from blood samples of the child and both the biological parents (trio) using the QIAmp DNA blood Midi Kit (Qiagen, Hilden, Germany) as per the manufacturer's instructions and subjected to whole exome sequencing. The quality and the quantity of the genomic DNA were assessed using the Qubit (ThermoFisher Scientific) and the NanoDrop (ThermoFisher Scientific).

### Library preparation, exon capture and sequencing

The samples (3 μg/sample) were sheared with the Picoruptor to a size of approximately 150–200 bp. The samples were cleaned with 1.8× AMPure beads (Agencourt) and end repaired at 20 °C for 30 min. The products were A tailed by incubation at 37 °C for 30 min, cleaned with AMPure beads again and ligated to index adapters at 30 °C for 10 min to make a pre-capture library using the Agilent Sureselect XT target enrichment system for Illumina. Enrichment was achieved by five rounds of PCR using Herculase II fusion DNA polymerase. The libraries were checked on an Agilent HS Bioanalyser chip and quantified by Qubit Assay. 750 ng of pre-capture library was used for the hybridization. Samples were lyophilized to attain the required volume. Libraries were then mixed with hybridization buffer, baits from the Human All Exon 5 kit and incubated overnight (24 h) at 65 °C. The samples were then mixed with washed streptavidin beads (Dynabeads MyOne Streptavidin T10) and the captured products were washed and pooled. The quantity and quality of the pool was assessed by Bioanalyzer and subsequently by qPCR using the Illumina Library Quantification Kit from Kapa on a Roche Light Cycler LC480II, according to manufacturer's instructions. The template DNA was denatured according to the protocol described in the Illumina cBot user guide and loaded at 300 pM concentration. Sequencing was carried out on one lane of an Illumina HiSeq4000 at 2 × 150 bp paired-end sequencing with v1 chemistry.

### Bioinformatics

The sequence data were aligned to the reference genome (GRCh37/hg19). Reads were mapped to the reference sequences using BWA mem version 0.7.5a (53) with default parameters. The mean depth of the coverage was 100×. In order to retain only confidently aligned reads, alignments were filtered to remove reads with a mapping quality lower than 10. The mapped reads were locally re-aligned to improve the alignments around small insertions/deletions (indels) using the Genome Analysis Tool Kit (GATK) version 2.1.13 (54). Base quality scores were

recalibrated using GATK Base Quality Score Recalibrator (BQSR). BQSR is a module of GATK to create more accurate base qualities, which in turn improves the accuracy of our variant calls. The variants identified were annotated using SnpEff. The variants present in at least 1% minor allele frequency in 1000 Genomes Project, Exome aggregation consortium (ExAC), dbSNP142 and NHLBI ESP exomes were excluded. The predicted deleterious variants included non-synonymous coding, splice site, frameshift and stop gain variants. The analysis of variants was performed using the ingenuity variant analysis (Qiagen bioinformatics) software. The identified potential variant segregating with the patient's phenotype was subsequently confirmed by Sanger sequencing.

### Mice

All mice were housed with a 12 h light/12 h dark cycle in a temperature- and humidity-controlled room (21 °C, 55% humidity) with constant access to food and water. Timed pregnancies were achieved by mating females and males overnight and, the presence of vaginal plug the following morning, was considered as embryonic day (e) 0.5. All experiments were conducted under the regulations, licenses and local ethical review of the UK Animals (Scientific Procedures) Act 1986.

### Immunohistochemistry

Paraffin-embedded human tissue samples at 6, 8 and 13 weeks of gestation were obtained from the Human Developmental Biology Resource (Institute of Genetic Medicine, Newcastle and Institute of Child Health, London; www.hdbr.org). Immunohistochemistry was performed by deparaffinization of the sections followed by rehydration through decreasing ethanol dilutions. Heat-induced antigen retrieval was performed with a microwave in 10 mM sodium citrate buffer (pH 6). Samples were left to cool down at room temperature before incubating them for 1 h in blocking buffer [1× PBS, 0.1% Triton X-100, 5% Normal Goat Serum (Vector Laboratories)]. Endogenous hFOXA2 was detected with a primary rabbit monoclonal antibody against hFOXA2 (Thermo Fisher Scientific; 701698; 1:250) followed by a secondary biotinylated goat anti-rabbit antibody (Vector Laboratories; BA-1000; 1:300). Staining was achieved using DAB Peroxidase Substrate Kit (Vector Laboratories; SK-4100). The colorimetric reaction was stopped with washes in water and the sections were counterstained using Haematoxylin (Sigma-Aldrich). Images were acquired using a Leica microscope and figures were done with Adobe Photoshop CS6.

### *In situ* hybridization

Wild type mouse embryos were collected at different embryonic stages of mouse development (e11.5, e12.5, e13.5, e15.5 and e18.5), fixed with 4% paraformaldehyde (PFA) and washed in PBS before proceeding with paraffin embedding. Paraffin-embedded mouse embryos were sectioned at 7 μm thickness for histochemical evaluation. In situ hybridization was performed by processing the slides with a pre-hybridization treatment. Sections were deparaffinised, rehydrated through decreasing ethanol dilutions, fixed with 4% PFA, incubated with proteinase K, fixed again with 4% PFA and finally incubated with 0.1 M triethanolamine, 0.1% acetic anhydride. The mouse *Foxa2* gene fragment (1567 bp) plasmid was kindly provided by www.hdbr.org. The digoxigenin-labeled anti-sense probe for m*Foxa2* was generated by *in vitro* transcription using T3 RNA polymerase (Roche). Hybridization with 100 ng of the digoxigenin-labeled probe was carried out overnight at 65 °C. Sections were washed in 0.1 M Tris-HCl Buffer (pH = 7.5, 0.15 M Sodium) followed by 1 h blocking at room temperature and overnight incubation at 4 °C with anti-Dig antibody (Sigma-Aldrich). Detection of murine *Foxa2* was achieved by colorimetric reaction using 4-Nitro blue tetrazolium chloride solution (NBT, Sigma-Aldrich) and 5-Bromo-4-chloro-3-indolyl phosphate disodium salt (BCIP, Sigma-Aldrich). Images were acquired using a Leica microscope and figures were done using Adobe Photoshop CS6.

### Plasmids and site-direct mutagenesis

Full length cDNA of human *FOXA2* (GENE Bank RefSeq NM 021784.4) was cloned in ORF mammalian expression vector pCMV3 (pCMV3-hFOXA2, Sino Biological Inc). *E. coli* DH5α competent cells were transformed with h*FOXA2* (cDNA size: 1392 bp). The detected mutation was introduced by site-directed mutagenesis using QuikChange II XL Site-Directed Mutagenesis Kit (Agilent Technologies) according to the manufacturer's instructions (primers used, Forward strand: 5′-CAAAGCCGCCC TACCCGTACATCTCGCTC-3′. Reverse strand: 5′-GAGCGAGATG TACGGGTAGGGCGGCTTTG-3′). Sanger sequencing confirmed the point mutation.

### Cell culture and luciferase assays

HEK293T cells were grown in Dulbecco's Modified Eagle Medium (DMEM) supplemented with 10% FBS. 2.5 x $10^5$ cells/well were seeded in 24-well plates. 200 ng of phGT2-294-promoter-luc reporter (kindly provided by Professor Yong-Ho Ahn) and 100 ng of Renilla SV-40 were transiently co-transfected with either i) equal amounts (50 and 75 ng) of Wt or mutant p.S169P hFOXA2 expression plasmids or ii) both Wt and mutant p.S169P hFOXA2 expression plasmid (25 or 37.5 ng of each plasmid) using Lipofectamine 2000 (Life Technologies) according to the manufacturer's instructions. The total amount of DNA transfected was kept constant at 500 ng by adding pBluescript plasmid. The cells were harvested 24 h after transfection and the luciferase activity was measured using the Dual-Luciferase Reporter Assay System (Promega) in a BMG LABTECH Microplate reader (Omega, Germany) according to manufacturer's instructions. Firefly luciferase activity was normalized to the Renilla luciferase expression from pRL-SV40 (Promega). The experiments were independently repeated four times in triplicates and statistical analysis was performed using one-way ANOVA.

### Western blotting

1.75 × $10^5$ cells/well were seeded in 24-well plates and transiently transfected with equal amounts (200 ng) of Wt or mutant p.S169P hFOXA2 expression plasmids using Lipofectamine 2000 according to the manufacturer's instructions. 300 ng of pBluescript plasmid were added to each transfection mix to maintain the total amount of DNA constant at 500 ng. The cells were harvested 24 h after the transfection in a lysis buffer containing 50 mM Tris-Base (pH 7.6), 150 mM NaCl, 1% Triton X-100, protease inhibitor cocktail (Complete Mini, EDTA-free tablets, Roche) at a 1:6 ratio and 1% phosphatase inhibitor Cocktail3 (Sigma-Aldrich). Samples containing 20 μg of total proteins were loaded on 12% polyacrylamide gel. The proteins were

transferred on a nitrocellulose membrane and nonspecific binding sites were blocked for 1 h with 5% dried skimmed milk in PBS-T (1× PBS, 0.1% Tween 20). The membrane was incubated overnight at 4 °C with the primary antibody (rabbit anti-FOXA2; Thermo Fisher Scientific; 701698, 1:5000 dilution in 5% dried skimmed milk in PBS-T), followed by one hour incubation with IRDye 800CW Donkey anti-rabbit antibody (LI-COR Biosciences; 1:5000). Anti-GAPDH (Santa Cruz; 1:5000, rabbit polyclonal) levels were used to normalize the total level of protein. Blots were analyzed using Odyssey 2.1 Imaging System (LI-COR Biosciences). The experiments were independently repeated six times and the statistical analysis was performed using one-way ANOVA.

### Immunofluorescence

$1 \times 10^5$ cells/well were seeded in 4-well cell culture slide (Millipore, Fisher Scientific) and transiently transfected with 200 ng of Wt or mutant p.S169P hFOXA2 expression plasmids and 300 ng of pBluescript plasmid using Lipofectamine 2000 according to the manufacturer's instructions. 24 h after transfection, the cells were fixed in 2% PFA in 1× PBS for 10 min and washed with 1× PBS three times. Samples were permeabilized with 0.1% Triton X-100 in 1× PBS for 30 min and blocked with blocking buffer (5% Normal Goat Serum in 1× PBS) for 30 min. The staining was performed by incubating the samples with α-FOXA2 antibody (Thermo Fisher Scientific; 701698, 2 μg/ml) in blocking buffer for 1 h, followed by a 30 min incubation with goat α-rabbit Alexa fluor 594 (ThermoFisher Scientific; 1:250) and α-PHALLOIDIN Alexa fluor 488 (Molecular Probes; 1:1000) antibodies. The cell nuclei were stained with DAPI (4′,6-diamidino-2-phenylindole). Images were acquired using a fluorescence microscope (Leica microsystem, Germany) and processed using Adobe Photoshop CS6.

## Acknowledgements

The human embryonic and fetal material was provided by the Joint Medical Research Council (MRC)/Wellcome Trust Human Developmental Biology Resource (www.hdbr.org) (Grant 099175). M.L.V, A.G., have been funded by Action Medical Research (Grant Number GN2272); Barts and the London Charity (BTLC; Grant Number 417/2238); V.S and C.G-M are currently funded by Early Career Fellowship from the Medical College of Saint Bartholomew's Hospital Trust and Action Medical Research. D.G is funded by a research grant from Sandoz (UK) limited through the University of Liverpool, UK (Grant number Jxg 70001); D.G and S.S thank the staff at Clinical Research Facility (CRF) at Alder Hey Children's NHS Foundation Trust, patients and families for supporting this study.

*Conflict of Interest statement*. None declared.

## References

1. Kelberman, D., Rizzoti, K., Lovell-Badge, R., Robinson, I.C.A.F. and Dattani, M.T. (2009) Genetic regulation of pituitary gland development in human and mouse. *Endocr. Rev.*, **30**, 790–829.
2. Mehta, A. and Dattani, M.T. (2008) Developmental disorders of the hypothalamus and pituitary gland associated with congenital hypopituitarism. *Best. Pract. Res. Clin. Endocrinol. Metab.*, **22**, 191–206.
3. Patel, L., McNally, R.J., Harrison, E., Lloyd, I.C. and Clayton, P.E. (2006) Geographical distribution of optic nerve hypoplasia and septo-optic dysplasia in Northwest England. *J. Pediatr.*, **148**, 85–88.
4. Birkebæk, N.H., Patel, L., Wright, N.B., Grigg, J.R., Sinha, S., Hall, C.M., Price, D.A., Lloyd, I.C. and Clayton, P.E. (2003) Endocrine status in patients with optic nerve hypoplasia: relationship to midline central nervous system abnormalities and appearance of the hypothalamic-pituitary axis on magnetic resonance imaging. *J. Clin. Endocrinol. Metab.*, **88**, 5281–5286.
5. Willnow, S., Kiess, W., Butenandt, O., Dorr, H.G., Enders, A., Strasser-Vogel, B., Egger, J. and Schwarz, H.P. (1996) Endocrine disorders in septo-optic dysplasia (De Morsier syndrome)–evaluation and follow up of 18 patients. *Eur. J. Pediatr.*, **155**, 179–184.
6. Dattani, M.T., Martinez-Barbera, J.P., Thomas, P.Q., Brickman, J.M., Gupta, R., Martensson, I.L., Toresson, H., Fox, M., Wales, J.K. and Hindmarsh, P.C. (1998) Mutations in the homeobox gene HESX1/Hesx1 associated with septo-optic dysplasia in human and mouse. *Nat. Genet.*, **19**, 125–133.
7. Wu, W., Cogan, J.D., Pfäffle, R.W., Dasen, J.S., Frisch, H., O'Connell, S.M., Flynn, S.E., Brown, M.R., Mullis, P.E., Parks, J.S., Phillips III, J.A. and Rosenfeld, M.G. (1998) Mutations in PROP1 cause familial combined pituitary hormone deficiency. *Nat.Genet.*, **18**, 147–149.
8. Tatsumi, K-i., Miyai, K., Notomi, T., Kaibe, K., Amino, N., Mizuno, Y. and Kohno, H. (1992) Cretinism with combined hormone deficiency caused by a mutation in the PIT1 gene. *Nat. Genet.*, **1**, 56–58.
9. Netchine, I., Sobrier, M.L., Krude, H., Schnabel, D., Maghnie, M., Marcos, E., Duriez, B., Cacheux, V., Moers, A. and Goossens, M. (2000) Mutations in LHX3 result in a new syndrome revealed by combined pituitary hormone deficiency. *Nat. Genet.*, **25**, 182–186.
10. Machinis, K., Pantel, J., Netchine, I., Léger, J., Camand, O.J.A., Sobrier, M.-L., Moal, F.D.-L., Duquesnoy, P., Abitbol, M., Czernichow, P. *et al.* (2001) Syndromic short stature in patients with a germline mutation in the LIM Homeobox LHX4. *Am. J. Hum. Genet.*, **69**, 961–968.
11. Semina, E.V., Reiter, R., Leysens, N.J., Alward, W.L.M., Small, K.W., Datson, N.A., Siegel-Bartelt, J., Bierke-Nelson, D., Bitoun, P., Zabel, B.U. *et al.* (1996) Cloning and characterization of a novel bicoid-related homeobox transcription factor gene, RIEG, involved in Rieger syndrome. *Nat. Genet.*, **14**, 392–399.
12. Dateki, S., Fukami, M., Sato, N., Muroya, K., Adachi, M. and Ogata, T. (2008) OTX2Mutation in a patient with anophthalmia, short stature, and partial growth hormone deficiency: functional studies using theIRBP, HESX1, andPOU1F1Promoters. *J. Clin. Endocrinol. Metab.*, **93**, 3697–3702.
13. Kelberman, D., Rizzoti, K., Avilion, A., Bitner-Glindzicz, M., Cianfarani, S., Collins, J., Chong, W.K., Kirk, J.M., Achermann, J.C., Ross, R. *et al.* (2006) Mutations within Sox2/SOX2 are associated with abnormalities in the hypothalamo-pituitary-gonadal axis in mice and humans. *J. Clin. Invest.*, **116**, 2442–2455.
14. Laumonnier, F., Ronce, N., Hamel, B.C.J., Thomas, P., Lespinasse, J., Raynaud, M., Paringaux, C., van Bokhoven, H., Kalscheuer, V., Fryns, J.-P. *et al.* (2002) Transcription factor SOX3 is involved in X-linked mental retardation with growth hormone deficiency. *Am. J. Hum. Genet.*, **71**, 1450–1455.
15. Woods, K.S., Cundall, M., Turton, J., Rizotti, K., Mehta, A., Palmer, R., Wong, J., Chong, W.K., Al-Zyoud, M., El-Ali, M. *et al.* (2005) Over- and underdosage of SOX3 is associated

with infundibular hypoplasia and hypopituitarism. *Am. J. Hum. Genet.*, **76**, 833–849.
16. Senniappan, S., Arya, V.B. and Hussain, K. (2013) The molecular mechanisms, diagnosis and management of congenital hyperinsulinism. *Indian. J. Endocrinol. Metab.*, **17**, 19.
17. Aguilar-Bryan, L., Nichols, C., Wechsler, S., Clement, J., Boyd, A., Gonzalez, G., Herrera-Sosa, H., Nguy, K., Bryan, J. and Nelson, D. (1995) Cloning of the beta cell high-affinity sulfonylurea receptor: a regulator of insulin secretion. *Science*, **268**, 423–426.
18. Thomas, P., Cote, G., Wohllk, N., Haddad, B., Mathew, P., Rabl, W., Aguilar-Bryan, L., Gagel, R. and Bryan, J. (1995) Mutations in the sulfonylurea receptor gene in familial persistent hyperinsulinemic hypoglycemia of infancy. *Science*, **268**, 426–429.
19. Nestorowicz, A., Wilson, B.A., Schoor, K.P., Inoue, H., Glaser, B., Landau, H., Stanley, C.A., Thornton, P.S., Clement, JPt., Bryan, J. *et al.* (1996) Mutations in the sulonylurea receptor gene are associated with familial hyperinsulinism in Ashkenazi Jews. *Hum. Mol. Genet.*, **5**, 1813–1822.
20. Thomas, P., Ye, Y. and Lightner, E. (1996) Mutation of the pancreatic islet inward rectifier Kir6.2 also leads to familial persistent hyperinsulinemic hypoglycemia of infancy. *Hum. Mol. Genet.*, **5**, 1809–1812.
21. Nestorowicz, A., Inagaki, N., Gonoi, T., Schoor, K.P., Wilson, B.A., Glaser, B., Landau, H., Stanley, C.A., Thornton, P.S., Seino, S. *et al.* (1997) A nonsense mutation in the inward rectifier potassium channel gene, Kir6.2, is associated with familial hyperinsulinism. *Diabetes*, **46**, 1743–1748.
22. Stanley, C.A., Lieu, Y.K., Hsu, B.Y.L., Burlina, A.B., Greenberg, C.R., Hopwood, N.J., Perlman, K., Rich, B.H., Zammarchi, E. and Poncz, M. (1998) Hyperinsulinism and hyperammonemia in infants with regulatory mutations of the glutamate dehydrogenase gene. *N. Engl. J. Med.*, **338**, 1352–1357.
23. Glaser, B., Kesavan, P., Heyman, M., Davis, E., Cuesta, A., Buchs, A., Stanley, C.A., Thornton, P.S., Permutt, M.A., Matschinsky, F.M. *et al.* (1998) Familial hyperinsulinism caused by an activating glucokinase mutation. *N. Engl. J. Med.*, **338**, 226–230.
24. Clayton, P.T., Eaton, S., Aynsley-Green, A., Edginton, M., Hussain, K., Krywawych, S., Datta, V., Malingré, H.E.M., Berger, R. and van den Berg, I.E.T. (2001) Hyperinsulinism in short-chain L-3-hydroxyacyl-CoA dehydrogenase deficiency reveals the importance of β-oxidation in insulin secretion. *J. Clin. Invest.*, **108**, 457–465.
25. González-Barroso, M.M., Giurgea, I., Bouillaud, F., Anedda, A., Bellanné-Chantelot, C., Hubert, L., de Keyzer, Y., de Lonlay, P., Ricquier, D. and Barsh, G.S. (2008) Mutations in UCP2 in congenital hyperinsulinism reveal a role for regulation of insulin secretion. *PLoS. One*, **3**, e3850.
26. Stanescu, D.E., Hughes, N., Kaplan, B., Stanley, C.A. and De León, D.D. (2012) Novel presentations of congenital hyperinsulinism due to mutations in the MODY genes: HNF1A and HNF4A. *J. Clin. Endocrinol. Metab.*, **97**, E2026–E2030.
27. Meissner, T., Otonkoski, T., Feneberg, R., Beinbrech, B., Apostolidou, S., Sipila, I., Schaefer, F. and Mayatepek, E. (2001) Exercise induced hypoglycaemic hyperinsulinism. *Arch. Dis. Child.*, **84**, 254–257.
28. Pinney, S.E., Ganapathy, K., Bradfield, J., Stokes, D., Sasson, A., Mackiewicz, K., Boodhansingh, K., Hughes, N., Becker, S., Givler, S. *et al.* (2013) Dominant form of congenital hyperinsulinism maps to HK1 region on 10q. *Horm. Res. Paediatr.*, **80**, 18–27.
29. Tegtmeyer, L.C., Rust, S., van Scherpenzeel, M., Ng, B.G., Losfeld, M.E., Timal, S., Raymond, K., He, P., Ichikawa, M., Veltman, J. *et al.* (2014) Multiple phenotypes in phosphoglucomutase 1 deficiency. *N. Engl. J. Med.*, **370**, 533–542.
30. Stanley, C.A. (2016) Perspective on the genetics and diagnosis of congenital hyperinsulinism disorders. *J. Clin. Endocrinol. Metab.*, **101**, 815–826.
31. Ang, S.L. and Rossant, J. (1994) HNF-3 beta is essential for node and notochord formation in mouse development. *Cell*, **78**, 561–574.
32. Weinstein, D.C., Ruiz i Altaba, A., Chen, W.S., Hoodless, P., Prezioso, V.R., Jessell, T.M. and Darnell, J.E. (1994) The winged-helix transcription factor HNF-3β is required for notochord development in the mouse embryo. *Cell*, **78**, 575–588.
33. Lee, C.S., Friedman, J.R., Fulmer, J.T. and Kaestner, K.H. (2005) The initiation of liver development is dependent on Foxa transcription factors. *Nature*, **435**, 944–947.
34. Wan, H., Dingle, S., Xu, Y., Besnard, V., Kaestner, K.H., Ang, S.L., Wert, S., Stahlman, M.T. and Whitsett, J.A. (2005) Compensatory roles of Foxa1 and Foxa2 during lung morphogenesis. *J. Biol. Chem.*, **280**, 13809–13816.
35. Gao, N., LeLay, J., Vatamaniuk, M.Z., Rieck, S., Friedman, J.R. and Kaestner, K.H. (2008) Dynamic regulation of Pdx1 enhancers by Foxa1 and Foxa2 is essential for pancreas development. *Genes. Dev.*, **22**, 3435–3448.
36. Friedman, J.R. and Kaestner, K.H. (2006) The Foxa family of transcription factors in development and metabolism. *Cell. Mol. Life. Sci.*, **63**, 2317–2328.
37. Jin, O., Harpal, K., Ang, S.L. and Rossant, J. (2001) Otx2 and HNF3beta genetically interact in anterior patterning. *Int. J. Dev. Biol.*, **45**, 357–365.
38. Mavromatakis, Y.E., Lin, W., Metzakopian, E., Ferri, A.L.M., Yan, C.H., Sasaki, H., Whisett, J. and Ang, S.-L. (2011) Foxa1 and Foxa2 positively and negatively regulate Shh signalling to specify ventral midbrain progenitor identity. *Mech. Dev.*, **128**, 90–103.
39. Treier, M., O'Connell, S., Gleiberman, A., Price, J., Szeto, D.P., Burgess, R., Chuang, P.T., McMahon, A.P. and Rosenfeld, M.G. (2001) Hedgehog signaling is required for pituitary gland development. *Development*, **128**, 377–386.
40. Lantz, K.A., Vatamaniuk, M.Z., Brestelli, J.E., Friedman, J.R., Matschinsky, F.M. and Kaestner, K.H. (2004) Foxa2 regulates multiple pathways of insulin secretion. *J. Clin. Invest.*, **114**, 512–520.
41. Sund, N.J., Vatamaniuk, M.Z., Casey, M., Ang, S.L., Magnuson, M.A., Stoffers, D.A., Matschinsky, F.M. and Kaestner, K.H. (2001) Tissue-specific deletion of Foxa2 in pancreatic beta cells results in hyperinsulinemic hypoglycemia. *Genes. Dev.*, **15**, 1706–1715.
42. Cha, J.Y., Kim, H., Kim, K.S., Hur, M.W. and Ahn, Y. (2000) Identification of transacting factors responsible for the tissue-specific expression of human glucose transporter type 2 isoform gene. Cooperative role of hepatocyte nuclear factors 1alpha and 3beta. *J. Biol. Chem.*, **275**, 18358–18365.
43. Dayem-Quere, M., Giuliano, F., Wagner-Mahler, K., Massol, C., Crouzet-Ozenda, L., Lambert, J.-C. and Karmous-Benailly, H. (2013) Delineation of a region responsible for panhypopituitarism in 20p11.2. *Am. J. Med. Genet. A*, **161**, 1547–1554.
44. Tsai, E.A., Grochowski, C.M., Falsey, A.M., Rajagopalan, R., Wendel, D., Devoto, M., Krantz, I.D., Loomes, K.M. and Spinner, N.B. (2015) Heterozygous deletion of FOXA2 segregates with disease in a family with heterotaxy, panhypopituitarism, and biliary atresia. *Hum. Mutat.*, **36**, 631–637.

45. Garcia-Heras, J., Kilani, R.A., Martin, R.A. and Lamp, S. (2005) A deletion of proximal 20p inherited from a normal mosaic carrier mother in a newborn with panhypopituitarism and craniofacial dysmorphism. *Clin. Dysmorphol.*, **14**, 137–140.
46. Kamath, B.M., Thiel, B.D., Gai, X., Conlin, L.K., Munoz, P.S., Glessner, J., Clark, D., Warthen, D.M., Shaikh, T.H., Mihci, E. *et al.* (2009) SNP array mapping of chromosome 20p deletions: genotypes, phenotypes, and copy number variation. *Hum. Mutat.*, **30**, 371–378.
47. Williams, P.G., Wetherbee, J.J., Rosenfeld, J.A. and Hersh, J.H. (2011) 20p11 deletion in a female child with panhypopituitarism, cleft lip and palate, dysmorphic facial features, global developmental delay and seizure disorder. *Am. J. Med. Genet. A*, **155**, 186–191.
48. Lo, F.S., Lee, Y.J., Lin, S.P., Shen, E.Y., Huang, J.K. and Lee, K.S. (1998) Solitary maxillary central incisor and congenital nasal pyriform aperture stenosis. *Eur. J. Pediatr.*, **157**, 39–44.
49. Ben-Shushan, E., Marshak, S., Shoshkes, M., Cerasi, E. and Melloul, D. (2001) A pancreatic -cell-specific enhancer in the human PDX-1 gene is regulated by hepatocyte nuclear factor 3 (HNF-3), HNF-1, and SPs transcription factors. *J. Biol. Chem.*, **276**, 17533–17540.
50. Wang, H., Gauthier, B.R., Hagenfeldt-Johansson, K.A., Iezzi, M. and Wollheim, C.B. (2002) Foxa2 (HNF3) controls multiple genes implicated in metabolism-secretion coupling of glucose-induced insulin release. *J. Biol. Chem.*, **277**, 17564–17570.
51. Lee, C.S., Sund, N.J., Vatamaniuk, M.Z., Matschinsky, F.M., Stoffers, D.A. and Kaestner, K.H. (2002) Foxa2 controls Pdx1 gene expression in pancreatic – cells in vivo. *Diabetes*, **51**, 2546–2551.
52. Ahlgren, U., Jonsson, J., Jonsson, L., Simu, K. and Edlund, H. (1998) beta-Cell-specific inactivation of the mouse Ipf1/Pdx1 gene results in loss of the beta-cell phenotype and maturity onset diabetes. *Genes. Dev.*, **12**, 1763–1768.
53. Li, H. and Durbin, R. (2010) Fast and accurate long-read alignment with Burrows-Wheeler transform. *Bioinformatics*, **26**, 589–595.
54. McKenna, A., Hanna, M., Banks, E., Sivachenko, A., Cibulskis, K., Kernytsky, A., Garimella, K., Altshuler, D., Gabriel, S., Daly, M. *et al.* (2010) The Genome Analysis Toolkit: a MapReduce framework for analyzing next-generation DNA sequencing data. *Genome. Res.*, **20**, 1297–1303.

Giri et al. International Journal of Pediatric Endocrinology (2017) 2017:8
DOI 10.1186/s13633-017-0047-9

International Journal of Pediatric Endocrinology

CASE REPORT Open Access

# Novel compound heterozygous *ASXL3* mutation causing Bainbridge-ropers like syndrome and primary IGF1 deficiency

Dinesh Giri[1,3], Daniel Rigden[2], Mohammed Didi[3], Matthew Peak[1,4], Paul McNamara[1] and Senthil Senniappan[1,3*]

## Abstract

**Background:** De novo truncating and splicing mutations in the additional sex combs-like 3 (*ASXL3*) gene have been implicated in the development of Bainbridge-Ropers syndrome (BRPS) characterised by severe developmental delay, feeding problems, short stature and characteristic facial features.

**Case presentation:** We describe, for the first time, a patient with severe short stature, learning difficulties, feeding difficulties and dysmorphic features with a novel compound heterozygous mutation in *ASXL3*.Additionally the patient also has primary insulin like growth factor-1 (IGF1) deficiency. The mutations occur in exon 11 and proximal part of exon 12 and are strongly conserved at the protein level across various species. *In-silico* analyses using PolyPhen-2 and SIFT predict the amino acid substitutions to be potentially deleterious to the protein function. Detailed bioinformatics analysis show that the molecular defects caused by the two compound heterozygous mutations synergistically impact on two points of the molecular interaction network of *ASXL3*.

**Conclusion:** We hypothesise that *ASXL3* potentially has a role in transcriptional activation of *IGF1* involved in signalling pathways that regulate cell proliferation and growth, which could be contributing to short stature encountered in these patients.

**Keywords:** *ASXL3*, Bainbridge-Ropers syndrome, IGF-1 deficiency

## Background

The use of next generation sequencing in children with undiagnosed or unidentified syndromic disorders is becoming more popular in recent years, increasing the diagnostic ability and discovery of novel genes and mutations contributing to novel clinical phenotypes.

Bainbridge-Ropers syndrome (BRPS: OMIM #615485) was described for the first time by Bainbridge and his colleagues in the year 2013 [1]. BRPS is caused by de-novo truncating mutations in the additional sex combs-like 3 (*ASXL3)* gene giving rise to characteristic phenotypic features such as short stature, severe intellectual deficit, feeding difficulties, failure to thrive and cranio-facial features. BRPS has been reported in 27 patients in the literature so far [1–4]. The majority of the patients had frameshift or truncating mutations in *ASXL3*. One patient has been reported to have a splicing mutation in *ASXL3* resulting in BRPS [3].

Bohring-Opitz syndrome (BOS: OMIM#605039) is a developmental syndrome characterised by a severe intellectual deficit, distinct posture and cranio-facial abnormalities, feeding problems and failure to thrive [5]. BOS is caused by de novo truncating mutations in *ASXL1*, which belongs to the same family as *ASXL3* [5]. BOS and BRPS have been found to have some overlap of their clinical phenotypes.

We describe, for the first time, a patient, with severe short stature secondary to IGF1 (Insulin Growth Factor 1) deficiency, developmental delay, intellectual deficit, cranio-facial abnormalities due to a novel compound heterozygous mutation in *ASXL3* identified by whole exome sequencing.

## Case presentation

The patient is a 16-year-old Caucasian British boy born at full term following an induction of labour to non-

* Correspondence: senthil.senniappan@alderhey.nhs.uk
[1]Institute in the Park, Alder Hey Children's NHS Foundation Trust, University of Liverpool, Eaton Road, Liverpool, UK
[3]Department of Paediatric Endocrinology, Alder Hey Children's NHS Foundation Trust, Liverpool, UK
Full list of author information is available at the end of the article

consanguineous Caucasian healthy British parents. The antenatal scans were normal and the birth weight was 4.1 kg (1.84 SDS). He was admitted to the neonatal unit due to respiratory distress. Whilst in the neonatal unit, he had persistent feeding difficulties and required tube feeding. He was noted to have scaphocephaly that required surgical fixation at 4 months of age. He also developed severe constipation from 5 weeks of age requiring daily bowel washouts from 18 months of age and colostomy at 3 years. He had bilateral undescended testes requiring orchidopexy. He has global developmental delay and complex learning difficulties requiring additional support at school. He also has been diagnosed with autism. At 7 years of age, he was referred to endocrinology for assessment of his severe short stature (−4.11 SDS for height, mid parental height: −1.1 SDS, weight: -2.30 SDS). He has dysmorphic features including prominent long nasal bridge and forehead, small lower jaw, thin lips, low set cupped ears, strabismus and down-slanting palpebral fissures (Fig. 1). He was found to have a normal growth hormone (GH) response (peak GH 11.7 μg/L) (Normal:>6.7 μg/L) to an arginine stimulation test. He had a bone age delay of 3 years and the IGF1 was persistently low at 4.9 nmol/L (−3.2 SDS). TSH (Thyroid stimulating hormone), Free T4 (thyroxine), ACTH (Adreno corticotrophic hormone), prolactin and cortisol concentrations were all within the normal range. A trial of rhGH (recombinant human growth hormone) (50 μg/kg/day) for a period of 1 year was ineffective in improving height velocity (Fig. 2a). An IGF1 (insulin growth factor-1) generation test after 33 μg/kg of rhGH did not produce any response. Subsequently, recombinant IGF1 (rIGF1) therapy (mecasermin) was commenced at 12.5 years which resulted in improvement of height velocity to -3SDS (Fig. 2a). He has a normal muscle tone and normal deep tendon reflexes. His cranial MRI scan of brain and spine were normal. The hearing has been normal. The echocardiogram and renal ultrasound did not identify any abnormalities. The plasma amino acids, urine organic acids, pyruvic acid analysis were within the normal limits. CGH microarray did not reveal any copy number changes. Targeted sequencing of *IGF1*, *IGF1R* and *GHR* did not reveal any mutations. Currently, the patient continues to require rIGF1 therapy to support growth. The weight gain continues to be suboptimal (Fig. 2b).

**Fig. 1** Dysmorphic features: prominent long nasal bridge and forehead, small lower jaw, thin lips, strabismus, down slanting palpebral fissures and low set cupped ears

## Material and methods

This study was given favourable ethical opinion by the North West - Liverpool Central Research Ethics Committee (REC Reference: 15/NW/0758) and site study approval was granted by the Clinical Research Business Unit at Alder Hey Children's NHS Foundation Trust, Liverpool, UK. Informed and written consent was obtained from the parents. DNA was extracted from blood samples of the child and both the biological parents (trio). Exons were captured using SureSelect XT Human All Exon V5 capture library and DNA sequencing was carried out using the Illumina HiSeq4000 at 2 × 150 bp paired-end sequencer. The sequence data were aligned to the reference genome (GRCh37/hg19). The variants present in at least 1% minor allele frequency in 1000 Genomes Project, dbSNP142, and NHLBI ESP exomes were excluded. The predicted deleterious variants included non-synonymous coding, splice site, frameshift, stop gain variants.

## Results

Two novel heterozygous mutations in *ASXL3* [NM_0 30632.1]: c.2965C > G, p.R989G inherited from the mother and c.3078G > C, p.K1026 N, inherited from the father were found in the patient. The mutations were subsequently confirmed by Sanger sequencing (Fig. 3). The mutations occur in exon 11 and proximal part of exon 12(Fig. 4). Multiple sequence alignment visualisation using the UCSC Genome Browser showed that both mutated positions are strongly conserved at the protein level across vertebrates as diverse as lemur, bat, fish and frog, implying that mutation could potentially affect the protein structure or function. *In silico* analyses using PolyPhen-2 and SIFT predict the amino acid substitutions to be potentially deleterious to the protein function.

## Discussion

Loss of function mutations in *ASXL3* in the form of de-novo truncating dominant mutations and splicing mutation have been implicated in BRPS. Here we report for the first time, a compound heterozygous *ASXL3* mutation in a patient with BRPS-like features and associated with primary IGF1 deficiency. Pathogenic mutations in *ASXL3* have been reported to occur predominantly in exon 11 and proximal part of exon 12. All the described mutations retain the ASXN and ASXH domains. The compound heterozygous mutations in our patient also lie on exon 11 and proximal exon 12, retaining the ASXN and ASXH domains similar to previously described mutations (Fig. 4).

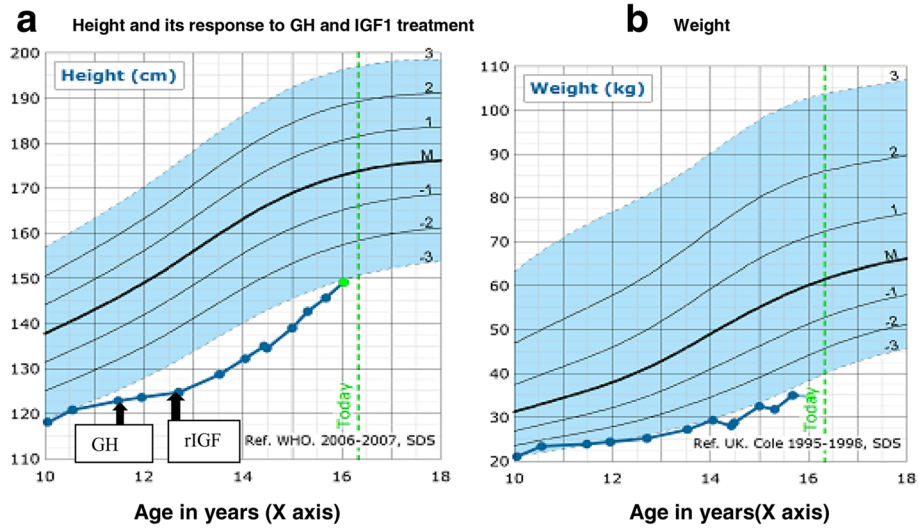


**Fig. 2** **a** Height and its response to GH and IGF1 treatment. **b** Weight

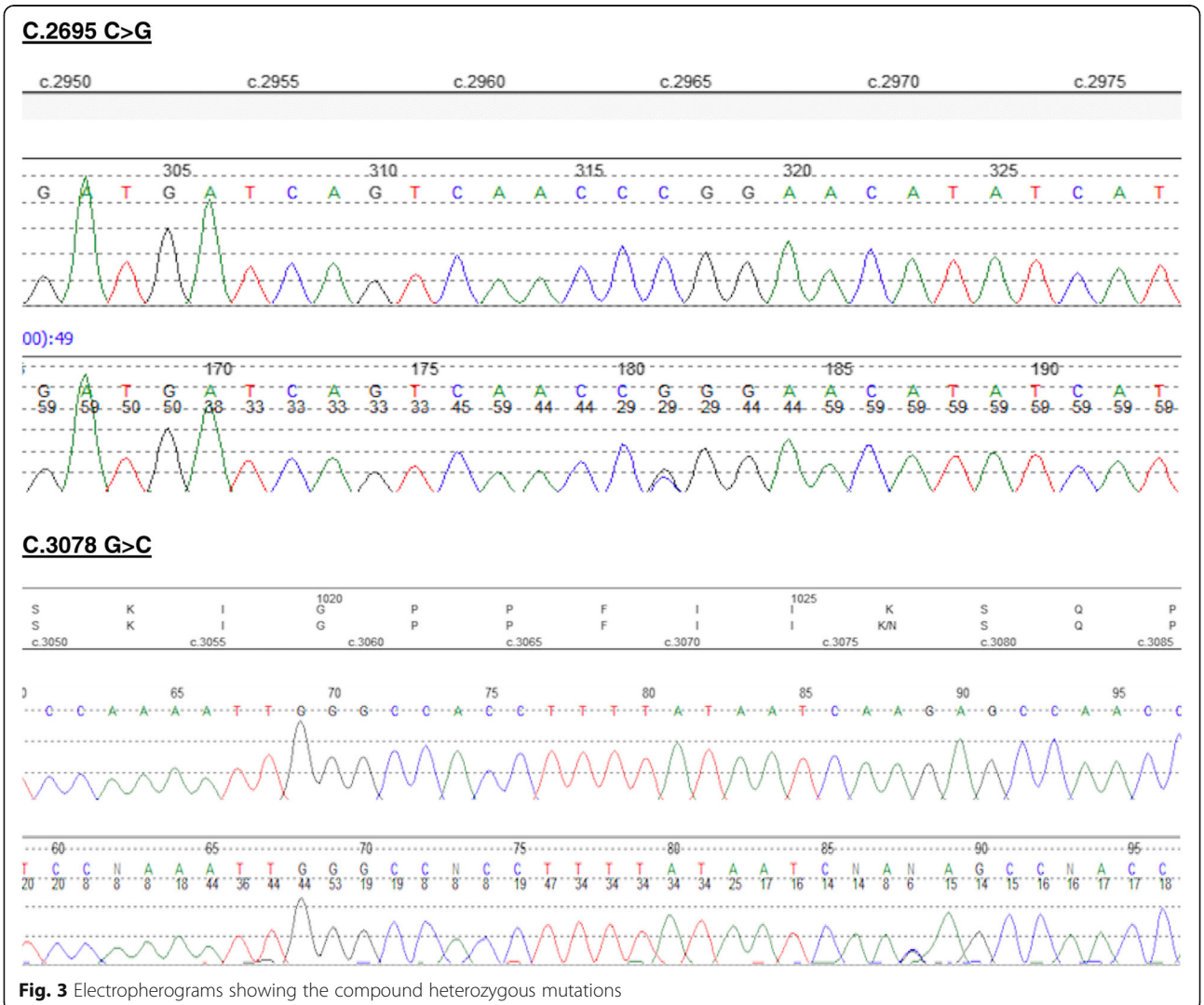


**Fig. 3** Electropherograms showing the compound heterozygous mutations

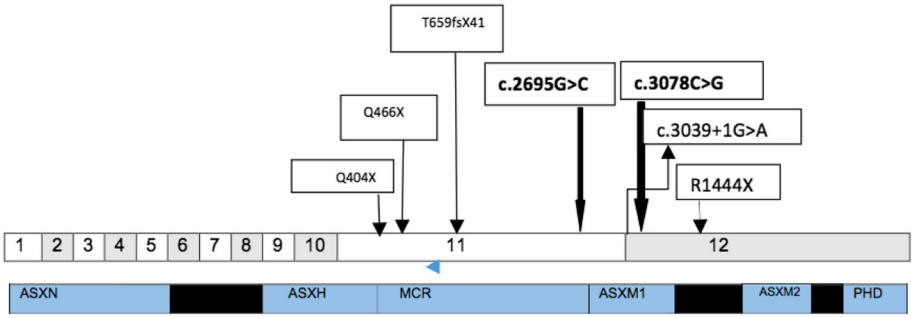


**Fig. 4** *ASXL3* gene with domains. 1–12 represents the exon numbers. Some of the previously reported mutations (frameshift and truncating) and splice site mutations have been shown. Compound heterozygous mutations in our patient have been highlighted in bold

Both these mutations occur on the conserved ASXM1 domain in *ASXL3* (Fig. 4). Both the variants are extremely rare and have a population frequency < 0.01, as indicated from the ExAC browser. The synergistic effect of both of these rare mutations potentially contributes to the loss of function of the protein contributing to the BRPS like phenotype. Our patient has multiple dysmorphic features that overlap with those described in previous reported cases of BRPS such as short stature, failure to thrive, feeding difficulties, cranio-facial features, developmental delay and learning difficulties (Table 1).

*ASXL3* belongs to the gene family of ASXL genes, the mammalian homologues of Drosophila Asx. ASXL includes three orthologues: *ASXL1*, *ASXL2* and *ASXL3* that encode the Putative Polycomb group (PcG) protein that has a role in regulating the homeotic genes (Hox) [6]. PcG proteins can act either as transcriptional repressors or activators of Hox genes [6]. The genes in the ASXL family share a common domain architecture consisting of ASXN, ASXH, ASXM1, ASXM2 domains and a PHD finger, and act by forming complexes with other proteins via methylation of histones [4, 6, 7]. *ASXL3* has been implicated in the deubiquitination of histone H2A lysine 119(H2AK119Ub1), a component of the polycomb repressive deubiquitination (PR-DUB) complex [4]. The formation of PR-DUB complex is critical for normal function. *ASXL3* interacts with BAP1, a ubiquitin terminal hydroxylase and removes the monoubiquitin (Ub1) from the H2AK119Ub1 [8]. Patients with BRPS have been found to have a significant increase in the H2AK119Ub1 in their fibroblasts because of the impaired deubiquitination [4]. *ASXL3* has a similar expression pattern in human tissues as *ASXL1* but at a relatively lesser levels, which may explain the overlap of some phenotypic features seen in BRPS and BOS [9]. Within the human brain, *ASXL3* expression has been found within the white matter, insula, cingulate gyrus and amygdala [10]. The spinal cord, kidney, bone marrow and liver also express *ASXL3*, but at a lower level when compared to *ASXL1* [9].

Detailed bioinformatics analysis suggests a possible molecular mechanism by which the first of the mutations R989G would lead to a functional defect. A scan against the ELM(Eukaryotic Linear Motif) database shows a stretch of amino-acid residues from the position 989 to 997 within the wild-type *ASXL3* that matches with an interaction motif (LIG_14–3-3_CanoR_1; Accession ELME000417) that describes canonical phosphopeptide binding motif of 14–3-3 group of proteins. 14–3-3 proteins are important cell regulators [11], best known for their role in cell cycle control. The mutated Arginine at position 989 together with a phosphorylated Serine residue, 3–5 residues downstream are the main determinants of interaction with 14–3-3 proteins. These proteins are also characterised as histone modification readers [12]. This links suggestively to the recently determined role of *ASXL3* in histone deubiquitination [4]. According to this hypothesis, mutation of R989 to glycine would prevent the interaction of *ASXL3* with an as-yet unidentified 14–3-3 protein, thereby damaging function through impairing its ability to scaffold epigenetic protein complexes [6]. Although the molecular mechanism of the second mutation K1026 N, is unclear it is possible that this mutation affects phosphorylation of *ASXL3* through its location within recognition motifs for kinases (PIKK group, motif from 1024 to 1030 or GSK3, motif from 1024 to 1031); The molecular defects caused by the two mutations would specify the disorder additively or synergistically by simultaneously impacting on two points of the molecular interaction network of *ASXL3* contributing to its loss of function.

The association of primary IGF1 deficiency in BRPS has not been described before. IGF-1 is a 70-amino acid peptide hormone and growth factor that is structurally homologous to proinsulin [13]. In normal individuals, IGF-1 circulates as part of a ternary complex with a molecular weight of 150 kDa. The complex consists of IGF-1, an acid-labile subunit (ALS), and a protein that binds IGF-1 (IGFBP-3). Primary IGF1 deficiency is defined as basal

**Table 1** Phenotypic comparison between our patient and other reported patients with BRPS

| Phenotype | Our Patient | Bainbridge et al. [1]. 4 patients | Dinwiddie et al. [2]. 1 patient | Srivastava et al. [4]. 3 patients | Hori et al. [3]. 1 patient | Balasubramanian et al. [17]. 12 patients | Kuechler et al. [18]. 6 patients |
|---|---|---|---|---|---|---|---|
| Clinical | | | | | | | |
| Feeding problems | + | + | + | + | + | 9/12 | 6/6 |
| Failure to thrive | + | + | + | + | + | | 3/6 |
| Short stature | + | + | | ND | + | 2/12 | 2/6 |
| IUGR | – | 3/4 | + | 2/3 | + | | – |
| Craniofacial | | | | | | | |
| Trigonocephaly | – | 1/4 | + | 1/3 | + | ND | ND |
| Microcephaly | – | 2/4 | + | – | + | + | 1/6 |
| Scaphocephaly | + | – | – | – | – | + | ND |
| Palate | High arched | 1/4 | ND | ND | ND | High arched (9/12) | High arched (5/6) |
| Prominent forehead | + | 2/4 | ND | 1/3 | ND | + | 5/6 |
| Prominent eyes | – | – | + | – | ND | ND | ND |
| Palpebral fissures | downslanting | | upslanting | downslanting (2/3) | – | downslanting-10/12 Upslanting-2/12 | downslanting |
| Nasal bridge | long | – | depressed | Broad (1/3) | depressed | long, prominent | 6/6 (prominent columella) |
| Low set ears | + | 1/4 | NA | 1/3 | – | + | ND |
| Posteriorly rotated ears | Cupped ears | 2/4 | + | + | – | + | ND |
| Anteverted nares | – | + | + | 1/3 | – | ND | 5/6 |
| Small chin | + | ND | ND | 2/3 | + | + | ND |
| Ophthalmic | | | | | | | |
| Strabismus | + | ND | ND | 1/3 | + | 7/12 | 5/6 |
| Astgmatism | myopia | ND | Myopia (1/3) | Hyperopia (1/3) | myopia | ND | |
| Neurological | | | | | | | |
| Developmental delay | + | + | + | + | + | 12/12 | 6/6 |
| Intellectual deficit | + | + | + | 2/3 | + | 12/12 | 5/6 |
| Seizures | – | – | + | 1/3 | | 3/12 | 2/6 |
| Autism | + | NA | NA | NA | + | 9/12 | not formally diagnosed |
| Other Features | | | | | | | |
| large fontanelle | + | 1/4 | ND | ND | ND | ND | ND |
| Undescended testes | + | 1/4 | ND | ND | ND | ND | ND |
| Chronic constipation | + | ND | ND | 1/3 | ND | ND | ND |

ND: not described. +: present. -: absent

IGF-1 and height of ≤ -3 SDS with normal or elevated levels of GH [13]. The primary action of IGF1 is mediated by binding to its specific receptor, the insulin-like growth factor 1 receptor (IGF1R), which is present in many tissues. IGF1R is a receptor tyrosine kinase and binding of IGF1 to IGF1R initiates intracellular signalling. IGF-1 is

one of the most potent natural activators of the Akt signalling pathway, which stimulates cellular growth and proliferation [14].

Transcriptome analysis of *ASXL3* fibroblasts from patients with BRPS examining the differentially expressed genes (DEGs) has shown that the genes regulating the cellular proliferation are downregulated [4]. IGF1 plays a vital role in activating the Akt signalling pathway, a potent stimulator for cell proliferation and growth [15]. We therefore hypothesise that *ASXL3* potentially has a role in transcriptional activation of *IGF1* involved in this pathway potentially via epigenetic mechanisms [16], which could be contributing to short stature encountered in these patients.

## Conclusions

The compound heterozygous mutations potentially contribute to the loss of function in *ASXL3*, causing a phenotype similar to BRPS. Although with our current knowledge, the molecular interaction between *ASXL3* and *IGF1* is unclear, it may important to look for IGF1 deficiency in the patients with *ASXL3* mutation.

## Consent

Written informed consent was obtained from the patient's legal guardian(s) for publication of this case report and any accompanying images. A copy of the written consent is available for review by the Editor-in-Chief of this journal.

### Abbreviations

ASXL3: additional sex combs-like 3; BAP1 : BRCA1 Associated Protein 1; BOS: Bohring-Opitz syndrome; BRPS: Bainbridge Ropers syndrome; ExAC: Exome Aggregation Consortium; GH: Growth hormone; IGF-1: Insulin Growth Factor-1; SDS: Standard deviation score; Ub1: mono-ubiquitin

### Acknowledgements

We thank the staff at Clinical Research Facility (CRF) at Alder Hey Children's NHS Foundation Trust for supporting this study.

### Funding

No funds were obtained for this case report.

### Availability of data and materials

Not applicable.

### Authors' contributions

DG wrote the initial draft of the manuscript. DR contributed to the bioinformatics section and the revision of the manuscript.PM, MP and MD edited, reviewed and revised the manuscript. SS oversaw the case report, reviewed and revised the manuscript. All authors read and approved the final manuscript.

### Ethics approval and consent to participate

This study was given favourable ethical opinion by the North West - Liverpool Central Research Ethics Committee (REC Reference: 15/NW/0758) and site study approval was granted by the Clinical Research Business Unit at Alder Hey Children's NHS Foundation Trust, Liverpool, UK. Informed and written consent was obtained from the parents.

### Consent for publication

A written informed consent was obtained from the parents regarding the publication of the case report and the images.

### Competing interests

The authors declare that they have no competing interests.

## Publisher's Note



### Author details

[1]Institute in the Park, Alder Hey Children's NHS Foundation Trust, University of Liverpool, Eaton Road, Liverpool, UK. [2]Institute of Intergrative Biology, University of Liverpool, Liverpool, UK. [3]Department of Paediatric Endocrinology, Alder Hey Children's NHS Foundation Trust, Liverpool, UK. [4]NIHR Alder Hey Clinical Research Facility for Experimental Medicine, Liverpool, UK.

Received: 8 May 2017 Accepted: 27 July 2017
Published online: 04 August 2017

### References

1. Bainbridge MN, Hu H, Muzny DM, Musante L, Lupski JR, Graham BH, Chen W, Gripp KW, Jenny K, Wienker TF, Yang Y, Sutton VR, Gibbs RA, Ropers HH. De novo truncating mutations in ASXL3 are associated with a novel clinical phenotype with similarities to Bohring–Opitz syndrome. Genome Med. 2013;5:11.
2. Dinwiddie DL, Soden SE, Saunders CJ, Miller NA, Farrow EG, Smith LD, Kingsmore SF. De novo frameshift mutation in ASXL3 in a patient with global developmental delay, microcephaly, and craniofacial anomalies. BMC Med Genet. 2013;6:32.
3. Hori I, Miya F, Ohashi K, Negishi Y, Hattori A, Ando N, Okamoto N, Kato M, Tsunoda T, Yamasaki M, Kanemura Y, Kosaki K, Saitoh S. Novel splicing mutation in the ASXL3 gene causing Bainbridge-ropers syndrome. Am J Med Genet A. 2016;170:1863–7.
4. Srivastava A, Ritesh KC, Tsan YC, Liao R, Su F, Cao X, Hannibal MC, Keegan CE, Chinnaiyan AM, Martin DM, Bielas SL. De novo dominant ASXL3 mutations alter H2A deubiquitination and transcription in Bainbridge-Ropers syndrome. Hum Mol Genet. 2016;25:597–608.
5. Bohring A, Oudesluijs G. G, Grange D. K, Zampino G, Thierry P.2006. New cases of Bohring-Opitz syndrome, update, and critical review of the literature. Am J Med Genet 140A: 1257–1263.
6. Katoh M. Functional proteomics of the epigenetic regulators ASXL1, ASXL2 and ASXL3: a convergence of proteomics and epigenetics for translational medicine. Expert Rev Proteomics. 2015;12:317–28.
7. Aravind L, Iyer LM. The HARE-HTH and associated domains: novel modules in the coordination of epigenetic DNA and protein modifications. Cell Cycle. 2012;11:119–31.
8. Di Croce L, Helin K. Transcriptional regulation by Polycomb group proteins. Nat Struct Mol Biol. 2013;20:1147–55.
9. Shmueli O, Horn-Saban S, Chalifa-Caspi V, Shmoish M, Ophir R, Benjamin-Rodrig H, Safran M, Domany E, Lancet D. Gene note: whole genome expression profiles in normal human tissues. C R Biol. 2003;326:1067–72.
10. Jones AR, Overly CC, Sunkin SM. The Allen brain atlas: 5 years and beyond. Nat Rev Revs. 2009;10:821–8.
11. Aghazadeh Y, Papadopoulos V. The role of the 14-3-3 protein family in health, disease, and drug development. Drug Discov Today. 2016;21:278–87.
12. Yun M, Wu J, Workman JL, Li B. 2011. Readers of histone modifications. Cell Res. 2011;21:564–78.
13. Cohen J, Blethen S, Kuntze J, Smith SL, Lomax KG, Mathew PM. Managing the child with severe primary insulin-like growth factor-1 deficiency (IGFD): IGFD diagnosis and management. Drugs R D. 2014;14:25–9.
14. Ashare A, Nymon AB, Doerschug KC, Morrison JM, Monick MM, Hunninghake GW. Insulin-like growth factor-1 improves survival in sepsis via enhanced hepatic bacterial clearance. Am J Respir Crit Care Med. 2008;178:149–57.
15. Manning BD, Cantley LC. AKT/PKB signaling: navigating downstream. Cell. 2007;129:1261–74.
16. Madonna R, De Caterina R, Geng YJ. Epigenetic regulation of insulin-like growth factor signaling: a novel insight into the pathophysiology of neonatal pulmonary hypertension. Vasc Pharmacol. 2015;73:4–7.
17. Balasubramanian M, Willoughby J, Fry AE, Weber A, Firth HV, Deshpande C, Berg JN, Chandler K, Metcalfe KA, Lam W, et al. Delineating the phenotypic spectrum of Bainbridge-Ropers syndrome: 12 new patients with de novo, heterozygous, loss-of-function mutations in ASXL3 and review of published literature. J Med Genet. 2017 Jan 18. pii: jmedgenet-2016-104360. doi:10.1136/jmedgenet-2016-104360. [Epub ahead of print].
18. Kuechler A, Czeschik JC, Graf E, Grasshoff U, Hüffmeier U, Busa T, Beck-Woedl S, Faivre L, Rivière JB, Bader I, et al. Bainbridge-ropers syndrome caused by loss-of-function variants in ASXL3: a recognizable condition. Eur J Hum Genet. 2017;25(2):183–91.